

NOVEL WATER SOLUBLE POLYMERS AS FLOCCULANTS

Novel Water Soluble Polymers as Flocculants

By

Huining Xiao

A Thesis

Submitted to the School of Graduate Studies

in Partial Fulfillment of Requirements

for the Degree

Doctor of Philosophy

McMaster University

© Copyright by Huining Xiao, December 1994

DOCTOR OF PHILOSOPHY (1994)

(Chemical Engineering)

McMASTER UNIVERSITY

Hamilton, Ontario, Canada

TITLE: Novel Water Soluble Polymers as Flocculants

AUTHOR: Huining Xiao, M. Eng., B. Eng. (Nanjing Institute of
Chemical Technology)

SUPERVISORS: Professors Robert H. Pelton and Archie E. Hamielec

**NUMBER OF
PAGES:** xviii, 257

ABSTRACT

High molecular weight poly(ethylene oxide) (PEO) is used in conjunction with a cofactor such as phenol formaldehyde resin (PFR) as flocculants for newsprint manufacture. The objectives of the work described in this thesis were to prepare flocculants superior to PEO and to determine the flocculation mechanism. A series of novel comb copolymers consisting of a polyacrylamide backbone with short pendant poly(ethylene glycol) (PEG) chains was prepared and characterized. Additionally, polymerization conversion curves and reactivity ratios were measured. An interesting finding was that the reactivity of the macromonomer in free radical copolymerization decreased with PEG chain length.

Flocculation results with both model latex dispersions and commercial wood pulp suspensions showed that copolymer chain length was the most important variable; molecular weights greater than 3 million were required for good flocculation. On the other hand, the PEG pendant chains could be as short as 9 ether repeat units. Also, only 1 to 2 PEG chains for every 100 acrylamide backbone moieties were required.

No published flocculation mechanisms could predict all the behaviors of the PEO or copolymer system. A new mechanism called complex bridging was proposed. According to this mechanism PEO or copolymer chains aggregate in the presence of cofactor to form colloiddally dispersed polymer complex which heteroflocculates with the colloidal particles.

Given in this work is the first explanation of the requirement for extremely high PEO or copolymer molecular weights for flocculation. It is proposed that polymer chains with molecular weights less than 10^6 collapse in the presence of PFR to an inactive precipitate before flocculation can occur whereas complexes based on very high molecular weight PEO collapse slowly enough to permit flocculation.

Published mechanistic studies are hindered by the fact that PFR has poorly defined structures. It is shown for the first time in this work that well-defined, linear, poly(p-vinyl phenol) (PVPh) is an effective cofactor.

ACKNOWLEDGMENTS

First and foremost, I am deeply grateful to Professor R.H. Pelton and Professor A.E. Hamielec, my supervisors, for their supervision, instruction, encouragement and support in successfully completing this dissertation. No words can sufficiently express my thanks.

Sincere appreciation is also extended to the following people for their support during the course of this thesis:

Professor J.M. Dickson and Professor J.R. Kramer, members of my supervisor committee, for their advice and help.

Professor A.D. Bain and G. Timmins for their help in NMR analysis.

Professor R.M. Epand and Dr. R.F. Epand for their help on the work of fluorescence.

G. McClung, G. Liu and M. Moore for their assistance in fluorescent microscopy, confocal microscopy and SEM.

Professors S. Zhu, K.C. Tam, X. Wu, P. Li, Drs. Y. Deng and T. Xie for their encouragement and helpful discussions.

D. Keller, L. Morine, J. Micalash, D. Anderson, M. Ajersch, M. Corak, B. Grosse, H. Ketelson, P. Miller, B. Wasmund, X. Zhao and Dr. L.K. Kostanski for their help, assistance and all the convenience to access research facilities.

Networks of Centres of Excellence, Mechanical and Chemimechanical Wood-pulps Network, Dorset Industrial Chemicals and Department of Chemical Engineering of McMaster University for their financial support.

Finally, my wife Baijing for her understanding and moral support through these years.

Table of Contents

	Page
Abstract	iii
Acknowledgments	v
List of Figures	xii
List of Tables	xvii
Introduction	1
CHAPTER 1: Preparation and Kinetic Characterization of Copolymers of Acrylamide and PEG (meth)acrylate Macromonomers	6
Abstract	6
Introduction	7
1.1 Experimental	
1.1.1 Materials	9
1.1.2 Copolymer characterization and monomer conversion measurements	9
1.1.3 Homopolymerization	10
1.1.4 Copolymerization	11
1.1.5 Solution properties of macromonomers	12
1.2 Results	12
1.2.1 Homopolymerization of macromonomer	12
1.2.2 Copolymerization	13
1.2.3 Reactivity of macromonomers toward acrylamide	13
1.2.4 Influence of polymerization temperature on the molecular weight of copolymers	16
1.2.5 Solution properties of macromonomers	16
1.3 Discussion	17
1.3.1 Homopolymerization	17
1.3.2 Copolymerization	21
1.3.3 Microstructure of the copolymers	23

Conclusions	24
References	25
Tables	28
Figures	33
CHAPTER 2: Interpolymer Association between Phenolic Resin and PEO or PAM-co-PEG Copolymers	41
Abstract	41
Introduction	42
2.1 Experimental	45
2.1.1 Materials	45
2.1.2 Potentiometric titration	45
2.1.3 PFR solubility	46
2.1.4 PEO/PFR precipitation experiments	46
2.1.5 Viscosity measurement	46
2.1.6 Fluorescent laser microscopy observation	47
2.2 Results	47
2.2.1 Characterization of PFR	47
2.2.2 Precipitation isotherms	48
2.2.3 Rheological properties of PEO/PFR mixtures	50
2.2.4 Morphology observations in complex formation	50
2.3 Discussion	51
2.3.1 Characterization of hydrogen bonding formation	52
2.3.2 Conceptual models of complex formation	54
2.3.3 An analogy between the oligomer/polymer complexation and the polymer adsorption	55
2.3.4 Conceptual model of precipitate formation	57
Conclusions	59
References	60
Figures	62

CHAPTER 3:	Flocculation of Polystyrene Latex by	78
	Polyacrylamide-co-poly(ethylene glycol)	
	Abstract	78
	Introduction	79
3.1	Experimental	80
3.1.1	Materials	80
3.1.2	Flocculation of polystyrene latex particles by dual-polymer	81
3.2	Results	83
3.2.1	Effect of polymer concentration on flocculation	83
3.2.2	Effect of composition of copolymers on latex flocculation	84
3.2.3	Effect of PEG pendant chain length on flocculation	85
3.2.4	Effect of molecular weight of copolymers on flocculation	85
3.2.5	Aging resistance of the copolymers in aqueous solution	85
3.3	Discussion	86
3.3.1	Copolymer structure and flocculation performance	86
3.3.2	Mechanistic implications	88
3.3.3	Aging resistance	91
	Conclusions	92
	References	93
	Tables	94
	Figures	97
CHAPTER 4:	Mechanism on Flocculation of Colloidal Particles	105
	by PEO and PAM-co-PEG Copolymers with Phenolic Resins	
	Abstract	105
	Introduction	106
4.1	Experimental	106

4.1.1	Materials	106
4.1.2	Polystyrene latex flocculation experiments	110
4.1.3	Adsorption isotherm measurements of phenolic resin and PEO latex surface	111
4.1.4	Electrophoretic characterization of PSL	111
4.1.5	Viscosity measurement	112
4.1.6	Imaging floc morphology	112
4.2	Results	113
4.2.1	Adsorption isotherms	113
4.2.2	Assessing flocculation	113
4.2.3	Effects of the flocculation on viscosity	121
4.2.4	Morphology of PSL flocs formed by dual-polymer systems	122
4.2.5	Summary of experimental results	123
4.3	Discussion	125
4.3.1	Network flocculation mechanism	125
4.3.2	Postulated mechanisms	127
	Conclusions	133
	References	133
	Tables	135
	Figures	141
CHAPTER 5:	Acrylamide-co-PEG Copolymers as Novel	162
	Retention Aids for Mechanical Pulps	
	Abstract	162
	Introduction	163
5.1	Experimental	165
5.2	Results	167
5.2.1	Influence of copolymer structure on fines retention	167
5.2.2	Influence of copolymer concentration	169
5.2.3	Aging effect of the polymers in aqueous solution	170

5.2.4	Effect of the shear stress on retention	170
5.3	Discussion	171
5.3.1	Copolymer retention mechanism	172
5.3.2	Interpreting DDJ induced shear degradation of polymer	176
	Conclusions	178
	References	179
	Tables	181
	Figures	183
CHAPTER 6:	Poly(p-vinyl phenol) as a Cofactor in Colloidal	192
	Particle Flocculation Induced by PEO Dual-Polymer Systems	
	Abstract	192
	Introduction	192
6.1	Experimental	194
6.1.1	Materials	194
6.1.2	Polystyrene latex flocculation	195
6.2	Results	196
6.2.1	Factors influencing the latex flocculation induced by PVPPh/PEO or copolymer systems	196
6.2.2	PAA/PEO compared with PVPPh/PEO system	199
6.2.3	Kinetic flocculation process	200
6.3	Discussion	200
6.3.1	Comparison between PVPPh and PFR as cofactors	200
6.3.2	Flocculation mechanism	201
6.3.3	Kinetic analysis	202
6.3.4	Microparticle flocculation system	205
6.3.5	PAA cofactor	206
	Conclusions	207

References	207
Tables	209
Figures	211
Appendix A1: Supplementary materials for chapter 1	220
Appendix A2: Supplementary materials for chapter 2	235
Appendix A3: Supplementary materials for chapter 3	244
Appendix A4: Supplementary materials for chapter 4	250
Appendix A5: Supplementary materials for chapter 5	255
Appendix A6: Supplementary materials for chapter 6	256

LIST OF FIGURES

		Page
Chapter 1		
Figure 1	Schematic structure of long PAM having short PEG pendant chains to give a comb copolymers.	33
Figure 2	Structure of PEG-(meth)acrylate macromonomer	33
Figure 3	¹ H NMR spectrum of copolymer synthesized from acrylamide and PEG macromonomer MA-9.	34
Figure 4	Conversion versus time for the homopolymerization of PEG-methacrylate macromonomers with different PEG pendant chain lengths	35
Figure 5	Conversion curves for AM and PEG-methacrylate macromonomer with PEG pendant chain length of 23.	36
Figure 6	Conversion curves for AM and PEG-acrylate macromonomer with PEG pendant chain length of 40.	37
Figure 7	AM conversion in copolymerization of AM with macromonomer with different PEG pendant chains length.	38
Figure 8	Fluorescence spectra of pyrene in SDS, MA-9, MA-23 and water.	39
Figure 9	Schematic description of shielding effect on propagating radicals.	40
Chapter 2		
Figure 1	A schematic for hydrogen bonding between PEO and PFR.	62
Figure 2	A schematic structure of comb copolymer with long PAM backbone and short PEG pendant chains.	62
Figure 3	Influence of pH and NaCl concentration on the solubility of the phenolic resin C-271.	63
Figure 4	Potentiometric titration of phenolic resins C-271.	64
Figure 5	Degree of ionization of PFR C-271 versus pH from the potentiometric titration.	65
Figure 6	Phenolic resins precipitate isotherm in PEO-309 and copolymer (56-107) solution.	66
Figure 7	Initial pH effects on the precipitated amounts of	67

	PFR C-271 on PEO-309.	
Figure 8	The viscosity behavior during interpolymer associations between PEO and phenolic resin C-271.	68
Figure 9	The viscosity behavior during interpolymer associations between copolymer and phenolic resin C-271.	69
Figure 10	Chemical structure of Acridine Orange.	70
Figure 11	Fluorescent microscopic observation on the mixture of Acridine Orange and PFR C-271.	71
Figure 12	Fluorescent microscopic observation on the mixture of Acridine Orange and PFR C-271 with PEO-309.	72
Figure 13	Fluorescent microscopic observation on the mixture of Acridine Orange and PFR C-271 with copolymer 56-107.	73
Figure 14	A schematic of flattening complex configuration in an oligomer/polymer system.	74
Figure 15	An analogy between the polymer adsorption on the solid surface and an oligomer/polymer complexation system.	74
Figure 16	A schematic of the complexation between PAM-co-PEG copolymer and PFR	75
Figure 17	Complex associations induced by uncharged cofactor and charged cofactor in PEO/cofactor system	76
Figure 18	A schematic of the complexation between PFR and PEO in three situations.	77
Chapter 3		
Figure 1	Structure of PAM-co-PEG copolymer.	97
Figure 2	Structure of PEG-macromonomer.	97
Figure 3	The effect of PEO concentration on latex flocculation at a constant concentration of phenolic resin.	98
Figure 4	The effect of copolymer concentration on latex flocculation at a constant concentration of phenolic resin of 2.0 mg/L.	99
Figure 5	Relative turbidity versus composition of copolymers.	100
Figure 6	Relative turbidity as a function of PEG pendant length n in copolymers.	101
Figure 7	The Influence of polymer aging on PSL flocculation.	102

Figure 8	A schematic of hydrogen bonding formation between phenolic resin and PAM-co-PEG Copolymer.	103
Figure 9	Complex formation between PAM-co-PEG copolymer and PFR	104
Chapter 4		
Figure 1	Structure of the comb copolymer of acrylamide and polyethylene glycol (PEG) methacrylate macromonomer.	141
Figure 2	PFR adsorption on polystyrene latex.	141
Figure 3	PEO adsorption on PS latex	142
Figure 4	Observations on latex flocculation induced by PEO and copolymer with PFR in turbidity measurements.	143
Figure 5	The influence of pH on PS latex flocculation by PEO/PFR.	144
Figure 6	Effect of NaCl concentration, i.e. conductivity, on the latex flocculation.	145
Figure 7	Effect of copolymer dosages on latex flocculation.	146
Figure 8	Effect of PEO dosages on latex flocculation.	147
Figure 9	The effect of PFR dosages on the flocculation of latex at constant PEO-309 dosage (1.0 mg/L).	147
Figure 10	The influence of total polymers concentration on latex flocculation at constant ratio of PEO-309/ PFR = 1/1 (wt).	148
Figure 11	The influence of PS latex particle size on flocculation.	149
Figure 12	The effect of initial PS latex concentration on flocculation.	150
Figure 13	The effect of fiber concentration on latex flocculation.	151
Figure 14	The effect of mechanical shearing on the latex flocculation induced by PEO/PFR in the absence of fibers.	151
Figure 15	Effects of interpolymer association between PEO and PFR on the system viscosity.	152
Figure 16	Effects of interpolymer association between copolymer (56-48) and PFR on the system viscosity.	153
Figure 17	Control morphology of fiber and latex without polymer.	154
Figure 18	Flocs of PS latex formed by PEO-309/PFR in the presence of fibers.	155
Figure 19	Spherical flocs formed by PEO-309/PFR.	156

Figure 20	Spherical flocs formed by copolymer 43-129/PFR.	157
Figure 21	PS Latex deposited on the bleached fibers caused by addition of cationic copolymer XB-54-15-1.	158
Figure 22	SEM observation on a single floc attached on the fiber.	159
Figure 23	A schematic of network flocculation proposed by Lindstrom et al.	160
Figure 24	A schematic of the formation of the complex aggregates and flocculation processes.	161
Chapter 5		
Figure 1	A schematic structure of long PAM having short PEG pendant chains to give a comb copolymers.	183
Figure 2	Structure of PEG-(meth)acrylate macromonomer	183
Figure 3	Effect of composition of copolymer on FPR.	184
Figure 4	Effects of Pendant PEG chain lengths on FPR.	185
Figure 5	Effects of amounts of copolymer 56-108 addition on FPR.	186
Figure 6	Effect of aging time on PSL Flocculation.	187
Figure 7	Effect of propeller speed on FPR for different polymers.	188
Figure 8	Effects of propeller speed on FPR for the copolymers with different PEG pendant chain lengths.	189
Figure 9	A schematic of hydrogen bonding between the PAM-co-PEG copolymer and phenolic resin.	190
Figure 10	A schematic of complex bridging retention process	191
Chapter 6		
Figure 1	Potentiometric titration of PVPh-30.	211
Figure 2	The pH effect on flocculation of latex for PEO-309/PVPh systems.	212
Figure 3	The effects of PVPh dosages on latex flocculation in the PEO/PVPH system.	213
Figure 4	The effect of PVPh MW at two level addition amounts on latex flocculation in the PEO/PVPH system.	214
Figure 5	Effect of conductivity on the latex flocculation.	215
Figure 6	Characterization of PVPh particle size in dispersion.	216
Figure 7	Effect of PEG on the latex flocculation induced by	217

	PEO/PVPh-30 and PEO/PFR.	
Figure 8	Kinetic process for latex flocculation induced by PEO/PVPh-1.	218
Figure 9	A schematic description for hydrogen bonding between PEO and PVPh.	219
Appendix		
Figure A1-1	¹ H NMR spectrum for methoxy poly (ethyleneoxy) ethyl acrylate A-10 macromonomer.	221
Figure A1-2	¹ H NMR spectrum for methoxy PEG monomethacrylate MA-9 macromonomer.	222
Figure A1-3	¹³ C NMR spectrum for methoxy poly (ethyleneoxy) ethyl acrylate A-10 macromonomer.	223
Figure A1-4	¹ H NMR spectrum for a mixture of PAM (molecular weight 5,000,000) and PEG macromonomer MA-23.	226
Figure A1-5	A normalized ¹ H NMR calibration curve for the mixtures of PEG macromonomer and polyacrylamide homopolymer.	227
Figure A1-6	AM conversion in inverse microemulsion polymerization.	231
Figure A2-1	UV absorbency of PFR at 286 nm versus PFR conc.	235
Figure A2-2	Transition Temperature measured by DSC.	237
Figure A2-3	A schematic of DSC thermogram for PEO solution.	239
Figure A2-4	Influence of PEO 309 concentration in aqueous solution on the fusion enthalpy.	240
Figure A2-5	pH effects on fusion enthalpy for PEO/PFR complex aqueous solution.	241
Figure A3-1	Calibration curve of the latex concentrations versus log(T_d/T_c).	245
Figure A3-2	Correlation between the experimental observed data of the latex relative turbidity after flocculation and the data predicted by the empirical equation.	246
Figure A4-1	Morphology of latex flocs formed by PEO/PFR flocculation system in the presence of silica beads.	251
Figure A4-2	TiO ₂ flocs formed by PEO-309 and C-271.	253
Figure A4-3	TiO ₂ flocs formed by copolymer 56-108 and C-271.	254

Figure A5-1	Correlation between PFR and relative turbidity.	255
Figure A6-1	Morphology of polystyrene latex flocs formed by PEO/PVPh flocculation system in the presence of bleached fibers.	257

LIST OF TABLES

	Page
Chapter 1	
Table 1	Recipes for copolymerization. 28
Table 2	$K_p/K_t^{1/2}$ data from MA-PEG macromonomers. 29
Table 3	Conversion data for AM and Macromonomers 30
Table 4	r_1 estimated from low conversion data. 31
Table 5	Molecular Weight of Comb Copolymers. 32
Chapter 3	
Table 1	Summary of the properties of the copolymers. 94
Table 2	Particle Size of Polystyrene Latex(PSL) measured by a BI-DCP(Disc Centrifuge Photosedimentometer) Particle Sizer. 95
Table 3	Influence of copolymer MW on latex flocculation. 95
Table 4	Effect of the polymer storage conditions of on the relative turbidity during the latex flocculation τ_R . 96
Chapter 4	
Table 1	Influence of copolymer MW on flocculation effect. 135
Table 2	Small diameter latex flocculation by high polymer dosage. 136
Table 3	Flocculation of PNIPAM latex. 136
Table 4	Flocculation of PS-g-PNIPAM latex. 137
Table 5	Effects of polymer addition order on the latex flocculation. 138
Table 6	The effect of addition mode of the bleached fiber on PS latex flocculation. 139
Table 7	Flocculation of PS latex pre-treated with PEO-309 and PFR. 139
Table 8	Flocculation of PS latex in the presence of silica beads. 140
Table 9	Relative ratios of collision or aggregation rates in the schematic Figure 24. 140

Chapter 5

Table 1	Effect of MW of copolymers on the FPR.	181
Table 2	Correlation between PS latex flocculation and pulp fines retention.	182

Chapter 6

Table 1	Effects of addition modes on the latex flocculation induced by PEO-309/PVPh-30.	209
Table 2	Effect of addition order of PEO, PVPh and latex on the flocculation.	209
Table 3	The effect of dispersion state of PVPh-1 on the latex flocculation.	210
Table 4	The effect of PVPh dispersed particle size on the flocculation of latex.	210

Appendix

Table A1-1	Average degree of polymerization, n , of PEG pendant chains in macromonomers.	224
Table A1-2	Copolymerization Recipes.	229
Table A1-3	Conversion data for AM and Macromonomers.	230
Table A1-4	recipes for semi-batch polymerization	233
Table A3-1	Database for estimating the empirical equation.	247
Table A3-2	Flocculation of the latex by polymers in the absence of phenolic resin.	248
Table A4-1	Latex flocculation in the absence of the fibers.	250
Table A4-2	Flocculation of PS latex in the presence of silica beads.	251
Table A4-3	Flocculation of by dual-polymer systems; Concentration of $\text{TiO}_2 = 48 \text{ mg/L}$.	252

INTRODUCTION

Water-soluble synthetic polymers have been widely used as flocculants in many industrial applications such as solid-liquid separation processes, mineral processes, enhanced oil recovery, biological applications, waste water treatment and paper-making processes.^{1,2,3} This thesis describes the preparation, kinetic characterization, and mechanism of novel polymeric flocculants in papermaking.

In the formation section of a paper making, the pulp suspension is filtered by the wire to form a paper sheet. In addition to the wood fibers, much smaller fine particles, such as fiber fragments and mineral fillers, are easily lost during sheet formation because they are too small to be filtered. Since it is desirable to retain fines in the sheet, polymeric flocculants are used to deposit colloidal materials onto the fiber surfaces. In the paper industry, polymeric flocculants are called retention aids.

In water, most fines and cellulose fibers bear an anionic surface charge. Thus, most retention aids have a cationic component to facilitate adsorption to the pulp-furnish surfaces. However, mechanically-derived pulps such as newsprint contain large quantities of dissolved and colloidal substances (DCS) which are anionic. Cationic polymers are not cost effective in furnishes based on mechanical pulps because much of the cationic polymer is consumed by neutralization of DCS. By contrast, nonionic poly(ethylene oxide) (PEO) is an especially effective retention aid for newsprint manufacture and other groundwood furnishes because it is not sensitive to DCS.⁴ However, PEO does

require a cofactor which can be phenolic resin, kraft lignin, modified kraft lignin, tannin or Cartafen (a sulfonated phenolic polymer).

Currently, commercial PEO retention systems consist of high molecular weight (MW) PEO and phenol formaldehyde resin (PFR). It was found that only PEO with very high MW (usually $> 4.0 \times 10^6$) is an effective retention aid. However, very high molecular weight PEO chains are susceptible to degradation resulting in lower molecular weight and thus lower effectiveness as retention aids. The degradation can be caused by either shear forces, biological and oxidative degradation.

In order to overcome the fragile properties of PEO, a series of the novel comb copolymers with long polyacrylamide (PAM) backbones and short poly(ethylene glycol) (PEG) pendant chains have been prepared in this work.⁵ The PAM backbone is relatively inexpensive and more robust than PEO homopolymer. The comb copolymers combine the beneficial features of PAM (inexpensive, robust) and PEO (flocculation through hydrogen bonding).

Part of the current work focuses on the mechanisms by which PEO and the new copolymers function. Understanding the roles of polymers in flocculation processes is very important for designing novel functional polymers, improving control strategies in wet-end process; and, for guiding mills in the choice of the best retention system. Mechanisms of polymer-induced flocculation of colloidal particles have been investigated over the years.

The objectives of this work were: 1) to synthesize a series of novel comb copolymers from free-radical copolymerization of acrylamide (AM) and poly(ethylene glycol) (meth)acrylate macromonomers in aqueous solution; 2) to relate the copolymer structures with flocculation efficiencies for polystyrene latex

(PSL) and mechanical pulp fines; 3) to elucidate details of the complex formation between phenolic resin and PEO or the copolymers; and, 4) to determine the mechanism of flocculation by nonionic dual-polymer retention systems.

The thesis consists of six chapters prepared as manuscripts for publication. The contents of each chapter are briefly described as follows:

The first chapter of the thesis describes the preparation and kinetic characterization of novel comb copolymers of acrylamide (AM) and PEG (meth)acrylate macromonomers. Copolymerization with macromonomers provided a series of PAM-co-PEG copolymers with well-defined structures. The reactivity ratios, r_1 , of acrylamide (M_1) toward PEG macromonomers (M_2) as well as rate constant ratios of $K_p/K_t^{1/2}$ for macromonomers in homopolymerization are described in this chapter. Effects of PEG pendant chain lengths on reactivities of macromonomers in both aqueous solution copolymerization and homopolymerization were determined.

The second chapter of the thesis describes studies of the interpolymer association (i.e. complexation) between phenolic resins and PEO or copolymers. The evidence of the complex formation through hydrogen bonding was observed from UV spectrometry, viscometry and fluorescent microscopy. The mechanism of the complex formation between phenolic resins and short PEG pendant chains in the comb copolymers was discussed.

The third chapter of the thesis describes the results from the polystyrene (PS) latex flocculation induced by the copolymers in conjunction with phenol formaldehyde resin. The relationship between the copolymer structures and the efficiency in latex flocculation was determined. The optimum structures of copolymers for latex flocculation, including molecular weight, PEG pendant

chain length and composition of copolymers (or PEG pendant chain density), were described. The influence of aging time on the polymer flocculation performance was also discussed.

The fourth chapter of the thesis describes the flocculation mechanism of colloidal particles by the phenolic resin and nonionic PEO or PAM-co-PEG dual-polymer systems. A new flocculation mechanism called "complex bridging" was developed in this chapter. The proposed mechanism was based on a preliminary kinetic analysis on several possible flocculation approaches and found to be in agreement with a number of experimental observations including the influence of flocculation conditions, polymer adsorption, rheological behavior and morphology of colloidal flocs. The molecular weight dependence of polymer in inducing latex flocculation was interpreted by a dynamic collapsing process of colloidal polymer complexes.

The fifth chapter of the thesis deals with the retention of mechanical pulp fines by PAM-co-PEG comb copolymer and phenolic resin dual-polymer systems. Retention measurements were conducted using a dynamic drainage jar (DDJ) and results for the different copolymers were linked to the structure of copolymer. Shear stress effects on mechanical pulp retention induced by copolymers and high molecular weight PEO homopolymers were investigated. The retention mechanism was also discussed.

The sixth chapter of the thesis describes results from studies of latex flocculation induced by PEO and poly(p-vinyl phenol) (PVPh). This is the first reported use of PVPh as a cofactor. The comparison between PVPh and PFR as cofactor under different flocculation conditions, such as pH, salt concentration and addition orders, was conducted. Kinetic analysis of the complex bridging

flocculation was carried out and results indicated that an orthokinetic process was involved. The similarity between PEO/cofactor dual-polymer flocculation system and microparticulate flocculation system was also discussed.

References:

- ¹ Dickinson, E., and Eriksson, L., *Adv. Colloid Interface Sci.* **34**, 1(1991).
- ² Bailey, F.E., Jr. and Koleske, J.V., in "Alkylene Oxide and Their Polymers," Marcel Dekker, New York, 1990.
- ³ Pelton, R.H., Allen, L.H. and Nugent, H.M., *Tappi*, **63**(11):89(1981).
- ⁴ Pelton R.H., Tay, C.H. and Allen, L.H., *J. Pulp & Paper Sci.*, **10**(1), 5(1984).
- ⁵ Pelton, R.H., Hamielec, A.E. and Xiao, H.N. Patents pending.

CHAPTER 1

Preparation and Kinetic Characterization of Copolymers of Acrylamide and PEG (meth)acrylate Macromonomers

ABSTRACT

Novel comb copolymers were prepared by free radical copolymerizing of acrylamide (AM) and poly(ethylene glycol) (PEG) macromonomers in aqueous solution using potassium persulfate as an initiator. The reactivity ratios of acrylamide (M_1) toward macromonomers (M_2), $r_1 = K_{p11}/K_{p12}$, were estimated at low conversion by using H^1 NMR and HPLC techniques. The values of r_1 ranged between 1.35 and 2.2 and were dependent on PEG pendant chain length in the macromonomers. The reactivity of the macromonomers in copolymerization, characterized by $(1/r_1)$, decreased with PEG pendant chain length. The reactivity of the macromonomer in homopolymerization, expressed as $K_p/K_t^{1/2}$, increased with the PEG pendant chain length. The changes of K_p and K_t are likely caused by the shielding effect on growing radicals due to macromonomer pendant chains. The molecular weight of copolymer was found to be sensitive to the polymerization temperature. Higher MW (> 3 million) copolymers were obtained at lower temperatures.

KEY WORDS: acrylamide, macromonomer, copolymerization, reactivity ratio, water soluble polymers, nonionic polymers.

Introduction

Polyethylene oxide (PEO) has been widely used in many technologies including waste water treatment, paper making and polymer processing. PEO with a molecular weight of 4.0×10^6 is effective as a flocculant (retention aid) for the production of newsprint.^{1,2} However, the requirement for high molecular weight causes problems in industrial applications because very high molecular weight PEO chains are susceptible to oxidative and hydrodynamic degradation resulting in lower molecular weights and lower flocculation efficiencies. Pelton et al.³ proposed more robust structures for high molecular weight flocculants consisting of long polyacrylamide (PAM) backbone with a few short poly(ethylene glycol) (PEG) pendant chains to give comb structures (see Figure 1).

One route to the desired comb copolymers is to graft PEG onto polyacrylamide (PAM). Possible grafting methods include γ -ray radiation polymerization⁴, redox radical polymerization,⁵ functional group condensation and coupling through water-soluble carbodiimides.⁶ The disadvantages of using these methods include: 1) the difficulty in controlling the density of graft and graft chain lengths; 2) the tendency to produce by-products; and 3) the cost would be too high for commercial applications.

For this work, free radical copolymerization of acrylamide with PEG macromonomers was used to produce the comb copolymer. PEG macromonomers are methoxy PEG esters of acrylic and methacrylic acid. The structures of PEG macromonomers used in this work are shown in Figure 2. Compared with the random grafting methods previously mentioned, the copolymerization potentially provides full control over the pendant chain length,

the number of pendant chains per macromolecule and molecular weight of copolymers.

A number of papers have been published on macromonomer copolymerizations.^{7,8} Most of the published works have involved hydrophobic monomers such as styrene and methyl methacrylate (MMA)^{9,10,11,12} and few studies have been reported on copolymerization of PEG macromonomers with hydrophilic monomers such as acrylamide and acrylic acid. Schulz et al.¹³ synthesized copolymers of nonylphenoxy PEG acrylate and acrylamide. Since nonylphenoxy poly (ethylene oxide) acrylate is surface active, no external surfactant was needed for the preparation of high MW acrylamide copolymers with 0.1-5 (mol) % hydrophobic content from nonylphenoxy PEG acrylate macromonomer. Schulz's work focused on the use of the lowest levels of nonylphenoxy PEG acrylate macromonomer necessary to achieve hydrophobic enhancement of viscosity. However, no polymerization kinetic measurements were reported.

The objectives of this work included preparation of a series of novel acrylamide-PEG macromonomer comb copolymers with well defined structures and the measurement of the reactivities of PEG macromonomers in copolymerization with acrylamide. NMR and HPLC techniques were used to elucidate the kinetics of polymerization. Factors studied were the influence of PEG pendant chain length on the reactivities of macromonomers in homopolymerization and copolymerization, as well as the effect of polymerization temperature on the molecular weight of the copolymers synthesized.

1.1 Experimental

1.1.1 Materials

Acrylamide (Aldrich Co.), methoxy poly (ethyleneoxy) ethyl acrylate (R = H in Figure 2) (Monomer-Polymer, Inc), methoxy poly(ethylene glycol) monomethacrylate (R = CH₃ in Figure 2) (Polysciences, Inc.), potassium persulfate (KPS) initiator (BDH Chemicals), hydroquinone (BDH Chemicals), sodium dodecyl sulfate (SDS) (BDH Chemicals) and pyrene (Aldrich Co.) were used as supplied. Milli-Q treated distilled water was used to prepare all aqueous solution.

Herein the macromonomers are represented as MA-n or A-n where MA refers to methacrylic ester and A is acrylic ester. The n value is the average degree of polymerization for the PEG pendant chains. For example, MA-23 represents the PEG macromonomer with n = 23 and R = CH₃ (see Figure 2). The macromonomer structures have been verified by ¹H and ¹³C NMR measurements. More details on characterization of macromonomers are described elsewhere.¹⁴

1.1.2 Copolymer characterization and monomer conversion measurements

1.1.2.1 HPLC

High performance liquid chromatography (HPLC) was used to measure residual acrylamide concentration during polymerization¹⁵. The HPLC system was fitted with a CN precolumn (particle size 5 mm, cartridge ID 8 mM, Waters), an ERC-3110 degasser (Erma Optical works), a U6K injection system (Waters) and a Beckman 160 UV detector set at 214 nm where acrylamide gives

maximum absorption. Milli-Q treated distilled water was used as a mobile phase at a flow rate of 2.0 mL/min.

1.1.2.2 NMR

A Bruker AC 200 NMR spectrometer (200 MHz, Bruker Co.) was used to measure the composition of the copolymers. Comb copolymer powder was dissolved in D₂O at a concentration about 0.5 wt % in thin wall 5 mM NMR tube. ¹H chemical shifts were reported relative to HDO peak at 4.6 ppm.

1.1.2.3 LALLS and GPC

Low angle laser light scattering (LALLS) and gel permeation chromatography (GPC) were used to characterize the molecular weight of comb copolymers. LALLS photometer Model Chromatrix KMX-6 is supplied by Thermoste Separation Products. Light scattering was measured at 25°C with a He-Ne unit operating system at the red wavelength of 633 nm.

GPC is LC Model 5000 from Varian, Column Set TSK G 3000 pw, G 5000 pw and G 6000 pw. TSK standard poly(ethylene oxide) samples, SE-2 to SE-150 with Mw/Mn < 1.17, were used for GPC calibration.

The techniques used in MW measurement, LALLS and GPC, are reported to give more reliable data than those obtained using a viscometer since non-Newtonian effects would likely be significant for high MW polyacrylamide¹⁶ where intrinsic viscosity measurements are made.

1.1.3 Homopolymerization

Homopolymerization of macromonomers was carried out at 40°C in deuterated water in 5 mM NMR tubes with potassium persulfate initiator (see Table 2 for details). Monomer conversion was monitored with proton NMR by

following the peak disappearance of the vinylic protons relative to terminal methoxy group OCH_3 .

1.1.4 Copolymerization

The copolymerizations were carried out in aqueous solution in a 1 L batch reactor equipped with a mechanical stirring paddle or in 50 mL test tubes which were stirred with a magnetic stirring bar. The temperature of polymerization was maintained at 25°C or 40°C . Between 2 and 8 hours were required for polymerization with initiator KPS at concentration of 3.0×10^{-3} mol/L. Table 1 summarizes the copolymerization recipes.

For the systems with total volumes over 250 mL, a 20 mL sample was collected every 20 to 30 min. during polymerization to permit measurements of the conversion and copolymer compositions. About 1 mL 0.1 % hydroquinone aqueous solution was immediately added to each collected sample to terminate polymerization. Between 0.2 and 0.5 mL of each sample was required for HPLC analysis; the remainder of the sample was precipitated into acetone.

The copolymer, precipitated with acetone, was washed with toluene to extract unreacted macromonomers. The washed copolymer was dried at 30°C in vacuum oven for 12 hours. The composition of the purified copolymers was measured by proton NMR. Conversion of the macromonomer in each sample was calculated from the composition of the copolymer and AM conversion.

An NMR spectrum for PAM-co-PEG copolymer is given in Figure 3 as an example. The peak assignments are described in Figure 3 as well. The composition of copolymer was estimated from the ratios of peak areas of OCH_2CH_2 in PEG pendant chains to CH-CH_2 in copolymer backbones. The

standard deviation, expressed as a percentage of the mean, ranged between 4 and 6 % for the same sample when repeats were made.

1.1.5 Solution properties of macromonomers

The luminescent molecule pyrene (Aldrich) was used to determine if the macromonomer solutions formed micelles. 1.0 mL saturated pyrene aqueous solution was mixed with 1.0 mL SDS or macromonomer solutions. The concentrations of SDS and the macromonomer are given in Figure 8. Synchronous scanings were conducted using an Aminco Luminescence Spectrometer (SLM Instruments Co.) at 25°C.

1.2 Results

1.2.1 Homopolymerization of macromonomer

Homopolymerizations of macromonomer were carried out to determine kinetic parameters and the results are shown in Figure 4. The points were measured and the continuous lines were predicted with the following kinetic model.

The rate expression for R_p in a free radical homopolymerization obeying the steady state hypothesis can be written as follows:¹⁷

$$R_p = -[M]_0 d(1-X)/dt = (K_p/K_t^{1/2})[M] (2f K_d[I])^{1/2} \quad (1)$$

where K_p and K_t are propagation and termination rate constants; f is the initiator efficiency; $[M]_0$ is the initial monomer concentration; X is monomer conversion at time t . $[M]$ and $[I]$ are the monomer and initiator concentrations at time t . K_d is

the decomposition rate constant of the initiator. For potassium persulfate at pH 7, the Arrhenius equation for K_d ¹⁸ is given by:

$$K_d = 3.53 \times 10^{16} \exp(-33320/RT) \text{ sec}^{-1} \quad (2)$$

and for isothermal polymerization (assuming $f = 1.0$),

$$[I] = [I]_0 \exp(-K_d/t) \quad (3)$$

When diffusion-controlled termination does not occur (K_t is only a function of temperature), integration of equation (1) gives the following expression:

$$\ln(1 - X) = -(K_p/K_t^{1/2}) (8f [I]_0/K_d)^{1/2} \{1 - \exp(-K_d t/2)\} \quad (4)$$

Two standard assumptions were made.¹⁹ First, the stationary-state hypothesis (SSH) is valid for radical reactions. Second, long chain approximation (LCA), i.e. chain lengths are sufficiently large that the total rate of monomer consumption may be equated to the rate of monomer consumption by the propagation reactions alone. $K_p/K_t^{1/2}$ values were obtained by fitting equation (4) to experimental conversion data. The results are summarized in Table 2 and predicted conversion curves are compared with experimental data in Figure 4. For comparison, $K_p/K_t^{1/2}$ values were also estimated from literature.^{20,21}

Compared to values for macromonomers, the reactivity of acrylamide, expressed as $K_p/K_t^{1/2}$, was six to eight times higher. For macromonomers with different pendant chain lengths, the reactivity increased with the pendant chain length. For example, $K_p/K_t^{1/2}$ for MA-23 was 0.663, but only 0.474 for MA-5. An even higher value for MA-67 was obtained by Ito (polymerization conditions for MA-67 are shown in Table 2). Compared with methyl methacrylate (MMA) polymerized in benzene, polymerization of PEG-methacrylate macromonomer conducted in water was an order of magnitude faster.

1.2.2 Copolymerization

Conversion data for the copolymerizations of AM and macromonomers with different PEG chain lengths and corresponding compositions of the copolymers are summarized in Table 3. The conversion of acrylamide was always higher than that of the macromonomer. This suggested that the reactivity of acrylamide was higher than that of PEG macromonomers at the same polymerization conditions. These results are also consistent with the $K_p/K_t^{1/2}$ values shown in Table 2.

AM and macromonomer conversion versus time data are plotted in Figures 5 and 6. In both cases the AM was consumed more quickly than macromonomers.

Figure 7 shows AM conversion curves obtained in the presence of three different macromonomers. The similarity of AM polymerization behavior in Figure 7 suggested that AM reactivity was independent of the type of macromonomers at mole ratios of AM to macromonomer higher than 50. By contrast, the macromonomers with different PEG pendant chain lengths behaved differently, as shown in the Figures 5 and 6. MA-23 reached a higher conversion than A-40 under the same conditions. For example, the conversion of MA-23 was about 42 % after 1.5 h polymerization, whereas the conversion of A-40 was about 20 % at the same time.

1.2.3 Reactivity of macromonomers toward acrylamide

For binary copolymerization which follows the terminal model, the instantaneous copolymer composition equation may be expressed as:

$$\frac{d[M_1]}{d[M_2]} = \frac{[M_1] r_1[M_1] + [M_2]}{[M_2] [M_1] + r_2[M_2]} \quad (5)$$

where M_1 is acrylamide and M_2 is the macromonomer. Reactivity ratios are defined as $r_1 = K_{p11}/K_{p12}$ and $r_2 = K_{p22}/K_{p21}$, where the rate constant nomenclature is illustrated with the following reactions:



With a very large molar excess of acrylamide, i.e. $[M_2]/[M_1] \ll 1$, equation (5) reduced to the simple form:

$$\frac{d[M_1]}{d[M_2]} = r_1 \frac{[M_1]}{[M_2]} \quad (8)$$

This equation can be used to estimate r_1 for macromonomers with different PEG chain lengths. The reciprocal ($1/r_1$) is a measure of the reactivity of the macromonomer towards the polyacrylamide radical. The parameter r_2 cannot be estimated due to the extremely low molar concentrations of macromonomer used.

It was assumed that the drift in copolymer composition was negligible at low monomer conversions (< 25 %), and the instantaneous composition was approximately equal to the composition in the accumulated copolymer. Under these conditions, equation (9) can be expressed in the following form:

$$r_1 = \frac{\ln(1-X_1)}{\ln(1-X_2)} \quad (9)$$

where X_1 and X_2 are the conversions of acrylamide and PEG macromonomer, respectively.

Table 4 shows r_1 data obtained by applying equation (9) to experimental conversion data. The results indicated that reactivity of macromonomer, measured by $1/r_1$, increased as the PEG pendant chain lengths decreased. For

example, the average $1/r_1$ for MA-5 was 0.74 while $1/r_1$ for MA-23 was 0.63. Similarly, the average $1/r_1$ for A-10 was 0.735, and for A-40 was 0.45.

1.2.4 Influence of polymerization temperature on the molecular weight of copolymers

Copolymerizations were carried out at 25°C and 40°C to investigate the temperature effect on the copolymer molecular weight. The results (see Table 5) suggested that the weight average molecular weight (Mw) of copolymer was temperature dependent. The copolymers with MW higher than 3×10^6 were obtained when aqueous solution copolymerization were carried out at a temperature of 25°C or lower. Polymerization at 40°C gave copolymers with MW of approximately 1.0×10^6 . No significant influence was observed for PEG pendant chain length on MW of copolymers. The molecular weights of acrylamide homopolymers obtained at 25°C and 40°C are compared with those of the copolymers in the Table 5. The PAM molecular weights herein are number average.

1.2.5 Solution properties of macromonomers

It has been reported in the literature that macromonomers can form micelles in water which would influence polymer structure and complicate the kinetic interpretation.²² To check for this, fluorescence measurements were performed using pyrene as a probe. Figure 8 shows the fluorescence emission spectra of pyrene in aqueous sodium dodecyl sulfate (SDS) which is known to form micelles. The strong emissions indicated the presence of hydrophobic domains capable of enhancing the solubility of pyrene. By contrast, neither of

the two macromonomer solutions showed any evidence of pyrene solubilization (see Figure 8).

1.3 Discussion

The results from present work have indicated that the reactivities of macromonomers in aqueous solution polymerization are PEG pendant chain length dependent. It is of interest to note that the influences of PEG pendant chain lengths in macromonomers on their polymerization behavior or reactivities are different in homopolymerization and copolymerization. This may suggest that the mechanisms of polymerization involved are not the same. A discussion of the possible mechanisms for both homo and copolymerization is now presented.

1.3.1 Homopolymerization

In homopolymerization, the $K_p/K_t^{1/2}$ values obtained using conversion measurements increased as the PEG pendant chain lengths (n) increased. This trend could have resulted from the increase of K_p or decrease of K_t with pendant chain length n , or with both happening simultaneously. It is clear that K_t falls more rapidly with n than K_p increases if it does at all.

The interpretation of the affect of pendant chain length on K_p and K_t can follow two approaches: 1) shielding effect of pendant group on growing radicals; 2) micelle formation of macromonomers.

The shielding effect on radicals can simultaneously reduce radical/radical termination and propagation of radical centers located on macromonomers. Research on the kinetics of polymerization of macromonomers has already revealed this.²³ We assume that there are two kinds of shielding effects in

macromonomer homopolymerization; they are: 1) backbone chain effect, which is the influence of the whole growing polymer chain on end radical; 2) pendant chain effect, which is the influence of the PEG pendant chain on the growing radical. Figure 9 schematically shows the two kinds of effects.

In the first situation, i.e., for the shielding effect caused by the entire growing backbone polymer chain, several models dealing with the dependence of termination rate constant K_t on the chain lengths of two reacting radical chains have already been developed.^{24,25} A simplified model for the effect of segmental diffusion was expressed as follows:²⁶

$$K_{t(n,m)} = K_{to(n,m)}^{-\alpha} \quad (10)$$

where $K_{t(n,m)}$ is the specific rate constant of termination between two radicals of sizes n and m and $K_{to(n,m)}$ is a constant. α is a parameter which describes the chain length dependence of K_t . Aqueous solution polymerizations done herein are too dilute for polymer translation diffusion to be a limiting factor.

With the pendant chain effect, i.e. the case in which the pendant chain is attached on the end growing radical may influence both propagation rate constant K_p and termination rate constant K_t . The increase in $K_p/K_t^{1/2}$ with pendant chain length is a result of the more rapid decrease of K_t compared to K_p as the pendant chain length increases. For example, K_p of MA-23 might be smaller than that of MA-5, but an even smaller K_t value for MA-23 (due to the pendant chain shielding effect) results in a larger $K_p/K_t^{1/2}$ value for MA-23. The radical lifetime for MA-23 may also be longer than that of the radical for MA-5 due to the smaller value of K_t .

The dependence of the reaction rate on chain length has been reported for other macromonomer systems. For example, in the homopolymerization of PMMA macromonomer in toluene with AIBN as an initiator, Masuda et al.²³ determined K_p and K_t values by using electron spin resonance (ESR) and found that K_t decreased much faster than K_p as the molecular weight of the macromonomer increased. It was suggested that the highly crowded pendant chain segment resulted in a very slow segmental diffusion-controlled termination.

Similar work with the styrene macromonomer, done by Tsukahara et al.,²⁷ showed a significant effect of MW of macromonomers on the diffusivity of the macromonomer in radical polymerization. Data after Tsukahara et al. indicated that when the degree of polymerization (DP) of the styrene macromonomer was increased from 54 to 59, K_p decreased from 18 to 4 L/mol·s. Meanwhile, coupling termination rate constant K_t decreased from 8400 to 1300 L/mol·s. However, $K_p/K_t^{1/2}$ value for the styrene macromonomer with DP 54 was 0.196 which was still higher than the $K_p/K_t^{1/2}$ value of 0.111 for styrene macromonomer with DP 59. These results differ from the current observations but still show that K_t falls faster than K_p with increasing macromonomer chain length.

An alternative explanation for the effect of PEG pendant chain length on $K_p/K_t^{1/2}$, proposed by Ito et al.²², was that the macromonomers formed micelles in water. Homogeneous polymerization kinetic expressions cannot apply to systems where one of the monomers is present as micellar aggregates. Ito et al. indicated that the micelle formed because of the amphiphilic structure of the macromonomer. They used light scattering technique to estimate the critical micelle concentration (CMC) and micellar sizes of the nonpolymerizable

models²⁸ for macromonomers. The hydrophobic heads of the model compounds used by Ito et al. were benzyl and isobutyryl, which will form hydrophobic domains or micelles much more easily than methacrylate heads used in this work. The CMC values for the models of the PEG vinylbenzyl macromonomers ranged from 1.8 to 7.1×10^{-5} M and the aggregation numbers were between 19 and 1800.

Fluorescence probes have been widely applied in micelle characterization.^{29,30} For example, Turro and Yekat proposed an excimer fluorescent method to estimate the CMC and the aggregation number for SDS micellar system³¹. Geetha et al.³² used this method to characterize macromonomer A-9. They claimed that the aggregation number was 20 and the CMC was 1.2×10^{-4} M. We believe the conclusion that A-9 micellizes is wrong for the following reasons.

Conventional PEG-based surfactants which readily form micelles have a hydrophobic head containing eight or more carbon atoms. Structures with smaller head groups either form micelles at very high concentrations or not at all. For example, Elworthy et al.³³ found the CMC value for $\text{OH}(\text{CH}_2)_4\text{EO}_3$ to be 0.8 M in aqueous solution at 20°C; molecules with smaller headgroups were not reported. Similarly, Corkill et al.³⁴ found the CMC value for $\text{OH}(\text{CH}_2)_6\text{EO}_3$ to be 0.1 M at 25°C and Donbrow et al.³⁵ found the CMC value for $\text{OH}(\text{CH}_2)_6\text{EO}_5$ to be 0.09 M at 20°C. Macromonomer A-9 has a headgroup based on 3 carbon atoms so it is inconceivable that micellization could occur. In support of this argument is our pyrene solubilization data for MA-9 and MA-23 (see Figure 8) which showed no evidence for micellization of the 4 carbon head macromonomer.

1.3.2 Copolymerization

In copolymerization the reactivities of macromonomers are a function of pendant chain length. The reactivity of the macromonomer toward polyacrylamide radical in copolymerization, as estimated by $1/r_1$, was found to decrease with increasing PEG pendant chain length. The majority of propagating radicals during copolymerization were acrylamide radicals because the molar concentration of AM was at least 20 times greater than that of macromonomers. As a result, the reactivity of macromonomers toward polyacrylamide radicals was controlled mainly by the effect of pendant chain length on the propagation constant.

The propagation rate constant K_{p12} in equation (8) describes the kinetic process of macromonomers reacting with polyacrylamide radicals. The segmental diffusion of the pendant chains on individual macromonomers may limit the propagation rate with polyacrylamide radicals. In other words, K_{p12} may be higher for macromonomers with short pendant chains as compared to macromonomers with long pendant chains whereas K_{p11} for acrylamide is independent of macromonomer pendant chain lengths. Therefore, the r_1 ($= K_{p11}/K_{p12}$) change was caused only by K_{p12} which is a function of pendant chain length of the macromonomer.

Decreased reactivity with increased PEG chain length has been reported for the copolymerization of PEG macromonomers with styrene in benzene. Ito et al.³⁶ explained the results by a thermodynamic repulsion between incompatible PEG and polystyrene. In the copolymerization of PEG macromonomers with maleic anhydride, Suzuki et al.³⁷ observed similar effects of PEG on MW. Suzuki suggested that one reason was the competitive complex formation of

MAN with the ether oxygen in the macromonomer, resulting in lower reactivity of macromonomers with longer PEG chains.

Since the total amount of macromonomer used in copolymerization was much lower than that in homopolymerization, the effect of micelle formation by macromonomer appears even less likely. Therefore, macromonomer behavior in copolymerization is mainly determined by its individual structure (or pendant chain length) and not due to aggregation of macromonomers to form micelles.

The molecular weight of the copolymer was found to be affected by polymerization temperature. The higher temperature gave a lower copolymer MW. This result is the same as for acrylamide homopolymerization, since low levels of macromonomers in copolymer chains may not significantly affect MW. Chain transfer to monomer and initiator have been found to be the major reasons for lowering of MW at higher polymerization temperature. Many earlier researches have revealed this. For example, the ratio of chain transfer to monomer rate constant to propagation rate constant ($C_m = K_{fm}/K_p$) in AM homopolymerization at 25°C was found to be 2.0×10^{-5} , as reported by Cavell et al.³⁸ and Fadner et al.³⁹ At a higher temperature of 40°C, the ratio became 5.8×10^{-4} , as reported by Kangfu.⁴⁰ By using least square estimating method, Shawki and Hamielec⁴¹ gave more accurate values of K_{fm}/K_p , which were 9.10×10^{-6} at 25°C and 2.04×10^{-5} at 40°C. Therefore, higher chain transfer constant at higher temperature led to a lower molecular weight. The same trends were found for chain transfer to initiator. Shawki et al. reported that the K_{fi}/K_p values were 1.58×10^{-3} and 4.41×10^{-3} , corresponding to 25°C and 40°C respectively.

The molecular weights for copolymers (Table 5) were lower than those of acrylamide homopolymers obtained at the same temperatures. Higher initiator

concentration used in the copolymer synthesis ($[I] = 3.0 \times 10^{-3}$ mol/L) was one reason. Another possible reason is that chain transfer to macromonomers is easier than chain transfer to acrylamide. This explanation has been proposed by Schulz et al.¹³

1.3.3 Microstructure of the copolymers.

The performance of the copolymers in applications such as flocculation could depend upon the chain microstructure. The distribution of pendant chains was characterized by the mean sequence lengths, μ_1 and μ_2 , calculated using the following equations⁴²,

$$\mu_1 = 1 + r_1[M_1]/[M_2] \quad (11)$$

$$\mu_2 = 1 + r_2[M_2]/[M_1] \quad (12)$$

where subscript 1 refers to acrylamide and 2 refers to the macromonomer. For example, sample 56-35 in Table 1 has $[M_1]/[M_2] = 60$, $r_1 = 1.63$ (MA-23 from Table 4). If it is assumed that $r_2 = 0.1$, then μ_1 and μ_2 calculated for 56-35 were 98.8 and 1.002, respectively. Since $[M_2]/[M_1] = 1/50 - 1/200$, equation (12) predicted that $\mu_2 \cong 1.0$. This meant that PEG pendant chains were separated by about 50 to 100 acrylamide repeat backbone units in the copolymers produced in this work.

Semi-batch polymerization process²⁰ is a more effective approach to minimize composition drift and more effective in the utilization of costly macromonomers. One possible semi-batch feed policy, i.e. Policy I, is the addition of all macromonomer and sufficient AM (to give the desired composition F_1 , i.e. mole % of AM in copolymers) to the reactor at time zero. Thereafter, the AM is fed to the reactor with a time-varying feedrate to maintain $[M_1]/[M_2]$ and F_1 constant with time. This method should provide copolymer chains with the same

composition. An alternative policy is called monomer-starved feed policy. With this method, the premixtures of AM and macromonomers at desired ratios are fed to a reactor. Addition rate is controlled at a lower rate so that $[M_1] \sim 0$, $[M_2] \sim 0$ and the copolymer composition spontaneously formed is the same as the feed composition. In order to maintain the initiator concentration constant in an isothermal polymerization, initiator potassium persulfate can also be continuously fed to the reactor in aqueous solution during polymerization.

Conclusions

The main conclusions from this work are:

1. Copolymers of AM and PEG macromonomers can be prepared by free homogeneous radical polymerization in aqueous solution.
2. The reactivity of the macromonomer (M_2) toward acrylamide (M_1) was pendant chain length dependent in both homopolymerization and copolymerization of the macromonomer. In copolymerization, longer PEG pendant chain lengths gave lower reactivity, as characterized by $(1/r_1)$. The homopolymerization rate of macromonomers increased as PEG pendant chain lengths increased, as estimated by $K_p/K_t^{1/2}$.
3. The shielding effect caused by pendant chains of macromonomers on growing polymer radicals was proposed to interpret the kinetic mechanism in polymerizations and it was observed that shielding reduced the radical/radical termination rate more than the propagation rate.
4. The molecular weights of the copolymers synthesized were sensitive to the polymerization temperature. Higher MW was obtained at the lower

lower temperatures which is similar to that found for AM

homopolymerization. The pendant chain length in the macromonomer did not show a significant effect on the copolymer MW.

- 5) Each PEG pendant chain, on average, was separated by 100 AM repeat units at feed ratio of $[M_1]/[M_2] \cong 60$. Semi-batch polymerization can provide a more effective approach to minimize composition drift with more effective use of costly macromonomers.

References

- 1 Pelton, R.H., Allen, L.H. and Nugent, H.M. Tappi, 1981, **63**(11), 89
- 2 Pelton, R.H., Allen, L.H. and Nugent, H.M. Svensk Papperstidning, 1980, **9**, 251
- 3 Pelton, R.H., Hamielec, A.E. and Xiao, H.N. Patents pending.
- 4 Ferloni, P., Magistris, A., Chiodelli, G., Faucitano, A. and Buttafava, A. Radiat. Phys. Chem., 1991, **37**, 615
- 5 Cakmak, I., Hazer, B. and Yagci, Y. Eur. Polym. J. 1991, **27**, 101
- 6 Douglas, R.L. and Charles, M.B. J. Polymer Sci. Polym. Chem. Edn. 1979, **17**, 3473
- 7 Rempp, P.F. and Franta, E. Adv. Polym. Sci. 1984, **58**, 1
- 8 Gnanou, Y. and Lutz, P. Makromol. Chem. 1989, **190**, 577
- 9 Ito, K., Tanaka, K., Tanaka, H., Imai, G., Kawaguchi, S. and Itsuno, S. Macromolecules, 1991, **24**, 2348
- 10 Cameron, G.G. and Chisholm, M.S. Polymer, 1986, **27**, 1420
- 11 Tsukahara, Y.; Hayashi, N., Jiang, X. and Yamashita, Y. Polymer J., 1989, **21**, 377
- 12 Meijs, G.F. and Rizzardo, E. Rev. Macromol. Chem. Phys. 1990, **C30**, 305

-
- 13 Schulz, D.N., Kaladas, J.J., Maurer, J.J., Bock, J. Pace, S.J. and Schulz, W.W. *Polymer*, 1987, **28**, 2110
 - 14 Xiao H.N. Ph.D thesis, McMaster University, 1994.
 - 15 Baade, W., Hunkeler, D. and Hamielec, A.E. *J. App. polym. Sci.* 1989, **38**, 185
 - 16 Shawki, S. and Hamielec, A. E. *J. Appl. Polym. Sci.* 1979, **23**, 3323
 - 17 Flory, P.J. in 'Principles of Polymer Chemistry', Cornell University Press, Ithaca, NY, 1953.
 - 18 Kim, C.J. and Hamielec, A. E. *Polymer*, 1984, **25**, 845
 - 19 Bamford, C. H. in 'Encyclopedia of Polymer Sci. and Tech.' v.13, Wiley-Interscience, New York, p.708, 1988.
 - 20 Kamachi, M. Liaw, D.J. and Nozakura, S. *Polymer J.* 1981, **13**, 41
 - 21 Dainton, F.S. and Tordoff, M. *Trans. Farad. Soc.* 1957, **53**, 499
 - 22 Ito, K., Tomi, Y. and Kawaguchi, S. *Macromolecules*, 1992, **25**, 1534
 - 23 Masuda, E., Kishiro, S. Kitarama, T. and Hatada, K. *Polymer J.* 1991, **23**, 847
 - 24 Hamielec, A.E., Macgregor, J.F. and Penlidis, A. *Makromol. Chem., Macromol. Symp.* 1987, **10/11**, 521
 - 25 Zhu, S and Hamielec, A.E. *Macromolecules*, 1989, **22**, 3093
 - 26 Mahabadi, H.K. *Macromolecules*, 1985, **18**, 1319
 - 27 Tsukahara, Y., Tsutsumi, K., Yamashita, Y. and Shimada, S. *Macromolecules*, 1990, **23**, 5201
 - 28 Imae, T and Ikeda, S. *J. Phys. Chem.* 1986, **90**, 5216
 - 29 Aoudia, M., Rodgers, M.A.J. and Wade, W.H. in 'Surfactants in Solution', v.4, Plenum Press, 1986
 - 30 Almgren, M. and Swarup, S. in 'Surfactants in Solution', Plenum Press, v.1, 1984
 - 31 Turro, N.J. and Yekta, A. *J. Am. Chem. Soc.* 1978, **100**, 5951
 - 32 Geetha, B., Mandal, A.B. and Ramasami, T. *Macromolecules*, 1993, **26**, 4083
 - 33 Elworthy, P.H. and Florence, A. T. *Kolloid-Z*, 1964, **195**, 23
 - 34 Corkill, J.M., Goodman, J.F. and Harrold, S.P. *Trans. Faraday Soc.* 1964, **60**, 202

-
- 35 Donbrow, M. and Jan, Z.A. J. Pharm. Pharmacol. 1963, **15**, 825
 - 36 Ito, K. Hasimura, K., Itsuno, S. and Yamada, A. Macromolecules, 1991, **24**, 3977
 - 37 Suzuki, T. and Tomono. T. J. Polym. Sci.: Polym. Chem., 1984, **22**, 2829
 - 38 Cavell, E.A.S. and Gilson, I.T. Makromol. Chem. 1962, **54**, 70
 - 39 Fadner, T.A. and Morawetz, H. J. Polym. Sci. 1960, **45**, 475
 - 40 Kwamgfu, C., Kobunshi Kagaku, 1972, **29**, 225
 - 41 Shawki, S.M. Ph.D Thesis, McMaster University, 1978.
 - 42 McCormick, C. and Chen, G.S. J. Polym. Sci. Polym. Chem. 1982, **20**, 832

Tables

Table 1 Recipes for copolymerization; Concentration of initiator
[KPS] = 3×10^{-3} mol/L.

Samples	Type of (M)A-n	Weight of AM (g)	Weight of PEG-M (g)	Mole Ratio AM/PEG-M	H ₂ O mL	Temp. °C
43-36	MA-23	9.20	2.84	50	300	40
56-35	MA-23	1.6	0.31	60	35	40
43-176	MA-23	12.8	0.99	200	286	25
56-48	MA-23	2.16	0.259	130	40	20
56-51	MA-9	2.21	0.177	88	40	25
43-71	MA-9	11.08	0.798	100	300	40
56-49	MA-5	2.19	0.166	56	40	25
43-16	A-40	11.36	6.07	50	400	40
23-170	A-40	16.0	8.44	50	475	40
56-36	A-20	1.61	0.369	60	35	40
56-1	A-20	12.82	0.968	200	285	25
43-22	A-10	12.78	1.99	50	385	40
23-160	A-10	16.0	9.99	14	500	40

Table 2 $K_p/K_t^{1/2}$ data from MA-PEG macromonomers. Polymerization were carried out in an NMR tube with D_2O at $40^\circ C$. Data are compared with MMA and Acrylamide.

Sample	$[Mo] \times 10^{-2}$ mol/L	n of PEG	$[I_0]$ mmol/L	$K_p/K_t^{1/2}$
MA-5	25.2	5	1.81	0.474*
MA-9	8.44	9	3.55	0.504*
MA-23	3.85	23	3.83	0.663*
MA-67	4.5	67	0.45 ^a	2.46 ^a
MMA	-	-	-	0.077 ^b
Acrylamide	-	-	-	5.57 ^c or 5.19 ^d

*: $K_p/K_t^{1/2}$ values were obtained from fitting the kinetic model Equation (5) to experimental data using least square fitting approach.

a: Data taken from K. Ito et al.²⁰ Polymerization was carried out at $60^\circ C$ in D_2O with initiator. 4,4'-azobis (4-cyanovaleric acid) (AVA). $K_d = 4.58 \times 10^{-5}$ (s^{-1}) for AVA was chosen in calculation. $K_p/K_t^{1/2}$ value was estimated from dX/dt at $t=0$.

b: Data taken from Kamachi et al.²⁰ Methyl Methacrylate was polymerized at $30^\circ C$ in benzene with initiator 2,2'-azobisisobutyronitrile (AIBN).

c: Data taken from Kim, C. J. Ph.D. Thesis, McMaster University, 1983.

d: Data calculated from equation $K_p/K_t^{1/2} = 57.0 \exp(-1500/2T)$.²¹

Table 3 Conversion data for AM and Macromonomers

# of Samples	Reaction Time (min.)	Conversion AM %	Conversion (M)A-n %	Type of (M)A-n	(M)A-n % (mol) in copolymers*
43-22	35	24.9	18.4	A-10	1.41
23-160	60	28.4	18.6	A-10	4.83
56-36	40	12.2	8.32	A-20	1.09
56-1	130	38.6	23.2	A-20	0.32
43-16	210	83.7	50.8	A-40	1.21
23-170	190	63.7	28.4	A-40	0.88
56-49	20	15.5	12.4	MA-5	1.51
43-63	250	69.9	53.0	MA-9	1.62
56-51	20	7.83	6.42	MA-9	1.0
43-176	30	19.3	13.4	MA-23	0.33
43-36	90	58.6	42.6	MA-23	1.36
56-35	20	13.8	9.65	MA-23	0.83

*: Average MW of the macromonomers were calculated using average chain length of PEG in the macromonomers obtained from proton NMR measurements.

Table 4. r_1 estimated from low conversion data. Error estimation are based on standard deviation of NMR composition measurement

Macromonomer	n of PEG	reactivity ratio r_1
PEG-MA-5	5	1.35 ± 0.11
PEG-MA-9	9	1.39 ± 0.15
PEG-MA-23	23	1.58 ± 0.13
PEG-A-10	10	1.36 ± 0.04
PEG-A-20	20	1.63 ± 0.18
PEG-A-40	40	2.20 ± 0.11

Table 5. Molecular Weight of Comb Copolymers

Samples	Mw x 10 ⁻⁶	polymerization temp. °C	Mole feed ratio of M1:M2	Type of macromonomer
43-36	1.2*	40	50:1	MA-23
43-48	1.0**	40	25:1	MA-23
PAM	1.06 ^a	40	---	---
43-129	3.7**	20	99:1	MA-23
43-176	3.4**	25	200:1	MA-23
56-48	4.5*	20	130:1	MA-23
56-51	5.1*	25	88:1	MA-9
PAM	5.3 ^b	25	---	---

*: Data from GPC measurement. **: Data from LALLS measurement.

Data for polyacrylamide (PAM) homopolymers was number average molecular weights obtained from Shawki, S. M., Ph.D Thesis, McMaster University, 1978.

a.: [AM] = 0.5 mol/L; [KPS] = 2.5 x 10⁻³ mol/L;

b.: [AM] = 0.5 mol/L; [KPS] = 1.0 x 10⁻³ mol/L.

Figures

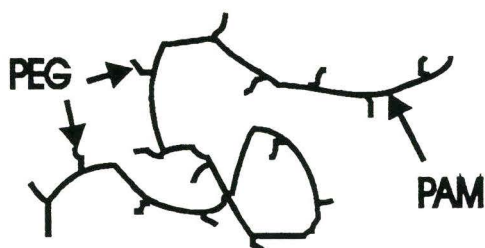
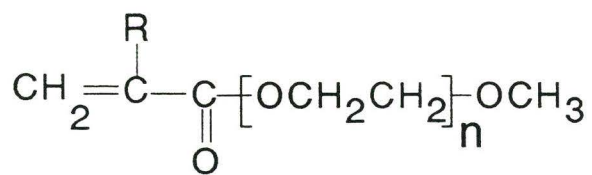


Figure 1. A schematic structure of long PAM having short PEG pendant chains to give a comb copolymer.



$n = 5 \text{ to } 40$

$\text{R} = \text{H}$ (A-n macromonomer)

or $\text{R} = \text{CH}_3$ (MA-n macromonomer)

Figure 2 Structure of PEG-(meth)acrylate macromonomer

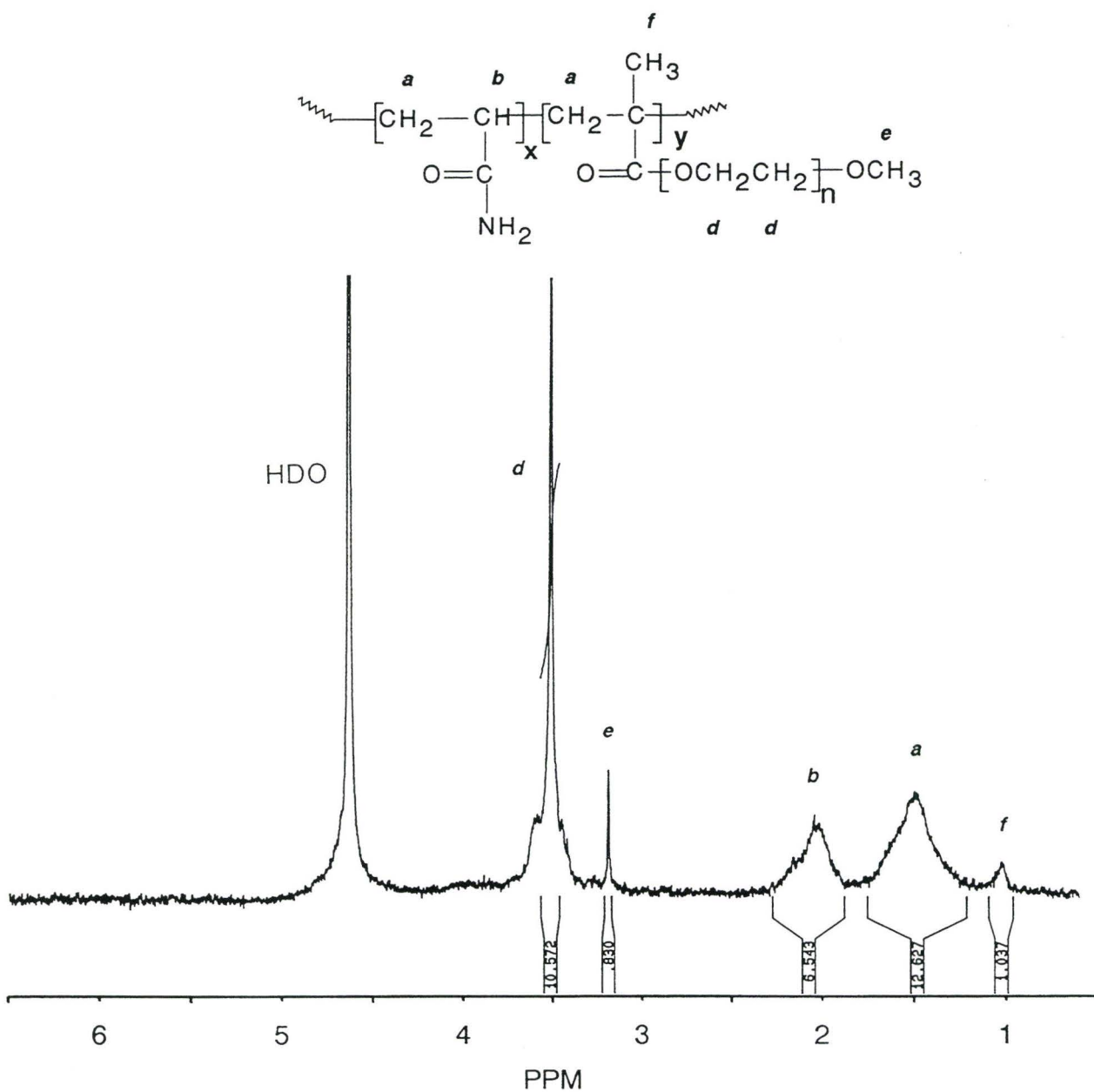


Figure 3. ^1H NMR spectrum of copolymer synthesized from acrylamide and PEG macromonomer MA-9.

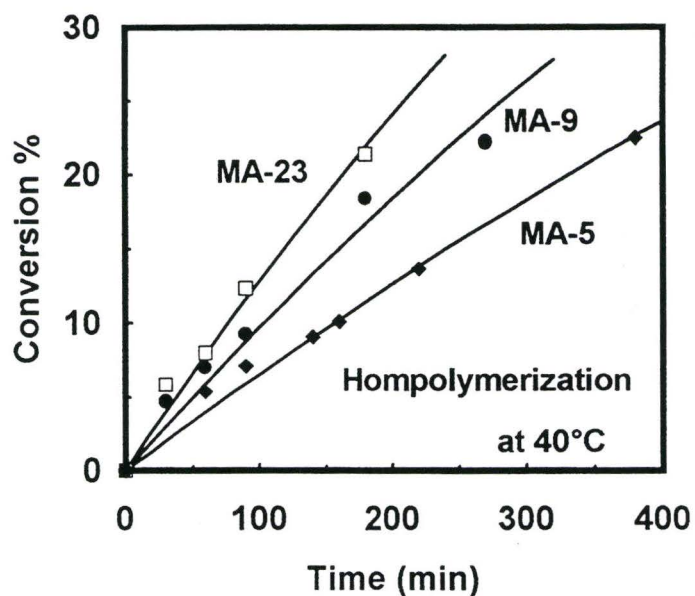


Figure 4. Conversion versus time for the homopolymerization of PEG-methacrylate macromonomers with different PEG pendant chain lengths (see Table 2). The fitted lines were obtained from the kinetic model summarized by Equation (4)

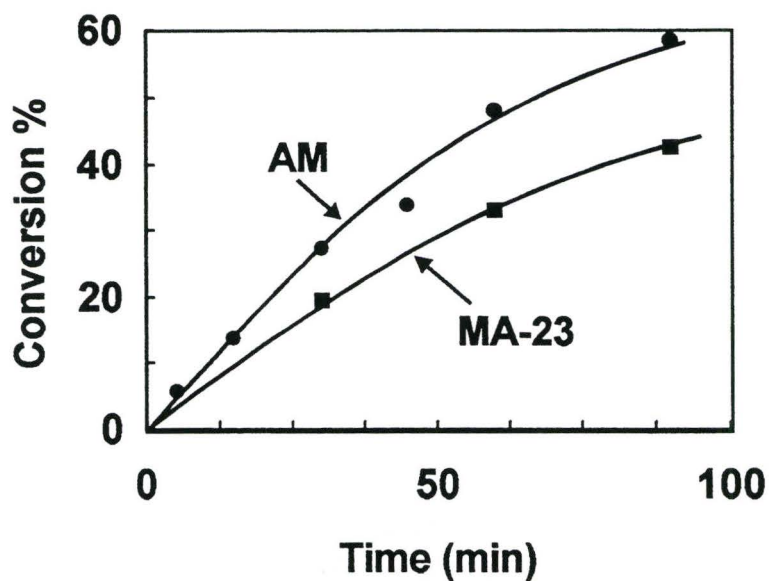


Figure 5. Conversion curves for AM and PEG-methacrylate macromonomer with PEG pendant chain length of 23. The corresponding recipe for copolymerization is given as recipe 43-36 in Table 1.

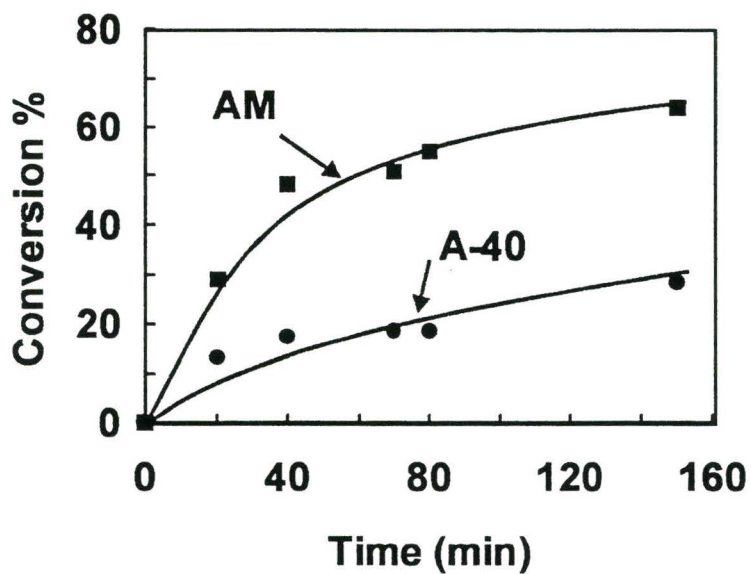


Figure 6. Conversion curves for AM and PEG-acrylate macromonomer with PEG pendant chain length of 40. The corresponding recipe for copolymerization is shown in 23-170 in Table 1.

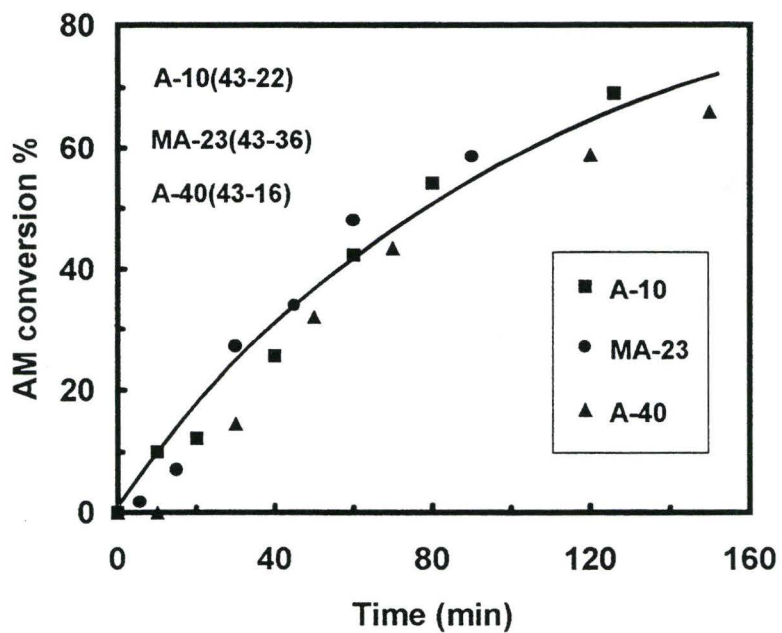


Figure 7. AM conversion in copolymerization of AM with macromonomer with different PEG pendant chains length. Molar ratios of AM to macromonomers were 50 all samples. Polymerizations were carried out at 40°C with the recipes (43-16, 43-22 and 43-36) shown in Table 1.

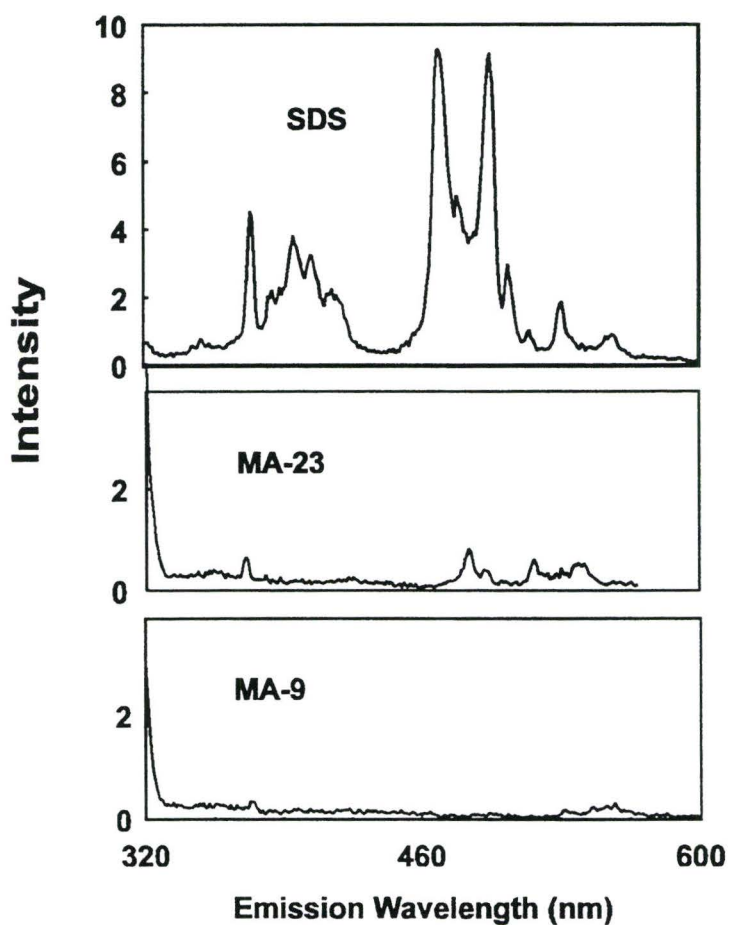


Figure 8. Fluorescence spectra of pyrene in SDS, MA-9, MA-23 and water. Concentrations of SDS, MA-9 and MA-23 in aqueous solution were 11.8, 11.4 and 8.86 mmol/L, respectively.

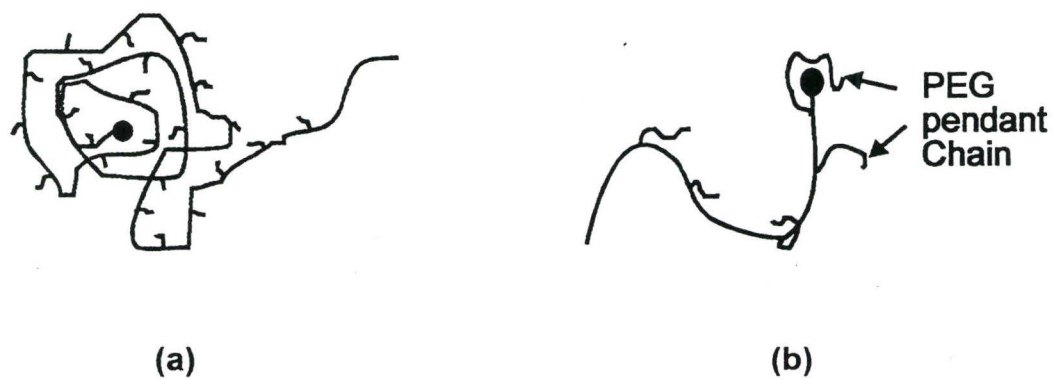


Figure 9. Schematic description of shielding effect on propagating radicals. (a) radical shielded by a growing polymer chain, i.e., growing chain effect; (b) radical shielded by a pendant chain in the macromonomer, i.e., pendant chain effect.

CHAPTER 2

Interpolymer Association between Phenolic Resin and PEO or PAM-co-PEG Copolymers

ABSTRACT

The complexation via hydrogen bonding between phenolic resins and poly(ethylene oxide) (PEO) or polyacrylamide (PAM)-co-poly(ethylene glycol) (PEG) copolymers has been investigated. Characterization of the complexes was conducted using precipitation isotherm, rheological behavior and fluorescent microscopic observations. The results indicated that interactions between phenolic resins and PEO or the copolymer led to the transient increase in viscosity, complex aggregation and precipitation. By contrast, PEG with a low MW of 2000 did not show the same evidence as observed for the high MW PEO/phenolic resins systems.

This work considered the complexation in analogy with polymer adsorption. Two parameters, the degree of linkage and the amount of binding, were required to characterize the complexes. Higher amounts of phenolic resin involved in the complexes at the higher PEO molecular weights were attributed to the dynamic collapse of colloidal complexes. Complexation between phenolic resin and copolymers with short PEG pendant chains (as low as 9 repeat units) is believed to arise from the simultaneous interactions of the phenolic resins with the short PEG chains bound to the same polymer backbone.

KEYWORDS: complexation; PEO; copolymer; phenolic resin; hydrogen bonding.

Introduction

The interpolymer association between a proton-donor polymer (e.g. poly(acrylic acid) and phenolic resins) and a proton-acceptor polymer (e.g. poly(ethylene oxide)(PEO) and polyacrylamide) has been extensively studied in past decades.¹ Two basic types of studies have been widely conducted. One has focused on the solid state polymer mixtures in which interpolymer association strongly influences the properties of polymers such as stress-strain behavior and glass transition temperature; another has concentrated on complexation occurring in organic or aqueous solutions.

Phenolic polymers, as proton-donor polyacids, have been recently studied in blends in the solid state. For example, interpolymer complexation between Poly(vinylphenol) and poly(N,N,-dimethylacrylamide) was reported by Suzuki et al.² Similar systems, such as blends of poly(vinylphenol)/poly(methyl acrylate)³ and poly(vinylphenol)/poly(vinyl acetate)⁴, and complexation of poly(N,N-dimethylacrylamide) and phenol-formaldehyde resins,⁵ have also been published. However, systematic studies on complex formation between phenolic polymer and poly(ethylene oxide) in aqueous solution are very limited.

Nevertheless, the complex formation in solvent, especially in aqueous solution, is very important. For example, a number of biological macromolecules produce aggregates or gels in aqueous solution due to association.⁶ PEO polymer used as a flocculant⁷ in papermaking processes is another important example for the complex formation occurring in aqueous solution. The flocculation processes, specifically, the fine particle retention for mechanical pulps, involve complicated macromolecular associations.

In this work, results on studies of the hydrogen bonding complexes between high molecular weight polyethers and water soluble phenolic polymers were reported. Our interest in these systems arises from the fact that these complexes are very effective flocculants (retention aids) in the production of newsprint and other papers based on mechanical wood pulps. The key feature of this application is that flocculation of suspended solids must occur in the presence of high concentrations of dissolved and colloidal substances (DCS) originating from the wood. Much of this dissolved material is anionic polyelectrolytes which form precipitates with conventional cationic flocculants. By contrast, high molecular weight poly(ethylene oxide), PEO, is not sequestered by the dissolved material and thus is effective as a colloidal flocculant at much lower dosages than the cationic polyelectrolytes.

A second polymeric component, herein called a cofactor, must be present for effective flocculation with PEO. Water soluble phenol formaldehyde resins are the standard cofactors used in industry. However, kraft lignin, sulfonated kraft lignin and abietic acid are also effective. All cofactors have phenolic hydroxyl groups which can form hydrogen bonding complexes with PEO. Stack and coworkers have published a series of papers^{8,9,10} on the complex formation between PEO and phenolic resins. They determined the factors affecting the formation of precipitated complex defined as that material which would not pass through a 76 μm screen. Comparing the precipitation behavior of different phenolic resins, they concluded that: 1) both Novolac and Resole resins can form complexes with PEO; however, they speculated that Novolac phenolic groups are more accessible to hydrogen bonding; 2) the tendency to form precipitate did not seem to depend upon the content of methylol groups whereas

resins with high hemiformal content gave the most precipitate; and, 3) they postulated that the structure shown in Figure 1 was representative of the hydrogen bonding interaction.

The effects of pH, ionic strength and PEO molecular weight were not entirely clear because many phenolic resins were phase separated in dilute aqueous solution at around pH 4 depending upon the salt concentration. In the presence of PEO there appears to be two precipitation regimes. At low pH values, near the PFR phase separation, the amount of precipitated PFR per PEO molecule increased with the PFR concentration. By contrast, at higher pH values, the PEO/PFR precipitate had a constant composition which was not sensitive to electrolyte concentration.

It has been shown that comb copolymers with polyacrylamide backbones and bearing 0.5 to 3 mole percent poly(ethylene glycol) (PEG) pendant chains function similarly to PEO as flocculants.¹¹ Whereas PEO molecular weights must be at least 4,000,000 for effective flocculation, good results were obtained when the pendant PEG chains on comb copolymers were as short as 9 repeat units. In this work we compare PEO, low molecular weight PEG and the PEG comb copolymers with respect to complex formation with phenolic resins. Several techniques have been used to characterize the interpolymer association in the present work. These include UV spectrometry, rheometry, and fluorescent microscopy.

2.1 Experimental

2.1.1 Materials

Poly(ethylene oxide) (PEO) homopolymers, Polyox-301 (PEO-301) and Polyox-309 (PEO-309) were supplied by Union Carbide. Weight average molecular weights (M_w) of PEO-301 and PEO-309 were 4 and 8 million respectively, as indicated by the supplier. Methoxy poly(ethylene glycol) (PEG) with a molecule weight of 2000 was obtained from Union Carbide. Copolymers with long polyacrylamide (PAM) backbones and short PEG pendant chains were synthesized in this work. Details on the copolymerization procedure and characterization have been described elsewhere.¹² The copolymer structure is schematically represented in Figure 2. The copolymer 56-107 used in this work contained 1.7 % (mole) of PEG pendant chains with chain length of 23 ether repeat units, and M_w was approximately 4.0 million.

Phenol formaldehyde resins (PFR) CASCOPHEN C-271 (40 % (wt) in aqueous solution) were obtained from Borden Chemicals. The average M_w of PFR was 13,000 based on gel permeation chromatography (GPC) measurement using PEO as standards.

2.1.2 Potentiometric titration

PFR C-271 titration was carried out with an ABU93 Triburette Radiometer (COPENHAGEN). The addition of acid, 0.1 N HCl, or base, 0.1 N NaOH, was automatically controlled by Aliquot software. NaOH was added first and the forward titration was stopped at pH 10.5; HCl was added for the back titration to give 90 data points for the titration curve. Hydroxyl content of the PFR C-271 was calculated from the reverse potentiometric titration curve.¹³ This curve was

also used to calculate the degree of ionization of C-271 as a function of pH using the method reported by Bloys van Treslong et al.¹⁴

2.1.3 PFR Solubility

The solubility of PFR at various pH and salt concentrations is given in Figure 3. Non turbid region occurred at the current conditions for precipitation isotherm, i.e., pH > 4.0, and [NaCl] = 10^{-3} M which corresponds to about 2.1 of log{conductivity ($\mu\text{S}/\text{cm}$)}. Therefore, no precipitate of PFR would be expected. These properties were similar to those observed by Stack et al.⁸

2.1.4 PEO/PFR precipitation experiments.

The pH and ionic strength of PFR and PEO stock solutions were adjusted by addition of HCl, NaOH, and NaCl. To a test tube containing 15 mL of PEO or copolymer solution (70 to 240 mg/L) was added between 0.02 and 0.2 mL of C-271 at the concentration of about 4000 mg/L. After shaking by hand the tubes were left for 20 minutes to allow the precipitated complex to settle. The C-271 concentration in the supernatant was measured by UV at 286 nm. The UV calibration curve obeyed Beer's law to a concentration of 200 mg/L; more concentrated PFR sample (3.7 % wt) was diluted before analysis.

2.1.5 Viscosity measurement

A Bohlin VOR Rheometer System (Bohlin, Sweden) was used to measure the rheological behavior of mixtures of the phenolic resin and PEO or copolymer. Measurements were conducted in a concentric cylinder with a measuring geometry of C25. Continuous viscosity and shear stress were recorded as a function of time at a constant strain. Shear rate was 146/s. The total sample volume was about 13 mL. In order to observe the influence of interpolymer

association on the system viscosity, one polymer (phenolic resin or PEO) was subjected to steady-state shear. After approximately 30 s the second component (PEO or phenolic resin) was added and data were collected for 120 to 150 s.

2.1.6 Fluorescent laser microscopy observation

Fluorescent microscopic observations of the interpolymer associations between PEO or PEG comb copolymer and phenolic resins were conducted using a Laborlux K Dage-Mti series Sit 66 microscopy system (Leitz) with a halogen laser source. Excitation wavelengths ranged between 450 and 490 nm, and the emission at 520 nm. Acridine Orange (Sigma) was used as a probe molecule in fluorescent microscopic observation. A solution mixture of phenolic resins and the probe molecule was first put in a watch glass. The PEO or copolymer solution, at pH 5, was then dropped on the glass and mixed with phenolic and Acridine Orange solution. Images were videotaped.

2.2 Results

2.2.1 Characterization of PFR

Figure 4 shows results from the potentiometric and conductivity titrations of PFR C-271. The potentiometric curve showed two inflection points. The first at pH 4.5 is assumed to indicate the presence of carboxyl groups in the phenolic resins. The second inflection point is at pH 10, which corresponds to the dissociation of hydroxyl groups in PFR. The conductivity curve agrees with the potentiometric curve.

To further elucidate the charge groups, the degree of ionization, σ , versus pH was calculated from the titration curve (see Figure 5). σ was defined as the

excess mM equilibrium base, relative to blank titration of 0.1 N HCl with 0.1 N NaOH, over phenolic resin concentration.

In plotting Figure 5, σ value was assumed to be zero at pH = 3. As pH increased, the degree of ionization increased. Corresponding to Figure 4, two inflection points also existed. The titration endpoints indicated that totally about 7 meq/g PFR of the charge content in the phenolic resin. Among them, about 5 meq/g PFR was attributed to the hydroxyl groups, and the remaining was from the carboxyl groups.

2.2.2 Precipitation isotherms

Precipitates formed when aqueous PEO was mixed with PFR. Figure 6 shows the mass of precipitate as a function of the amount of added PFR. The experimental conditions are summarized in the figure caption and the mass of PFR in the precipitate was divided by the total mass of polyether (i.e. PEO or copolymer) to give a dimensionless quantity. The mass of precipitated PFR increased linearly with the amount of added C-271. Similar results were reported by Stack et al.⁸ for a different PFR dissolved in 0.01 M KNO₃.

The data in Figure 6 also show that the amounts of precipitated PFR in the copolymer complexes (based on total amount of the copolymer) were lower than those in PEO-309 complexes. For example, the amount of precipitated PFR in PEO-309 was about 0.12 mg/mg PEO at about 0.6 mg/mg PEO addition dosage, whereas the amount of precipitated PFR bound to the copolymer 56-107 was approximately 0.04 mg/mg copolymer at the same PFR addition dosage. However, it should be noted that the copolymer used contained only about 21 % (wt) of macromonomers with an average PEG chain length of 23 moles. Therefore, when the estimation was based on the total amount of the

effective ether repeat units, the amount of bound PFR in the copolymer was 0.19 mg/mg copolymer at the same PFR dosage. This suggested that the PEG pendant chains in the copolymer appeared to be more effective than PEO at precipitation of PFR. The similar complex precipitate was also observed for the copolymer 56-108 which PEG pendant chain length was as low as 9 ether repeat units.

The mass of precipitated PFR in Figure 6 did not reach a constant value which should occur when the PEO is saturated with bound PFR. Higher PFR dosages were required for saturation.

When initial PEO concentration was low (about 70 mg/L), the different precipitation behavior was observed upon PFR addition. The results are shown in Figure 7. The important features include: 1) precipitated PFR amount is a function of pH; 2) PEO saturation was observed. An interesting phenomenon was that the precipitate did not form until PFR addition dosage exceeded 1.8 mg/mg PEO.

The precipitation amounts PFR were also pH dependent. At an initial pH of 4.4 the maximum mass of precipitated PFR was 1.3 mg/mg PEO. At a higher initial pH value of 7.2, a lower amount (\cong 1.0 mg/mg PEO) of the precipitated PFR was observed. The results suggested that acid conditions were more favorable for complex formation. The scattering in the data in Figure 7 may reflect the broad molecular weight distribution of PEO. Stack et al. have shown that the maximum amount of bound PFR increases with PEO MW.⁸

Many attempts were made to form precipitate by mixing PEG 2000 and phenolic resin C-271. No indication of precipitate was observed at PEG concentrations of 40.5 and 251 mg/L.

2.2.3 Rheological properties of PEO/PFR mixtures

It has been suggested that the addition of PFR to PEO aqueous solution forms a transient water swollen network. To test for this, the viscosity and shear stress was measured as a function of time at constant shear rate. The results, as indicated in Figure 8, show that a spike in the viscosity was observed after the PFR was added into the PEO solution. After approximately 30 seconds, the system viscosity was reduced to close to the initial PEO-309 homopolymer aqueous solution value. Similar result was obtained for the copolymer/C-271 complex (Figure 9).

2.2.4 Morphology observations in complex formation

Fluorescent microscopy was used to observe the water soluble PEO/PFR complex. Acridine Orange (3,6-bis[dimethylamino]acridine·HCl), a cationic water soluble dye, was used as a probe. The dye structure is given in Figure 10.

Figure 11 shows a photomicrograph of the mixture of phenolic resin C-271 and Acridine Orange. The dye concentration was 30 mg/L, which is lower than the limit of solubility (50 to 100 mg/L). PFR concentration was 275 mg/L. The white spots in the Figure indicate that the fluorescent emission from the probe was uniformly dispersed. It was assumed that the cationic dye formed electrostatic complexes with the negatively charged PFR.

When Acridine Orange was mixed with PEO in the absence of phenolic resins similar photomicrographs were obtained. However, when PEO or the copolymer was added to the mixture of Acridine Orange and phenolic resin, highly fluorescent aggregates with sizes greater than 10 μm were immediately observed. Figure 12 shows such an example. It is assumed that the large white fluorescent spot indicates the concentrated PFR complexed with PEO. Figure

13 shows the luminescent aggregate formed by copolymer 56-107 in the presence of PFR.

It should be noted that the PFR concentrations used in these measurements (275 mg/L) were much higher than those used in flocculation applications (2 mg/L). If polymer concentrations were reduced to 25 mg/L, no luminescent aggregates were observed under the present instrumental conditions.

The results of Lindstrom et al.¹⁵ and the rheological results presented herein suggest that soluble PFR/PEO complexes undergo synergistic interaction to form a precipitate. However, Acridine Orange labeled complex showed no tendency to collapse, aggregate or precipitate under microscope. Perhaps the dye introduced excess positive charges which solubilized the complexes.

When PEG (MW = 2000) or PEG macromonomer was added to the mixture of Acridine Orange and phenolic resin, no aggregation was observed under fluorescent microscope. This result suggested that low MW PEG did not cause aggregation of phenolic resin in the measurement conditions.

It was also found that Acridine Orange did not interfere with the ability of PEO/PFR complex to flocculate polystyrene latex. This has been demonstrated by effective flocculation of PS latex by PEO/PFR dual polymer in the presence of the same concentration of Acridine Orange (2.0 mg/L).

2.3 Discussion

Interpolymer association between a polyacid and a polybase can produce the water soluble complexes and/or water insoluble complexes. For example, the complex between PEG (MW > 1000) and polyacrylic acid (PAA) is water

soluble. By contrast, in this work it was found that the high MW PEO and phenolic resins formed a visible insoluble complex at a weight ratio of 1:1 with total polymer concentrations being greater than 16 mg/L.

Water soluble PEO/PFR complexes must form either at extreme ratios of the two polymers or immediately after mixing as a prelude to phase separation. The only direct evidence for soluble complex formation is the fluorescent labeled complex observed in this work. Unfortunately, the cationic dye is likely to perturb the complex structure and properties.

In this work, the formation of insoluble complex is emphasized because it has been measured and because colloidal flocculation with the PEO/PFR system occurs in the precipitation regime. In the following paragraphs, complex formation, starting from the molecular level (hydrogen bonding) and ending with a description of the formation of macroscopic precipitate, is discussed.

2.3.1 Characterization of hydrogen bonding formation

The schematic description of hydrogen bonding between PEO and PFR has been shown in Figure 1. There exists a great deal of evidence from related systems to support the concept of hydrogen bonding between PEO and PFR. For example, solution NMR has been used in the complex systems such as the PEO/PAA¹⁶ and PAA/polyacrylamide¹⁷. Chemical shifts in ¹H and ¹³C spectra were attributed to complexation and the change of ionization conditions.

In potentiometric titration of aqueous solution of PMMA,¹ the addition of PEG with MW of 3000 or higher was accompanied by a rapid increase in pH at [PMAA]/[PEG] mole ratio = 1 or above. This result is also an indication of the formation of hydrogen bonding.

Fuchs and Rupprecht⁶ reported the investigation on interaction of phenolic compounds with PEG in nonpolar solvents (CCl_4 and $\text{C}_2\text{H}_2\text{Cl}_4$) using IR spectroscopy. In the mixture of PEG 1500 and hexylresorcinol, a broad and strong band with a maximum at 3375 cm^{-1} was found in IR spectrum. This was attributed to the strong hydrogen bonding of the phenolic hydroxyl groups with the polyether oxygens of the PEG.

In the complexation of poly(N-dimethylacrylamide) and phenolic resins, differential scanning calorimetry (DSC) has been used in analyzing the hydrogen bonding association and determining the T_g of the blends. It has been found that the glass transition temperature of the complex was higher than the T_g values of either polymer components.⁶

Hemker et al.¹⁸ reported using pyrene-end-labeled poly(ethylene glycol) to investigate the complexation between PEG and PAA or PMAA. The effect of pH was particularly noted. The hydrophobic pyrene fluorescence labels interacted with the hydrophobic α -methyl groups of PMAA and caused enhanced complexation. Iliopoulos et al. used 9-aminoacridine labeled PAA in fluorescence polarization measurements.¹⁹ The method included a fluorescence probe which was covalently bonded to a macromolecule. Information about the local viscosity of the medium and polymer conformation can be obtained by determining the motion of a fluorescent labeled macromolecules. The resulting complexation led to a significant reduction in the mobility of the labeled molecules.²⁰

There is no direct evidence for hydrogen bonding between PEO and PFR in water. However, all changes such as increasing pH which should decrease hydrogen bonding also completely eliminate the ability of the PEO/PFR complex

to precipitate and to coagulate colloids. Thus based upon a great deal of circumstantial evidence there is general agreement in the literature that hydrogen bonding is the basis for PEO/PFR complex formation.

2.3.2 Conceptual models of complex formation

A number of investigations of the PEG/PAA and PEG/PMAA system have been published. The usual approach is to describe the experimental results by one parameter θ , the degree of linkage, which is defined as the concentration of hydrogen bonded carboxyl groups divided by the total concentration of carboxyl groups.^{21, 22, 23}

Experimentally, θ is estimated by the following equation:²⁴

$$\theta = 1 - ([H^+]/[H^+]_0)^2$$

where $[H^+]$ and $[H^+]_0$ are the proton concentration in the presence and absence of the PEG, respectively. For the PAA/PEG system θ increases with increasing PEG MW and temperature.

The usual approach is to calculate a complex stability constant K from θ using:

$$K = \theta / C_0(1 - \theta)^2$$

where C_0 is the normality of the polymeric acid.

An important feature of the PEO/PFR system is that the chain length of PEO was about 10^5 whereas the chain length of PFR was only 120. Kabanov et al. have developed models for this situation.²⁵ An interesting assumption for this model was that the low molecular weight polymers (or oligomers) were either free in solution or completely bonded (i.e. $\theta_{\text{oligomer}} = 1$) to the high molecular weight polymer. This is illustrated in Figure 14.

The main predictions on the basis of Kabanov's analysis included: 1) the stability constant K exponentially increased as oligomer chain length exceeded a critical value ($\cong 40$ repeat units for PEG in PEG/PMAA system and $\cong 200$ for PEG in PEG/PAA system); and, 2) very weak segment/segment interactions can lead to complex formation.

When considering the binding of two different polymers it is conceivable that a fraction, θ_1 , of the possible binding sites on one polymer binds with θ_2 sites on the second. Most of the models describing the PEG/PAA system assume that all the polyether oxygens participate in hydrogen bonding (i.e. $\theta_{\text{PEG}} = 1$) whereas θ_{PAA} values were determined experimentally. The phenolic resin used in this work is believed to be branched and the polyether molecular weights were very high so it is unlikely that either θ value equaled one and that complex formation can be adequately described by 1 parameter.

2.3.3 An analogy between the oligomer/polymer complexation and the polymer adsorption

The basis of the following analysis is that there should be many similarities between the interaction of polymers with other polymers and the interactions of polymers with surfaces. Adsorbed polymers can have a spectrum of configurations.²⁶ In one extreme, the adsorbed polymer can lie completely flat along a surface. In the other, the adsorbed polymer interacts only through a few contacts and the adsorbed configuration is similar to the random coil form of the polymer in solution. The usual situation, between the extremes, is illustrated in Figure 15(a).

By analogy, a polymer in a complex can be stretched out to give the commonly assumed "zipper" structures or, in contrast, only a few of the polymer

sites participate in bonding to give configurations such as those illustrated in Figure 15 (b). If these configurations exist in polymer/polymer complexes, then two experimental parameters are required to characterize the average properties of a complex formed from two monodisperse polymers. For example, in polymer adsorption the two common parameters are the mass of adsorbed polymer per unit area and the fraction of adsorbed segments which are directly bound to the surface. For polymer complexes two potentially measurable parameters are the mass of one polymer per unit mass of the other in the complex, Γ_{12} , and the θ value for either polymer. Similarly, measurement of both θ values gives the same information. There have been no reported measurements of either θ value in the PEO/PFR system whereas Γ values were measured in this work and by Stack et al.⁸

An interesting result in this work was that PAM-co-PEG copolymer formed precipitate with PFR when the PEG pendant chain lengths were as short as 9 repeat units (MW of about 400). This was attributed to the simultaneous interaction of more than one PEG chain with a phenolic resin molecule. Figure 16 (a) shows one possible structure in which a PFR is simultaneously bonded to neighboring PEG chains on the PAM backbone. However, if the copolymer contained less than 1.0 % (mole) of macromonomers and copolymer chains were fully extended, this case would seldom occur because PFR only contained roughly 100 phenolic repeat units. Figure 16 (b) shows how complex formation could result in intramolecular crosslinking whereas Figure 16 (c) shows a PFR molecule binding two different copolymer molecules. These two cases were the more realistic configuration of complexes, compared with the case in Figure 16 (a).

2.3.4 Conceptual model of precipitate formation

The formation of soluble complex is usually mass transport limited and thus is very fast whereas the conversion to precipitated complex can be slow. A number of different types of interactions can influence precipitate formation and these are summarized in Figure 17. In case 1, cofactor (i.e. PFR) binds together two PEO molecules via hydrogen bonding. With continued inter and intramolecular crosslinking of the long PEO chains, a point may be reached where the complex becomes insoluble.

Case 2 shows bonding via hydrophobic association of cofactor molecules. This possibility may distinguish the hydrophilic PEG/PAA system from the PEO/PFR system which has a much greater tendency to form precipitates.

Finally, case 3 shows the situation where if the cofactor is highly charged and the ionic strength is low, electrostatic repulsion will prevent aggregation and precipitation.

Stack et al.⁸ found that higher MW of PEO allowed higher amounts of PFR into the complex. However, no satisfactory explanation on the PEO MW effects was given. The following arguments explain the molecular weight results.

Consider an isolated PEO chain exposed to PFR. The phenolic molecules will diffuse to the polyether and bind by hydrogen bonding. After the first few phenolic molecules are attached the complex may appear as shown in Figure 18 (a) - note that many of the potential hydrogen bonding sites on the phenolic resin are not involved in the initial attachment. At this point two processes can occur simultaneously. The first is the further attachment of PFR molecules and the second is the re-arrangement of the PEO chain to give

intramolecular crosslinking (see Figure 18 (b)). The more intramolecular crosslinking that occurs, the fewer new PFR molecules that can be accommodated on the PEO backbone. In the other extreme, if molecular rearrangement for crosslinking is much slower than diffusion of additional PFR molecules, the maximum PFR content would be attained (Figure 18 (c)).

Finally, it seems reasonable to propose that the highest molecular weight PEO molecules exhibit the slowest rearrangement required for intramolecular crosslinking. By contrast, short PEO chains will have high mobility and thus crosslinking (i.e. Figure 18 (b)) will be favored.

Similar arguments can be used to speculate about the role of cofactor molecular weight. For a constant cofactor concentration, the size and number of cofactor chains increase with decreasing molecular weight.

At low MW the cofactors easily diffuse into the PEO chains, and the higher number of the cofactor increased the interaction possibility. Therefore, the rate of complex collapse is also increased.

At high MW, diffusion of the cofactor into the PEO coils becomes difficult. The lower number of cofactor also decreases the number of available interaction sites. Therefore, the collapse rate decreases and a high degree of linkage results.

If the cofactor is added in two steps: half a dose of PFR is added first, and, after a sufficiently long period of time to allow collapse of the complex, the remaining half dose of PFR is then added, it will be expected that the bound amount of PFR is lower due to a previous collapse of the complex. Therefore, one step addition of cofactor should be more effective than two step addition.

Conclusions

The investigations on interpolymer association between phenolic resins and PEO or PAM-co-PEG comb copolymer have been conducted by several different approaches. The conclusions are as follows:

1. Precipitated isotherms for PFR on PEO or the copolymer indicated that the bound amount of phenolic resin was a function of initial pH. The higher saturated amount of bound PFR was produced at lower pH.
2. Interpolymer associations between PEO/PFR and the copolymer/PFR caused a transient viscosity increase.
3. Complex aggregates were formed between phenolic resins and PEO or the copolymer in the presence of Acridine Orange.
4. Complexation was considered to be analogous to polymer adsorption in PEO/PFR as well as the similar oligomer/polymer systems. Two parameters, the degree of linkage and binding amount, were required to completely describe the complexation in these systems.
5. Effects of PEO MW on the PFR bound amounts were caused by the time dependence of collapse and aggregation of the polymer complexes.
6. There was no evidence indicating PEG (MW 2000) forming complex with PFR. However, when the same or shorter length PEG chains were incorporated into copolymers, the simultaneous interactions of many short PEG chains on the same polymer backbone with phenolic resin significantly increase the number of sites available for association and the possibility of enhancing the stability of complex.

References

- ¹ Tsuchida, E. and Abe, K., *Adv. in Polym. Sci.*, **45**, 1(1982).
- ² Suzuki, T., Pearce, E.M. and Kwei, T.K., *Polymer Commun.*, **33**, 198(1992).
- ³ Zhang, X., Takegoshi, K. and Hikichi, K., *Macromolecules*, **24**, 5756(1991).
- ⁴ Moskala, E.J., Howe, S.E., Painter, P.C. and Coleman, M.M., *Macromolecules*, **17**, 1671(1984).
- ⁵ Yang, T.P., Pearce, E.M., Kwei, T.K. and Yang, N.L., *Macromolecules*, **22**, 1818(1989).
- ⁶ Fuchs G. and Rupprecht, H., *Colloids and Surfaces*, **6**, 175(1983).
- ⁷ Pelton, R.H., Allen, L.H. and Nugent, H.M., *Pulp & Paper Can.*, **80**(12), 25(1979).
- ⁸ Stack, K.R., Dunn, L.A. and Roberts, N.K., *Colloids and Surfaces*, **61**, 205(1991).
- ⁹ Stack, K.R., Dunn, L.A. and Roberts, N.K., *J. of Wood Chem. and Tech.*, **12**, 283(1993).
- ¹⁰ Stack, K.R., Dunn, L.A. and Roberts, N.K., *Colloids and Surfaces*, **70**, 23(1993).
- ¹¹ Xiao, H.N., Chapter 3, Ph.D. Thesis,, McMaster University, 1994.
- ¹² Xiao, H.N., Chapter 1, Ph.D. Thesis,, McMaster University, 1994.
- ¹³ Pelton, R.H., *J. Polym Sci.: Part A: Polym. Chem.*, **22**, 3944(1984).
- ¹⁴ Bloys van Treslong, C.J. and Staverman, A.J., *J. R. Netherlands Chem. Soc.*, **93**, 171(1974).
- ¹⁵ Lindstrom, T. and Glad-Nordmark, G., *J. Colloid Interface Sci.*, **97**, 62(1984).
- ¹⁶ Maunu, S.L., Korpi, T. and Linberg, J.J., *Polym. Bull.*, **18**, 172(1987).
- ¹⁷ Garces, F.O., Sivadasan, K., Somasundaran, P. and Turro, N., *Macromolecules*, **27**, 272(1994).
- ¹⁸ Kondo, T., Sawatari, C., Manley, R.J. and Gray, D.G., *Macromolecules*, **27**, 210(1994).
- ¹⁸ Hemker, D.J., Garza, V. and Frank, C.W., *Macromolecules*, **23**, 4411(1990).
- ¹⁹ Iliopoulos, I., Halary, J.L. and Audebert, R., *J. Polym. Sci.: Part A: Polym. Chem.*, **26**, 275(1988).
- ²⁰ Ohno, H. and Tsuchida, E., *Makromol, Chem. Rapid Commun.*, **1**, 585(1980).

-
- ²¹ Tsuchida, E., Osada, Y. and Ohno, H., *J. Macromol. Sci. Phys.*, **B17**, 683(1980).
- ²² Iliopoulos, I. and Audebert, R., *Macromolecules*, **24**, 2566(1991).
- ²³ Subotic, D., Ferguson, J. and Warren, B.C.H., *Eur. Polym. J.*, **25**,1233(1989).
- ²⁴ Osada, Y. and Sato, M., *J. Polym. Sci. Letters Ed.*, **14**, 129(1976).
- ²⁵ Kabanov, V.A.and Papisov, I.M., *Vysokmol. Soyed.*, **A21**, 243(1979).
- ²⁶ Vincent. B., *Adv. Colloid & Interface Sci.*, **4**, 193(1974).

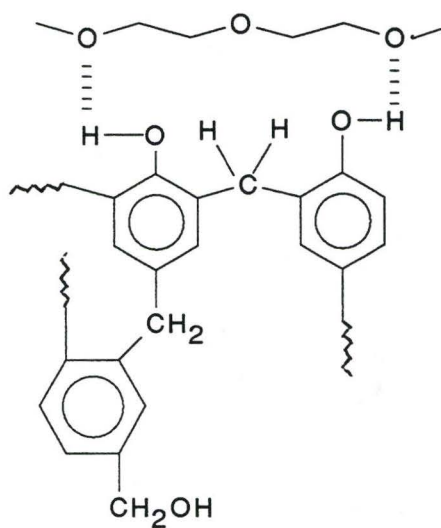
Figures

Figure 1. A schematic for hydrogen bonding between PEO and PFR

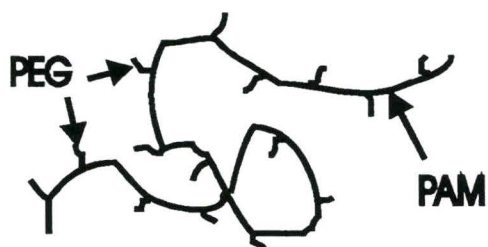


Figure 2. A schematic structure of comb copolymer with long PAM backbone and short PEG pendant chains.

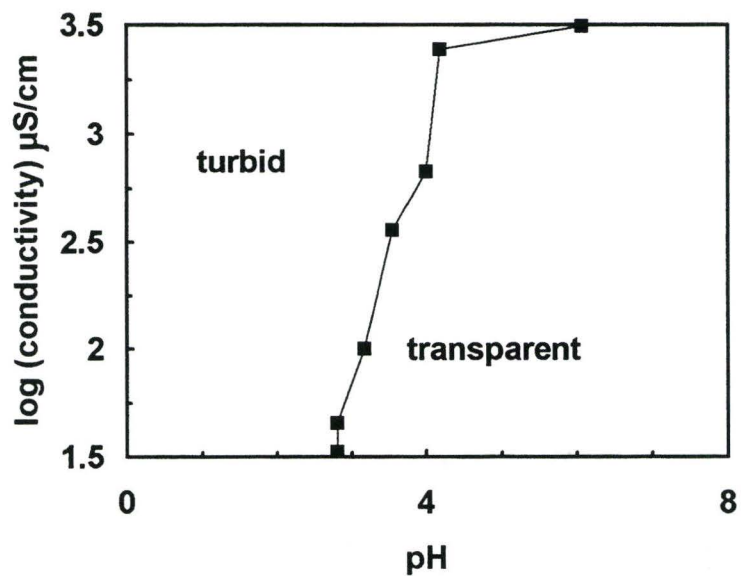


Figure 3 Influence of pH and NaCl concentration on the solubility of the phenolic resin C-271

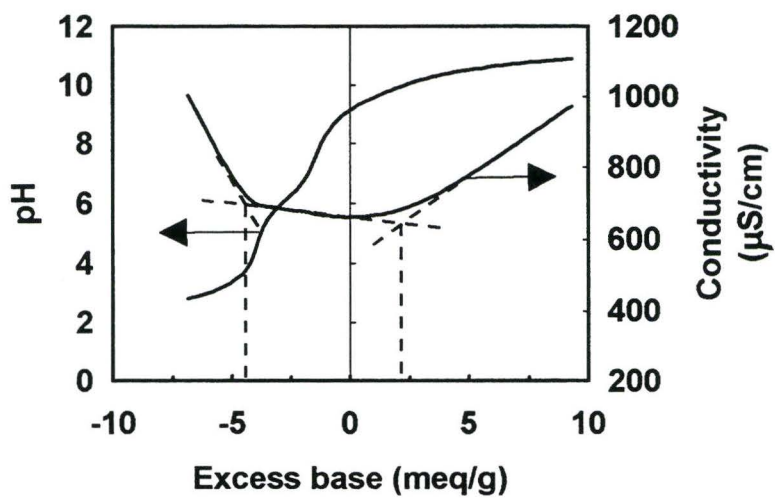


Figure 4 Potentiometric titration of phenolic resins C-271. Concentration of C-271 was 0.476 g/L. Total volume 120 mL.

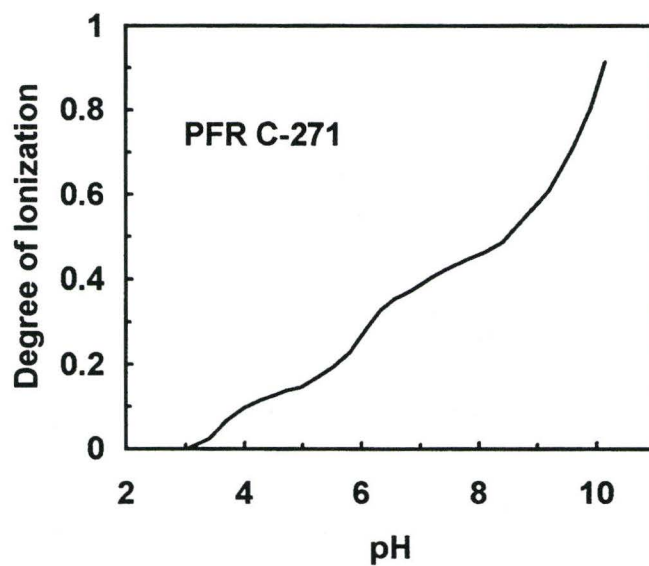


Figure 5 Degree of ionization of PFR C-271 verse pH from the potentiometric titration.

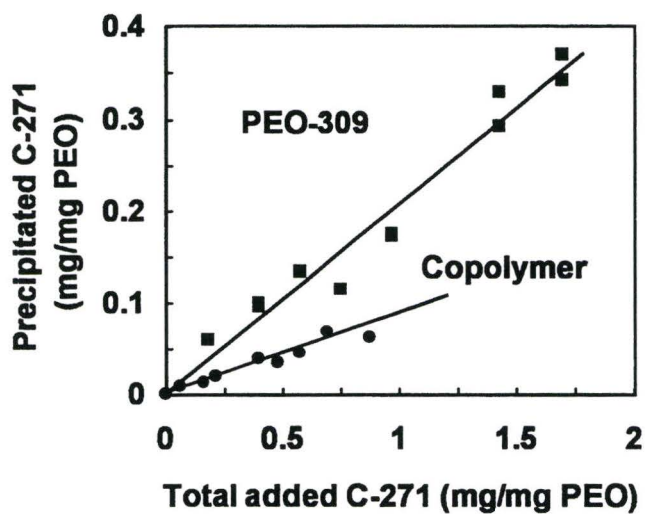


Figure 6 Phenolic resins precipitate isotherm in PEO-309 and copolymer (56-107) solution. PEO-309 concentration = 230 mg/L; copolymer concentration = 249 mg/L. Initial pH = 5, [NaCl] = 10^{-3} M.

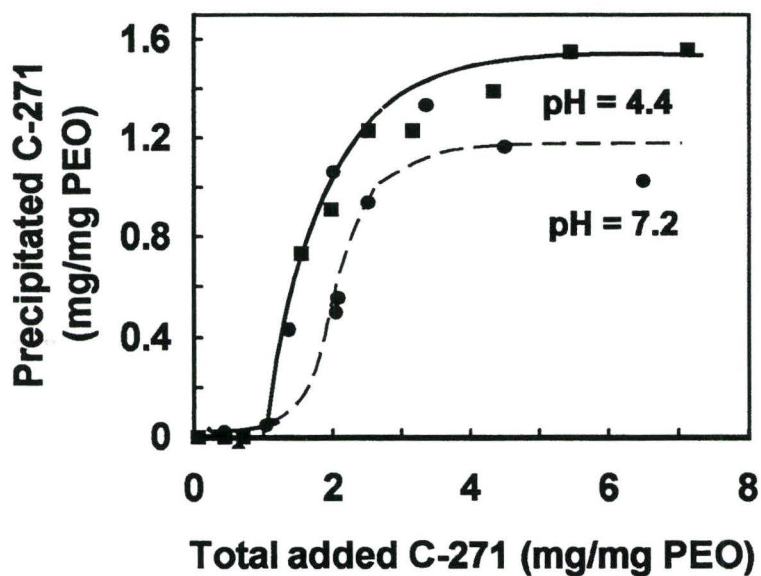


Figure 7 Initial pH effects on the precipitated amounts of PFR C-271 on PEO-309. Measurement conditions: ■ initial pH = 4.4; [PEO-309] = 71.9 mg/L; ● initial pH = 7.2, [PEO-309] = 74.7 mg/L. [NaCl] = 10^{-3} M for both cases.

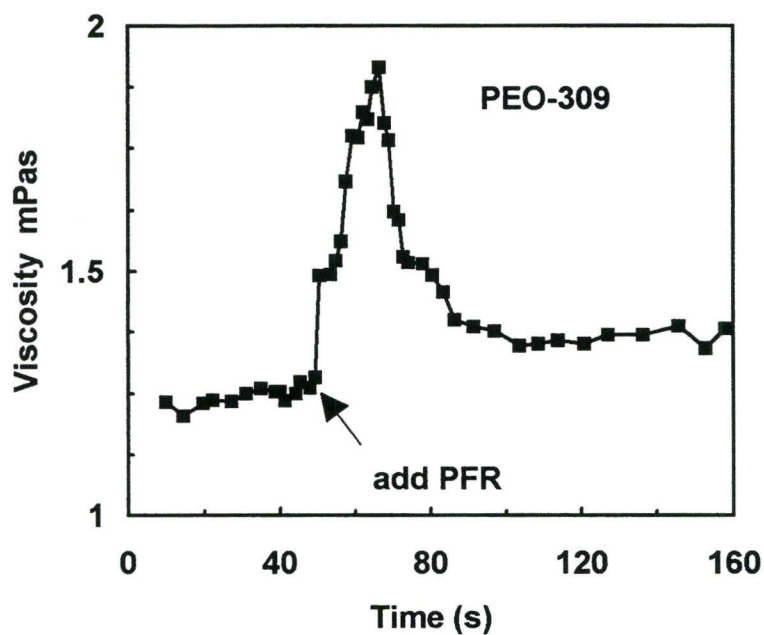


Figure 8 The viscosity behavior during interpolymer associations between PEO and phenolic resin C-271. Experimental conditions: PEO-309 conc. = 60 mg/L; [C-271] = 60 mg/L; pH ~ 5.0; temperature = $23 \pm 0.1^\circ\text{C}$; shear rate = 146 sec^{-1} ; and, constant shear strain. Adding PFR at time = 30 seconds.

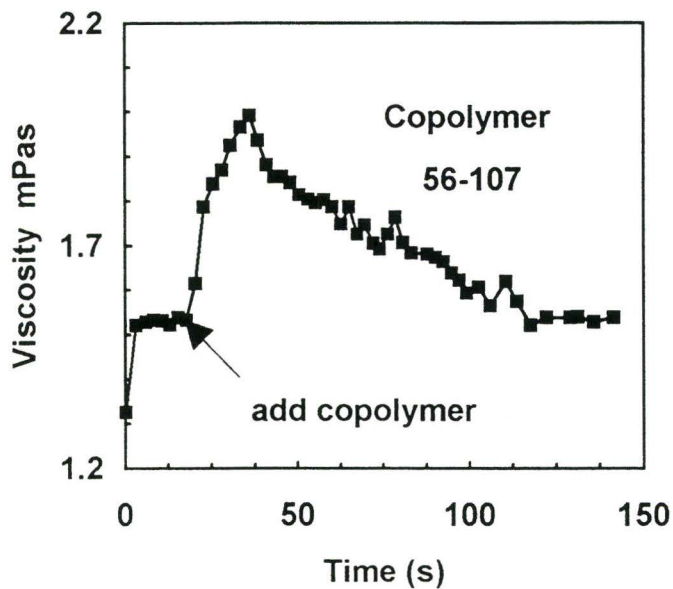


Figure 9 The viscosity behavior during interpolymer associations between copolymer and phenolic resin C-271. Experimental conditions: copolymer conc. = 60 mg/L; [C-271] = 60 mg/L; pH ~ 5.0; temperature = $23 \pm 0.1^\circ\text{C}$; shear rate = 146 sec^{-1} ; and, constant shear strain. Adding copolymer at time = 20 seconds.

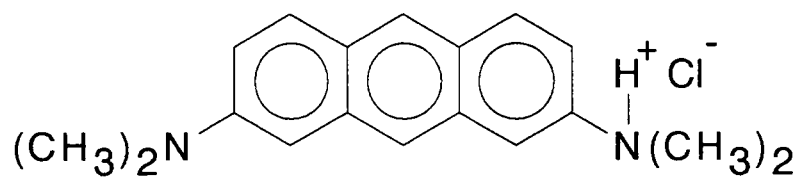


Figure 10 Chemical structure of Acridine Orange

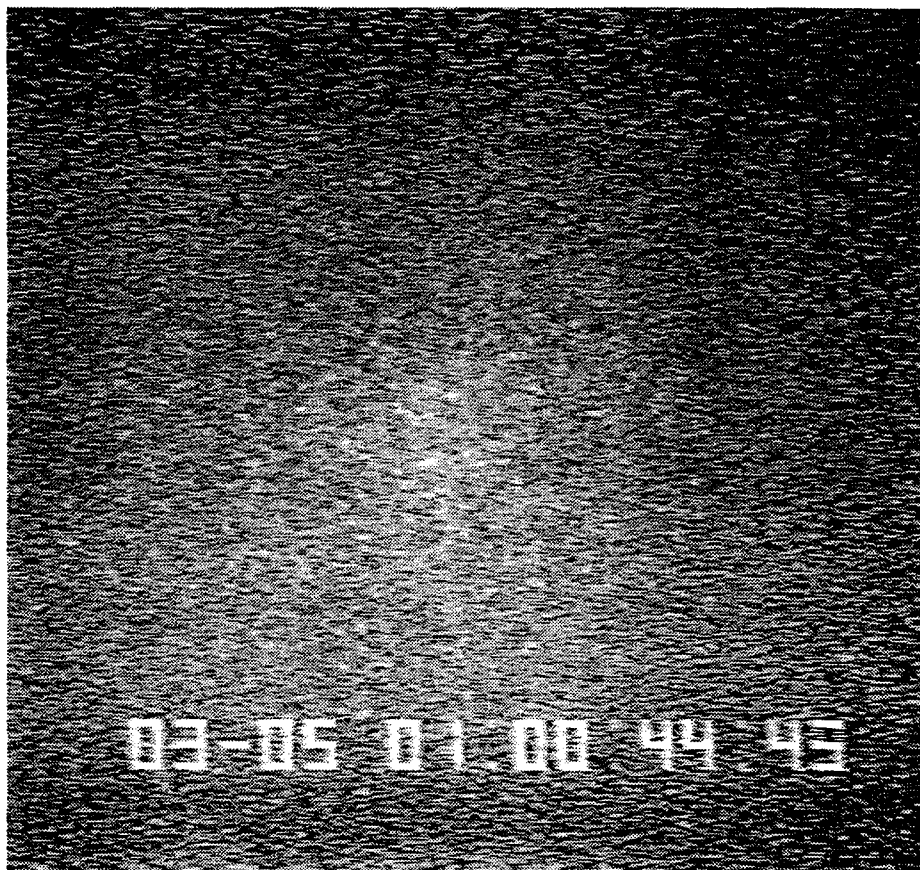


Figure 11 Fluorescent microscopic observation on the mixture of Acridine Orange and PFR C-271; [Acridine Orange] = 30 mg/L; [PFR] = 275 mg/L.

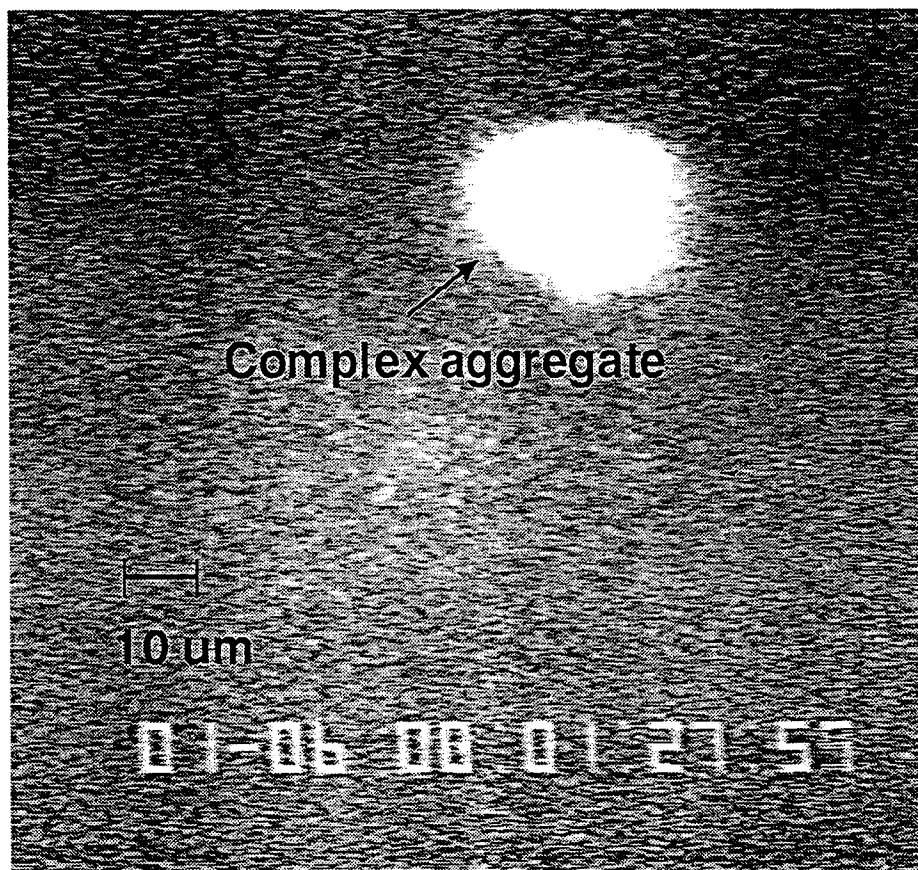


Figure 12 Fluorescent microscopic observation on the mixture of Acridine Orange and PFR C-271 with PEO-309; [Acridine Orange] = 30 mg/L; [PFR] = 275 mg/L; [PEO] = 230 mg/L. Luminescent polymer complex aggregates were formed in this case.

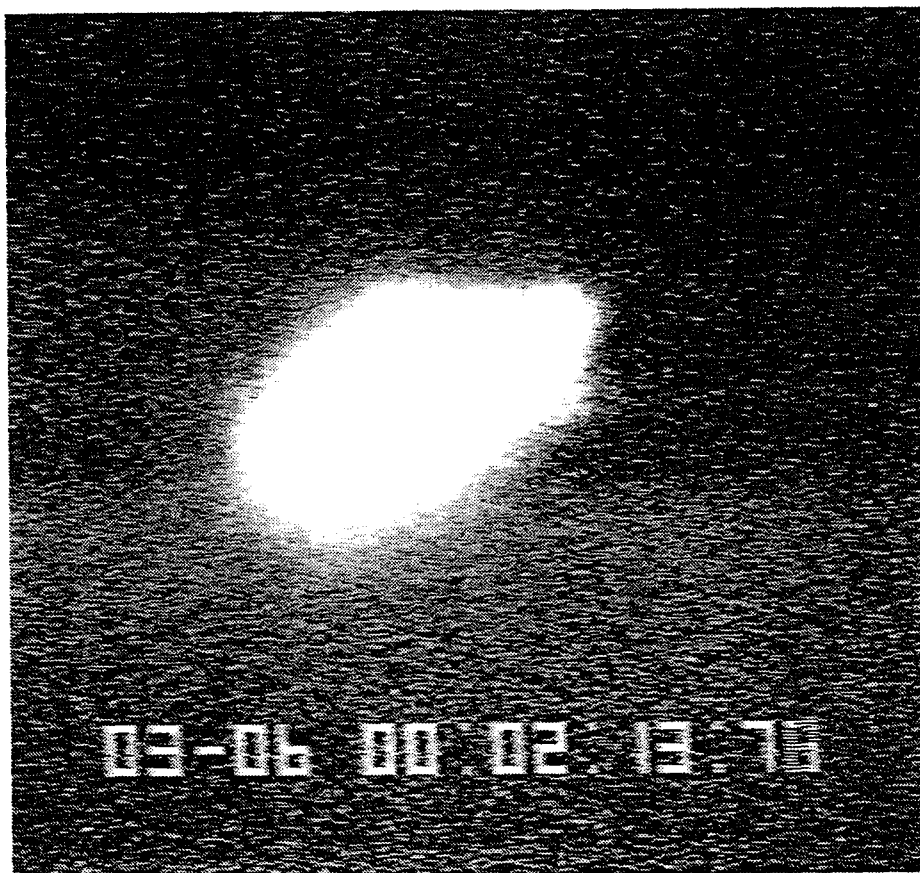


Figure 13 Fluorescent microscopic observation on the mixture of Acridine Orange and PFR C-271 with copolymer 56-107; [Acridine Orange] = 30 mg/L; [PFR] = 275 mg/L; [copolymer] = 490 mg/L. Luminescent aggregates were formed in this case. Copolymer 56-107 containing 1.7 % (mol) of PEG macromonomers with average PEG chain length of 23 repeat units.

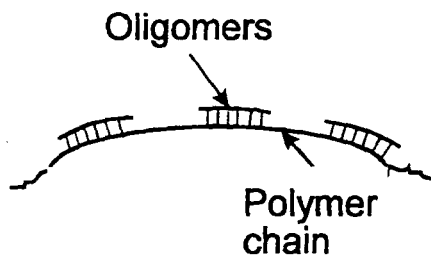


Figure 14 A schematic of flattening complex configuration in an oligomer/polymer system

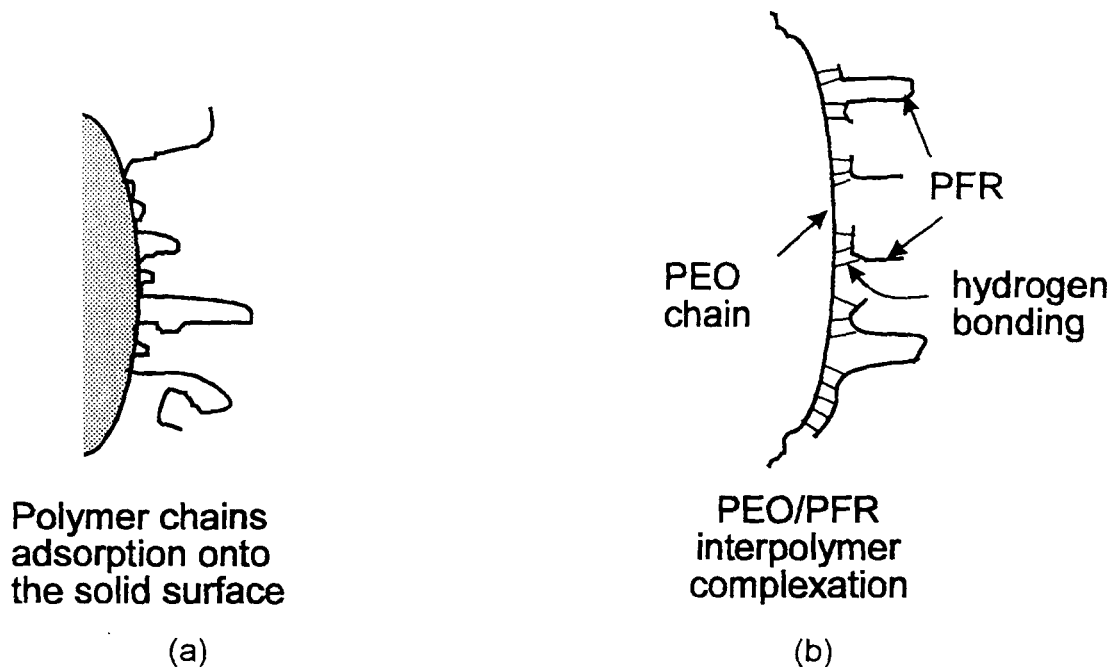


Figure 15 An analogy between the polymer adsorption on the solid surface and an oligomer/polymer complexation system

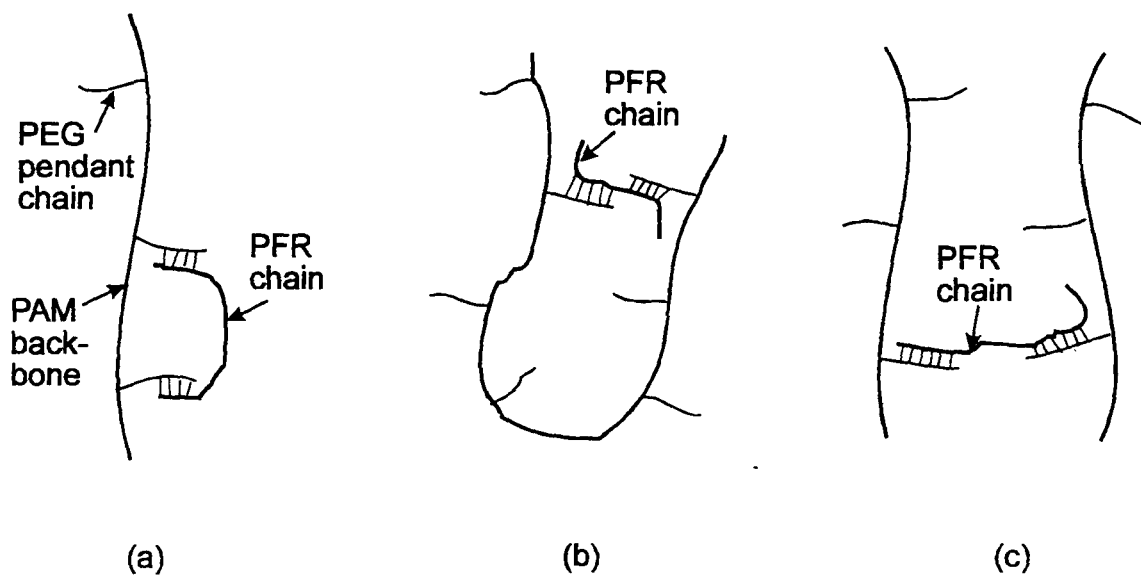


Figure 16 A schematic of the complexation between PAM-co-PEG copolymer and PFR

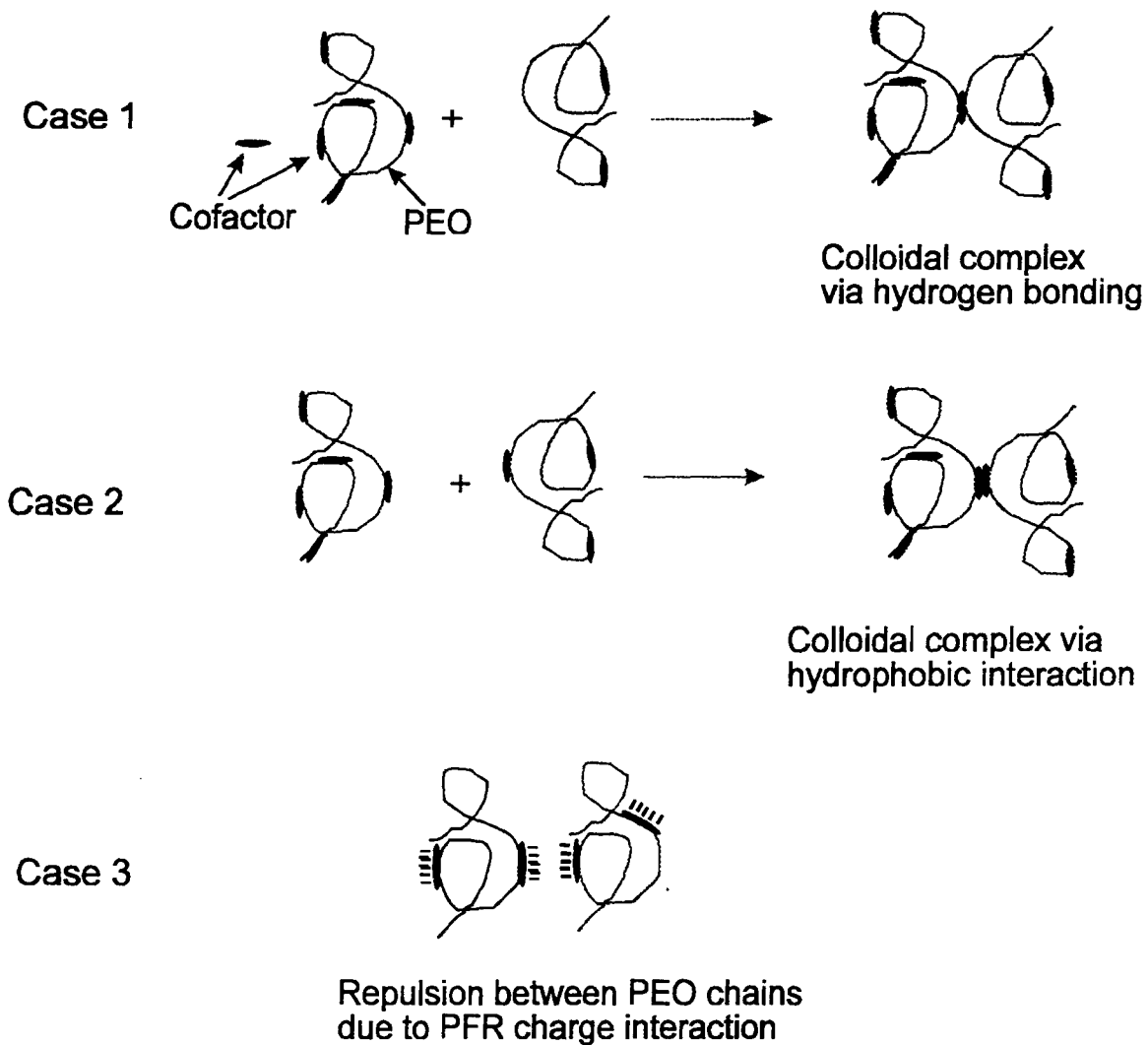


Figure 17 Complex associations induced by uncharged cofactor and charged cofactor in PEO/cofactor system

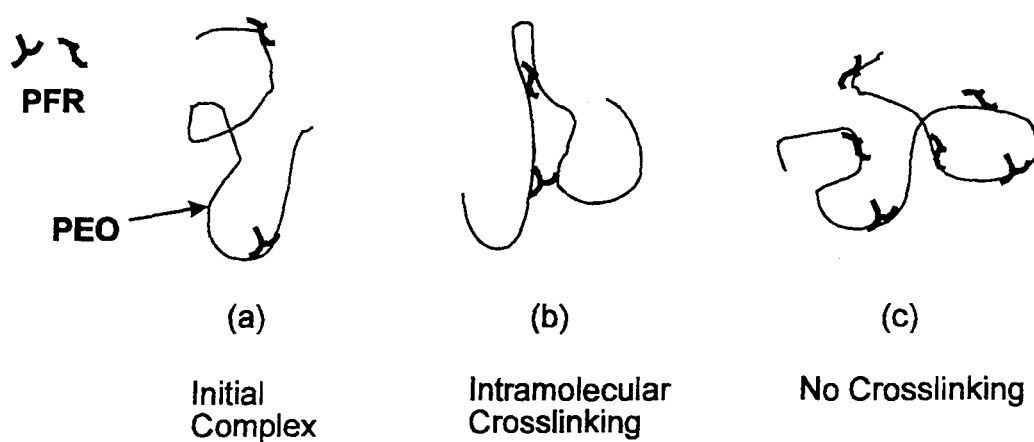


Figure 18 A schematic of the complexation between PFR and PEO in three situations

CHAPTER 3

Flocculation of Polystyrene Latex by Polyacrylamide-co-poly(ethylene glycol)

ABSTRACT

Comb copolymers with long polyacrylamide (PAM) backbones and short poly(ethylene glycol) (PEG) pendant chains were used to flocculate aqueous latex in conjunction with a phenol-formaldehyde resin (PFR). Flocculation efficiency was determined as a function of molecular weight (MW), PEG content and PEG pendant chain length. The results indicated that high copolymer MW was crucial. More than 70 % of polystyrene latex particles in latex-fiber suspensions were flocculated by copolymer with MW higher than 3 million. Moreover, only 0.3 to 0.8 % (mole) of macromonomers were required to be incorporated in the high MW copolymers. The minimum PEG pendant chain length for successful removal of the latex was as low as 9 ether repeat units. An empirical equation to relate the flocculation efficiency and the copolymer structures has been derived.

The copolymers exhibited similar flocculation performance to poly(ethylene oxide) (PEO) (molecular weight > 4 million). However, the copolymers did not exhibit the loss of flocculation ability with aging time.

KEYWORDS: comb copolymer; flocculation; PEG macromonomer; PEO; latex.

Introduction

Poly(ethylene oxide) (PEO), a water-soluble nonionic polymer, is widely used in waste water treatment, mineral processing and papermaking.^{1,2,3} In the manufacture of the newsprint paper, PEO is used as a flocculant or "retention aid".⁴ The advantage of using PEO is that the flocculation performance is not affected by the presence of wood based dissolved and colloidal substance (DCS) which bear anionic surface charges.⁵ By contrast, DCS causes the excess consumption of conventional cationic flocculants.

In many uses PEO flocculants require the presence of a cofactor, such as phenolic resin, tannic acid or kraft lignin. All effective cofactors have phenolic groups which can form hydrogen bonds with PEO. The nature of the complexation and the flocculation mechanism are discussed elsewhere.^{6,7}

The molecular weight (MW) of PEO is important. Only PEO with MW higher than 4 million gave significantly improved flocculation. However, very high molecular weight PEO is expensive and susceptible to degradation which lowers the molecular weight and thus the flocculation efficiency. PEO is particularly susceptible to degradation when in aqueous solution. The degradation can be caused by either shear forces or oxidation. Thus, in commercial applications, PEO solution must be freshly prepared and carefully handled.

In order to overcome the fragile properties of PEO, a series of the novel comb copolymers with long polyacrylamide (PAM) backbones and short poly(ethylene glycol) (PEG) pendant chains have been developed in our work. The chemical structure of the copolymer is presented in Figure 1. Details of the copolymer synthesis and characterization have been described elsewhere.⁸

The objective of this work was to correlate the flocculation performance to the structures of the copolymers. The following three structural factors were investigated: 1) the density of PEG pendant chains on the PAM backbone; 2) the PEG pendant chain length; and, 3) the backbone chain length. An empirical equation describing the relationship between flocculation and the three structural parameters was derived. Aging resistance of the copolymers was compared with the resistance of high MW PEO.

The flocculation system used in this work was a mixture of polystyrene latex (PSL), phenol-formaldehyde resin (PFR) and bleached kraft pulp fibers. PEO homopolymers, Polyox 301 and Polyox 309, were benchmarks for evaluating the performance of copolymers.

3.1 Experimental

3.1.1 Materials

The copolymers were synthesized by copolymerization of acrylamide (AM) and PEG macromonomers which are low molecular weight PEG esters of (meth)acrylic acid. Two series of macromonomers based on poly(ethylene glycol) were used in this work. Methoxy poly(ethyleneoxy) ethyl acrylate was supplied by Monomer-Polymer, Inc. Methoxy poly(ethylene glycol) methacrylate was supplied by Polysciences, Inc. The structures of macromonomers are shown in Figure 2. The acrylate based ($R = H$ in Figure 2) macromonomers are designated herein as A-n, where n is the average degree of polymerization or pendant chain length of PEG. The average pendant chain lengths of PEG in the A-n samples were 10, 20 and 40. Similarly, MA-n is used to denote the

methacrylate based ($R = \text{CH}_3$ in Figure 2) macromonomer. The corresponding n values for the average degree of polymerization of PEG in MA- n were 5, 9 and 23.

Copolymerizations were conducted in aqueous solution at 25°C or 40°C. Details of the polymerization have been given elsewhere.⁸ and Table 1 summarizes the properties of the copolymers used in this work.

PEO-301 (Polyox 301) with MW of 4 million and PEO-309 (Polyox 309) with MW of 8 million were obtained from Union Carbide Corporation. Phenol formaldehyde resin (PFR), Cascophen C271, (40 % in aqueous solution) was supplied by Borden Chemical.

The polystyrene latex (PSL) particles were synthesized in this work by the surfactant-free emulsion polymerization, using the method described by Goodwin et al.⁹ The recipe consisted of: styrene 73 g, potassium persulfate 0.53 g and deionized and distilled water 670 g. The polymerization was carried out at 70°C for 12 hours. The particle size of polystyrene latex was measured using a BI-DCP (Disc Centrifuge Photosedimentometer) Particle Sizer (Brookhaven Instrument Co.). The results are given in Table 2.

The cellulose fiber used in PSL flocculation experiments was bleached softwood kraft pulp supplied by Noranda Forest Co. The pulp stock was prepared by blending the bleached fibers with distilled water in a Commercial Blender (Waring Products). The consistency of the pulp was approximately 1.0 % (wt).

3.1.2 Flocculation of polystyrene latex particles by dual-polymer

Flocculation of PSL particles was induced by sequential addition of small quantities (1.0 - 4.0 mg/L) of copolymer or PEG and phenolic resin, in the

presence of the bleached fibers. For a flocculation experiment, the 35 mL Milli-Q treated distilled water, 5 mL bleached fiber pulp of 1.0 % consistency, and 1 mL 0.25 %(wt.) PS latex were added to a 50 mL test tube. pH of the solution was adjusted to approximately 5 by adding 0.1 mL 0.02 N HCl. To maintain the electrolyte at a concentration of 2.0×10^{-3} M, 0.1 mL of 1 N NaCl was added . Then 0.4 mL 0.25 % (wt.) phenolic resin was added to give a concentration of 2.0 mg/L. The transmittance for the control was measured by using HP 8452A UV Spectrophotometer (Hewlett-Packard) at a wavelength of 500 nm. Finally, copolymer or PEO aqueous solution at 0.025 - 0.05 % concentration was added to give a total volume of 50 mL. The samples were vigorously shaken by hand for 3 to 5 seconds and suspended solids were allowed to settle for 1 hour at room temperature. The supernatant was decanted and filtered through a 200 mesh screen to remove suspended fiber fragments. The extent of latex removal by flocculation and sedimentation was determined by the relative turbidity, τ_R , calculated from the following expression:

$$\tau_R = \log(100/T_c/100/T_s)$$

where T_c and T_s were the percent transmittances of the control and the supernatant after flocculation, respectively. The lower relative turbidity indicates that more latex particles are removed.

3.2 Results

3.2.1 Effect of polymer concentration on flocculation

The influence of the concentration of the copolymers or PEO on the latex flocculation was investigated at a fixed concentration of phenolic resin (2.0 mg/L). Figure 3 shows the relative turbidity of the latex as a function of concentration of two commercial PEO homopolymers. Relative turbidity is a measure of the concentration of unflocculated latex; lower relative turbidity indicates better flocculation. Both PEO-301 and PEO-309 had an optimum concentration of 2 mg/L which allowed the lowest relative turbidity or maximum removal of the latex. At PEO concentrations lower than 2 mg/L, the relative turbidities of the latex decreased as PEO concentrations were increased. At PEO concentrations in excess of 2 mg/L, the relative turbidity of the latex increased as PEO concentrations were further increased. The optimum weight ratio of PEO/phenolic resin was found to be 1:1 which agrees with that obtained by Lindstrom et al¹⁰.

Figure 4 shows the relative turbidity of the latex as a function of copolymer concentration. Compositions of the copolymers are given in the Figure caption. Copolymer concentrations yielding the minimum relative turbidity values were between 2 and 4 mg/L. Higher copolymer concentration caused flocculation to deteriorate. The dependence of latex flocculation on copolymer concentration was similar to PEO, i.e., the relative turbidity showed a minimum where flocculant concentration was varied. One exception was 23-144. The removal of latex was increased with polymer concentration up to 8 mg/L, the highest studied.

The lowest optimum dosage and the best flocculation result in Figure 4 corresponded to the highest MW samples. By contrast, the PEO data in Figure 3 did not show a MW dependence on optimum polymer dosage.

3.2.2 Effect of composition of copolymers on latex flocculation

The density of PEG pendant chains on the comb copolymer backbone has influence on the flocculation efficiency as shown in Figure 5. Two series of data represent the results from two series of copolymers which were polymerized at 25 and 40°C. Previous work has shown that the copolymer molecular weight was sensitive to polymerization temperature. The two continuous lines were from an empirical equation which will be discussed later.

A minimum relative turbidity was observed for the copolymers that were prepared at 40°C (diamonds in Figure 5). By contrast, the higher molecular weight series, prepared at 25°C, showed no minimum in the flocculation experiments. Comparison of the two datasets shows that less amount of macromonomer was required for the copolymer synthesized at lower temperature. For example, in order to have 65 % of PS latex flocculated, 0.8 % (mole) of MA-23 was necessary for copolymers prepared at 40°C, while only 0.3 % (mole) of MA-23 was required for copolymers prepared at 25°C.

The scatter in the experimental data points, in particular for the copolymers prepared at 40°C, was attributed to the difficulty in preparing a series of copolymers of varying compositions but constant MW. It was reported that the chain transfer to PEG macromonomers occurred during polymerization.¹¹ As a result, the copolymer MW may be decreased as the macromonomer contents increased which in turn lowers flocculation efficiency.

No latex flocculation was observed for the PFR/PAM homopolymer with a MW of 5 million. The result confirmed the significant role of the PEG pendant chains in copolymers.

3.2.3 Effect of PEG pendant chain lengths on flocculation

The relationships between latex flocculation and PEG chain lengths in copolymers were investigated using a series of copolymers containing about 0.9 % (mole) macromonomer with PEG chain lengths from 5 to 40 repeat units. The results are summarized in Figure 6 where the two sets of data represent polymerizations carried out at 25°C and 40°C. The efficiency of flocculation increased with the PEG pendant chain lengths. The higher molecular weight series, prepared at 25°C, gave the best flocculation.

3.2.4 Effect of molecular weight of copolymers on flocculation

The effects of molecular weights of copolymers and PEO on latex flocculation are summarized in Table 3. It was extremely difficult to vary the total copolymer chain lengths at constant composition so the macromonomer contents are also given in Table 3. Latex flocculation by copolymers in this system significantly increased with molecular weight. For example, in comparing copolymer 56-48 with 43-36, the former has the higher MW whereas the latter has the higher macromonomer content. The higher MW copolymer, 56-48, gave the best flocculation.

3.2.5 Aging resistance of the copolymers in aqueous solution

One impetus for this work was to develop flocculants with improved stability toward decomposition upon aging. Figure 7 shows relative turbidity of the flocculated latex versus flocculant aging time. Both PEO homopolymers

showed severe degradation between 3 and 10 days with almost complete loss of efficiency after 20 days. By contrast, the copolymer showed no loss in efficiency over the same time period.

Another interesting phenomenon was that the copolymer 43-129 sample gave excellent flocculation (relative turbidity = 0.33, as shown in Table 4) after it had been stored at 1.0°C for over 6 months. Further aging data are given in Table 4. The aging properties of copolymers did not show significant dependence on their structures. Flocculation performance of the MA-n copolymer series was similar to that of the A-n series.

3.3 Discussion

3.3.1 Copolymer structure and flocculation performance

Synthetic polymers such as polyethyleneimine, cationic polyacrylamide, and anionic polyacrylamide are used routinely as retention aids in paper industry.¹² Comb copolymers prepared in this work, in conjunction with phenolic resins consisting of a nonionic dual-polymer system, are potentially a new class of flocculants.

The copolymer/PFR system maintained the advantage of PEO/PFR system in providing effective flocculation for colloidal particles in the presence of DCS. The flocculation results indicated that the amounts of the latex removal induced by most of copolymer samples with high MW (> 3 million) were higher than those by the PEO-301 and close to PEO-309.

There are two potential advantages from using the copolymers instead of PEO homopolymers. First, the copolymer produced more robust polymer

backbones which improved the its aging resistance in aqueous solution as well as shear resistance. Second, the copolymers were acrylamide-based and hence are possibly less expensive to manufacture than very high MW PEO. Furthermore, PAM polymerizations are carried out by many companies. Thus, the comb copolymer preparations can be easily incorporated in existing production facilities. By contrast, PEO is relatively expensive because extremely high MW of PEO is a low volume specialty chemical.

To achieve the most effective copolymer, three important factors regarding the copolymer structure have been investigated. These were: 1) MW of copolymers; 2) PEG pendant chain length (i.e. n in Figure 1); and, 3) macromonomer mole % content or density of PEG pendant chains (i.e. y in Figure 1). The three factors interacted with each other and determined the performance of the copolymers as flocculants.

Key observations from the experiments in this work included:

- 1) Latex flocculation was very sensitive to copolymer MW. To obtain an effective flocculation, the copolymer MW must be higher than 3 million. No significant improvement in latex flocculation was observed for the lower MW (< 1 million) samples.
- 2) Excellent latex flocculation was observed even when PEG pendant chain lengths were as short as 9 repeat units. Longer pendant chain lengths gave better flocculation; however, the long PEG chains were less cost effective at the same pendant chain density.
- 3) Only 0.3 to 0.8 mole % macromonomers were required in copolymer compositions to induce effective latex flocculation, whereas without any PEG

pendant chains (i.e. PAM homopolymer), no latex flocculation was induced even with a PAM MW as high as 5 million.

The experimental turbidity data for both acrylate and methacrylate based copolymers were fitted to the following empirical equation:

$$\tau_R = 0.078C^{-0.48} + 0.005C + 0.156(n/10)^{-0.65} + 0.006(n/10) + 0.19(M/X)^{-0.91}$$

where τ_R is the relative turbidity; C is the mole % of macromonomer in the copolymers, ranging from 0.1 % to 4.0 %; n is the number of repeat units of PEG pendant chain in the macromonomers, ranging from 1 to 40; and M is molecular weight of the copolymers, ranging between 0.1 to 8 million; and X is a scaling parameter equal to 1×10^6 Dalton. The predicted relative turbidity curves versus the compositions of the copolymers and PEG pendant chain lengths are shown as solid lines in Figures 5 and 6. The correlation coefficient for the predicted and observed data was 0.96. The equation is not valid when the C , n and M values are out of the ranges mentioned above.

In summary, the flocculation efficiencies of PS latex induced by the PFR/copolymers can be calculated from parameters of the copolymers: MW, pendant chain length and composition.

3.3.2 Mechanistic implications

Studies on the flocculation mechanism of PEO/PFR or PAM-co-PEG copolymer/PFR have shown that complex formation between PEO and PFR is necessary for flocculation.⁶ It is widely accepted that the origin of complex formation is hydrogen bonding between phenolic hydroxyls on PFR and polyether oxygens on PEO. The same interaction is believed to occur between phenolic hydroxyl groups on PFR and the short pendant PEG chains on the

copolymer. The phenomena associated with complexation in the PEO/PFR system, such as transient viscosity increase and complex precipitation, have been observed with the copolymers; these are described elsewhere.⁷ A possible structure of the complex between the PEG in the copolymer and PFR is given in Figure 8.

An interesting observation was that ungrafted short PEG chains did not form complexes with PFR whereas PEG chains of the same length that are bound to a PAM backbone (i.e. the copolymer) formed complexes. This possibly arises from the fact that simultaneous interactions of many short PEG chains on the same polymer backbone with a PFR molecule increased the number of sites available for association.

There are three extreme topologies possible for the PFR/copolymer complexes: 1) PFR bound to neighboring PEG chains on the PAM backbone; 2) PFR bound to non-adjacent pendant PEG chains; and, 3) PFR bound to PEG chains on different copolymer molecules. These are illustrated in Figure 9.

The effective copolymers in latex flocculation usually contained about 1 % (mole) of PEG pendant chains. Thus, on average, two pendant PEG chains were separated by about 100 PAM repeat units. If the copolymer chains were fully extended, case 1 would seldom occur because the PFR chain length was about 100 phenolic repeat units. However, a more realistic configuration of the copolymer would be a coil which could lead to case 2. Intrapolymer crosslinking was produced in case 2 whereas interpolymer crosslinking occurred in case 3.

The minimum PEG pendant chain length in the copolymer for the effective latex flocculation was 9 ether repeat units. This implies that a minimum of 5

hydrogen bonds in a PEG are required to form interpolymer association based on the hydrogen bonding structure described in Figure 8.

Latex flocculation induced by copolymer/PFR is a consequence of complexation. The flocculation mechanism called complex bridging has been presented elsewhere.⁶ The key point in this mechanism was that the high MW PEO or copolymer molecules aggregated in the presence of a cofactor (e.g. PFR) to form colloiddally dispersed polymer complexes which heteroflocculated with the latex particles. Complex bridging mechanism successfully interpreted most of the experimental observations with the exception of the requirement for extremely high MW for good flocculation.

The high MW dependence in conventional bridging flocculation is because the adsorbed bridging polymer must extend beyond the effective distance of electrostatic repulsion in order to adsorb onto a second particle. However, this is difficult to visualize for a dual-polymer system because the complex formation between copolymer and PFR can give multilayer adsorption on the latex surface. This multilayer can extend beyond the electrostatic repulsion distance.

A possible explanation for the MW effects involves the dynamics of the complex collapse.⁶ Mixing of aqueous copolymer with PFR results in the formation of a precipitate. Latex flocculation must occur before the dual polymer complex collapses into a precipitate. However, the rate of complex collapse should be MW dependent. The origin of the molecular weight dependence in complex collapse may be that extremely high MW chains take longer to fold back upon themselves to give a precipitate. Also, it may be more difficult for the

small PFR chains to reach the center of very high molecular weight copolymer or PEO coils.

3.3.3 Aging resistance

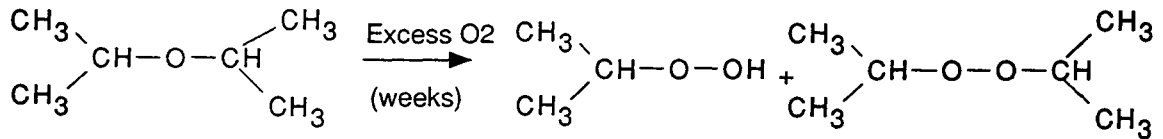
The ability of high MW PEO to flocculate colloids decreased with PEO aging time. Other studies have shown that the viscosity of PEO solution decreases with aging.¹³ This can be explained by either the slow untangling of PEO chains or the degradation of PEO into lower molecular weight fragments.

The slow untangling of PEO was described by Polverari and van de Ven.¹⁴ They used dynamic light scattering to monitor the PEO size change during storage and found that PEO clusters were formed in aqueous solution. It was proposed that the non-aggregated PEO adsorbed preferentially onto the latex surfaces whereas the PEO clusters did not. However, the PEO molecular weights in their work ranged between 100,000 and 555,000 which were much lower than those of PEO used in this work.

Many studies dealing with the mechanism of degradation of PEO induced by temperature, oxidation and radiation have been published.^{15,16} It has been found that trace amounts of metal ions¹⁷ and peroxides could generate hydroxyl radicals which further attack polymer chains in aqueous solution. Therefore, extreme caution with contamination from metal ions and impurities must be taken in preparing PEO solutions.

Polymer chain oxidation occurring in aqueous solution might be the main reason for the degradation of PEO in storage. The peroxide group -C-O-O-C- results from the original -C-C-O- backbone due to autoxidation which is the free-radical chain oxidation of organic molecules by oxygen. This has been demonstrated in low molecular weight ethers. For instant, the peroxide formed

from diethyl ether and tetrahydrofuran under the autoxidation.¹⁸ The autoxidation of diisopropylane ether¹⁹ is given in the following as an example:



The improved aging resistance of PAM-co-PEG copolymers can be attributed to the -C-C- backbones which are less sensitive to the autoxidation than polyether backbones. Because of this, the stable copolymer backbone (i.e. total polymer chain length) would maintain the flocculation efficiency as expected.

Conclusions

The main conclusions obtained from this work are:

1. Copolymers prepared from the copolymerization of PEG-macromonomer and acrylamide in conjunction with phenol formaldehyde resin provided a promising novel dual-polymer system for colloidal particle flocculation.
2. Only copolymers with a molecular weight greater than 3 million gave good flocculation.
3. Good flocculation was observed with copolymers containing 0.5 to 1.0 mole % macromonomer.
4. Flocculation was observed with copolymers having PEG pendant chain lengths as low as 9. An optimal PEG chain length appeared to be 23.
5. In contrast to PEO, the copolymer showed no decrease in flocculation ability with aging time.

References

- ¹ Molyneux, P., "Water-Soluble Synthetic Polymers: Properties and Behavior" , Vols, I and II, CRC Press, Boca Raton, FL 1984.
- ² Dickinson, E. and Eriksson, L., *Adv. Colloid Interface Sci.*, **34**, 1(1991).
- ³ Pelton, R.H., Allen, L.H. and Nugent, H.M., *Tappi*, **63**(11), 89(1981).
- ⁴ Pelton, R.H., Allen, L.H. and Nugent, H.M., *Svensk Papperstidning*, **9**, 251(1980).
- ⁵ Pelton, R.H., Allen, L.H. and Nugent, H.M., *Pulp and Paper Canada*, **81**(1), 54(1980).
- ⁶ Xiao, H.N., Chapter 4, Ph.D. Thesis, McMaster University, 1994.
- ⁷ Xiao, H.N., Chapter 2, Ph.D. Thesis, McMaster University, 1994.
- ⁸ Xiao, H.N., Chapter 1, Ph.D. Thesis, McMaster University, 1994.
- ⁹ Goodwin, J.W., Hearn, J., Ho, C.C. and Ottewill, R.H., *Colloid Polym. Sci.*, **252**, 464(1974).
- ¹⁰ Lindstrom, T. and Glad-Nordmark, G., *J. Colloid Interface Sci.*, **97**, 62(1984).
- ¹¹ Schulz, D.N., Kaladas, J.J., Maurer, J.J., Bock, J., Pace, S.J. and Schulz, W.W., *Polymer*, **28**, 2110(1987).
- ¹² Horn, D. and Linhart, F., "Paper Chemistry," Ed by Roberts, J.C., Blackie, Glasgow and London, 1991.
- ¹³ McGary, C.W., *J. of Polymer Sci.*, **46**, 51(1960).
- ¹⁴ Polverari, M. and van de Ven, T.G.M., "Dynamic light scattering of suspensions of PEO coated polystyrene latex"., 67th Colloid and Surface Sci. Sympo., University of Toronto, June 21-23, 1993.
- ¹⁵ Crouzet, C. and Marchal, J., *Makromol. Chem.*, **166**, 99(1973).
- ¹⁶ Decker, C. and Marchal, J., *Makromol. Chem.*, **166**, 155(1973).
- ¹⁷ Ramsden, D.K. and McKay, K., *Polymer Degradation and Stability*, **14**, 217(1986).
- ¹⁸ Carey, F.A. and Sundberg, R.J., "Advanced Organic Chemistry," p.694, 3rd. Ed., Plenum Press, New York and London, 1991.
- ¹⁹ Wade, L.G., "Organic Chemistry," p.509, Prentice-Hall, New Jersey, 1987.

Tables

Table 1. Summary of the properties of the copolymers in this work. Syntheses and characterizations have been described elsewhere⁸

# of Samples	Type of (M)A-n	MW x 10 ⁻⁶ of copolymer	(M)A-n %(mol) in copolymers
43-131	A-40	0.42	0.38
23-144	A-40	0.76	0.56
43-95	MA-23	1.1	1.18
56-121	MA-23	2.8	2.40
43-176	MA-23	4.3	0.41
43-36	MA-23	1.2	0.85
56-110	MA-23	3.7	1.40
56-48	MA-23	4.5	0.47
43-149	MA-23	5.1	0.14
43-129	MA-23	3.7	0.65
43-55	MA-23	3.4	0.23
56-113	A-10	2.1	0.70
43-22	A-10	0.63	1.10
56-108	MA-9	4.6	0.69
43-134	MA-9	0.9	0.70
43-71	MA-9	0.70	0.41
43-133	MA-5	0.45	0.60
56-49-2	MA-5	3.1	1.51
56-72	MA-1	3.0	2.3

Table 2 Particle Size of Polystyrene Latex(PSL) measured by a BI-DCP(Disc Centrifuge Photosedimentometer) Particle Sizer.

Average	Size (μm)	Std DEV
Number Average	0.629	0.110
Surface Area Average	0.667	0.112
Weight Average	0.685	0.110

Table 3 Influence of copolymer MW on latex flocculation. Two PEO homopolymer samples were given for comparison. PFR concentration was 2.0 mg/L for all samples. The * labeled samples were added at 4.0 mg/L, the remaining samples were added at 2.0 mg/L.

Sample No.	MW of copolymer	Type of macro-monomer	mole % of macro-monomers	Relative Turbidity τ_R
43-36*	1.2×10^6	MA-23	0.85	0.36
43-55	3.4×10^6	MA-23	0.23	0.35
43-129	3.7×10^6	MA-23	0.65	0.29
43-149*	5.1×10^6	MA-23	0.14	0.34
56-48	4.5×10^6	MA-23	0.47	0.27
43-71	7.0×10^5	MA-9	0.41	0.55
56-108*	4.6×10^6	MA-9	0.69	0.25
43-22*	6.3×10^5	A-10	1.10	0.59
PEO-309	8.0×10^6	---	---	0.23
PEO-301	4.0×10^6	---	---	0.37

Table 4 Effect of the polymer storage conditions of on the relative turbidity during the latex flocculation τ_R . The copolymer properties are given in Table 1.

Samples	Type of (M)A-n	Stored conc. %(wt)	Aging Time	Stored Temp(°C)	Initial τ_R	τ_R after aging
56-108	MA-9	0.024	42 days	1 ± 0.2	0.25	0.25
56-110	MA-23	0.024	4 months	1 ± 0.2	0.23	0.47
43-129	MA-23	0.29	6.5 months	1 ± 0.2	0.29	0.33
43-95	MA-23	0.025	20 days	24 ± 2.0	0.37	0.47
56-113	A-10	0.54	24 days	1 ± 0.2	0.28	0.33
43-131	A-40	0.043	3 days	24 ± 2.0	0.61	0.66
43-131	A-40	0.043	9 days	24 ± 2.0	0.61	0.76

Figures

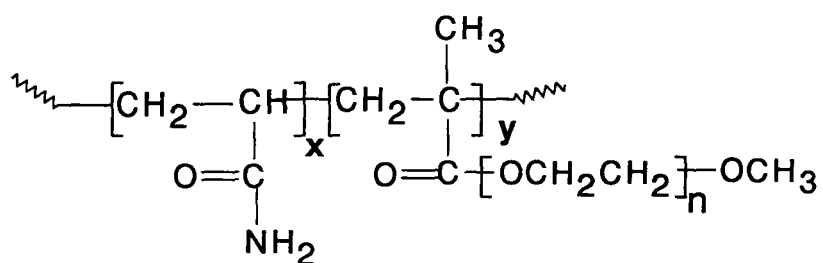
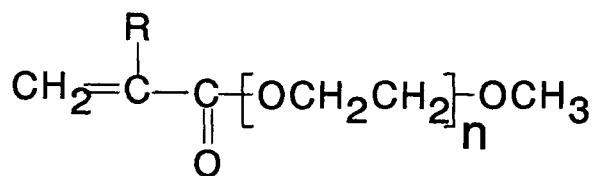


Figure 1. Structure of PAM-co-PEG copolymer



$$n = 5 \text{ to } 40$$

$$R = \text{H or } \text{CH}_3$$

Figure 2 Structure of PEG-macromonomer

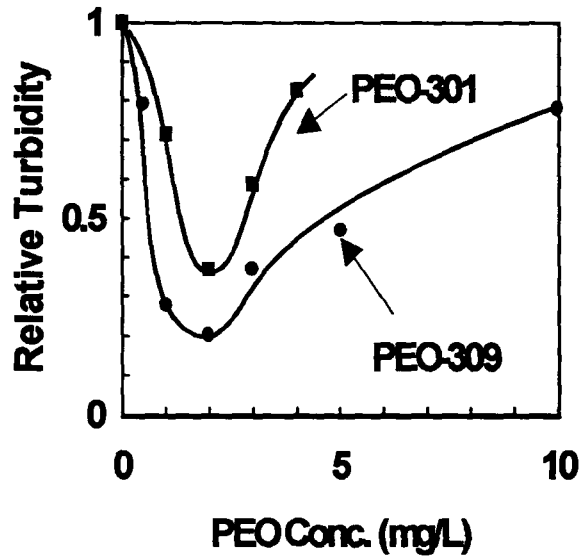


Figure 3 The effect of PEO concentration on latex flocculation at a constant concentration of phenolic resin of 2.0 mg/L. PSL concentration was 50 mg/L and fiber consistency was 1.0 g/L.

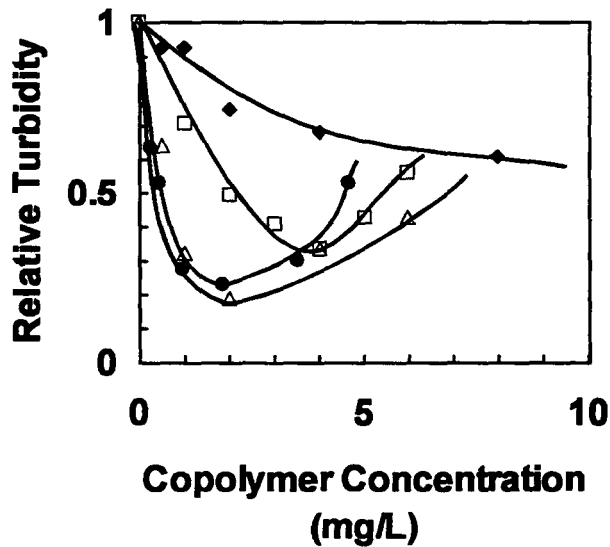


Figure 4 The effect of copolymer concentration on latex flocculation at a constant concentration of phenolic resin of 2.0 mg/L.

- 43-36: Copolymer containing 0.85 %(mole) MA-23 and MW 1.2×10^6
- ◆ 23-144: Copolymer containing 0.56 %(mole) A-40 and MW 7.6×10^5
- △ 56-48: Copolymer containing 0.47 %(mole) A-23 and MW 4.5×10^6
- 56-110: Copolymer containing 1.40 %(mole) A-23 and MW 3.7×10^6

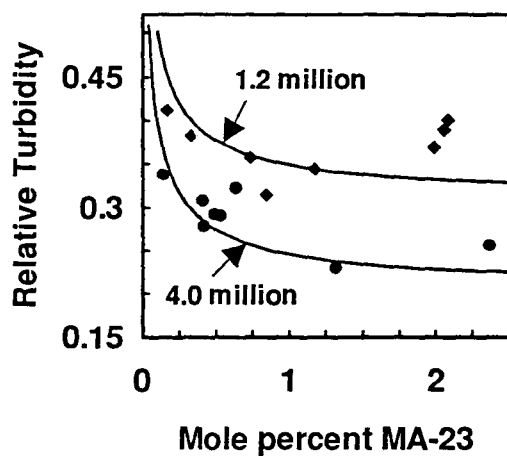


Figure 5 Relative turbidity versus composition of copolymers. Copolymerizations of AM and MA-23 were conducted at 25°C(●) and 40°C(◆). The curves were calculated from the empirical Equation for a pendant chain length of 23 and the molecular weight values shown in the figure.

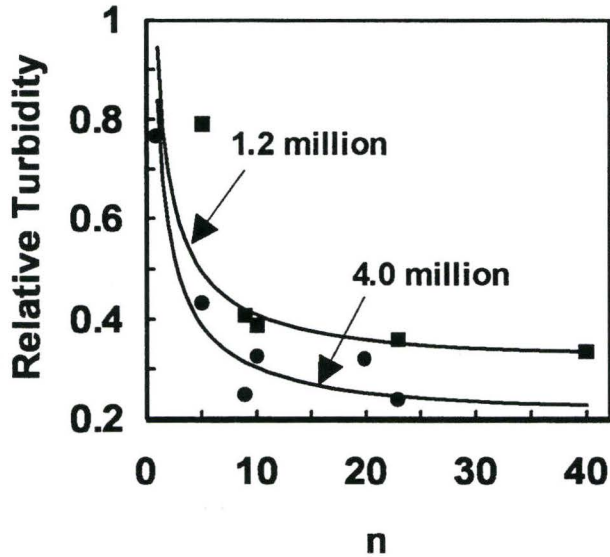


Figure 6 Relative turbidity as a function of PEG pendant length n in copolymers which were polymerized at 25°C(●) and 40°C(■). The curves were calculated from the empirical Equation assuming constant composition of 0.9 % (mole) macromonomer and the molecular weight values shown in the figure.

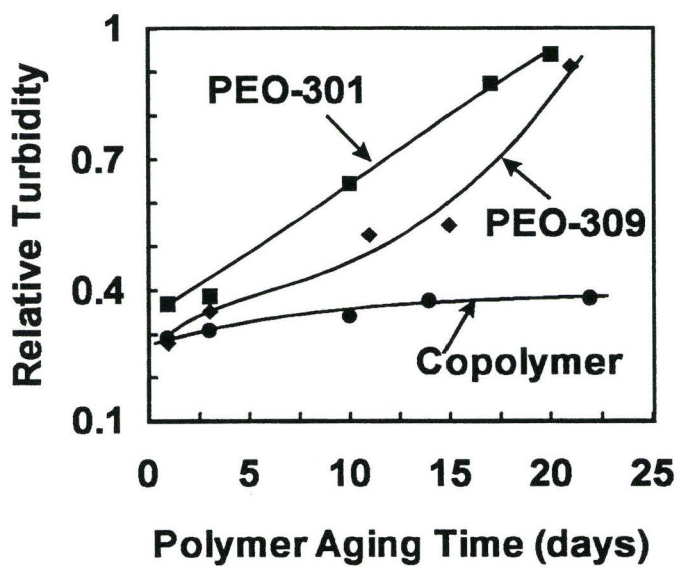


Figure 7 The Influence of Polymer Aging on PSL Flocculation. Polymer conc. = 0.025 %(wt) and stored at room temperature.

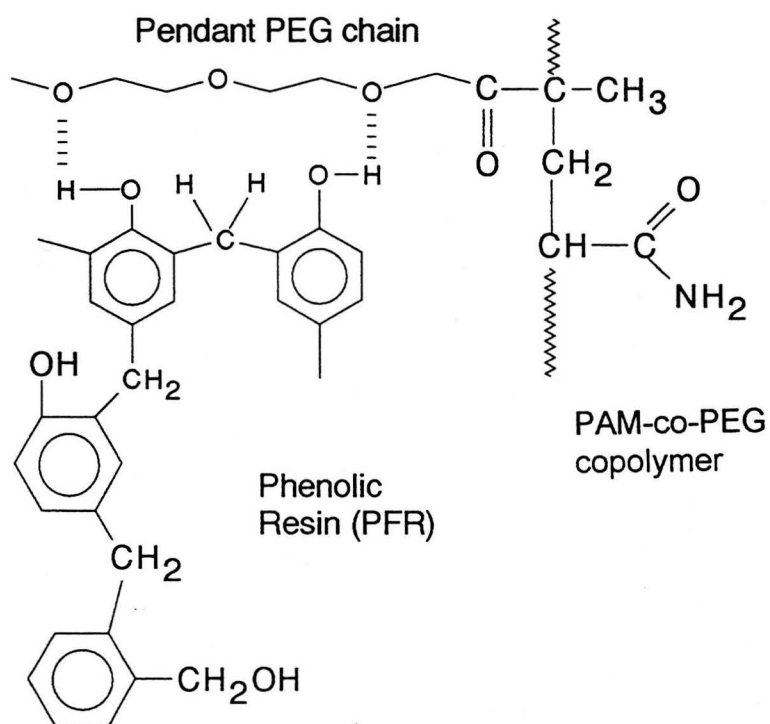


Figure 8 A schematic of hydrogen bonding formation between phenolic resin and PAM-co-PEG Copolymer

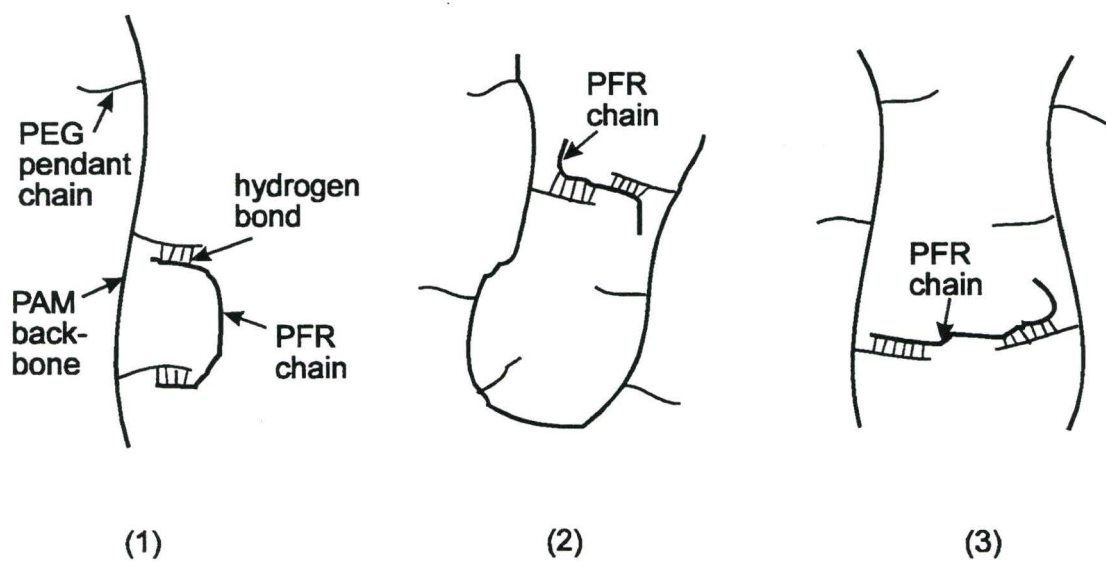


Figure 9. Complex formation between PAM-co-PEG copolymer and PFR

CHAPTER 4

Mechanism on Flocculation of Colloidal Particles by PEO and PAM-co-PEG Copolymers with Phenolic Resins

ABSTRACT

The mechanism of colloidal flocculation induced by nonionic dual-polymer systems was investigated. A new mechanism called “complex bridging flocculation” was proposed. With this mechanism PEO molecules aggregate in the presence of cofactor to form colloidal dispersed polymer complex which heteroflocculates with the colloidal particles. Most of the features of PEO/phenolic resin (PFR) dual-polymer in inducing the polystyrene latex flocculation were in agreement with the proposed mechanism. In particular, the experimental results support the contention that adsorption of cofactor (e.g. PFR) or PEO onto the latex surface is required for flocculation.

The molecular weight sensitivity of PEO/PFR flocculants perhaps resulted from the dynamics of the complex collapse. Flocculants based on low molecular weight PEO may collapse too quickly for flocculation to occur. The new polyacrylamide-co-poly(ethylene glycol) copolymers showed the same trends as PEO and thus likely function by the same mechanism.

KEYWORDS: flocculation; PEO; phenolic resin; complex bridging; latex.

Introduction

Flocculants are routinely used in papermaking to help retain colloidal additives in the sheet during papermaking process. However, mechanically-derived wood pulps contain large quantities of anionic dissolved and colloidal substances (DCS) which interfere with the performance of conventional retention aids (flocculants) based on cationic polyelectrolytes. On the other hand, very high molecular weight polyethylene oxide (PEO) is an effective retention aid for newsprint and other mechanical pulp furnishes. For flocculation, PEO requires a second polymer called cofactor. In some pulps, part of the DCS fraction acts as a cofactor whereas in other cases a synthetic cofactor must be added.^{1,2,3}

There are problems associated with the use of PEO as a retention aid. PEO is expensive compared to many synthetic flocculants. Also, PEO chains are susceptible to degradation which results in lowering the molecular weight and thus flocculation efficiency. Degradation can be caused by either shear forces or extended storage.

In order to overcome the fragile properties of PEO, a novel comb copolymer with long polyacrylamide (PAM) backbones bearing short polyethylene glycol (PEG) pendant chains, i.e. PAM-co-PEG, has been developed in our laboratory.⁴ The copolymers in conjunction with phenolic resin provided a novel series of retention aids for mechanical pulps with improved aging and shear resistances. This paper describes the results of our investigation on the mechanism of latex flocculation induced by PEO or PAM-co-PEG copolymer and cofactor.

The literature contains other discussions of the PEO/cofactor system.^{1,2} In the earliest work, the synergistic effects of cofactor was attributed to polymer-

polymer complex formation arising from hydrogen bonding between polyether oxygen and phenolic hydrogen as a cofactor. The best evidence supporting this view was the observation that flocculation ceased at high pH when the phenolic groups dissociated and could not participate in hydrogen bonding.

A mechanism called network flocculation was first postulated by Lindstrom and Glad-Nordmark in 1984.^{5,6} The basic idea of this mechanism is that colloids are mechanically trapped by a macroscopic transient polymer network formed by PEO and cofactor. Examples of flocculation systems that have been explained by the network mechanism include PEO plus phenolic resins, PEO plus tannic acid and PAM plus tannic acid. This type of mechanism has also been investigated by Lapin et al.^{7,8} They postulated that a supermolecular network is formed during the mixing of PEO and a cofactor (the condensate of naphthalenesulfonic acid with formaldehyde). The network fulfilled the role of a three-dimensional filter for kinetic particles of the suspension, and flocculation is accomplished by fibrillar formation of the polymer complex.⁸

Presented in this work are new experimental results aimed at clarifying the flocculation mechanisms for PEO/phenolic resins or PAM-co-PEG copolymer/phenolic resin. A new mechanism called "complex bridging" is presented as a better explanation of the results than the network flocculation mechanism.

4.1 Experimental

4.1.1 Materials

Copolymer flocculants based on long polyacrylamide (PAM) backbones with pendant polyethylene glycol (PEG) short chains were synthesized and their structures are shown in Figure 1. The PEG (meth)acrylate macromonomers, represented by (M)A-*n*, were used in copolymerizations. For example, MA-23 represents the PEG methacrylate macromonomer with PEG repeat units $n = 23$. Details on the copolymerization procedure have been described elsewhere.⁹

The polystyrene latex (PSL) particles were synthesized in this work by the emulsifier-free polymerization, using the method described by Goodwin et al.¹⁰ The recipe consisted of: styrene 73 g, potassium persulfate 0.53 g and deionized and distilled water 670 g. The polymerization was carried out at 70°C for 12 hours. The weight average size of PSL, measured by a BI-DCP Particle Sizer (Brookhaven Instrument Co.), was $0.69 \pm 0.11 \mu\text{m}$. Mobility results, measured by electrophoresis, will be given later. Other PSL with different sizes ($110 \pm 3 \text{ nm}$, $390 \pm 6 \text{ nm}$ and $1.09 \pm 0.038 \mu\text{m}$), used in studying latex size effect, were obtained from Polysciences Co.

Polystyrene latex grafted with poly(N-isopropylacrylamide) (PNIPAM) was synthesized from polymerization of NIPAM in the presence of the well-defined PSL. Details on the grafting polymerization have been reported by Pelton.¹¹ Proton NMR analysis indicated that PSL contained approximately 1 to 1.5 % (wt) of PNIPAM based on total amount of latex. The size of bare PSL before being grafted is 400 nm (intensity average), determined by dynamic light scattering using a fixed angle NICOMP 370 Sub-micro Particle Sizer (Pacific Scientific).

PNIPAM homopolymer latex prepared in previous work was also used as model latex for comparison.¹²

Polyethylene oxide (PEO) (Union Carbide) and phenol formaldehyde resin (PFR) CASCOPHEN C271 (40 % in aqueous solution) (Borden Chemical) were used as supplied. Weight average molecular weights (Mw) of PEO-301 and PEO-309 were 4 and 8 million respectively, as indicated by the supplier. Mw of C271 was approximately 13,000 as measured by GPC in this work.

Poly(p-vinyl phenol) (PVPh) with MW of 30,000, was obtained from Polysciences Co. PVPh was dissolved in a 50/50 (wt) of methanol/water mixture solution for use in flocculation measurements.

Low molecular weight samples of methoxy polyethylene glycol (PEG) 350 to 5000 were supplied by Union Carbide.

Cationic polymer XB-54-15-1 (Allied Colloid Canada), which was a poly(acrylamide-co-DADMAC) with charge density of 38 % and MW higher than 1 million, was used for comparison of flocculation performance with nonionic dual-polymer systems.

The cellulose fiber used in PSL flocculation experiments, was bleached softwood kraft pulp supplied by Noranda Forest Co. The fibers are 1 - 3 mm in length and approximately 20 to 30 μm in diameter. The pulp stock was prepared by blending the bleached fibers with distilled water in a Commercial Blender (Warring Products). The consistency of the pulp was approximately 1.0 % (wt). Another type of substrate used in flocculation characterization was silica beads, obtained from Orlick Industries. Coarse beads (#3) had sizes ranging from 590-840 μm . Fine beads had sizes ranging from 88-140 μm . Both bleached fibers and silica beads are called substrates in this work.

4.1.2 Polystyrene latex flocculation experiments

Flocculation of the polystyrene(PS) latex particles was caused by sequential addition of small quantities (1.0 - 4.0 mg/L) of two mutually interacting copolymer or PEO and phenolic resin components in the presence of the bleached fiber. 35 mL water and 10 mL bleached fiber pulp of 0.5 % consistency were added to a 50 mL test tube. 1 mL of 0.25 %(wt.) PSL was then added and the pH of the solution was adjusted to about 5 by adding 0.1 mL 0.02 N HCl. 0.1 mL 1 N NaCl was also added to maintain the electrolyte at concentration of 10^{-3} M. After 0.4 mL 0.25 %(wt.) phenolic resin was added, the transmittance of the control was measured using UV spectroscopy (Hewlett Packard) at wavelength of 500 nm. Finally, 0.2 - 1.0 mL copolymer or PEO aqueous solution at concentration of 0.025 - 0.05 % (wt) was added with water to make total volume of 50 mL. The samples were shaken vigorously for 3 to 5 seconds and then allowed to settle for about 1 hour. The supernatant was decanted and filtered with a 200 mesh screen to separate suspended fragment of fiber and the transmittance was measured at 500 nm. It was assumed that the turbidity of the supernatant was proportional to unflocculated latex concentration. In cases where small latex aggregates remained in solution this assumption breaks down.

Turbidity results were expressed as relative turbidities defined as:

$$\tau_R = \log(100/T_S) / \log(100/T_C)$$

where T_S was the transmittance of the sample and T_C the transmittance of the control which was a stable latex without flocculant. A lower relative turbidity indicates that more latex particles are flocculated.

4.1.3 Adsorption isotherm measurements of phenolic resin and PEO on latex surfaces

Adsorption isotherms of PFR on PSL were measured by an UV spectroscope. The adsorption measurements were conducted at room temperature (23°C) with PSL concentration of 2.5 g/L. Phenolic resin was added to the latex to give concentrations ranging from 2 to 200 mg/L. After mixing followed by 30 minutes of equilibrium time, the mixture was separated in a L7-55 Ultracentrifuge (Beckman) at 40,000 rpm for 40 min. PFR concentration in supernatant was measured by UV at a wavelength of 286 nm. The adsorbed amount of PFR was estimated from the differences between the latex sample and the control without latex.

PEO adsorption on PSL was measured using a Bruker AC 200 NMR spectrometer (200 MHz, Bruker Co.). Sample preparation was similar to phenolic resin described above. The concentration of PEO in supernatant was determined by ^1H NMR using methanol as internal reference. A calibration curve following peak ratios of PEO and methanol was obtained. The adsorption amount of PEO after being added to latex then was estimated from the calibration curve.

4.1.4 Electrophoretic characterization of PSL

Electrophoretic mobilities of PSL were measured with a Coulter Doppler Electrophoretic Light Scattering Analyzer (DELSA) 440 using the software version 1.36. For PSL grafted with PNIPAM as well as the mixture of PSL with phenolic resins, the same technique was used in determining the properties of PSL after being grafted or mixed.

4.1.5 Viscosity measurement

Bohlin VOR Rheometer System (Bohlin, Sweden) was used to determine the rheological properties of the complex formed between PEO or copolymer and phenolic resin. Measurements were conducted in a concentric cylinder with a measuring geometry C25. Continuous viscosity and shear stress were recorded as a function of time at a constant shear rate of 581/s. Total sample volume was about 13 mL. In order to observe the influence of polymer association on the system viscosity, one polymer (phenolic resin or PEO) was added first with fibers and latex. After measurement had been carried out for approximately 30 seconds, second component (PEO or phenolic resin) was then added with the viscometer running.

4.1.6 Imaging floc morphology

Polystyrene latex flocs were observed by optical microscopy and scanning electron microscopy (SEM). In optical microscopy observation, latex floc size and distribution on fibers immersed in water were observed with a Axioplan Optical Microscope (Zeiss) at magnifications of 200 to 400. Microscope images were connected to a Kontron Vidasplus Image Analysis System via an Hamamatsu C2400 video camera, running IBAS 2.0 software (Zeiss). The Philips 501 B scanning electron microscopy (SEM) was used to observe the latex flocs at magnifications of 5000 and 10000.

4.2 Results

4.2.1 Adsorption isotherms

Adsorption isotherms for PEO and phenolic resins on PSL surfaces are given in Figures 2 and 3. Figure 2 describes the adsorption of phenolic resin on PSL with a diameter of approximately $0.69\ \mu\text{m}$. Saturated adsorption amounts of $4.3 \pm 0.2\ \text{mg/m}^2$ occurred when the equilibrium concentration reached approximately $70\ \text{mg/L}$.

Additional evidence for phenolic resin adsorption on PSL was obtained from electrophoresis measurements. The mobility of PSL, determined at the diluted suspension ($= 50\ \text{mg/L}$) in the presence of $10^{-3}\ \text{M}$ NaCl and pH 5, was approximately $-3.1 \times 10^{-8}\ \text{m}^2/\text{V}\cdot\text{s}$. After the $10\ \text{mL}$ diluted latex was mixed with $0.01\ \text{mL}$ PFR ($0.11\ \%$), the mobility of the latex was increased to about $-3.6 \times 10^{-8}\ \text{m}^2/\text{V}\cdot\text{s}$. The increase in mobility was attributed to adsorbed phenolic resins bearing some anionic groups such as carboxyl groups which were found from potentiometric titration.

Figure 3 shows the adsorption isotherm for PEO on latex. The saturated coverage of PEO adsorbed on PSL surfaces was $1.0 \pm 0.2\ \text{mg/m}^2$ which agrees with the values given by Couture and van de Ven.¹³

In summary, both PEO and phenolic resin were found to adsorb onto PSL surfaces. However, the maximum amount of phenolic resin which could adsorb onto the latex surface was four times that of PEO homopolymer.

4.2.2 Accessing flocculation

Effective flocculation was usually obvious from visible inspection of the test tubes. Figure 4 presents examples for the latex particles before and after flocculation by PEO and copolymer. It is clear that the turbidity in the test tubes

are different and the fiber sedimentation volume also varied. In control sample (left in Figure 4), the supernatant appeared to be turbid. After the latex flocculation was induced by PEO/PFR, the supernatant (middle in Figure 4) become clear which suggested that most of the latex particles were flocculated and deposited onto the fiber surfaces. In the copolymer/PFR flocculation system, clear supernatant (right in Figure 4) was also observed. However, the fiber sedimentation in copolymer sample appeared to be more loose than those in the control and PEO samples. There are many factors affecting the flocculation processes; the details are presented as follows.

4.2.2.1 The influence of pH

Latex flocculation with PEO/PFR system was studied as a function of pH and the results are summarized in Figure 5. Excellent flocculation was obtained for pH ranging from 2 to 5. However, latex removal was decreased when the pH was above 5.5. For example, relative turbidity of the latex increased from 0.25 at pH below 5 to about 0.6 at pH 7 to 9.5.

Similar results have also been reported by Lindstrom et al for the latex flocculation induced by PEO/tannic acid system.⁶ The optimal pH range for this system was between 5 and 6.

4.2.2.2 Effects of the electrolyte concentration

Sodium chloride addition was used to control ionic strength. However, addition of NaCl in the systems was found to show rather complicated effects on flocculation. The results are presented in Figure 6 and details of experimental conditions are described in the Figure caption. Polyvinyl phenol with MW of 30,000, instead of phenolic resin, was used as the cofactor.

It was found that the presence of salt induced instability of the latex even without polymer addition. The results, as shown by the upper curve in Figure 6, indicate that an inflection point occurs at $\log(\text{conductivity, } \mu\text{S/cm})$ equal to about 2, which may correspond the critical coagulation concentration (CCC) for the latex particles. When PEO/PFR induced flocculation was conducted in the range of $\log(\text{conductivity})$ below the CCC, flocculation processes appeared to be insensitive to NaCl. The pH in Figure 6 ranged between 3.2 and 3.8.

In PEO/tannic acid flocculation system, Lindstrom et al.⁶ reported that the significant effect of aluminum chloride concentration on latex removal. The relative turbidity of latex with diameter of 1.1 μm was decreased from about 0.8 at $6 \times 10^{-8} \text{ M } [\text{Al}]_{\text{tot}}$ to about 0.3 at $10^{-5} \text{ M } [\text{Al}]_{\text{tot}}$.

4.2.2.3 Effects of polymer molecular weights

The effects of polymer MW on latex flocculation are presented in Table 1. Both copolymer and PEO samples show that higher MW gave a greater amount of latex particle removal. The copolymer with higher MW but lower density of PEO pendant chains, e.g. sample 56-48, was more effective than the copolymer 43-36 which has higher density of PEO pendant chains but lower MW.

The same trend occurred in PEO/PFR flocculation systems. The PEO-309 with highest MW (i.e. 8 million) produced the maximum latex removal in the three PEO samples. When the MW of PEO was less than 1 million (e.g. 300,000 in Table 1), almost no latex flocculation was observed.

The same PEO MW effect has been reported by Pelton et al.¹ in the pulp fine retention induced by PEO/PFR system. The results, obtained from a systematic studies on a series of PEO homopolymers with MW ranging from 1000 to 5 million, indicated that only PEO with MW of 5 million was effective in

improving the pulp fine particle flocculation. In single polymer flocculation of silica or latex particles, it has also been reported that higher MW of PEO homopolymer produced more effective bridging between particles and induced flocculation.^{14,15}

It was found that there were no significant differences in flocculating latex with phenolic resins which were fractionated by dialysis. The separation was carried out by using Spectra membranes with a MW cut-off of 12,000 - 14,000. About 51 % of PFR was fractionated after dialysis for 6 days. The results show no significant differences in latex flocculation caused by the original phenolic resin and the fractionated resin with cut-off of MW below 12,000.

4.2.2.4 Effects of polymer dosage

It has been found that there is an optimum range for the weight ratios between PEO and cofactor from both our work and Lindstrom's result. At constant total amount of polymer addition (2 mg/L), Lindstrom et al.⁵ changed the ratio of PEO to cofactor phenolic resin or tannic acid and found that maximum flocculation occurred at weight ratio 1:1 of PEO to cofactors in both systems. Similarly, flocculation measurements were conducted in this work at a PFR constant concentration of 2.0 mg/L and the results are shown as a function of copolymer concentration in Figure 7. The ratio for maximum flocculation for copolymers with molecular weights over 3 million was approximately 1:1. With the same type of cofactor (i.e. PFR), the ratios for maximum flocculation in PEO-301/PFR and PEO-309/PFR were also found at 1:1 (wt) (see Figure 8). The results are in agreement with that reported by Lindstrom et al.⁵

The effects of phenolic resin concentration on latex flocculation were investigated at constant PEO dosage (2 mg/L) and the results are presented in

Figure 9. PFR concentration as low as 0.2 mg/L gave good flocculation whereas without PFR no flocculation was observed. Maximum flocculation was observed at phenolic resin concentration equal to 2.0 mg/L, which corresponded the weight ratio of PEO-309 to phenolic resins at 1:1. However, higher dosages up to 16 mg/L of phenolic resins were not detrimental to flocculation efficiency. This result was in contrast to the behaviors of PEO and copolymer where relative turbidity increased significantly at higher polyether dosage (see Figures 7 and 8).

An interesting observation was that, at constant optimum ratios of the copolymer or PEO to phenolic resin, increasing both polymer and phenolic resin gave significantly enhanced flocculation efficiency. The results, shown in Figure 10, indicate that the relative turbidity decreased from 0.42 to 0.09 when the PEO/phenolic resin concentrations were increased from 1/1 to 14/14 mg/L.

4.2.2.5 Influence of latex size and concentration

The influence of latex sizes on flocculation, at the same polymer flocculant concentration, is shown in Figure 11. The results obtained by Lindstrom et al.⁵ were also presented in the Figure for comparison. The flocculation operation conditions in the present work and Lindstrom's work were similar. Experimental details are given in the Figure caption. Flocculation induced by PEO/PFR was observed for the smaller latex particles with diameter of 0.109 μm in the present work. By contrast, no flocculation was reported in Lindstrom's results for this size range of latex particles. When the larger particles were used, more latex particles were removed by the same flocculant system, which was consistent with Lindstrom's data.⁵ It should be noted that Lindstrom stated surfactant was used in their system to prevent PEO adsorption

on latex. They used the size dependent removal of latex particles as the primary evidence for network flocculation.

In another experiment in this work, it was found that at high polymer concentration such as PEO/PFR = 5/10 mg/L, more than 80 % (wt) of small latex particles (0.11 μm in diameter) were removed with a latex concentration of 5 mg/L (see Table 2). The results suggested that smaller latex particles can be significantly flocculated at higher polymer dosage.

Although the latex size influenced its flocculation by dual-polymer systems, the initial latex concentration indicated no significant effects. Figure 12 shows flocculation as a function of initial latex concentrations. Even when PSL concentration was as high as 300 mg/L, approximately 60 % of latex was removed by polymer addition. Similar work was also reported by Lindstrom et al.⁵ who found that the same fraction of latex removal was maintained when the latex concentration was increased from 25 mg/L to 200 mg/L.

4.2.2.6 Influence of PS-g-PNIPAM latex

a) Microgel particles

A key postulate in Lindstrom's network flocculation mechanism is that the network polymers do not adsorb on the latex surface. Since PEO does adsorb on the polystyrene latex used in this work, a microgel latex composed of cross-linked poly(N-isopropylacrylamide) (PNIPAM) was used in flocculation experiments.¹⁶ The advantage of this colloid was that PNIPAM does not interact with PEO in water¹⁷, therefore we anticipate that PEO adsorption on the microgel does not occur. The results are shown in Table 3. Less than 17 % of PNIPAM latex was flocculated by PEO or copolymer whereas more than 60 % of PSL with the similar size (390 nm) was removed.

b) Microgel coated PSL

In related experiments, flocculation of the PSL colloids with grafted PNIPAM was investigated. The results in Table 4 are particularly interesting. At most 40 % of the PNIPAM grafted latex was flocculated compared with 65 % of the bare latex. The results indicated that the grafted PNIPAM on the latex surface inhibited polymer adsorption and thereby decreased amount of the grafted latex being flocculated.

4.2.2.7 Order of polymer addition

Various sequences of polymer addition were used in this work to investigate the flocculation process. The following summary can be made from the results in Tables 5 and 6.

- 1) PEO addition before or after PFR gave almost the same amounts of latex removal. Similar results were found for the copolymer samples. When PFR was added before copolymer 43-129, relative turbidity was 0.29; when the copolymer was added before PFR, the relative turbidity was also 0.30. The results agree with observations obtained by Lindstrom.⁵
- 2) Addition of fiber after the polymers influenced flocculation. When fibers were added 45 seconds after polymers, improved flocculation performance of polymers was still maintained. Similarly, with a larger size latex system (diameter of 1.09 μm) and at higher polymer dosage, good flocculation was observed when fibers were added 180 seconds after the polymers. These results were in contrast with the observation by Lindstrom et al.⁵ who indicated that in PEO-301/PFR flocculation system, the flocculation ability of polymers was almost lost when the fibers were added 30 seconds after polymers. In this work, decreased flocculation performance was only

observed when the fibers were added 15 minutes after PFR and PEO additions.

- 3) When PSL was added 30 seconds after fibers, polymers and other components, flocculation was poor. For example, with the PEO/PFR system only about 18 % of latex particles were flocculated.
- 4) An interesting result shown in Table 5 was that flocculation was poor (relative turbidity = 0.79) when PEO was pre-mixed with PFR.

4.2.2.8 Influence of pre-treated latex with PFR or PEO

To further study the effects of the addition mode on flocculation efficiency, flocculation of latex pre-treated with PFR or PEO was investigated. In the pre-treatment processes, PFR or PEO was mixed with PSL at high concentration and the un-adsorbed polymer was removed. The results, presented in Table 7, show that about 44 % of the PFR pre-treated latex particles were flocculated and that about 38 % of the PEO pre-treated latex particles were flocculated. The values are lower than those of latex removal in the standard procedure.

4.2.2.9 Influence of substrates

Wood fibers were used in the flocculation experiments because the research was directed at papermaking. The effects of fiber concentration were investigated and the results are shown in Figure 13. Latex flocculation processes are fiber content dependent. As the fiber concentrations were increased from 0.5 g/L to 2.0 g/L, the relative turbidity decreased linearly. Further increase in fiber concentration from 2.0 g/L to 2.5 g/L, however, did not give a significant improvement for flocculation. The cofactor used in these experiments was poly(vinyl phenol) with MW 30,000.

In order to elucidate the role of substrate in latex flocculation, silica beads with two level sizes were used instead of bleached fibers. It was found that silica beads also promoted PSL flocculation. The data in Table 8 indicate that higher amounts of beads gave greater latex removal. Furthermore, more efficient flocculation was observed for fine beads than coarse beads. This result suggested that latex removal was not sensitive to the surface chemistry of substrates.

2.2.10 Mechanical shearing induced flocculation

It has been found in this work that even in the absence of fiber or other substrates, latex flocculation induced by PEO/PFR can be significantly enhanced by high shear stress. Figure 14 describes flocculation under mechanical shearing induced by a stirring propeller in a Dynamic Drainage Jar (DDJ). The flocculation was conducted as a function of propeller speed. The results indicated that higher shear stress (i.e. higher propeller speed) produced a higher flocculation of latex (i.e. lower relative turbidity). Many visible large latex flocs precipitated after stirring. However, without polymer addition the latex exposed to the same shearing conditions in DDJ did not show any instability.

4.2.3 Effects of the flocculation on viscosity

Flocculation experiments were conducted in a rheometer to get evidence for network flocculation. Figure 15 shows the viscosity changes resulting from the interaction of dual-polymer flocculants. One curve represents the experiments conducted in the presence of latex and fibers; another represents the results in the absence of latex and fibers. With latex and fiber, the curve indicates that steady shear viscosity of a mixture of latex, fibers and PEO was maintained until about 30 seconds later as PFR was added to initiate the

flocculation. A rise in viscosity was observed immediately after PFR addition and viscosity reached a maximum 10 to 15 seconds later. However, the viscosity was reduced to the initial value in about 30 seconds. Similar results were observed without latex and fibers. Lindstrom et al.⁵ mentioned the viscosity increasing phenomena, but did not give any data.

Lapin et al.⁷ reported similar viscosity measurements in the absence of latex and fibers. An abrupt increase in system viscosity occurred upon mixing PEO and cofactor. Maximum viscosity was reached at about 15 seconds after mixing.

Figure 16 describes the rheological behavior for copolymer systems. In this measurement, the copolymer 56-48 (MW of 4.5 million and containing 0.47 % (mol) MA-23) was added after all other components to give a dramatic increase in system viscosity. After approximately 20 seconds, the system viscosity was reduced to a steady state.

4.2.4 Morphology of PSL flocs formed by dual-polymer systems

4.2.4.1 Optical microscopy

Suspensions of fibers with latex dispersion were withdrawn from the test tube and transferred to watch glass which was placed under a microscope. The results in Figure 17 shows the PSL particles before being flocculated. This picture indicates only a few latex particles being attached on the fibers. Unattached latex particles were obvious because they underwent Brownian motion.

Figure 18 shows the PSL flocs formed by PEO-309 and phenolic resin. The dominant features are roughly spherical flocs between 15 and 25 μm in

diameter. Careful inspection reveals that small flocs and single particles were also attached to the fibers.

Figures 19 and 20 give higher magnification views of a single latex floc attached to the fibers. Figure 19 shows the floc formed by PEO/PFR; Figure 20 shows the floc formed by copolymer 43-129 (MW of 3.7 million and containing 0.65 % (mole) MA-23) and PFR. The large, spherical latex flocs obtained with the dual polymers were different from latex deposited on bleached fiber caused by cationic polyacrylamide copolymer XB-54-15-1. Figure 21 shows that the cationic polymer gave smaller size latex aggregates. Since the flocculation mechanisms for cationic polymer and nonionic dual-polymer system are different, the result suggests that the difference in flocculation mechanism also leads to the difference in flocs morphology.

4.2.4.2 Scanning electron microscopy

SEM micrograph latex flocs were taken and a typical result is shown in Figure 22. The deposited latex was mainly present as large flocs roughly the size of a fiber diameter.

4.2.5 Summary of experimental results

In this section the results are summarized as follows in three groups to clearly identify what is new, what is old and what is controversial.

4.2.5.1 Results confirming published data

1. PEO or copolymer must have a molecular weight greater than 3×10^6 for good flocculation.
2. The best flocculation occurred when the pH was below 6.
3. Optimum flocculation occurred at a weight ratio of PEO to cofactor equal to 1.
4. Flocculation was independent of the latex particle concentration.

5. Good flocculation was observed if either the PEO or cofactor were added last.
6. Transient viscosity peaks were observed when PEO and PFR were mixed either with or without the presence of latex particles and fibers.
7. When PEO and PFR were added at a constant weight ratio, the higher the dosage, the better the flocculation.

4.2.5.2 Results contradicting published data

1. Both PEO and PFR adsorbed onto the PSL surface.
2. Flocculation was not very sensitive to salt concentration.
3. Flocculation was not significantly affected by the latex particle size.

4.2.5.3 New results

1. Latex coated with PNIPAM, which prevented PEO adsorption, was much less efficiently removed by PEO/PFR than was untreated latex.
2. No flocculation was observed if latex was added last.
3. Flocculation was much improved in the presence of substrate (fiber or silica); however, the advantage of fiber addition was lost if it was added more than 15 minutes after everything else.
4. The latex aggregated to form roughly spherical flocs containing hundreds of particles.
5. PAM-co-PEG copolymers showed the same trends as PEO in all flocculation experiments.
6. Good flocculation was observed without substrate if the system was vigorously mixed.

7. Pre-treating latex with PEO or PFR followed by removal of un-adsorbed polymer gave poor flocculation when the second component was added.

4.3 Discussion

4.3.1 Network flocculation mechanism

The flocculation of colloiddally dispersed latex with a mixture of two polymers and cellulose fibers is complicated because many interactions are possible. The transient polymer network flocculation mechanism proposed by Lindstrom and Glad-Nordmark is frequently used to describe this system.⁵ The mechanism assumes that an open polymeric network forms from the hydrogen bonding interaction of PEO and cofactor and that the network is fixed to the cellulose fibers. With mixing, the fibers “sweep” the network through the suspension and latex particles are mechanically entrapped like fish in a net. The network flocculation process is illustrated in Figure 23

Network flocculation was justified on the basis that it explained the following observations: 1) flocculation was sensitized by the presence of substrate (e.g. fibers); 2) latex removal was independent of particle or latex concentration, and 3) flocculation efficiency was strongly dependent on the latex size; the larger particles being more easily removed (see Figure 11). The latexes used in the Swedish study were chosen to have surfactant on the surfaces to inhibit PEO adsorption on the latex.¹⁸

The network mechanism was discussed by Lapin et al.⁸ who suggested that PEO and cofactor formed macroscopic fibrils which caused flocculation by the network mechanism. Wagberg and Lindstrom¹⁹ also applied the network

flocculation mechanism to interpret polymer-induced cellulose fiber flocculation in turbulent suspensions. In their work, the flocculation process was extremely rapid, and virtually completed in less than two seconds.

The network mechanism also can explain some of the experimental results herein. For example, the rheology results indicate a short-lived supermolecular structure. The observation that flocculation was not very sensitive to latex concentration also fits the transient network theory. However, many of the current results are not consistent with the network flocculation mechanism. These include:

- 1) Latex coated with PNIPAM which prevented PEO adsorption, was much less efficiently removed by PEO/PFR than was untreated latex. (Table 4). According to the network flocculation model, particle removal is mechanical and should not depend upon the latex surface chemistry.
- 2) In this work, small diameter latex particles ($0.11\ \mu\text{m}$) were also efficiently removed.
- 3) The volume fraction of available network was too small. Extending Lindstrom's fishing analogy, the net is much smaller than the ocean. This can be illustrated by the following simple analysis. If the PEO concentration was $2\ \text{mg/L}$, the volume fraction occupied by spherical PEO molecules was only 0.005 based on a radius of gyration of $93\ \text{nm}$. Thus, however a macroscopic network is formed from the PEO units, the network will be much smaller than the volume to be swept.
- 4) In the following sections a kinetic analysis will show that the rate of network formation must be much lower than other competing processes.

Based on the above arguments the network flocculation mechanism originally proposed by Lindstrom and coworkers does not explain the experimental observations. Alternative explanations are presented in the following sections.

4.3.2 Postulated mechanisms

4.3.2.1 A schematic of flocculation processes

In the standard flocculation experiment PEO is added to an aqueous mixture of latex, PFR and fibers. Figure 24 illustrates the most important possible events upon PEO addition. The latex is shown coated with PFR because it was assumed that saturation adsorption occurred before the PEO was added. Ten possible steps are shown in Figure 24. Below each step is explained and then kinetic arguments are made to identify the most important steps.

Step 1: A PEO molecule forms a primary soluble polymer complex with one or more cofactor molecules.

Step 2: A PEO molecule adsorbs onto a latex surface.

Step 3: Primary PEO complex aggregates to form a time dependent distribution of colloidal sized species called colloidal complex.

Step 4: Colloidal complex adsorbs onto PSL.

Step 5: The bridging of two latex particles by colloidal complex.

Step 6: Formation of a macroscopic transient network from the association of colloidal complex.

Step 7: Continuing heterocoagulation of latex and colloidal complex. Steps 5 and 7 constitute a mechanism herein called "complex bridging".

Step 8: The mechanical entrapment of PSL in the transient network. Steps 6 and 8 portray the main features of the transient network flocculation mechanism.

Step 9: The deposition of large latex flocs onto the substrate surface.

Step 10: The syneresis and aggregation of colloidal complex to give a dense precipitated complex.

In order to identify the most important steps in Figure 24, estimations on the relative rates are made below. The system considered was: 2.0 mg/L PEO, 2.0 mg/L PFR and 50 mg/L PSL (0.7 μm in diameter) and 1.0 g/L bleached fibers. The pH and NaCl concentration were 5.0 and 10^{-3} M, respectively. With a total latex surface area of 0.41 m^2/L , about 12 % of the added PFR was not adsorbed assuming a saturation PFR coverage of 4.3 mg/m^2 . Similarly, if the latex surface was fully covered with a single layer of PEO (i.e. the case with no PFR present), then only about 20 % of the added would be adsorbed.

To simplify the kinetic analysis it was assumed that all the steps in Figure 24 were in the rapid coagulation regime. That is, every collision resulted in a coagulation event. Under these conditions the collision frequency can then be calculated by the Smoluchowski's expression for orthokinetic flocculation:²⁰

$$J_{ij} = (4/3)n_i n_j G(a_i + a_j)^3 \quad (1)$$

where a_i and a_j are the radii of the coagulating particles i and j , G is the shear rate; and, J_{ij} is the number of i - j collisions occurring in a unit volume per unit time.

To apply Equation 1 to the steps in Figure 24 many assumptions were made about the size and concentrations of the various species. The initial (maximum) rate of rapid latex flocculation in the absence of any energy barriers

was chosen as the basis for comparison. This rate equals the initial rate of Step 5 if adsorbed complex does not increase the latex diameter and if Step 4 is much faster. The latter requirement ensures that any two colliding latex particles had sufficient PEO complex adsorbed on the surface to give coagulation.

The results are summarized in Table 9. The first row gives the initial latex concentration and size. By definition, the relative rate was 1. The second row describes the initial rate of step 1. The high initial concentration of PEO chains and the very high concentration of PFR chains (relative to the latex concentration) ensured that rate of complex formation between PEO and un-adsorbed PFR was 5 orders of magnitude faster than the initial maximum rate of latex flocculation. By contrast, the initial rate of un-complexed PEO adsorption onto latex, Step 2, was only three orders of magnitude faster than Step 5. Therefore, the first conclusion is that Step 2 is unlikely to be an important process.

The initial homocoagulation rate of PEO molecules (Step 3) was 4 orders of magnitude faster than Step 5 and so should be considered an important process. Step 4 is more difficult to describe in this simple analysis. The maximum possible rate would correspond to the case when all the PEO was present as isolated molecules; this is identical to Step 2. However, the aggregation of PEO (Step 3) will quickly slow to the same order of magnitude as Step 5. For example, the bottom row in table 9 shows the rate if all the PEO were present in aggregates of 10 molecules bound together by PFR. In this situation the rate of step 4 decreased to 225.

The rate of complex syneresis to dehydrated precipitate (Step 10) could not be calculated. However, this process occurs if no latex is present. Indeed,

no latex flocculation occurs if it was added 2 minutes after everything else. In this situation the PEO was removed by Step 10 before flocculation could occur.

The formation of macroscopic polymer network (Step 6) was not amenable to simple kinetic analysis. However, the rate of formation of macroscopic gels containing 10^5 to 10^6 PEO chains must be much slower and thus is less likely than the other processes outlined in Figure 24. Therefore, the most likely aggregation mechanism is complex bridging which encompasses Steps 1, 3, 4, 5, 7 and 9 in Figure 24. With one exception every experimental observation in this and previous work can be explained directly by complex bridging. The exception is the extreme sensitivity of flocculation to PEO molecular weight which is addressed below.

It is well documented that bridging flocculants required a high molecular weight. However, the molecular weight dependence with the PEO/PFR system is extreme. In this work we have shown that PEO 301 with a molecular weight of 4 million gives good flocculation whereas 300,000 MW PEO did not. Since a 300,000 MW has about the same degree of polymerization as a 500,000 MW polyacrylamide, it is surprising that the PEO is ineffective.

The usual argument for the molecular weight dependence in bridging flocculation is that the adsorbed bridging polymer must extend beyond the effective distance of electrostatic repulsion in order adsorb onto a second particle. Lafuma et al.²¹ identified three situations: Case 1 - the equilibrium adsorbed layer thickness is greater than the closest distance of approach so flocculation occurs; Case 2 - the initial adsorbed layer configuration is large enough to give flocculation; however, with time the adsorbed flocculant rearranges to a more compact configuration and flocculation stops; and, Case 3

- the initial adsorbed configuration of flocculant is too compact to give flocculation at any time.

With dual polymer flocculant systems such as PEO/PFR the requirement for high molecular weight is more difficult to understand because PEO can adsorb in multilayers which are bound together with PFR. Thus, a process could be envisaged where with the continued adsorption of complex on the latex surface would result in the adsorbed layer of complex growing beyond the electrostatic repulsion distance.

A possible explanation for the molecular weight sensitivity is that the cooperative nature of hydrogen bonding with PFR requires very high molecular weight. For example, it is known in the PEG/polymethacrylic acid system that complex formation does not occur if the PEG molecular weight is less than 1000.²² In work published elsewhere we have shown that low molecular weight polyethylene glycols up to a molecular weight of 5000 do not form complexes with phenolic resins.²³ On the other hand, 300,000 MW PEO does form complexes but does not give good flocculation so the molecular minimum for complex formation does not seem to be the explanation.

The only remaining explanation of the molecular weight effect involves the dynamics of the complex collapse. Mixing of PEO with PFR forms a precipitated coacervate phase. With PEO 309 the time scale for this collapse was less than 30 seconds since latex added 30 seconds after PEO and PFR did not flocculate (Table 5). Also, the rheology results in Figure 15 suggests that the complex collapsed in the 30 s time scale. Thus, flocculation must occur before the complex collapses. Perhaps the rate of complex collapse is molecular weight dependent. That is, PEO/PFR complexes based on PEO with molecular weight

in the range 10^4 to 10^5 collapse too quickly for flocculation to occur. This appears to be the most likely explanation for the molecular weight sensitivity of the PEO/PFR and the PAM-co-PEG/PFR flocculants. More work is required to prove it.

Conclusions

Based on the analysis of the results of this work and published data it is proposed that PEO/cofactor dual polymer flocculation mechanism is a process herein called "Complex Bridging". In this mechanism, PEO molecules aggregate in the presence of cofactors to form colloiddally dispersed polymer complexes which heteroflocculate with the latex particles. The new PAM-co-PEG copolymers showed the same trends as PEO and thus function by the same mechanism.

Although Lindstrom's network flocculation mechanism explains some of the features of the PEO/PFR system, inadequacies of the model do not justify its use. In particular, the results herein support the contention that adsorption of PEO on the latex surface is a required for flocculation.

A difficulty with the fundamental investigation of the PEO/PFR system is that commercial phenolic resins are mixtures of poorly defined structures. In this work we have shown that poly(p-vinyl phenol), a much better defined material, is an effective cofactor. Details on this cofactor will be published in a separate paper.

References

- ¹ Pelton, R.H., Allen, L.H. and Nugent, H.M., *Svensk Papperstidning*, **9**, 251(1980).
- ² Pelton, R.H., Allen, L.H, and Nugent, H.M., *Tappi*, **64**(11), 89(1981).
- ³ Tay, C.H., and Cauley, T.A., "Studies on Polyethylene Oxide as a Retention Aid in Wood Fibre Stock Systems", *Tappi Papermakers Conf.*, 1(1982).
- ⁴ Pelton, R.H., Hamielec, A.E. and Xiao, H.N., Patents pending

-
- ⁵ Lindstrom, T. and Glad-Nordmark, G., *J. Colloid Interface Sci.*, **97**, 62(1984).
 - ⁶ Lindstrom, T. and Glad-Nordmark, G., *Colloids and Surfaces*, **8**, 337(1984).
 - ⁷ Lapin, V.V., Fedyukin, A.V., Teslenko, V.V., Danilova, D.A. and Dem'yanenko, A.T., *Colloid J. of The USSR*, **53**, 880(1992).
 - ⁸ Lapin, V.V. and Fedyukin, A.V., *Colloid J. of The USSR*, **54**, 640(1992).
 - ⁹ Xiao, H.N., Chapter 1, Ph.D. Thesis, McMaster University, 1994.
 - ¹⁰ Goodwin, J.W., Hearn, J., Ho, C.C. and Ottewill, R.H., *Colloid Polym. Sci.*, **252**, 464(1974).
 - ¹¹ Pelton, R.H., *J. Polym. Sci., A: Polym. Chem.*, **26**, 9(1988).
 - ¹² McPhee, W., Tam, K.C. and Pelton, R., *J. Colloid Interface Sci.*, **156**, 24 (1993).
 - ¹³ Couture, L. and van de Ven, T.G.M., *Colloids and Surfaces*, **54**, 252(1991).
 - ¹⁴ De Witt, J.A and van de Ven, T.G.M., *Adv. in Colloidal and Interface Sci.*, **42**, 41(1992).
 - ¹⁵ Pelssers, E.G.M., Cohen Stuart, M.A. and Fleer, G.J., *Colloid and Surface*, **38**, 15(1989).
 - ¹⁶ Pelton, R.H. and Chibante, P., *Colloids and Surfaces*, **20**, 247(1986).
 - ¹⁷ Wu, X., Pelton, R.H., Hamielec, A.E., Woods, D.R. and McPhee, W., *Colloid & Polymer Sci.*, **272**, 467(1994).
 - ¹⁸ Lindstrom, T., private communication (discussion)
 - ¹⁹ Wagberg, L and Lindstrom, T., *Nordic Pulp Paper Res. J.*, **2**, 49(1987).
 - ²⁰ Gregory, J., *Critical Rev. in Enviro. Control*, **19**(3), 185(1989).
 - ²¹ Lafuma, F., Wong, K. and Cabane, B., *J. of Colloidal and Interface Sci.*, **143**, 9(1991).
 - ²² Tsuchida, E., Osada, Y. and Ohno, H., *J. Macromol. Sci.-Phys.*, **B17**, 683(1980)
 - ²³ Xiao, H.N., Chapter 2, Ph.D. Thesis, McMaster University, 1994.

Tables

Table 1. Influence of copolymer MW on latex flocculation. Experimental conditions: [Latex] = 50 mg/L; diameter of latex = 0.69 μm . Bleached fiber = 1.0 g/L; pH = 5.0 and [NaCl] = 0.002 N; [PFR] = 2.0 mg/L; [PEO] = 2.0 mg/L; [copolymers] = 2.0 - 4.0 mg/L.

Polymers	MW	Macro-monomers	Composition mol % MA-23	Relative Turbidity
43-36	1.2×10^6	MA-23	0.85	0.36
56-48	4.5×10^6	MA-23	0.47	0.27
43-149	5.1×10^6	MA-23	0.14	0.34
43-71	7.0×10^5	MA-9	0.41	0.55
56-108	4.6×10^6	MA-9	0.69	0.25
43-22	6.3×10^5	A-10	1.10	0.59
56-113	2.1×10^6	A-10	0.70	0.30
PEO-309	8.0×10^6	-	-	0.23
PEO-301	4.0×10^6	-	-	0.37
PEO	3.0×10^5	-	-	0.89

Table 2. Small diameter latex flocculation by high polymer dosage. Data was compared with the latex of 0.69 μm in diameter

PEO-309 (mg/L)	PFR C-271 (mg/L)	PS latex (mg/L)	Diameter of Latex (μm)	Relative Turbidity
5	10	50	0.69	0.124
5	10	50	0.11	0.209
2	2	5	0.11	0.196
1	2	50	0.69	0.29

Table 3 Flocculation of PNIPAM latex. Diameter of the latex was 370 nm. Data was compared with the similar size PS latex. Polymer dosage: 2 mg/L. 56-108-2 and 8-24-1 both are MA-23 types of copolymers. Bleached fiber = 1.0 g/L.; pH = 5.0 and [NaCl] = 0.002 N.

Polymer	Type of latex	Relative turbidity
PEO-309	PNIPAM latex	0.83
56-108-2	PNIPAM latex	0.86
PEO-309	PS latex	0.38
8-24-1	PS latex	0.25

Table 4. Flocculation of PS-g-PNIPAM latex. Diameter of the bare latex was 400 nm. Bleached fiber = 1.0 g/L.; pH = 5.0 and [NaCl] = 0.002 N.

Polymer	Latex	Flocculation Temperature °C	Relative Turbidity
PEO-309	not grafted	21.4	0.35
PEO-309	grafted	21.4	0.61
PEO-309	grafted	23.2	0.70
56-108-2	grafted	21.4	0.57
56-110-1	grafted	23.2	0.78

Table 5. Effects of polymer addition order on the latex flocculation. Experimental conditions: [Latex] = 50 mg/L; diameter of latex = 0.69 μm . Bleached fiber = 1.0 g/L.; pH = 5.0 and [NaCl] = 0.002 N. PEO-309 conc. = 2.0 mg/L; Copolymer 43-129 conc. = 2.0 mg/L; PFR conc. = 2.0 mg/L and PVPh-30 conc. = 6.0 mg/L.

1st addition	2nd addition	3rd addition	4th addition	Relative Turbidity
fiber	PS latex	PFR	PEO-309	0.24
fiber	PS latex	PEO-309	PFR	0.27
fiber	PS latex	PFR	43-129	0.29
fiber	PS latex	43-129	PFR	0.30
fiber	PS latex	pre mixtures*		0.79
fiber	PEO-309	PS latex	PFR	0.46
no fiber	PS latex	PFR	PEO-309	0.60
fiber	C	PEO-309	PS latex**	0.815

*: PEO-309 and PFR solutions (0.025 % wt) were premixed before addition.

** : PS latex was added approximately 30 seconds after addition of polymers.

Table 6. The effect of addition mode of the bleached fiber on PS latex flocculation. The interval times between the mixing of PFR and PEO and the later addition of the bleached fiber(fiber conc. = 1.0 g/L) are given.

[Latex] mg/L	Size of latex μm	[PEO] mg/L	[PFR] mg/L	Relative Turbidity	Time of addition(s)
50	0.69	1	2	0.30	45
12.5	0.69	5	10	0.66	900
9	1.09	10	20	0.08	180

Table 7. Flocculation of PS latex pre-treated with PEO-309 and PFR. [Latex] = 50 mg/L; diameter of latex = 0.69 μm . Bleached fiber = 1.0 g/L.; pH = 5.0 and [NaCl] = 0.002 N. For the latex pretreated with PEO, PFR was added last and [PFR] = 2.0 mg/L. For the latex pretreated with PFR, PEO-309 was added last and [PEO] = 1.0 mg/L.

Pretreatment Polymers	Dosage (g/g PS)	Relative Turbidity
PEO-309	0.4/0.3	0.61
PFR C-271	0.1/0.3	0.56

Table 8. Flocculation of PS latex in the presence of silica beads. PEO-309 and phenolic resin were used at 2 mg/L for all measurements. pH = 5 and [NaCl] = 10^{-3} M.

Average diameter of silica beads (μm)	Weight beads (g)	Relative Turbidity
715	2.1	0.31
715	8.2	0.24
114	2.4	0.12
114	5.6	0.13
no silica beads	-	0.68

Table 9. Relative ratios of collision or aggregation rates in the schematic Figure 24. PEO* is the primary complex.

Step	$a_i(\text{nm})$	$a_j(\text{nm})$	$n_i (\#/L)$	$n_j(\#/L)$	species i	species j	$(J_{ij})_{oi}/(J_{ij})_{o5}$
5	350	350	2.65×10^{11}	2.65×10^{11}	latex	latex	1
1	60	1.55	3.01×10^{14}	1.11×10^{16}	PEO	PFR(12%)	1.3×10^5
2	60	350	3.01×10^{14}	2.65×10^{11}	PEO	Latex	913
3	60	60	3.01×10^{14}	3.01×10^{14}	PEO*	PEO*	2.6×10^4
4	204	350	3.01×10^{13}	2.65×10^{11}	10 PEO	latex	225

Figures

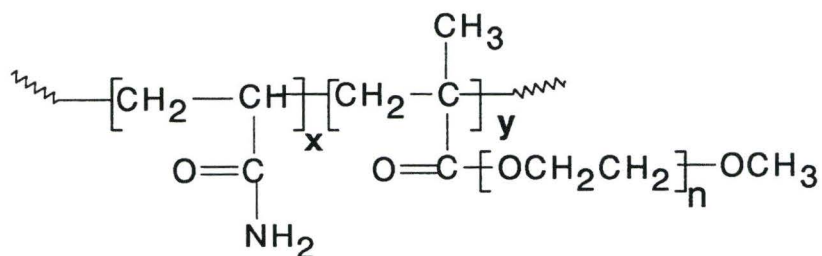


Figure 1. Structure of the comb copolymer of acrylamide and polyethylene glycol (PEG) methacrylate macromonomer.

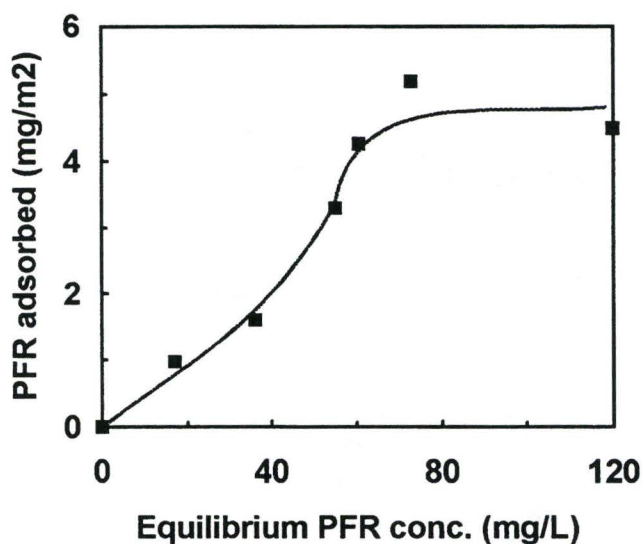


Figure 2. PFR adsorption on polystyrene latex. Experimental conditions: [Latex] = 2.48 g/L with 0.69 μm in diameter and temperature at 23°C.

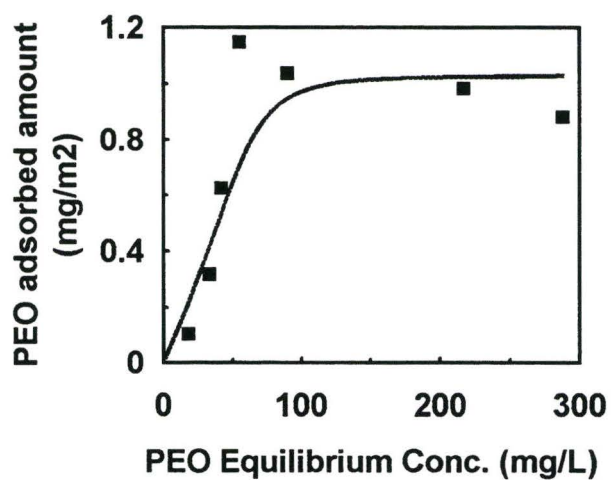


Figure 3. PEO adsorption on PS latex. Experimental Conditions: [Latex] = 3.64 g/L with 0.61 μm in diameter and temperature at 23°C.

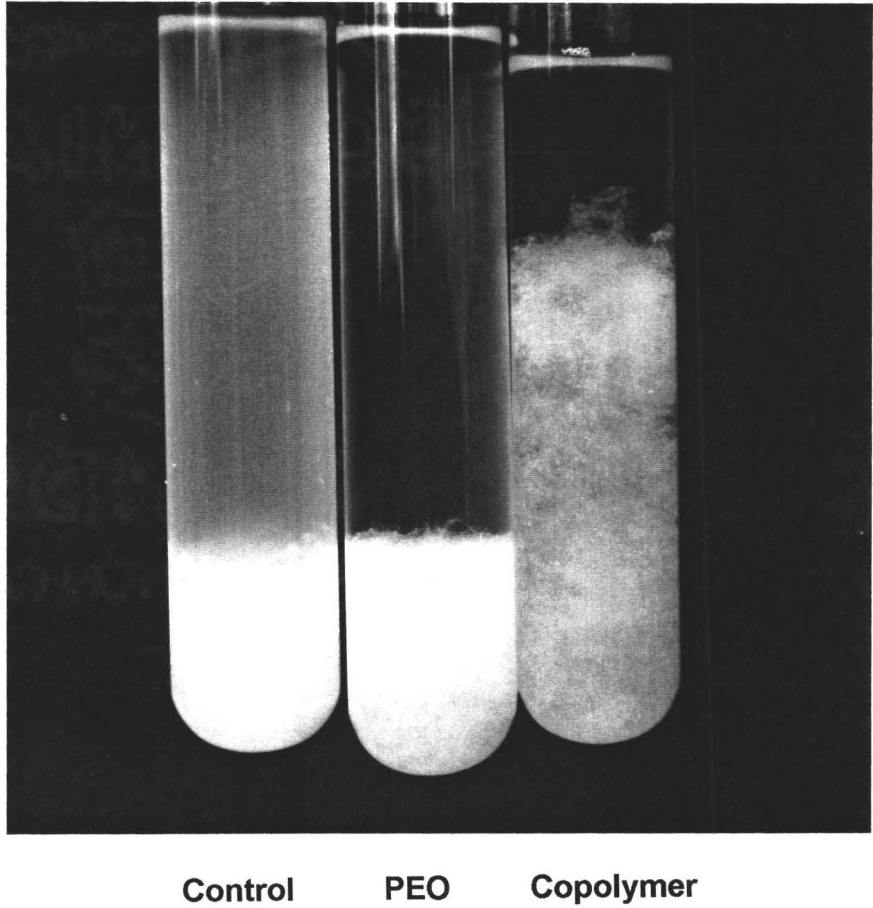


Figure 4. Observations on latex flocculation induced by PEO and copolymer with PFR in turbidity measurements. Concentrations of polymers and PFR were 2.0 mg/L.

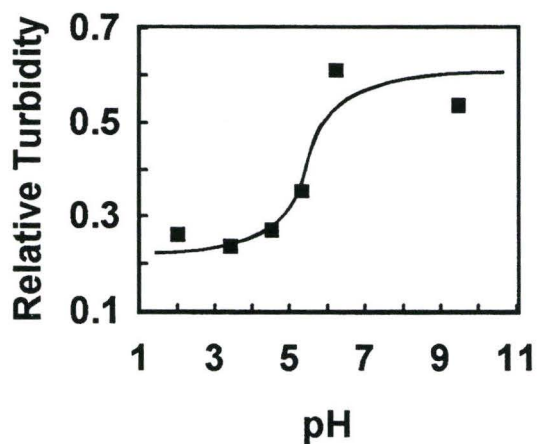


Figure 5. The influence of pH on PS latex flocculation by PEO/PFR system. pH adjusted by adding HCl or NaOH. Experimental conditions: [Latex] = 50 mg/L; diameter of latex = 0.69 μm . Bleached fiber = 1.0 g/L. [PEO 309] = 1.0 mg/L; and [PFR] = 2.0 mg/L.

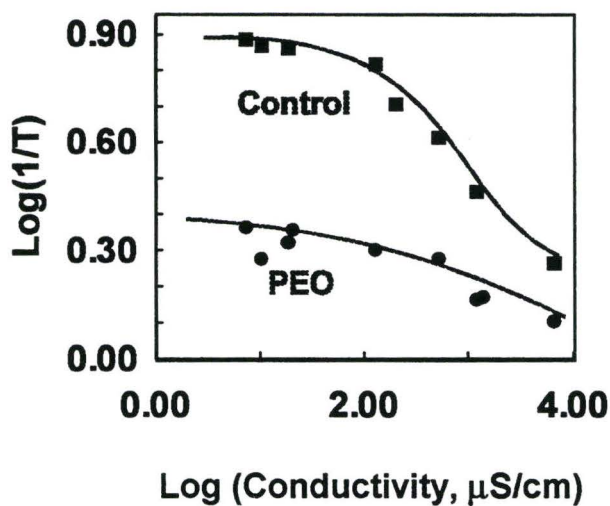


Figure 6. Effect of NaCl concentration, i.e. conductivity, on the latex flocculation. Experimental conditions: PEO-309 conc. = 2.0 mg/L; [PVPh] = 4 mg/L; MW of PVPh = 30,000; [Latex] = 50 mg/L; diameter of latex = 0.69 μm ; and, bleached fiber = 1.0 g/L; pH range of 3.2 to 3.8; T is transmittance, expressed in the fraction of T for pure water. $\log(1/T)$ is proportional to turbidity. solvent (water); conductivity unit is $\mu\text{s/cm}$.

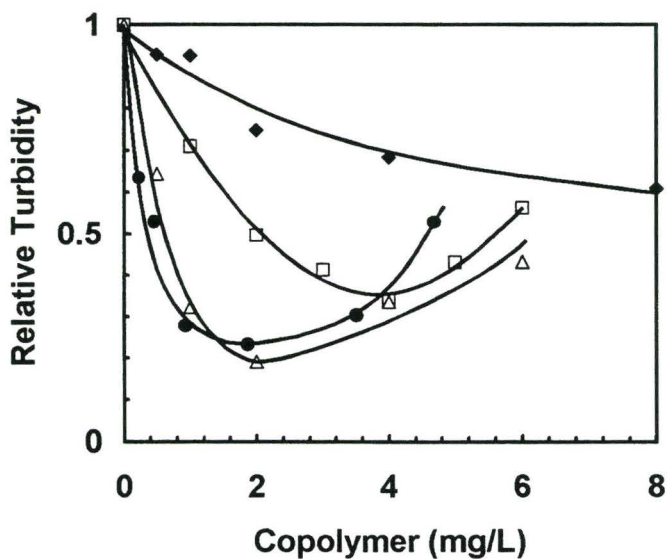


Figure 7. Effect of copolymer dosages on latex flocculation at constant concentration of phenolic resin 2.0 mg/L. [Latex] = 50 mg/L; diameter of latex = 0.69 μm ; and, bleached fiber = 1.0 g/L. pH = 5; [NaCl] = 0.002 N.

- 43-36: Copolymer containing 0.85 %(mole) MA-23 and MW 1.2×10^6
- ◆ 23-144: Copolymer containing 0.56 %(mole) A-40 and MW 7.6×10^5
- △ 56-48: Copolymer containing 0.47 %(mole) A-23 and MW 4.5×10^6
- 56-110: Copolymer containing 1.40 %(mole) A-23 and MW 3.7×10^6

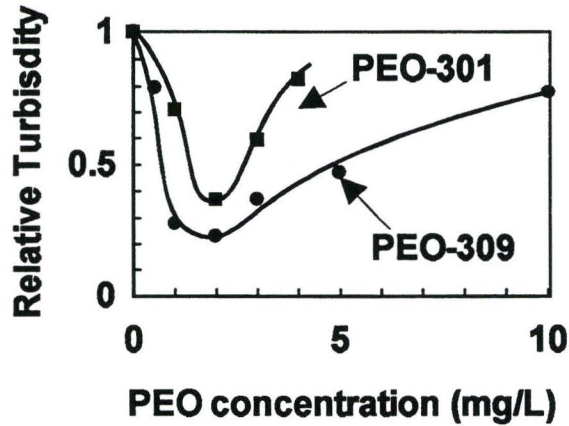


Figure 8. Effect of PEO dosages on latex flocculation at constant concentration of phenolic resin 2.0 mg/L. [Latex] = 50 mg/L; diameter of latex = 0.69 μm ; and, bleached fiber = 1.0 g/L. pH = 5; [NaCl] = 0.002 N.

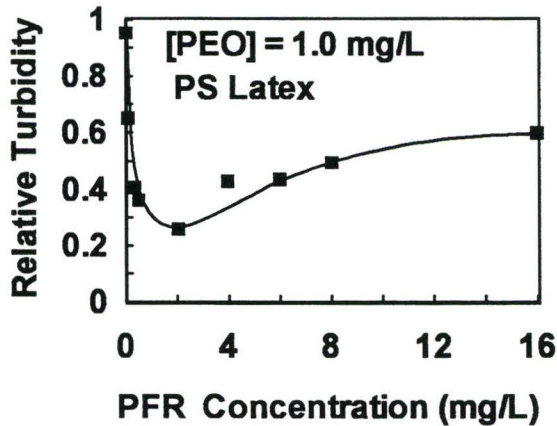


Figure 9. The effect of PFR dosages on the flocculation of latex at constant PEO-309 dosage (1.0 mg/L). Bleached fiber conc. = 1.0 g/L. [latex] = 50 mg/L; Diameter of latex = 0.69 μm . pH = 5.0 and [NaCl] = 0.002 N.

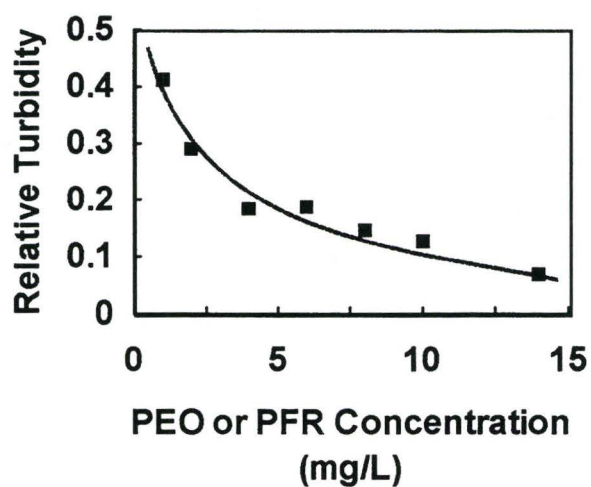


Figure 10. The influence of total polymers concentration on latex flocculation at constant ratio of PEO-309/ PFR = 1/1 (wt). [latex] = 50 mg/L; Diameter of latex = 0.69 μ m. pH = 5.0 and [NaCl] = 0.002 N.

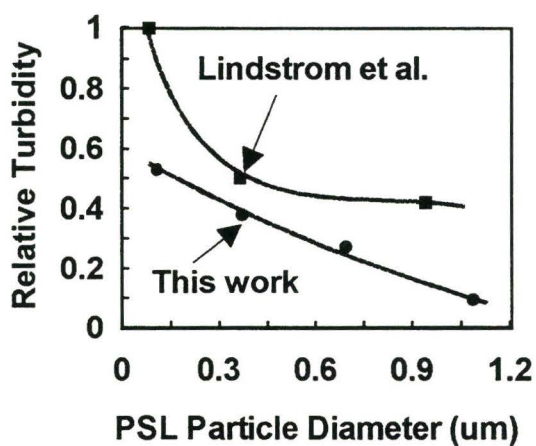


Figure 11. The influence of PS latex particle size on the latex flocculation. Experimental conditions for Lindstrom's data: cellulose fiber conc. = 1 g/L; [latex] = 25 mg/L; pH = 5.2; Polyox 301 conc. = 1.0 mg/L; and, [PFR] = 1.0 mg/L. Experimental conditions for this work: bleached fiber conc. = 1 g/L; [latex] = 50 mg/L; pH = 5.0; [NaCl] = 0.002 N; Polyox 309 = 1.0 mg/L; and, [PFR] = 2.0 mg/L.

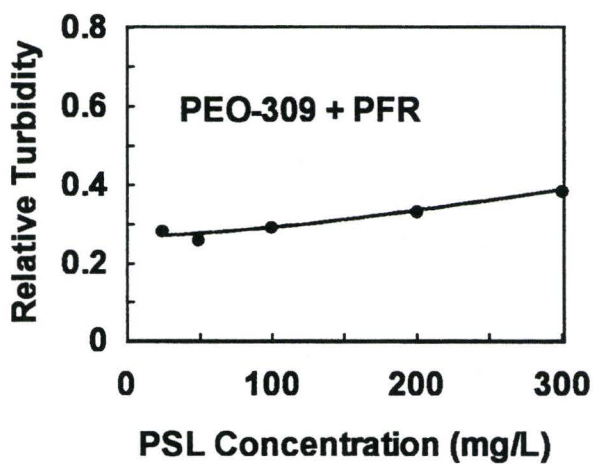


Figure 12. The effect of initial PS latex concentration on the flocculation. Diameter of latex = 0.69 μm . Experimental conditions: [PEO] = 1.0 mg/L; [PFR] = 2.0 mg/L; pH = 5.0; and, [NaCl] = 0.002 N. Bleached fiber concentration = 1.0 g/L.

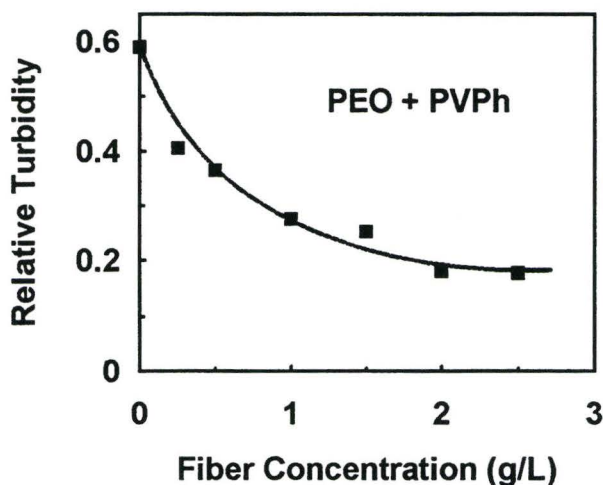


Figure 13. The effect of fiber concentration on latex flocculation. Cofactor used was polyvinyl phenol (PVPh-30) with MW of 30,000. Experimental conditions: [Latex] = 50 mg/L; Diameter of latex = 0.69 μm . [PEO] = 2.0 mg/L; [PVPh-30] = 6.0 mg/L; pH = 5.0; and, [NaCl] = 0.002 N.

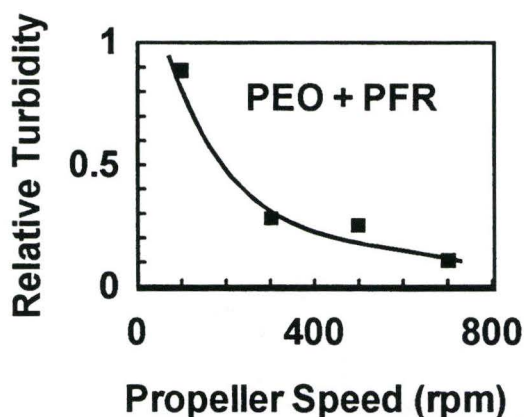


Figure 14. The effect of mechanical shearing on the latex flocculation induced by PEO/PFR in the absence of fibers. Experimental conditions: [Latex] = 50 mg/L; diameter of latex = 0.69 μm . [PEO-309] = 1.2 mg/L; [PFR] = 2.0 mg/L; pH = 5.0; and, [NaCl] = 0.002 N.

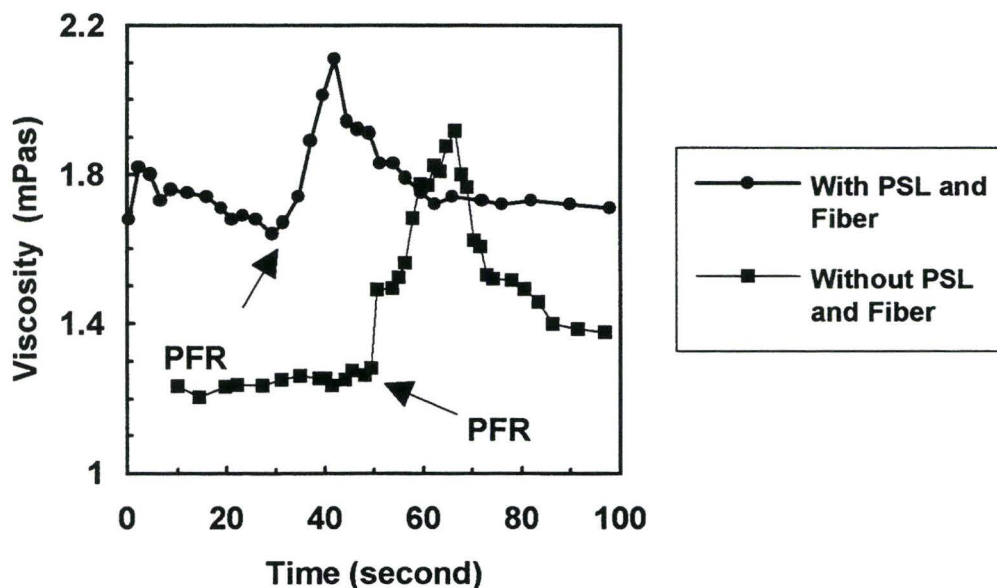


Figure 15. Effects of interpolymer association between PEO and PFR on the system viscosity in the presence and absence of the fibers and PSL.

Experimental conditions:

In the presence of PSL and fibers: PEO-309 conc. = 6.0 mg/L; [PFR] = 12 mg/L; pH = 5.0; temperature = $22 \pm 0.3^\circ\text{C}$; shear rate = 581 sec^{-1} ; and, constant shear strain. Adding PFR at time = 30 seconds.

In the absence of PSL and fibers: PEO-309 conc. = 60 mg/L; [PFR] = 60 mg/L; pH = 5.0; temperature = $22 \pm 0.3^\circ\text{C}$; shear rate = 146 sec^{-1} ; and, constant shear strain. Adding PFR at time = 50 seconds.

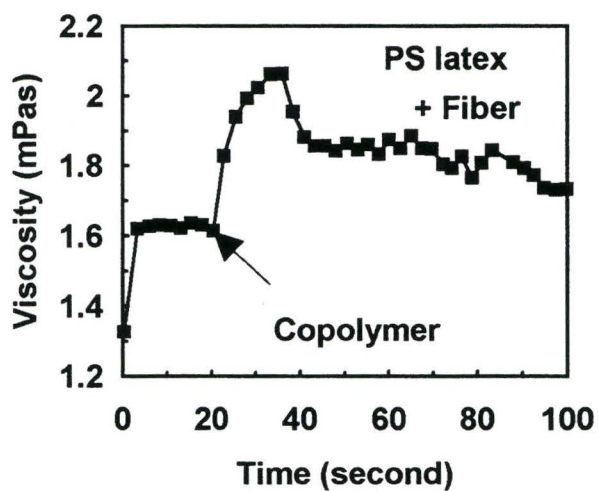


Figure 16. Effects of interpolymer association between copolymer (56-48) and PFR on the system viscosity in the presence of fiber and PS latex. Experimental conditions: copolymer conc. = 30 mg/L; [PFR] = 30 mg/L; pH = 5.0; temperature = $22.6 \pm 0.2^\circ\text{C}$; shear rate = 581 sec^{-1} ; and, constant shear strain. Adding copolymer at time = 20 seconds.

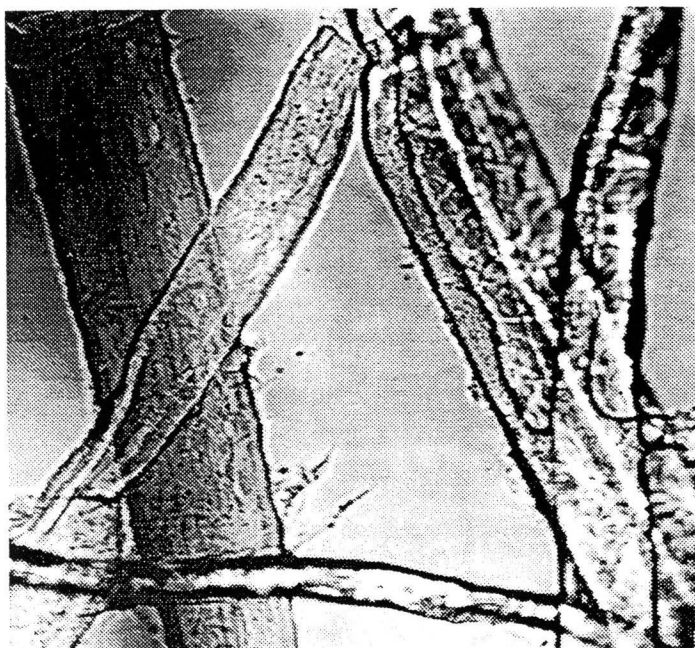


Figure 17 Control morphology of fiber and latex without polymer addition

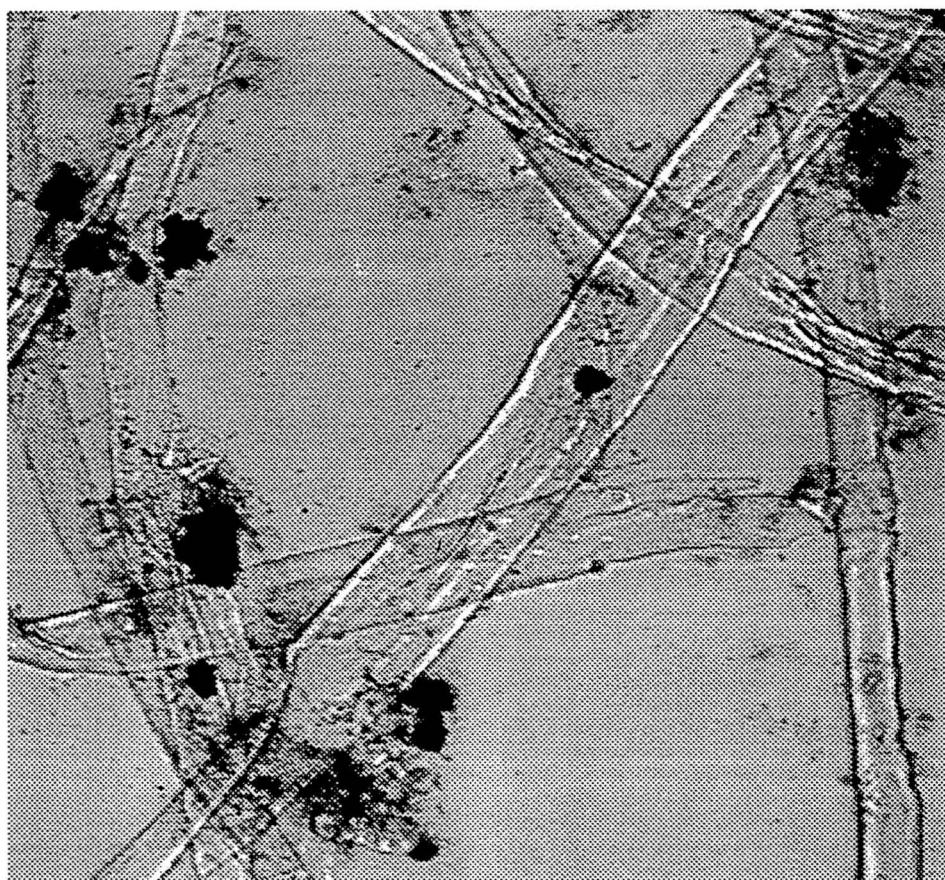


Figure 18 Flocs of PS latex formed by PEO-309/PFR in the presence of fibers

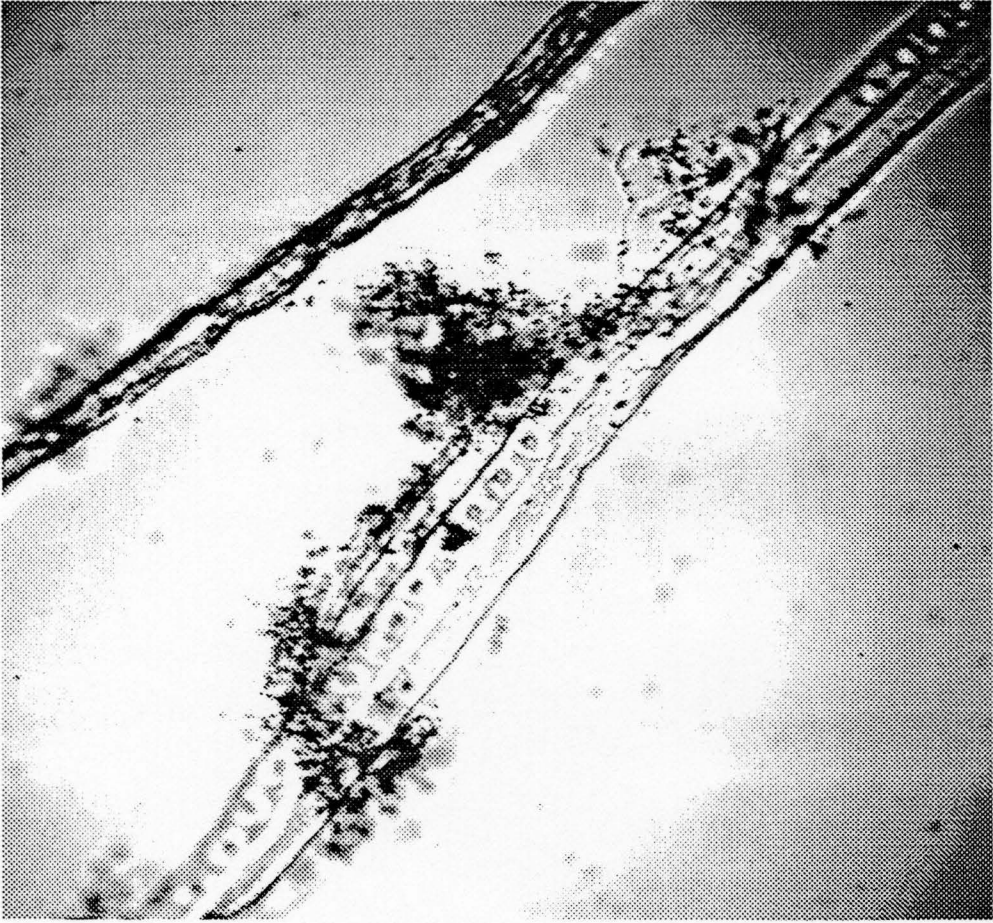


Figure 19 Spherical flocs formed by PEO-309/PFR



Figure 20 Spherical floes formed by copolymer 43-129/PFR

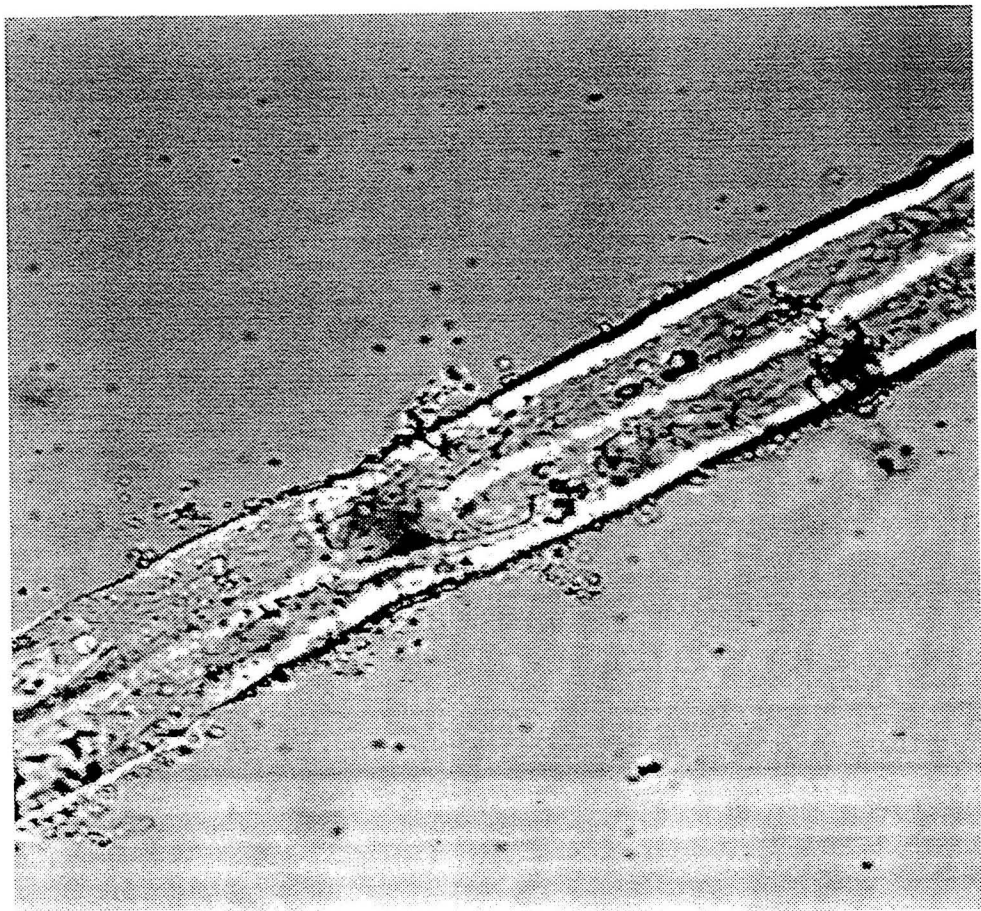


Figure 21 PS Latex deposited on the bleached fibers caused by addition of cationic copolymer XB-54-15-1. Polymer conc. = 32 mg/L.

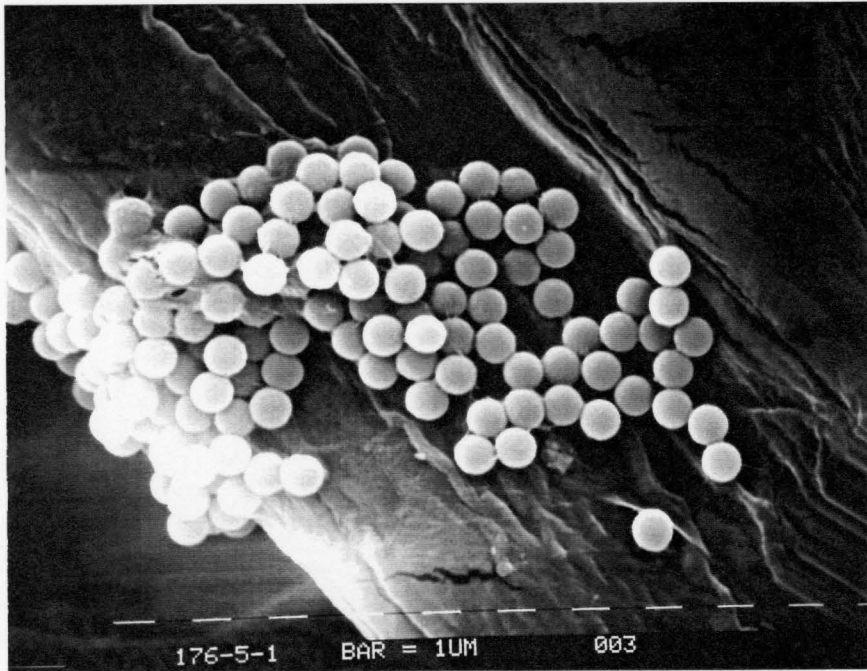


Figure 22. SEM observation on a single floc attached on the fiber. Floc was formed by copolymer 43-176 and phenolic resin. The copolymer with $MW = 4.3 \times 10^6$ and containing approximately 0.41 % (mol) MA-23. PS latex size = $1.09 \mu\text{m}$.

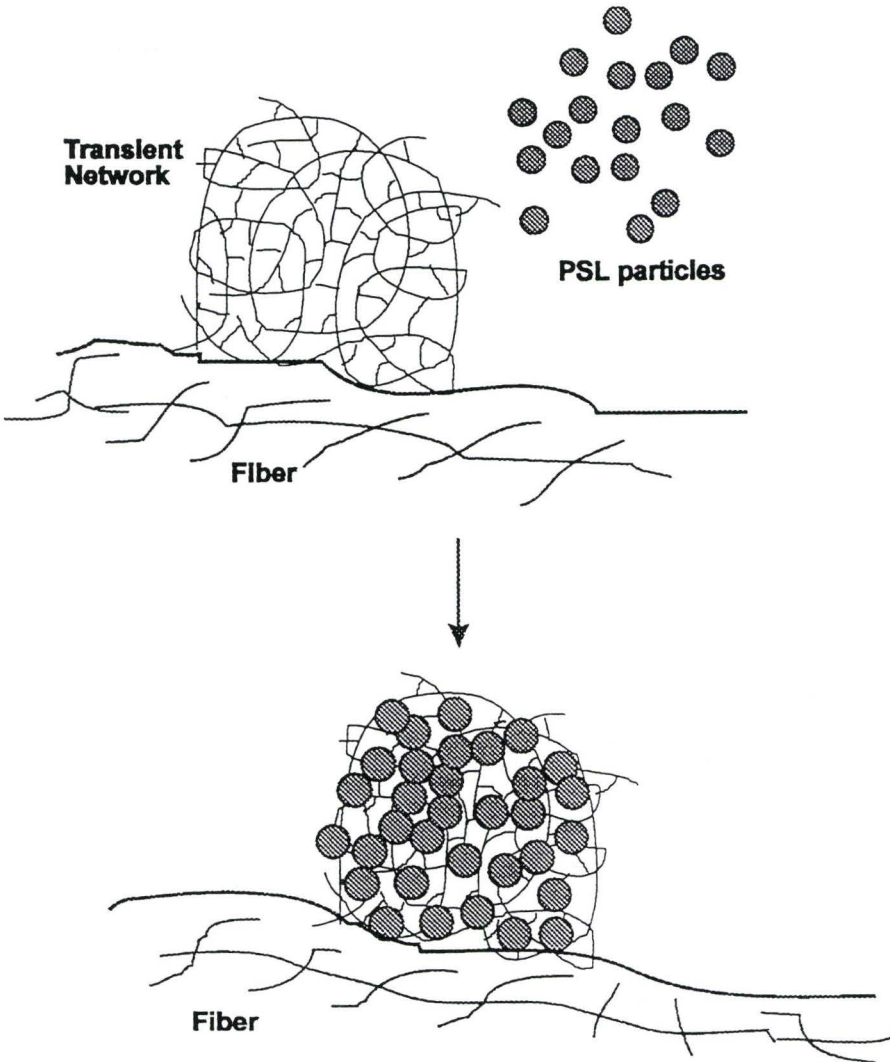


Figure 23 A schematic of network flocculation proposed by Lindstrom et al.

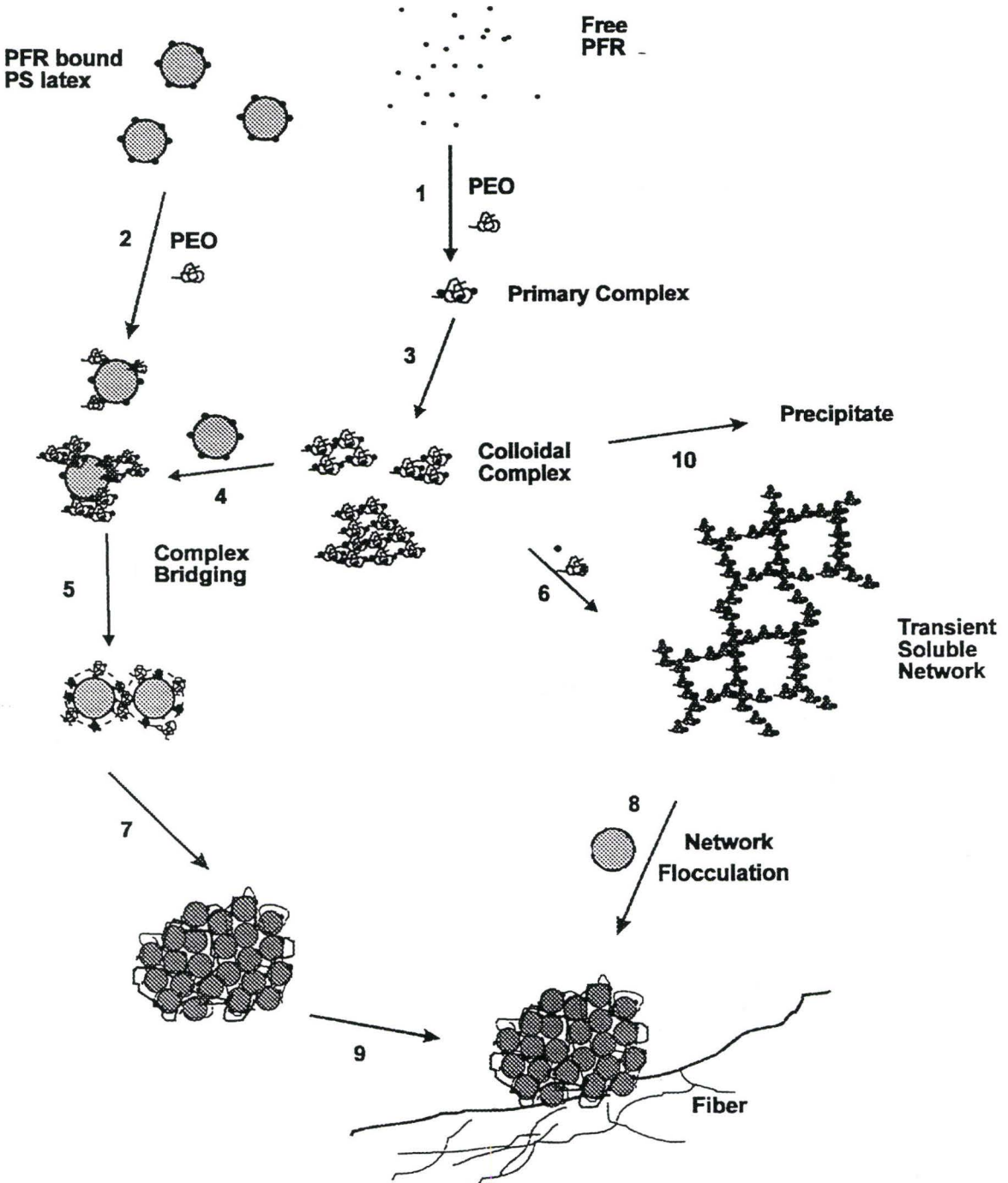


Figure 24 A schematic of the formation of the complex aggregates and flocculation processes

CHAPTER 5

Acrylamide-co-PEG Copolymers as Novel Retention Aids for Mechanical Pulp

ABSTRACT

Acrylamide and poly(ethylene glycol) (PEG) macromonomer copolymers, in conjunction with phenolic formaldehyde resin (PFR), were evaluated as novel retention aids for newsprint pulps. The first-pass retention (FPR) of the pulp fines was increased from 37 % without polymer to nearly 90 % with copolymer addition. This retention performance was similar to that of the high molecular weight poly(ethylene oxide) (PEO)/phenolic resin dual-polymer systems. However, the copolymers exhibited improved aging resistance and produced a higher fines retention than PEO ($M_w = 8$ million) under high shear stress.

The retention performance of the copolymers was very sensitive to the molecular weight. At high MW (e.g. 4.6 million), copolymer with only 0.69 % (mole) of PEG pendant chains as short as 9 repeat units gave 90 % fines retention. A new retention mechanism called complex bridging was proposed to explain the retention effects.

KEYWORDS: retention aids; fines; newsprint pulp, comb copolymer; PEO; acrylamide; macromonomer.

Introduction

Paper is formed by the rapid fibrillation of a dilute slurry of wood pulp fibers and mineral fillers. However, more than 50 % of the suspended solids are small enough to pass through the pores of the forming wire. Retaining these fine particles and fillers in the sheet during formation is important to the strength and optical quality of the product.^{1,2} This is accomplished by the addition of retention aids. Most mills³ nowadays use polymeric retention aids which cause the fine particles or fillers to stick on the fibers, or to form aggregates large enough to be filtered during papermaking. Polymer flocculants are not only used in the manufacture of fine papers but also in less expensive papers such as newsprint.

For bleached chemical pulps, cationic polymers are effective. However, for papermaking suspensions containing mechanical pulps, cationic polymers are not cost effective due to a large quantity of the dissolved and colloidal substances (DCS) originating from wood. The negatively charged DCS molecules form complexes with cationic retention aids causing excessive consumption of polymers. Since the origin of DCS-cationic retention aid interaction is electrostatic, nonionic polymeric retention aids, such as poly(ethylene oxide) (PEO), are less sensitive to the presence of DCS.

Pelton and co-workers were the first to report that very high molecular weight PEO was an effective retention aid in some mechanical pulps.⁴ It was discovered that some pulps had a crucial component of the DCS which worked in conjunction with PEO. This second component is herein called a cofactor. For pulps without an indigenous cofactor, phenolic resins or kraft lignin⁵ are

effective cofactors. PEO/phenolic resins dual-polymer retention systems have been widely used.^{6,7,8}

The advantage of using nonionic PEO as a retention aid for mechanical pulp is that DCS is not detrimental to the PEO performance. However, the problems with PEO use include: 1) it is susceptible to high shear stress⁹; 2) it undergoes oxidative degradation^{10,11}; and 3) it is relatively expensive because extremely high molecular weight of PEO is a low volume, specialty chemical which is only manufactured by a few companies. To solve these problems, novel copolymers with long polyacrylamide(PAM) backbone supporting short poly(ethylene glycol) (PEG) as pendant chains have been designed and synthesized in our laboratory.¹² Figure 1 illustrates the copolymer structure. The functional PEG pendant chains provide the associating sites for interaction with phenolic resins in the dual-polymer retention system.

The new copolymers were prepared by copolymerization of acrylamide and PEG (meth)acrylate macromonomers. The macromonomers had PEG pendant chains with 5 to 40 ether repeat units and a vinyl (-C=C-) reactive end group. Details on preparation of the copolymer have been presented elsewhere.¹²

The objectives of this work were: 1) to correlate the copolymer structures such as pendant PEG chain lengths copolymer composition and molecular weight to their performances as retention aids for newsprint pulps; 2) to compare the copolymer retention performance under high shear stress with that of conventional high MW of PEO; and, 3) to compare newsprint fines retention with flocculation of polystyrene latex which is a model colloid used in studying flocculation mechanism.

5.1 Experimental

Novel copolymers with long PAM backbone and short poly(ethylene glycol) (PEG) pendant chains were synthesized by copolymerization of acrylamide (Aldrich Co.) with PEG macromonomers.¹² The macromonomers used in the syntheses were supplied by Polysciences Inc. and Monomer-Polymer Inc. Chemical structures of the macromonomers are given in Figure 2. The acrylate based PEG macromonomers are designated herein as A-n, where n is the number of repeat units of the PEG pendant chain which was 10, 20 and 40. Similarly, MA-n is used to denote the methacrylate PEG macromonomers with n of 5, 9 and 23.

Phenol formaldehyde resin, CASCOPHEN C271 (40% wt solids content in aqueous solution), was supplied by Borden Chemicals. High molecular weight poly(ethylene oxide) samples were obtained from Union Carbide Corporation. PEO-301 (Polyox 301) had a weight average molecular weight (MW) of 4 million and PEO-309 (Polyox 301) had a MW of 8 million.

The newsprint pulp (Abitibi Price Co; Iroquois Falls) was based on 65 % stone groundwood and 35 % high yield sulfite pulps (70 % yield, acid sulfite). The pulps were made from a mixture of mostly black spruce plus a few percent jackpine and white spruce. Fines content of the pulp, defined as total fine particles capable of passing through the 76 μm mesh size stainless steel plate was 58 % (wt).

Evaluation of the copolymers as retention aids was carried out in a Dynamic Drainage Jar (Paper Research Materials Inc.) which was fitted with a perforated stainless steel plate containing 0.6 mm holes. The first-pass retention (FPR) was measured at 50°C with the propeller speed ranging from

250 to 1000 rpm. Detailed operating procedures were the same as described by Pelton et al.¹³ The standard deviation of FPR values was 5 - 8 % of the mean values based on 4 duplicates.

To prepare retention samples, 250 mL of newsprint pulps (about 1.0 % consistency) were diluted to 500 mL with water and heated up to 50°C. The pH of the pulp was adjusted to 5 by adding 1.0 mL 0.02 N HCl solution; 4.0 mL (0.025 % wt) phenol formaldehyde resin C271 was then added. Finally, 2.0 to 10. mL of PEO or the copolymer (0.025 % wt in aqueous solution) was added. Collection of the first 100 mL white water was initiated 2 minutes after PEO or copolymer addition.

Flocculation of the polystyrene(PS) latex particles was conducted by addition of small quantities(1.0 - 4.0 mg/L) of phenolic resin and PEO or copolymer in the presence of bleached fiber. 35 mL of Milli-Q treated distilled water and 10 mL bleached kraft pulp of 0.5 % consistency were added to a 50 mL test tube, followed by 1 mL 0.25 %(wt.) of PS latex. The pH of the solution was adjusted to about 5 by adding 0.1 mL 0.02 N HCl. Subsequently, 0.1 mL 1 N NaCl was also added to maintain the electrolyte at concentration of 10^{-3} M. Transmittance for the control was measured by using a UV spectrophotometer (Hewlett Packard) at a wavelength of 500 nm after 0.4 mL 0.25 %(wt.) phenolic resin had been added. Finally, copolymer or PEO aqueous solution at a concentration of 0.025 - 0.05 % was added with water to give a total volume of 50 mL and the mixtures was vigorously shaken for 3 to 5 seconds. After 1 hour sedimentation time, the supernatant was collected and filtered with a 200 mesh steel plate to separate suspended fiber fragments.

The supernatant transmittance was measured and relative turbidity was calculated by:

$$\tau_R = \log(100/T_C)/\log(100/T_S)$$

where T_C and T_S were transmittances of the control and the sample respectively. In the analysis of the data, it was assumed that the relative turbidity represented the fraction of latex not removed by flocculants.

5.2 Results

5.2.1 Influence of copolymer structure on fines retention

5.2.1.1 Effect of polymer molecular weight

Table 1 lists the first-pass retention of newsprint pulp in the presence of the copolymers or PEO with different MW. Phenolic resin was used for all measurements. More than 80 % of fines retention was reached by addition of the copolymers with a MW higher than 3.5 million. Polyox 309, the highest MW PEO homopolymer, produced similar fines retention. By contrast, the FPR without polymer addition was 37 %. The copolymer with a MW of about one million gave limited retention improvement whereas copolymers with MW lower than one million (such as sample 23-149) showed almost no improvement even though this sample contained more macromonomer A-10 (1.42 % mole). Therefore, flocculation appeared to be more sensitive to the MW of copolymers than the content of macromonomers.

First-pass retention values for PEO homopolymers also showed a strong dependence on polymer MW. FPR for PEO-301, which had a MW of 4 million, was 70%. When the MW of PEO was doubled, the FPR was increased to 83.7 %. This result has been reported by many other workers. For example, Pelton

et al.⁶ reported the effects of PEO molecular weight ranging from 1000 to 5 million on the pulp fines retention. The results indicated that only PEO with a MW of 5 million increased fines retention.

5.2.1.2 Effect of the copolymer composition

Figure 3 shows the first-pass retention as a function of the density of PEG pendant chains expressed as mole fraction of macromonomer in the copolymer. The two curves in Figure 3 represent results from two series of copolymers with different macromonomers. The curve labeled "low MW" in Figure 3 (□ points) was obtained using a series of copolymers from copolymerization of macromonomer A-10 and AM to give a molecular weight of approximately 1 million. When as little as 0.8 %(mole) A-10 macromonomer was incorporated into the copolymer, a significant enhancement of FPR was achieved. Further increase of the A-10 amount in the copolymers did not substantially increase FPR.

The curve labeled "high MW" in Figure 3 (■ points) was obtained using a series of copolymers based on MA-23 and AM to give a MW of approximately 4 million. The FPR increased to 75 % when only 0.8 % (mole) macromonomer was incorporated into the copolymer. From 0.8 % (mole) to 2.0 % (mole), FPR increased linearly up to 90 % as the composition of MA-23 in the copolymer increased. No further significant improvement was observed for composition above 2.0 % (mole) and up to 5.0 % (mole). Economics would dictate the use of the lowest levels of macromonomer possible. The scatter in the data points may reflect the difficulty in preparing a series of copolymers of varying composition but constant MW.

5.2.1.3 Effect of PEG pendant chain lengths

The influence of PEG pendant chain length in copolymers, obtained from copolymerization of MA-n macromonomer and AM, on FPR is shown in Figure 4 for two MW series. By comparing Figure 3, Figure 4 and the data in Table 1, it is clear that fines retention is much more sensitive to MW than the content of PEG or PEG pendant chain length at the higher levels of these quantities. Economics would dictate the use of the macromonomers with the shortest chain lengths.

It is remarkable that significantly increased retention was observed with a copolymer containing PEG chains with only 5 ether repeat units and located on average every 65 repeat units along the PAM backbone. Further increase in the PEG pendant chain length, for example, from 20 to 40, gave only limited improvement in the first-pass retention. The data point for zero chain length was for a polyacrylamide (PAM) homopolymer. As was shown years ago, high MW PAM is not an effective retention aid for newsprint pulps.⁴

5.2.2 Influence of polymer concentration

Figure 5 describes the influence of copolymer concentrations on FPR for newsprint pulps at constant phenolic resin concentration (= 2.0 mg/L). The copolymer used was 56-108 which contained approximately 0.69 % (mole) MA-9 PEG pendant chains and a MW of 4.6 million. Fines retention increased with copolymer concentration to a maximum of 90 % at a concentration of 2.0 mg/L. Beyond 2.0 mg/L, there was little increase in retention.

Fundamental studies on retention mechanism have been done in our¹⁴ and other¹⁵ laboratories using polystyrene latex and bleached kraft pulps as model systems. Latex flocculation is evaluated using a relative turbidity. The lower the relative turbidity, the more latex particles have been flocculated.

Latex flocculation results are compared with newsprint fines retention results in Figure 5. In both cases, optimal flocculation was obtained at 2 mg/L. Correlation between fines retention and latex flocculation is further illustrated by the results in Table 2. The two quantities were linearly related with a correlation coefficient of 0.995. Therefore, it seems likely that the mechanism described for latex flocculation with the copolymer will apply to fines retention.

5.2.3 Aging effect of the polymers in aqueous solution

Figure 6 shows the effects of aged aqueous polymer solutions on latex flocculation. The curves show the degree of latex flocculation induced by copolymer 43-129 or PEO as a function of storage time at room temperature. The copolymer showed no change in flocculation performance, whereas the PEO homopolymer gave poorer flocculation with longer storage time. Indeed, after having been stored for about 20 days, the PEO almost totally lost its ability to induce latex flocculation. By contrast, no significant decrease in latex flocculation was observed for the copolymer sample over the same period. Chemical changes associated with PEO aging have been described elsewhere.¹⁶

5.2.4 Effect of the shear stress on retention

There are several variables which affect FPR measurements using DDJ. These include propeller speed, screen hole size, pulp consistency and temperature. Generally, a low propeller speed, small screen hole size and high temperature resulted in higher first-pass retention for either the control or the samples with polymer addition. Details on the relationship between these factors and FPR results have been fully elucidated by Pelton et al.¹⁷ Of these

factors, propeller speed is the most important since this gives some indication of the sensitivity of the retention system to hydrodynamic forces.

Figure 7 shows the effect of propeller speed on the FPR of newsprint pulp. The data includes results from using copolymer 43-129, PEO-309 and the control (i.e. no polymer addition). Both copolymer and PEO gave lower retention at higher propeller speed. However, the copolymer seemed to be less sensitive to hydrodynamic forces than PEO homopolymer.

In Figure 8, retention performances for three kinds of copolymers, with different pendant chain lengths and MW, are compared as functions of DDJ propeller speed. Copolymer 56-108 with the highest MW (4.6 million) gave the best retention at low RPM but showed the largest decrease at high RPM. This behavior was similar to PEO-309. Sample 23-145, which had the lowest MW (1.1 million) among the three samples, exhibited no significant decrease in retention efficiency under higher shear rate compared with sample 56-108.

5.3 Discussion

First-pass retention measurements have provided an effective technique for characterizing polymer retention for mechanical pulps. However, systematic studies on the retention mechanism based on mechanical pulps appeared difficult firstly because the pulp fines were not well defined, and secondly, the retention results were not reproducible due to the DCS fraction changing with time and mills.¹⁸

The advantages of using PSL particles as model substances for pulp fines were that the PSL particles were well defined and that flocculation performance was reproducible. The properties of the latex, such as particle

size, size distribution and charge density, were not dependent on storage time due to the stability of the latex. Furthermore, the PSL was negatively charged which was the same as the charge carried in mechanical pulp fines. On the other hand, polystyrene latex in distilled in water is stabilized by electrostatic forces only whereas it has been shown that DCS from mechanical pulps can sterically stabilize colloidal particles.⁶ This effect occurs when wood based hydrophilic polymer adsorbed onto the particle surfaces. There are natural model colloids that contain some surface hydrophilic polymers such as polygalacturonic acid¹⁸ which has been used in some pulps.

5.3.1 Copolymer retention mechanism

5.3.1.1 Complexation between the copolymers or PEO and cofactors

Complex formation occurs as a result of hydrogen bonding which takes place between two interacting polymer components: copolymer and phenolic resin, or PEO and phenolic resin. This interpolymer association is crucial for dual-polymer flocculation systems. The copolymer or PEO alone showed no improvement on the retention of pulp fines unless the phenolic resin was present to achieve a synergistic effect. To illustrate the interpolymer association, the structure of the hydrogen bonding complex between phenolic resin and PAM-co-PEG copolymer, based on that proposed by Stack et al.,¹⁹ is given in Figure 9.

It has been found that complex association via hydrogen bonding not only occurs between the copolymer or PEO and synthetic phenolic resins. Some wood polymer species, such as dissolved and colloidal substances, may also complex with PEO or the copolymer to exhibit synergistic effects. Pelton et al.²⁰ attributed this synergism to the combining of polyether oxygens in PEO with the acidic protons on the secondary polymer molecule, which may form a precipitate.

Rahman and Tay²¹ suggested that the phenolic hydroxyl groups are primary adsorption sites for PEO bridging to take place. Leung and Goddard⁷ also claimed that bridging and flocculation are favored by phenolic sites on the fibers and fines.

An interesting result obtained in this work was that short PEG chains (MW ≤ 5000) did not form complexes with cofactor PFR. However, after PEG was bound to long PAM chains (i.e. the copolymer), a complex with PFR was formed. Polymer complexes were required for latex flocculation. To reach the same flocculated amount of latex particles, it was found that PEO homopolymers required chain lengths greater than 10^5 , whereas the minimum PEG pendant chain length in the copolymers needed only to be greater than 9 repeat units. Moreover, to reach the effective complexation for latex flocculation, the minimum amount of PEG pendant chains could be as low as 0.8 % (mole) of the backbones. This particular feature was attributed to the simultaneous interaction of the short PEG chains along the PAM backbone with the phenolic resin.²² In this case, PEG pendant chain length appeared less important to flocculation than the total polymer chain length and the density of pendant chains. Therefore, flocculation performance was not very sensitive to the PEG pendant chain length. The use of lower molecular weight macromonomer would, of course, lower the cost of the copolymer.

In most respects, latex flocculation and fines retention with copolymer/phenolic resin showed the same trends as the PEO/phenolic resin system. For example, the effects of MW, pH and polymer concentration were often similar. Consequently, the implication for the retention mechanism is the same for both the PEO/phenolic resin and the copolymer/phenolic resin systems.

5.3.1.2 Complex bridging retention mechanism

The mechanism of pulp fines retention induced by nonionic dual-polymer system has been discussed for years. One mechanism, called network flocculation, was first postulated by Lindstrom and Glad-Nordmark in 1984.²³ They proposed that flocculation is caused by a transient polymer network formed by the mutual interaction between two components. Cellulose fibers served to stabilize the transient network and sweep through it to gather colloidal particles.

Recent mechanistic studies indicate that a number of experimental phenomena cannot be interpreted by this network flocculation mechanism. Therefore, a novel flocculation mechanism called "complex bridging" has been proposed.¹⁴

Complex bridging occurs in several steps. A schematic description of complex bridging is given in Figure 10. Details for each step are discussed as follows:

- Step 1. Phenolic resins adsorb onto fine particles or filler surfaces or are free in solution.
- Step 2. As copolymer or PEO is added, they will either interact with the phenolic resins bound on the fine particles or the free phenolic resins in solution to form primary or colloidal polymer complexes.
- Step 3. Complex bridging occurs as copolymer or PEO bound particles collide with each other, or the colloidal polymer complexes adsorb onto more than two fine particles. In this case, the polymer complex thickness is beyond the electrostatic repulsion range for particle stabilization.
- Step 4. Fine particle aggregates are continuously colliding with each other and accumulate in flocs and then deposit on the fiber surfaces.

Important features for this mechanism include:

- 1) Adsorption of phenolic resins or complex aggregates on the fine particle surfaces is important whereas the polymer flocculant adsorption on the fiber surface is not necessary. Fine particles are aggregated into sufficiently large flocs which are then incorporated into the paper forming sheet by mechanical entrapment.
- 2) Two-step addition of polymer flocculant is crucial. If the copolymer or PEO were pre-mixed with PFR, and then added to the pulp, retention would be virtually nonexistent because the colloidal complex collapses to give an inactive precipitate.
- 3) In contradiction to the prediction of the network flocculation model small latex particles are also flocculated.

In complexation, one undesirable side reaction is the complex collapse resulting in a precipitate. This is important because the precipitated complex was not effective in inducing fines retention. Therefore, the flocculation must occur before the colloidal polymer complex collapses. Extremely high MW requirements have been found in both copolymer/cofactor and PEO/cofactor systems. The explanation proposed is that the rate of PFR penetration into PEO coils to give an undesirable precipitate is molecular weight dependent. That is, only the highest MW PEO or copolymer collapsed slowly enough to give an effective flocculation.¹⁴ In contrast, low MW PEO or copolymer produced colloidal complexes which collapsed too quickly for effective fines retention to occur.

5.3.2 Interpreting DDJ induced shear degradation of polymer

It has been found that shear rates in the DDJ are of the same order as those generated in the wet end.²⁴ Therefore, retention results obtained in this work under different shear rates in the DDJ provided a database to usefully evaluate the shear resistance of polymers. As expected, higher propeller speeds led to lower first-pass retention values. The reduction of FPR was possibly caused by shear degradation of polymers and/or weak flocs.

There have been a number of earlier reports concerning the shear degradation of water soluble polymers^{9,25} as well as solvent soluble polymers.^{26,27} In general, the stability of polymer chains to shear stress was characterized by measuring the change in polymer MW as a function of the shear stress applied.²⁸

Abdel-Alim and Hamielec²⁵ proposed an empirical correlation for the critical MW as a function of degrading shear stress for polyacrylamide with the formula:

$$M_c = 3.59 \times 10^8 / \tau^{0.41}$$

where M_c , the critical MW, is the maximum molecular weight present at the specified shearing condition and this was obtained by the GPC measurements. τ is the applied shear stress in dynes/cm². The relation indicates that only polymers with extremely high MW would be degraded. For example, M_c was 21.1 million at a τ value of 1000 dynes/cm².

The mechanism of mechanical degradation, proposed by Bueche's theory²⁹, indicated that chain scission only occurred in the central portion of the chain (instead of taking place randomly) where extending forces were maximum.

Buchholz and Wilson³⁰ used three types of viscometers to study the shear degradation of polymers with different ranges of MW at varying shear rates. They found that the higher MW polymers were more sensitive to shear stress. For example, when poly(acrylamide-co-sodium acrylate) with an extremely high MW of 14 million was exposed to very high shear rates ($= 10^6 \text{ s}^{-1}$) in a Savant viscometer, the polymer MW was decreased from 14 million to 4.7 million. However, no significant change in MW and viscosity was found for the same copolymer with a moderate MW ($= 141,000$).

Polymers used in the current work had high MW, such as PEO-309 with a MW of 8 million and copolymer 56-108 with a MW of 4.6 million. According to Bueche's theory and results of other workers, when these polymers are exposed to high shear stress, polymer degradation should be expected. By contrast, for a copolymer with a lower MW, chain degradation would not be so significant. This is at least in qualitative agreement with the retention behavior shown in Figures 7 and 8.

The shear rates generated in the DDJ did not reach values as high as 10^6 s^{-1} . This has been demonstrated by Tam Doo et al.³¹ who used laser anemometry to measure the mean velocity profile in the DDJ. They found that the maximum fluid shear rates, G_f , in the DDJ ranged only from 1×10^3 to $6 \times 10^3 \text{ (s}^{-1}\text{)}$ with propeller speeds ranging from 250 to 1000 rpm. Therefore, it is unlikely that individual polymer chains in solution would be broken based on Buchholz and coworkers' work discussed above. By contrast, Tanaka et al.³² found the scission of polymer chains occurred when the cationic polyacrylamide transferred from the latex and fiber surfaces to the pulp suspension under the shearing induced in DDJ at propeller speeds ranging from 1000 to 1500 rpm.

The cleavage of polymer chains was particularly observed for high MW cationic PAM (MW = 2.8×10^6). Since the shear conditions in this work were closer to those used by Tanaka et al., chain scission cannot be ruled out due to the use of extremely high MW PEO. On the other hand, the large decreases in FPR may partly result from the breakup of flocs by hydrodynamic forces.

Conclusions

The main conclusions of this work are:

1. Copolymers with long polyacrylamide backbones and short poly(ethylene glycol) pendant chains are novel and effective retention aids for high yield newsprint pulps.
2. To obtain the optimum retention performance, MW of the copolymers must fall between 3 to 5 million. With these MW, it is only necessary for the copolymer to contain 0.8 to 1.0 % (mole) PEG pendant chains. No significant effect of pendant chain length on retention performance was observed for pendant PEG chain lengths in the range 9 to 40.
3. These copolymers were more aging resistant and shear resistant than high MW PEO. Polymers of higher MW were more susceptible to shear in DDJ measurements.
4. Pulp fines retention follows the complex bridging flocculation mechanism which was postulated in our previous work.
5. PSL flocculation correlated linearly with FPR measurement at 250 rpm.

References

- ¹ Muller, F. and Beck, U., *Das Papier* **33**(10A): 89(1979).
- ² Bolmer, E., "Filling and Loading", *Pulp and Paper: Chemistry and Chemical Technology*, v.3, J.P. Casey, Ed., Wiley-Interscience, 1981.
- ³ Boucher, G. and Pikulik, I.I., *Pulp and Paper Can.* **95**(7): 41(1994).
- ⁴ Pelton, R.H., Allen, L.H. and Nugent, H.M., *Pulp and Paper Can.* **81**(1): 54(1980).
- ⁵ Pelton, R.H., Allen, L.H. and Nugent, H.M., U.S. Patent, 4,313,790 (1982).
- ⁶ Pelton, R.H., Allen, L.H. and Nugent, H.M., *Svensk Papperstidning*, **9**: 251(1980).
- ⁷ Leung, P.S. and Goddard, E.D., *Tappi*, **70**(7): 115(1987).
- ⁸ Unbehend, J.E., "Pulp and Paper Manufacture," 3rd. Ed. Joint Textbook Com. of Paper Ind.,v.6, 1992.
- ⁹ Wade, J.H.T. and Kumar, P., *J. Hydronautics*, **6**: 40(1972).
- ¹⁰ Crouzer, C. and Marchal, J., *Makromol. Chem.* **166**: 99(1973).
- ¹¹ Decker, C. and Marchal, J., *Makromol. Chem.* **166**: 155(1973).
- ¹² Xiao, H.N., Chapter 1, Ph.D. Thesis, McMaster Univeristy, 1994.
- ¹³ Pelton, R.H., Allen, L.H. and Nugent, H.M., *Pulp Paper Can.* **81**(1): 9(1980).
- ¹⁴ Xiao, H.N., Chapter 4, Ph.D. Thesis, McMaster Univeristy, 1994.
- ¹⁵ Lindstrom, T. and Glad-Nordmark, G., *J. Colloid Interface Sci.*, **97**: 62(1984).
- ¹⁶ Xiao, H.N., Chapter 3, Ph.D. Thesis, McMaster Univeristy, 1994.
- ¹⁷ Pelton, R. H., Allen, L.H. and Nugent, H., *Pulp Paper Can.* **80**(12): 25(1979).
- ¹⁸ Sundberg, K., Thornton, J., Ekman, R. and Halmbom, B., *Nordic Pulp and Paper Res.* **9**: 125(1994).
- ¹⁹ Stack, K.R. and Dunn, L.A. and Roberts, N.K., *Colloids and Surfaces*, **61**: 205(1991).
- ²⁰ Pelton, R. H., Allen, L.H. and Nugent, H., *Tappi*, **64**(11): 89(1981).
- ²¹ Rahman, L. and Tay, C.H., *Tappi*, **69**(4): 100(1986).
- ²² Xiao, H.N., Chapter 2, Ph.D. Thesis, McMaster Univeristy, 1994.
- ²³ Lindstrom, T. and Glad-Nordmark, G., *Colloids and Surfaces*, **8**: 337(1984).
- ²⁴ Pelton, R.H., *Tappi*, **67**(9): 116(1984).
- ²⁵ Abdel-Alim, A.H. and Hamielec, A.E., *J. Appl. Polym. Sci.*, **17**: 3769(1973).
- ²⁶ Nagashiro, W. and Tsunodam, T., *J. Appl. Polym. Sci.*, **21**: 1149(1977).

-
- ²⁷ Porter, R., Cantow, M and Johnson, J., J. Polym. Sci. **C16**: 1(1967).
- ²⁸ Yu, J.F.S., Zakin, L. and Pattenson, G.K., J. Appl. Polym. Sci., **23**: 2493(1979).
- ²⁹ Bueche, F., J. Appl. Polym. Sci., **4**: 101(1960).
- ³⁰ Buchholz, F.L. and wilson, L.R., J. Appl. Polym. Sci., **32**: 5399(1986).
- ³¹ Tam Doo, P.A., Kerekes, R.J. and Pelton, R.H., J. Pulp Paper Sci., **10**(4): 80(1984).
- ³² Tanaka, H., Swerin, A. and Odberg, L., J. Colloid Interface Sci., **153**: 13(1992).

Tables

Table 1. Effect of MW of copolymers on the FPR; Propeller speed at 250 rpm and at 50°C

Polymer	Types of Macro-Monomer	M _w of Polymers 1 x 10 ⁻⁶	Composition mol % of (M)A-n	FPR %
56-108	MA-9	4.6	0.69	90.6
43-129	MA-23	3.7	0.65	81.5
56-110	MA-23	3.7	1.40	87.5
23-145	A-40	1.1	2.84	61.3
23-157	A-10	1.3	0.71	58.7
23-149	A-10	0.7	1.42	40.5
Polyox-309	-	8.0	-	83.7
Polyox-301	-	4.0	-	70.0

Table 2. Correlation between PS latex flocculation and pulp fines retention. Propeller speed was maintained at 250 rpm in FPR measurement.

The fitted equation:
$$\text{FPR \%} = 129.5 - 161.3 \times \tau_R$$

(The regression was based on all data in the table except for the control)

Sample	Relative Turbidity τ_R	FPR %
56-108	0.25	90.6
43-129	0.29	81.5
23-145	0.42	61.3
23-157	0.44	58.7
Polyox-309	0.27	83.7
Polyox-301	0.37	70.0
Control	1.0	37.0

Figures

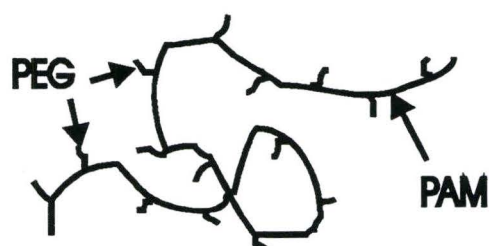
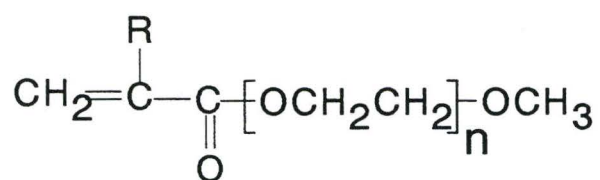


Figure 1. A schematic structure of long PAM having short PEG pendant chains to give a comb copolymers.



$n = 5 \text{ to } 40$

$\text{R} = \text{H}$ (A-n macromonomer)

or $\text{R} = \text{CH}_3$ (MA-n macromonomer)

Figure 2 Structure of PEG-(meth)acrylate macromonomer

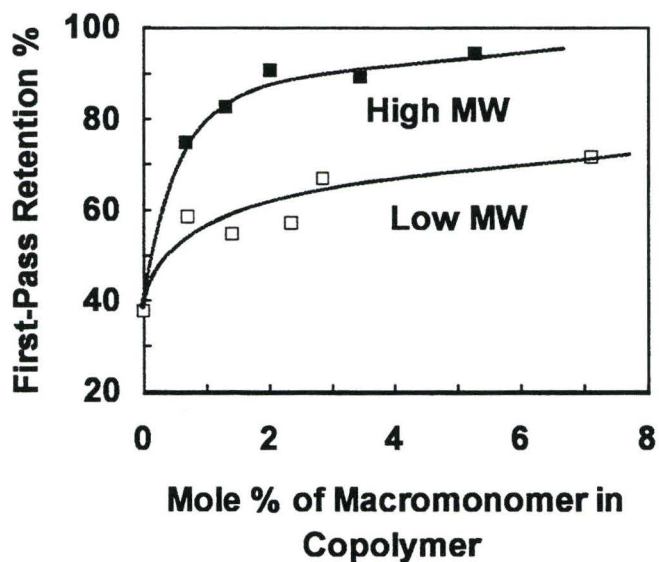


Figure 3. Effect of composition of copolymer on FPR. Lower MW copolymers (□ points) were obtained at 40°C with mole feed ratios of A-10 to AM from 1.0 to 10 %. High MW copolymers (■ points) were obtained at 25°C with mole feed ratios of MA-23 to AM from 1.0 to 7.0 %. The propeller speed was 250 rpm for both samples.

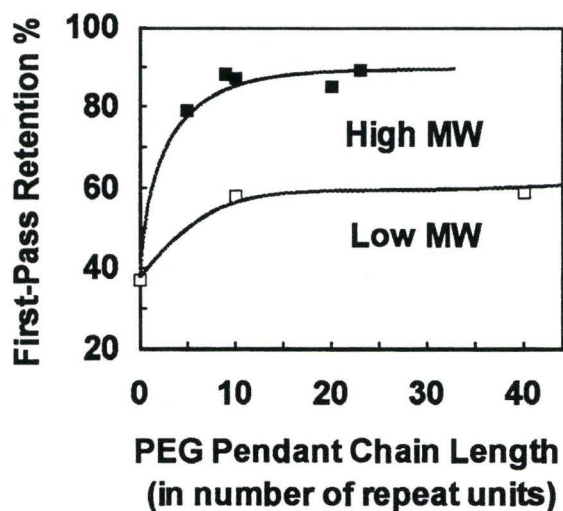


Figure 4. Effects of Pendant PEG chain lengths on FPR. Lower MW copolymers (□ points) were obtained at 40°C. High MW copolymers (■ points) were obtained at 25°C. The measurements were conducted at 50°C with propeller speed 250 rpm.

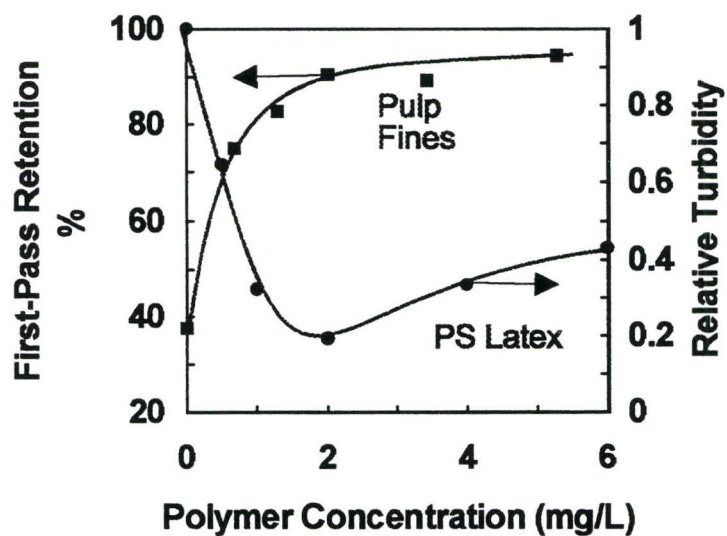


Figure 5 Effects of amounts of copolymer 56-108 addition on FPR (Squares). Phenolic resin was fixed at 2 mg/L. The measurements were conducted at 50°C with propeller speed 250 rpm. Circle points represent the effects of the copolymer amounts on the PS latex flocculation.

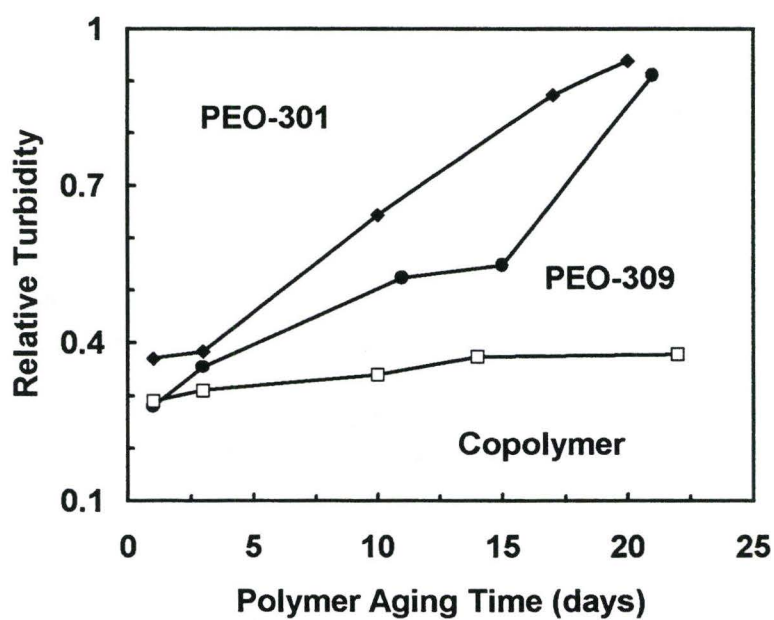


Figure 6. Effect of aging time on PSL Flocculation. Polymer concentration = 0.025 % (wt) and stored at room temperature; the copolymer sample was 43-129.

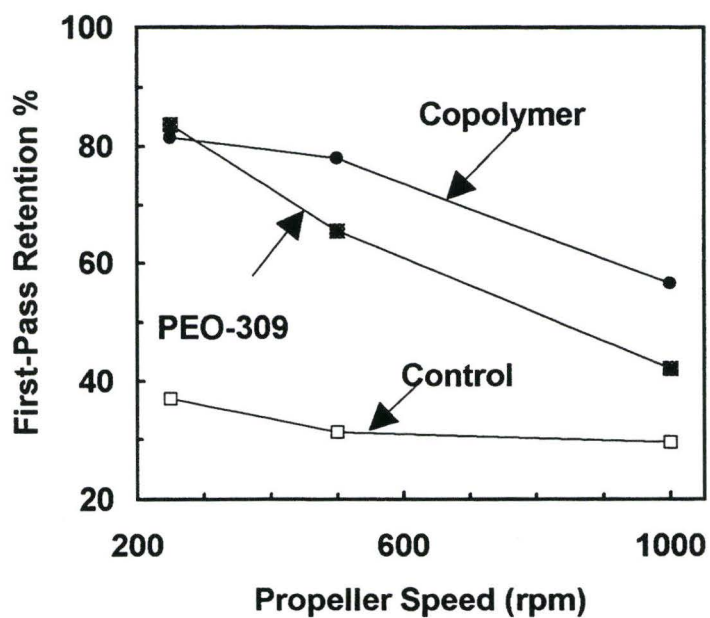


Figure 7. Effect of propeller speed on FPR for different polymers. copolymer sample was 43-129.

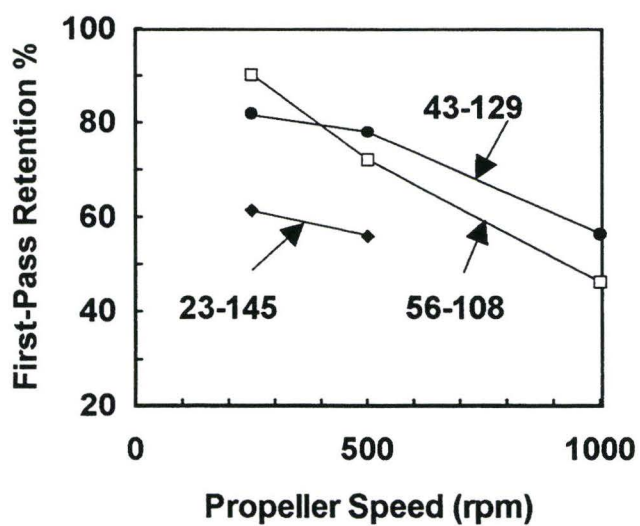


Figure 8. Effects of propeller speed on FPR for the copolymers with different PEG pendant chain lengths. FPR measurements were conducted at 50°C. The structure information regarding the copolymers are shown in Table 1.

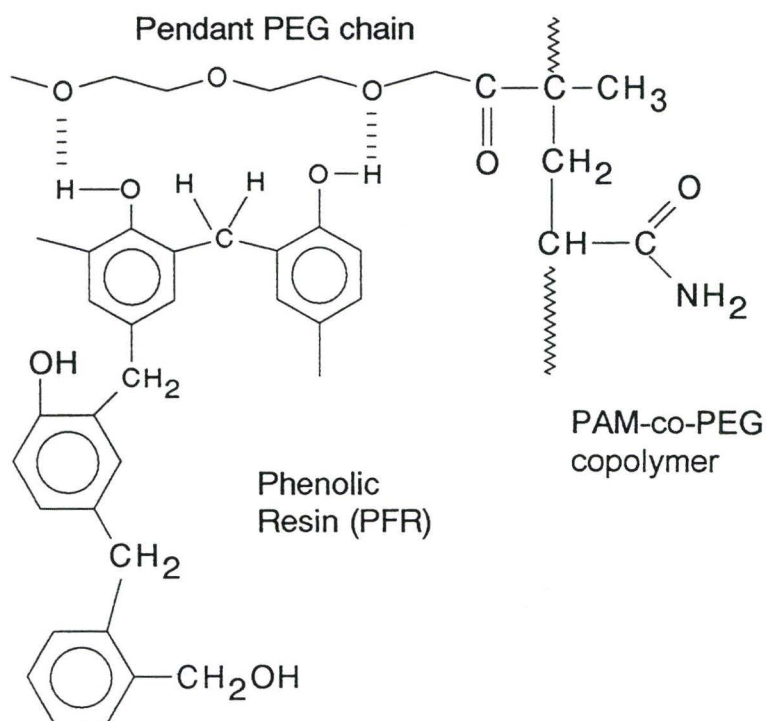


Figure 9 A schematic of hydrogen bonding between the PAM-co-PEG copolymer and phenolic resin

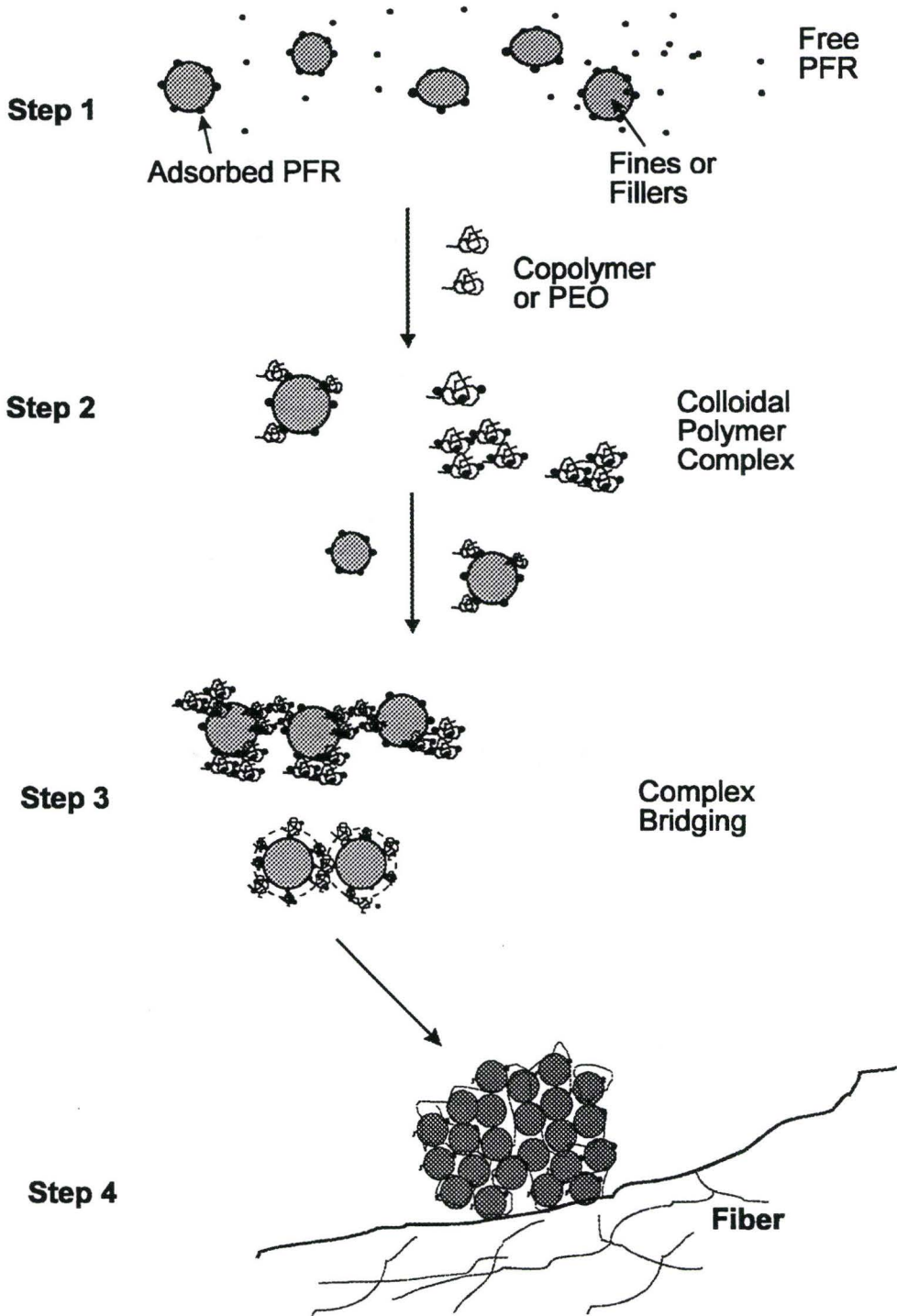


Figure 10 A schematic of complex bridging retention process

CHAPTER 6

Poly(p-vinyl phenol) as a Cofactor in Colloidal Particle Flocculation Induced by PEO Dual-Polymer Systems

ABSTRACT

Poly(p-vinyl phenol) (PVPh), was evaluated in conjunction with PEO as a flocculant for polystyrene latex. PVPh was an effective cofactor and performed similarly to a standard cofactor based phenol formaldehyde resin (PFR). Kinetic analysis indicated that flocculation was an orthokinetic collision process. Since PVPh in water was present as 1.3-1.7 μm microparticles, it was proposed that the fundamental flocculation mechanism for microparticulate flocculation systems is the same as for PEO/cofactor dual-polymer flocculants.

KEYWORDS: poly(vinyl phenol); PEO; flocculation; complexation; bridging; microparticles.

Introduction

High molecular weight polyethylene oxide (PEO) has been widely used as a flocculant in papermaking processes.¹ A cofactor capable of forming a complex with PEO is required for effective flocculation. Water soluble phenol

formaldehyde resin (PFR) is the standard cofactor for this purpose, however, some pulps contain natural cofactor. This comes from dissolved and colloidal substances (DCS) originating from wood pulps and containing phenol groups which complex with PEO. Other reported cofactors with PEO are kraft lignin² and tannic acid.³

The role of PFR is important. However, the interaction between PFR and PEO is not completely understood. PFR, which is prepared by condensation between phenol and formaldehyde using acid or base catalyses, has a complicated structure which may be branched and has a broad molecular weight distribution. Poorly defined PFR structure limits our ability to understand the details of the flocculation mechanisms with PEO/PFR molecules.

Described in this work is the use of poly(p-vinyl phenol) (PVPh)^{4,5,6} as an alternative to PFR for the PEO/PFR system. PVPh has been used as a proton donor polymer in polymer blends.⁷ However, there are no results on the interaction of the poly(vinylphenol) with PEO in water.

Flocculation studies of polystyrene latex with bleached kraft pulp mixture were conducted in this work using PEO as a flocculant and PVPh as a cofactor. The latex serves as a model for colloids in pulp; this has been used in our⁸ and other³ laboratories.

The objectives of this work were 1) to investigate the factors influencing the PVPh/PEO performance in flocculating latex particles, which included pH, PVPh concentration, PVPh molecular weight, salt concentration, addition order and dispersed state; 2) to compare the performance of PVPh with PFR in the latex flocculation; and 3) to reveal the possible flocculation mechanisms involved in the PVPh/PEO systems.

6.1 Experimental

6.1.1 Materials

Poly(p-vinyl phenol) (PVPh) was obtained from Polysciences Co. Three samples with different molecular weights were used. To distinguish the PVPh with different MW used in this work, PVPh with a MW of 1500-7000 was denoted as PVPh-1. Similarly, PVPh with a MW of 9000 was denoted as PVPh-9 and PVPh with a MW of 30,000 as PVPh-30. PVPh stock solutions were prepared in 50/50 % (wt) methanol/water solutions.

Potentiometric and conductometric titrations of PVPh were carried out with an ABU93 Triburette Radiometer (COPENHAGEN). The addition of acid, 0.1 N HCl, or base, 0.1 N NaOH, was automatically controlled by an Aliquot software. NaOH was added first and the forward titration was stopped at pH 11.5; HCl was added for the back titration to give 70 data points for the titration curves. The hydroxyl content of PVPh was calculated from the reverse titration curve. A titration curve for PVPh-30 is given in Figure 1. The results indicated that the dissociation of phenolic groups started at pH 11.4. The hydroxyl group content of PVPh-30 was 8.2 meq/g PVPh from the conductometric titration compared with a theoretical value of 8.33 meq/g PVPh.

The sizes of precipitated PVPh were measured using a BI-DCP (Disc Centrifuge Photosedimentometer) Particle Sizer (Brookhaven Instrument Co.). PVPh was initially dissolved in methanol at a concentration of about 1 - 3 % (wt), and then dispersed in water to give concentrations ranging from 200 to 700 mg/L which was used in determining the particle size. Homogeneous mode was adapted in measurement. The density of PVPh was assumed to be 1.05 g/cm³. The estimated particle sizes were based on volumement mean values.

Polyethylene oxide (PEO) (Union Carbide) was used as supplied. The weight average molecular weights (MW) of PEO-301 and PEO-309 were 4 and 8 million respectively, as indicated by the supplier. Methoxy polyethylene glycols (PEG) with MW of 2000 and 5000 were also supplied by Union Carbide.

Phenol formaldehyde resin (PFR) CASCOPHEN C271 (40 % in aqueous solution), a standard cofactor for dual-polymer retention systems, was supplied by Borden Chemical. Titration and molecular weight data have been given elsewhere.⁹ The concentrated PFR (40 % wt) was initially diluted to 3.7 % (wt) aqueous solution in the storage. This solution was further diluted to 250 mg/L for the flocculation experiments.

Polyacrylic acid with a MW of 2×10^5 , obtained from Polysciences, was also used as a cofactor.

Polystyrene latex (PSL) was synthesized in our laboratories. Details on preparation of PS latex have been reported elsewhere.⁸ The diameter of the latex particles was 606 nm (intensity average with 17 % of standard deviation), measured by dynamic light scattering using a fixed angle NICOMP 370 sub-micro particle Sizer (Pacific Scientific). Some flocculation experiments were conducted using a PSL size of 685 nm (weight average), measured using BLDCP.

The bleached fibers were softwood kraft pulp supplied by Noranda Forest Co.

6.1.2 Polystyrene latex flocculation

Flocculation of the PSL particles was induced by sequential addition of 0.4 to 1.0 mL polyvinyl phenol (0.05 % (wt) in 50/50 methanol/water mixture) and 0.2 to 0.6 mL PEO or copolymer aqueous solution (0.025 % (wt)). Measurements

of latex relative turbidity, τ_R , during flocculation were conducted on an UV Spectrophotometer and transmittance at a wavelength of 500 nm were recorded. The details have been described elsewhere.

6.2 Results

6.2.1 Factors influencing the latex flocculation induced by PVPh/PEO or copolymer systems

The extent of latex flocculation with the PEO/PVPh dual-polymer system depended upon pH, PVPh concentration, PVPh molecular weight, salt concentration, polymer addition order, state of PVPh dispersion and the presence of low MW PEG. These factors are described below.

6.2.1.1 pH Effects

It was found that the latex flocculation induced by the PEO/PVPh systems was pH sensitive. Figure 2 shows the extent of latex flocculation as a function of pH. The relative turbidity τ_R is roughly proportional to the concentration of latex not removed by flocculation. For PVPh-1 (10 mg/L) and PVPh-30 (6 mg/L), the maximum latex flocculation occurred at a pH 5. By contrast, when PVPh-1 was used at a low concentration (2.25 mg/L) and the PEO concentration was also reduced by half, the amounts of the latex removal were increased as the pH decreased.

6.2.1.2 PVPh concentration and MW effect

Latex flocculation with the three PVPh samples are compared with a standard cofactor PFR, as shown in Figure 3. The PEO concentration was 2

mg/L for all experiments. For PVPh-30, the flocculation efficiency increased as PVPh concentrations were increased up to 6 mg/L. Higher PVPh-30 concentrations caused an increase in relative turbidity from 0.3 to 0.35. For PVPh-1, the influence of its concentration on relative turbidity was similar to that for PVPh-30. For both polymers the optimal concentration was at 6 mg/L. By contrast, the optimal concentration for PVPh-9 was 2.3 mg/L. Relative turbidity increased as PVPh-9 concentration (> 2.3 mg/L) increased.

Under optimal concentrations, PVPh-30 was the most effective poly(vinyl phenol). However, phenolic resin C-271 was more effective.

There was no clear relationship between MW of PVPh and flocculation performance. This is illustrated in Figure 4 which compares the three polymers at two concentrations.

6.2.1.3 NaCl effect

Flocculation efficiency was measured as a function of ionic strength at pH 3.2 to 3.8. The ionic strength was varied by adding NaCl and conductivity was used to characterize the solution. The results are presented in Figure 5. It was found that the presence of salt induced latex coagulation without polymer addition. The results, as shown by the upper curve in Figure 5, indicate that $\log(1/T)$ decreased at $\log(\text{conductivity, } \mu\text{S/cm})$ values greater than 2 which corresponds to the critical coagulation concentration (CCC) for the latex. Below the CCC flocculation with PEO/PVPh appeared to be insensitive to ionic strength.

6.2.1.4 Effect of addition orders of flocculation components

Effects of the addition order in PEO/PVPh flocculation systems were evaluated and the results are summarized in Tables 1 and 2. Two series of

experiments were conducted. In the first series (Table 1), latex, water, salt, HCl and fibers were mixed first. Then, either PEO or PVPh was added. The results indicated that flocculation was not sensitive to the relative order of addition of PEO and PVPh. For example, at 6.0 mg/L concentration of PVPh-30, the relative turbidity was 0.64 when PEO (2.0 mg/L) was added last whereas the relative turbidity was 0.63 when PVPh was added last.

In the second series of experiments the latex was added at different steps. The results in Table 2 indicate that a much poorer flocculation occurred when the PS latex was added last. For example, about 67 % of latex particles were removed by PEO/PVPh-30 when latex was added before the flocculant. By contrast, only 40 % latex particles were removed when latex was added last. With PFR as cofactor the difference was more obvious ($\tau_R = 0.24$ vs. $\tau_R = 0.89$)

6.2.1.5 Dispersed state effect

Table 3 describes the influence of the states of the PVPh when added to the latex. It was found that if PVPh powder was directly added to water it gave a coarse aqueous suspension at pH values lower than 8. The suspension gave almost no flocculation. The concentrated PVPh solutions in methanol containing dispersed particles were prepared as described in the Table 3 caption. When this mixture of dissolved and colloidal dispersed PVPh was used, the latex removal amount was higher than with the coarse PVPh suspension. When PVPh was completely dissolved in methanol (concentration around 10 g/L) and then dispersed fiber/latex suspensions, good flocculation was observed with PVPh concentration of 20 mg/L in aqueous solution as shown in Table 3.

In an effort to prove that colloiddally dispersed PVPh were present in the flocculation experiments, the following experiment was conducted. A

concentrated PVPh solution (e.g. 29 g/L) in methanol was added to water to give a relatively diluted PVPh suspension (e.g. 0.69 g/L). The resulting suspension was split into two parts. The first was characterized with a disc centrifugal particle sizer whereas the second was used in a latex flocculation experiment. The two procedures were conducted as quickly as possible so it was reasonable to assume that the dispersion characterized in the disc centrifuge was the same as that in flocculation experiment. The particle size characterization for two PVPh samples are shown in Figure 6 and the results are summarized in Table 4.

Both PVPh concentrations were 6.0 mg/L in the flocculation experiments whereas the PEO-309 was 2.0 mg/L. The results also indicate that the smaller PVPh colloidal particles (1.3 μm from PVPh-9) produced slightly better flocculation ($\tau_R = 0.35$) than the larger PVPh particles (1.7 μm from PVPh-30, $\tau_R = 0.40$).

6.2.1.6 Effect of the presence of low MW PEG

Figure 7 shows the results of latex flocculation caused by PEO/PVPh-30 and PEO/PFR systems in the presence of low molecular weight polyethylene glycol (PEG). The MW of PEG in the PEO/PVPh system was 2000; MW of PEG in the PEO/PFR system was 5000. When the PEG concentrations were similar to those of PVPh or PFR, the flocculation efficiency was not influenced by PEG. When PEG concentration was higher than 10 mg/L, τ_R was increased from 0.4 to 0.6 for the PEO/PVPh-30 system.

6.2.2 PAA/PEO compared with PVPh/PEO system

Polyacrylic acid (PAA) is known to form hydrogen bond complexes with PEO. Therefore, PAA was evaluated as a cofactor. It was found that no

significant latex flocculation was induced. For example, with 10 mg/L concentration of PAA with MW of 10^5 and 2 mg/L concentration of PEO-309, the relative turbidity was close to 1.0. Thus, PAA has no activity as a cofactor.

6.2.3 Kinetic flocculation process

A kinetic characterization of PEO/PVPh induced flocculation process was conducted by following the system turbidity as a function of time. The results are given in Figure 8 along with some data from the literature. N_1 and N_0 herein were the number of latex particles after and before flocculation ($N_1/N_0 \cong$ relative turbidity). In PEO/PVPh system, N_0 was equal to 2.7×10^{11} which corresponded to the 50 mg/L latex concentration in 1 liter system under the assumption of monodispersed latex size. As indicated by the N_1/N_0 decay curve, the latex flocculation initially occurred very quickly. Most of latex (70 % wt) was removed within the initial 40 seconds. There was little further flocculation. By contrast, the bridging flocculation of PS latex, which was induced by the PEO homopolymer, was much slower (see Figure 8) even though the latex concentration was an order of magnitude greater.¹⁰

6.3 Discussion

6.3.1 Comparison between PVPh and PFR as cofactors

PVPh is a linear, well defined homopolymer which is only soluble in water at pH values greater than 9. For most of the flocculation experiments, PVPh was added to latex and fiber suspensions as a solution in methanol. By contrast, the

PFR used in this work was a branched water soluble polymer with a charge content of about 2 meq/g PFR which we believed to be due to carboxyl groups.

In spite of the differences in structures and properties, the behavior of PVPh as a cofactor was similar to that of PFR. Common features include:

1. Better flocculation was obtained at low pH. This suggested that hydrogen bonding was involved in the flocculation processes.
2. There existed optimum weight ratios between PEO and PVPh for flocculation which reflected bridging behavior in latex flocculation.
3. Flocculation was not sensitive to the cofactor MW.
4. Flocculation was not sensitive to the addition order of the cofactor and PEO.
5. Flocculation was complete a few second after the second polymer component was added.

Based on the above similarity it is proposed that the flocculation mechanism of PEO/PVPh was the same as that for the PEO/PFR system.

6.3.2 Flocculation mechanism

PVPh is a proton donor polymer so hydrogen bonding takes place between PVPh and PEO to give a complex. Figure 9 shows a possible structure of hydrogen bonding for the complex formation. A similar hydrogen bonding structure for PEO/PFR has been reported by Stack et al.¹¹

A novel flocculation mechanism called complex bridging flocculation has been proposed¹² to explain the PEO/PFR system. The mechanism proposes that flocculation occurs over several steps. First, a cofactor (e.g. PFR) adsorbs onto the latex surface with excess remaining free in the solution. Colloidally dispersed polymer complexes and complexes bound onto the latex surface are

formed when high MW PEO is added. Complex bridging occurs as PEO bound particles collide with each other.

In contrast to conventional bridging where bridging species is a single layer of adsorbed PEO, the bridging species in complex bridging can be a spectrum of PEO/cofactor sizes up to the same size scale as the latex particles.

Mixing of PEO with cofactor in water gives a precipitate. Thus, in the presence of colloids, the rate of colloidal flocculation must be greater than the rate of collapse of complex to a precipitate. The results in Table 2 show that if latex is added last, flocculation does not occur presumably because a precipitate has already been formed.

This work shows that the details of cofactor structure do not seem too important for flocculation. Whereas PFR molecules can adsorb onto the latex, it is unlikely that insoluble PVPh molecules will. Therefore, the important fraction of the cofactor is that which is dispersed in water.

6.3.3 Kinetic analysis

Complex bridging flocculation occurs much faster than does the conventional bridging induced by single high MW polymer. This has been demonstrated in this work (Figure 8). To further illustrate the difference between the complex bridging and conventional bridging, a preliminary kinetic discussion is given as follows.

It has been found that polymer induced colloidal particle flocculation is a complicated process. There are at least three important steps any of which may control the flocculation rate. They are: 1) adsorption of polymer on the particles; 2) re-conformation of polymer on the particle surface; and, 3) collision between particles adsorbed with polymers by bridging to produce the flocs.

In the bridging flocculation process as described by Pelssers et al,¹⁰ step 2 (i.e. re-conformation of polymer chains on the particle surface) occurred due to the low collision rate. As a result, flocculation did not occur until salt was added. In the present dual-polymer flocculation system, complexation produced high polymer attachment rate and the re-conformation of polymers had no effect on the flocculation rate. In this case, the flocculation rate may be determined by step 3, i.e. the collision among particles or between the particles and polymer colloidal complexes as described in the complex bridging mechanism.

In the absence of interparticular forces, the rate of flocculation is usually determined by the particle transport mechanism. Smoluchowski derived the following expression for the rate of diffusion controlled (perikinetic) flocculation of an initially monodispersed suspension of particles:¹³

$$-dn_T/dt = (4kT/3\mu)n_T^2 = k_F n_T^2 \quad (1)$$

where $k_F (= 4kT/3\mu)$ is the flocculation rate constant; n_T is the total particle concentration at time t ; T is the absolute temperature; μ is the viscosity, and k is the Boltzmann constant. For aqueous dispersions at 25°C, k_F equals to $6.13 \times 10^{-18} \text{ m}^3\text{s}^{-1}$. This equation can be integrated to give the n_T as a function of time:

$$n_T = n_o / (1 + k_F n_o t) \quad (2)$$

The characteristic flocculation time t_F , defined as the time in which the number of particles is reduced to half of the initial value (i.e. n_o), is given by:

$$t_F = 1/k_F n_o \quad (3)$$

Based on this equation and with the assumption of flocculation efficiency equal to one, t_F was 600 s for PEO/PVPh system and 71 s for the conditions described by Pelssers et al.¹⁰ at 25°C. However, the experimental data in Figure 8 indicated that t_F must be less than 10 s for the PEO/PVPh system and that t_F

must be higher than 2100 s for the PEO system. Therefore, analysis based on the perikinetic flocculation appeared to be invalid for the both systems.

Our pervious work showed that the extent of flocculation with the PEO/PFR system increased with hydrodynamic stress.⁸ This implied that the complex bridging flocculation followed an orthokinetic collision process instead of the perikinetic process.

In orthokinetic flocculation, fluid motion is the particle transport mechanism. The flocculation rate can be enormously increased by intensifying shearing. In this case, characteristic flocculation time t_F is given by:¹³

$$t_F = 3/16Gn_0a^3 \quad (4)$$

where n_0 is the initial number concentration of particles; a is the particle radius of the monodispersed particles; G is the shear rate.

The ratio of collision rate constants for the early stages of orthokinetic and perikinetic flocculation is given as follows:¹³

$$k_F(\text{ortho})/k_F(\text{peri}) = 4G\mu a^3/kT \quad (5)$$

The ratio equals one for particles with radii of about 0.5 μm at a low shear rate of 10 s^{-1} . However, this ratio should be much greater than one at high shear rates. Based on equations (5) and (3), the shear rate required in the present PVPh/PEO system can be estimated as follows:

At the same initial number of latex particles,

$$k_F(\text{ortho})/k_F(\text{peri}) = t_F(\text{peri})/t_F(\text{ortho}) \quad (6)$$

$t_F(\text{peri}) = 600$ s and $t_F(\text{ortho}) = 10$ s, which were previously discussed. Thus,

$$k_F(\text{ortho})/k_F(\text{peri}) = 60$$

This ratio was 1.0 where $G = 10 \text{ s}^{-1}$ and $a = 0.5 \text{ }\mu\text{m}$, as mentioned above. Therefore, when the latex radius is $0.3 \text{ }\mu\text{m}$ (as used in this work), shear rate G must be as high as $2.8 \times 10^3 \text{ s}^{-1}$ to keep the ratio of $k_F(\text{ortho})/k_F(\text{peri}) = 60$.

6.3.4 Microparticle flocculation system

Microparticulate systems emerged on the market as a new type of dual polymer retention aid (i.e. flocculant) in the last decade.¹⁴ There are two microparticulate retention systems most often referred to in the literature. One is bentonite plus high molecular weight polyacrylamide or PEO; another is colloidal silica plus cationic starch system. Additionally, the aluminum based microparticulate retention aids system, consisting of anionic colloidal aluminum hydroxide/cationic starch, has been reported.¹⁵ Since microparticulate systems have only been in use for about 10 years, there is a lack of systematic scientific information on the mechanism of action for these systems. To date, only a few experimental papers on microparticulate retention aid systems have been published.^{16,17,18,19}

PVPh samples used in this work were not water soluble at neutral or acidic pH conditions. After the PVPh in methanol/water mixture was added to the flocculation system, micrometer sized PVPh particles were produced (see Table 4). Indeed, the PVPh particle size was comparable the bentonite particles in polyacrylamide/bentonite system.

The basic principle in microparticulate retention systems is that the bridging formation takes place with the microparticles instead of the cationic polymer segments. For example, in the PAM/bentonite system, bentonite particles are considered to act as the bridges between adjacent sites on the PAM chains attached to the fines in pulp stock suspensions.²⁰ The rigidity of

microparticles allows for a reversible flocculation process. Under high shear forces, flocs are broken down at the particle-fiber interface instead of fracturing the bentonite particles.

Similarly, in PEO/PVPh system, PEO could adsorb onto the latex surface (this has been confirmed from our previous experiments). The latex bridging took place with the PVPh microparticles via complexation between the PVPh and the PEO bound to latex. At the same concentration, smaller PVPh particle size produced higher number of macroparticle which may enhance the interaction possibility with the PEO. Therefore, the induced flocculation was slightly better for 1.3 μm PVPh particles than the PVPh with diameter of 1.7 μm .

It has been shown that the PEO/PFR system behaves like the PEO/PVPh system in which PVPh is present as colloidal particles. Perhaps all microparticulate retention systems function by complex bridging flocculation. Furthermore, the fact that one of the components is a particle is irrelevant. Instead, the key property may be that the rate of complex collapse to a precipitate must be slower than the rate of flocculation.

6.3.5 PAA cofactor

For dual-polymer systems, flocculation requires interpolymer association. However, complexation may not result in flocculation. PEO/PAA is known to form water soluble hydrogen bonded complexes. However, no latex flocculation was induced by this system. The possible reasons for this included: 1) PAA cannot be adsorbed onto the latex surface due to the electrical repulsion arising from both the PAA and latex being negatively charged; 2) PAA is too soluble to form microparticles.

Conclusions

The main conclusions from this work are:

1. PVPh, a well-defined linear polymer, was an effective cofactor for PEO flocculation.
2. At pH < 10, PVPh was insoluble. However, it was an effective cofactor if present as colloiddally dispersed particles.
3. No significant differences were observed in the flocculation behaviors of PEO/PVPh and PEO/PFR, indicating that the flocculation mechanisms were the same.
4. Kinetic analysis indicated that the complex bridging flocculation induced by PEO/PVPh dual-polymer systems was an orthokinetic collision process.
5. Since the effective form of PVPh in water was as microparticles, perhaps the fundamental flocculation mechanism for microparticular flocculation systems is the same as for PEO/cofactor dual-polymer flocculants.
6. The poor flocculation results with polyacrylic acid as cofactor show that hydrogen bonding between cofactor and PEO, although necessary, is not sufficient for flocculation.

References

- ¹ Pelton, R. H., Allen, L.H. and Nugent, H., *Tappi*, **64**(11), 89(1981).
- ² Pelton, R. H., Allen, L.H. and Nugent, H., U.S. Patent, 4,313,790 (1982).
- ³ Lindstrom, T. and Glad-Nordmark, G., *Colloids and Surfaces*, **8**, 337(1984).
- ⁴ Pomposo, J.A., Cortazar, M. and Calahorra, E., *Macromolecules*, **27**, 252(1994).
- ⁵ Moskala, E.J., Howe, S.E., Painter, P.C. and Coleman, M.M., *Macromolecules*, **17**, 1671(1984).

-
- ⁶ Suzuki, T., Pearce, E.M. and Kwei, T.K., *Polym. Commun.*, **33**, 198(1992).
 - ⁷ Zhang, X., Takegoshi, K. and Hikichi, K., *Macromolecules*, **24**, 5756(1991).
 - ⁸ Xiao, H.N., Chapter 2, Ph.D. Thesis, McMaster University 1994
 - ⁹ Xiao, H.N., Chapter 3, Ph.D. Thesis, McMaster University 1994.
 - ¹⁰ Pelssers, E.G.M., Cohen Stuart, M.A. and Fler, G.J., *Colloids and Surfaces*, **38**, 15(1989).
 - ¹¹ Stack, K.R. and Dunn, L.A. and Roberts, N.K., *Colloids and Surfaces*, **61**, 205(1991).
 - ¹² Xiao, H.N., Chapter 4, Ph.D. Thesis, McMaster University 1994.
 - ¹³ Gregory, J., *Critical Reviews in Enviro. Control*, **19**, 185(1989).
 - ¹⁴ Langley, J.G. and Cutts, P.K. "Dewatering Additives of the 1990's", *Tappi Papermakers Conference*, 377 (1990).
 - ¹⁵ Lindstrom, T. Hallgren, H, and Hedborg, F., *Nordic Pulp and Paper Res J.*, **4**, 99(1989).
 - ¹⁶ Swerin, A., Sjodin, U. and Odberg, L., *Nordic Pulp and Paper Research J.*, **8**, 389(1993).
 - ¹⁷ Andersson, K, Sandstrom, A., Strom, K and Barla, P., *Nordic Pulp and Paper Research J.*, **1**(2), 26(1986).
 - ¹⁸ Wagberg, L., Zhao, X.P., Fineman, I. and Li, F. N.L, *Tappi*, **73**(4), 177(1990).
 - ¹⁹ Wall, S., Samuelsson, P., Degerman, G., Skoglund, P and Samuelsson, A., *J. Colloid Interface Sci.*, **151**, 178 (1992).
 - ²⁰ Unbehend, J.E., "Pulp and Paper Manufacture" v.6, p.135, *The Joint Textbook committee of the Paper Industry* 1992.

Tables

Table 1. Effects of addition modes on the latex flocculation induced by PEO-309/PVPh-30. Experimental conditions: pH = 5.0, [NaCl] = 0.002 N, the bleached fiber conc. = 1.0 g/L. PSL concentration = 50 mg/L and size of 0.61 μm .

1st Addition	2nd Addition	PVPh Dosage (mg/L)	Relative Turbidity
PVPh-30	PEO	6	0.64
PEO	PVPh-30	6	0.63
PVPh-30	PEO	10.8	0.48
PEO	PVPh-30	10.8	0.51

Table 2. Effect of addition order of PEO, PVPh and latex on the flocculation. Experimental conditions were the same as in Table 1.

1st Addition	2nd Addition	3rd Addition	Relative Turbidity
PS latex	PEO	PVPh-30	0.33
PEO	PVPh-30	PS latex	0.60
PS latex	PEO	PFR C271	0.24
PEO	PFR C271	PS latex	0.89

Table 3. The effect of dispersion state of PVPh-1 on the latex flocculation. Mixture of dissolved and colloidal dispersed PVPh was made by adding 4.45 mL 0.445%(wt.) of PVPh in methanol to 40 mL water led to a PVPh concentration of 200 mg/L.

PVPh (mg/L)	PEO-309 (mg/L)	PVPh stock solution	Relative Turbidity (τ_R)
40	5	coarse suspension	0.89
20	5	solution in MeOH	0.18
200	10	colloidal dispersed	0.40

Table 4. The effect of PVPh dispersed particle size on the flocculation of latex. PVPh was dissolved in MeOH, then dispersed in water. PEO-309 concentration was 2 mg/L.

PVPh samples	Conc. in MeOH (g/L)	Conc. in water (mg/L)	Volumement mean particle size (μm)	Conc. in flocculation (mg/L)	Relative Turbidity (τ_R)
PVPh-9	29.4	690	1.3 ± 0.2	6	0.35
PVPh-30	17.6	264	1.7 ± 0.6	6	0.40

Figures

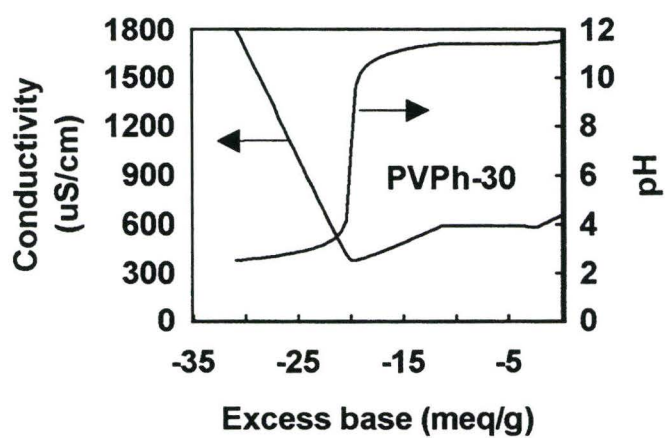


Figure 1 Potentiometric titration of PVPh-30. Initial total volume = 150 mL, PVPh concentration = 0.29 g/L.

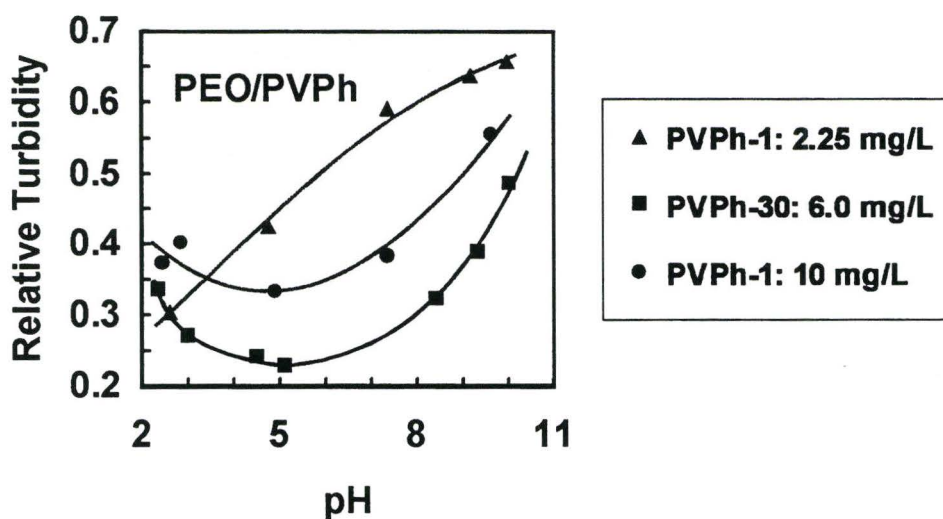


Figure 2 The pH effect on flocculation of latex for PEO-309/PVPh systems. [latex] = 50 mg/L; bleached fiber = 1.0 g/L. PVPh-1 was added at two levels. One was PEO/PVPh-1 = 1.0 /2.3 mg/L and [NaCl] = 0.002 N. Another was PEO/PVPh-1 = 2/10 mg/L. For PEO/PVPh-30 system [NaCl] = 0.01 N. [PEO] = 2.0 mg/L for all experiments.

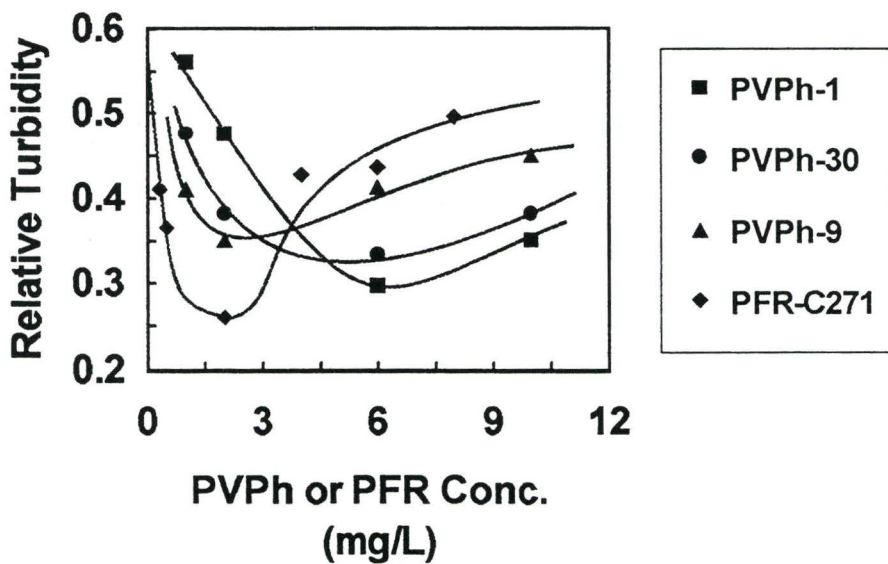


Figure 3 The effects of PVPh dosages on latex flocculation in the PEO/PVPH system. [PEO-309] = 2 mg/L. pH = 5.0, [NaCl] = 0.002 N. The bleached fiber 1.0 g/L, and [Latex] = 50 mg/L.

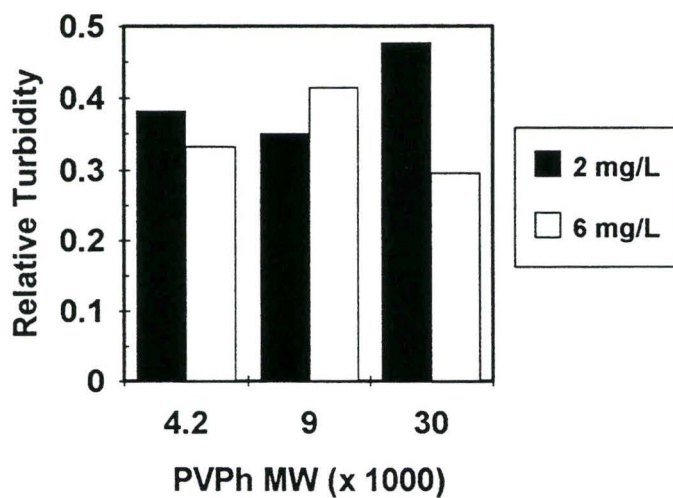


Figure 4 The effect of PVPPh MW at two level addition amounts on latex flocculation in the PEO/PVPH system. pH = 5.0, [NaCl] = 0.002 N. The bleached fiber 1.0 g/L, and [Latex] = 50 mg/L with size of 0.69 μm .

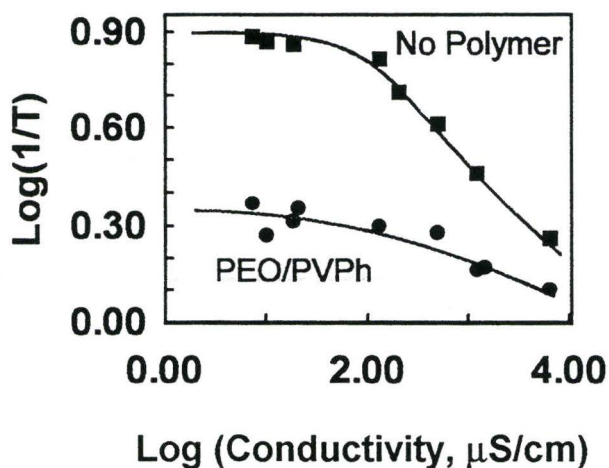


Figure 5 Effect of conductivity on the latex flocculation. Conductivity was varied by NaCl addition. Experimental conditions: [PEO-309] = 2.0 mg/L; [PVPh-30] = 4 mg/L; [Latex] = 50 mg/L; bleached fiber = 1.0 g/L; and pH ranged between 3.2 to 3.8. T is transmittance measured against a water blank.

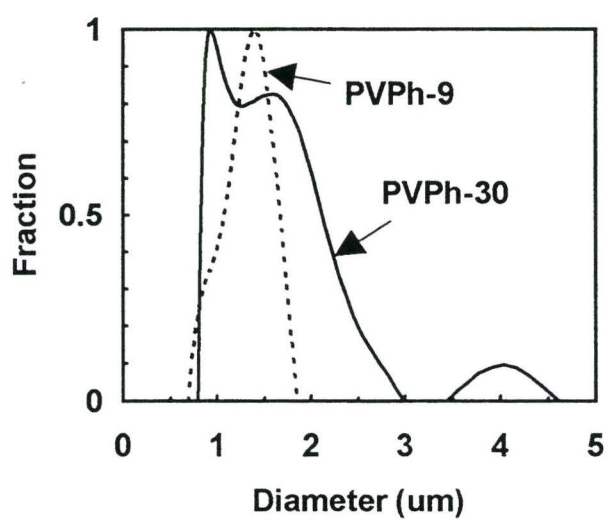


Figure 6. Characterization of PVPh particle size in dispersion

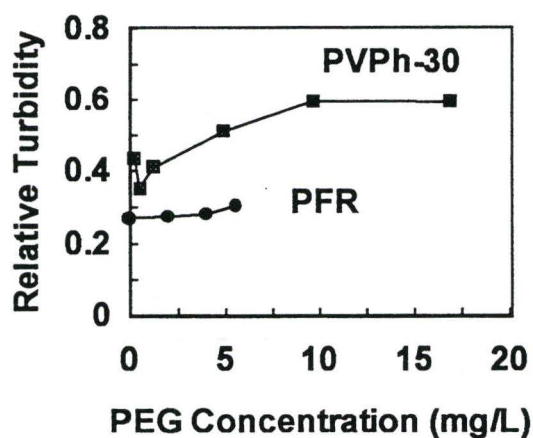


Figure 7 Effect of PEG on the latex flocculation induced by PEO/PVPPh-30 and PEO/PFR. MW of PEG in PEO/PVPPh system was 2000; MW of PEG in PEO/PFR system was 5000. pH = 5.0, [NaCl] = 0.002 N, the bleached fiber 1.0 g/L, and [latex] = 50 mg/L.

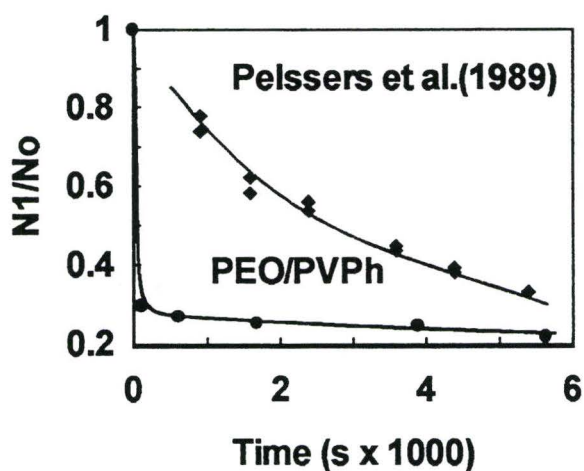


Figure 8 Kinetic process for latex flocculation induced by PEO/PVPh-1.

Data were compared with the result obtained by Pelssers et al.¹⁰

Experimental conditions:

PEO/PVPh system: [PEO-309] = 2 mg/L; [PVPh-1] = 10 mg/L; pH = 5.0, [NaCl] = 0.002 N, the bleached fiber 1.0 g/L, and $N_0 = 2.7 \times 10^{11}/L$.

Pelssers system: PEO MW = 6×10^5 , PEO addition amount = 0.83 mg/m²; $N_0 = 2.3 \times 10^{12}/L$ and [KNO₃] = 0.01 M.

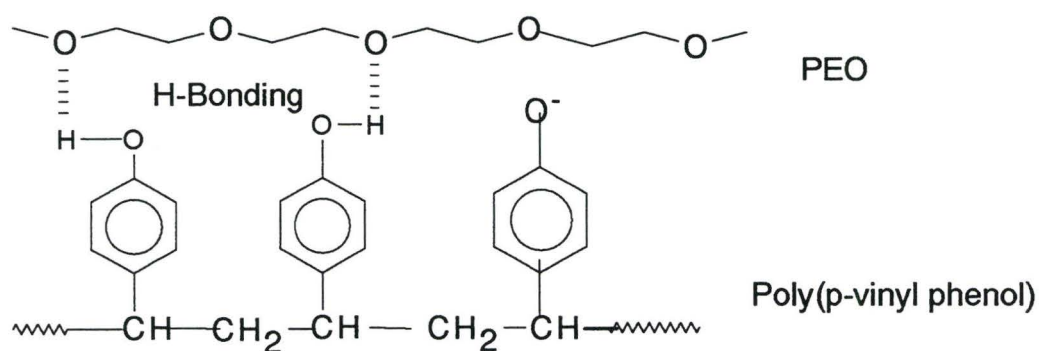


Figure 9 A schematic description for hydrogen bonding between PEO and PVP

Appendix A1: Supplementary materials for chapter 1

1. Characterization of macromonomers

The macromonomers were used as supplied without further purification. According to the suppliers, the average pendant chain lengths of PEG in methoxy PEG ethyl acrylate (A-n) were 10, 20 and 40 moles respectively. The average pendant chain lengths of PEG in methoxy PEG monomethacrylate (MA-n) were 5, 9 and 23 moles respectively. To verify the structures of PEG macromonomers, NMR analyses of the macromonomers were conducted. The proton NMR spectra for A-10 and MA-9 are shown in Figures A1-1 and A1-2. A-10 macromonomer NMR spectrum shows multiple peaks at 5.5 and 6.0 ppm which correspond to the protons attached to the carbon double bonds. The multiple peaks resulted from proton-proton couplings in $\text{CH}=\text{CH}_2$. Two single peaks at 5.5 and 6.0 ppm were observed for MA-9 macromonomer NMR spectrum, which correspond to the protons in $-\text{C}=\text{CH}_2$. The other proton peaks in OCH_2CH_2 and OCH_3 were clearly distinguished for both AM-9 and A-10 as indicated.

To further verify the structure of the PEG macromonomer, A-10 macromonomer was also analyzed by ^{13}C NMR. The result is given in Figure A1-3. The peak assignments are also presented in the Figure. Both ^1H and ^{13}C spectra proved the existing of $-\text{CH}=\text{CH}_2$, OCH_2CH_2 , $-\text{C}=\text{O}$ and OCH_3 groups in the macromonomers.

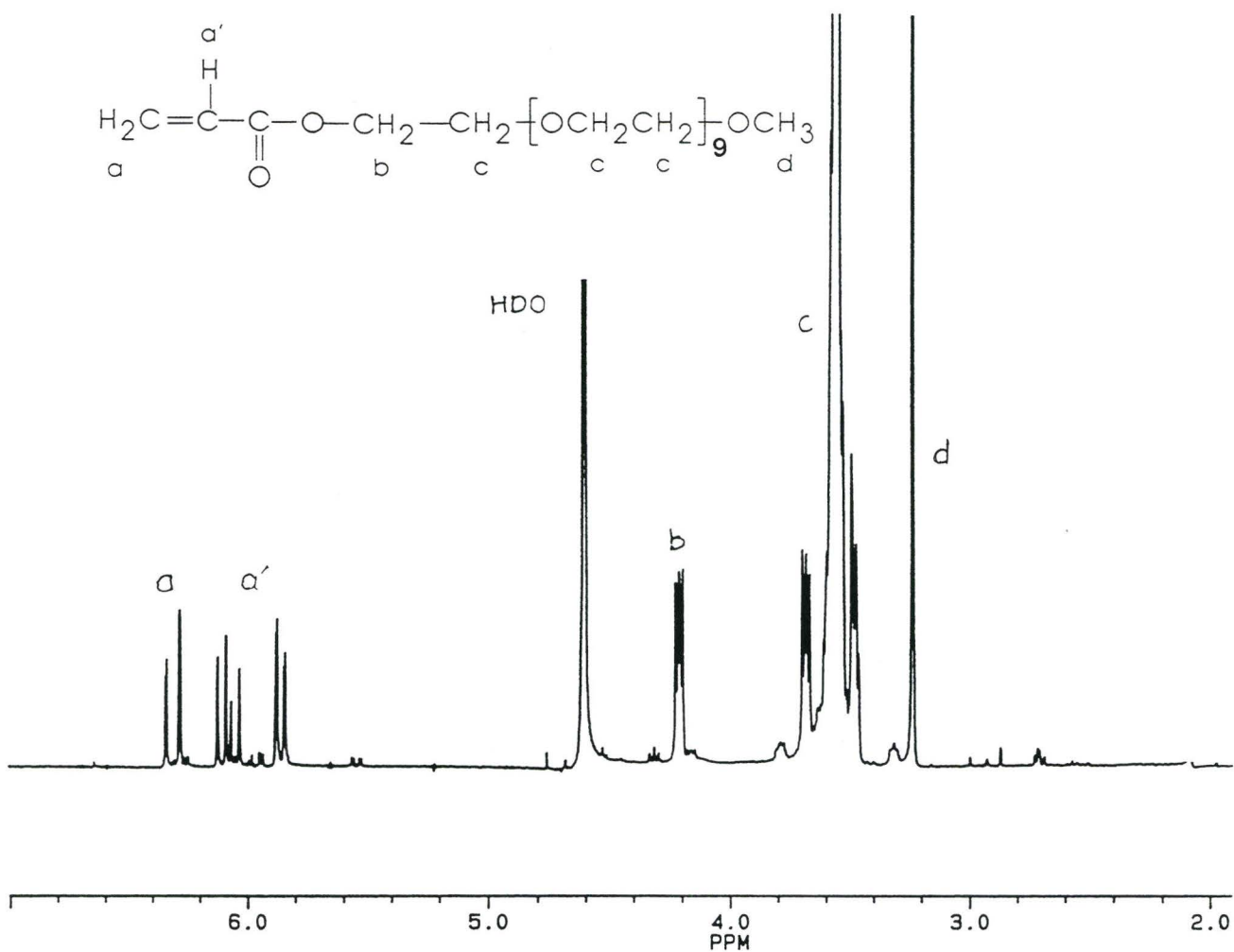


Figure A1-1. ^1H NMR spectrum for methoxy poly (ethyleneoxy) ethyl acrylate A-10 macromonomer.

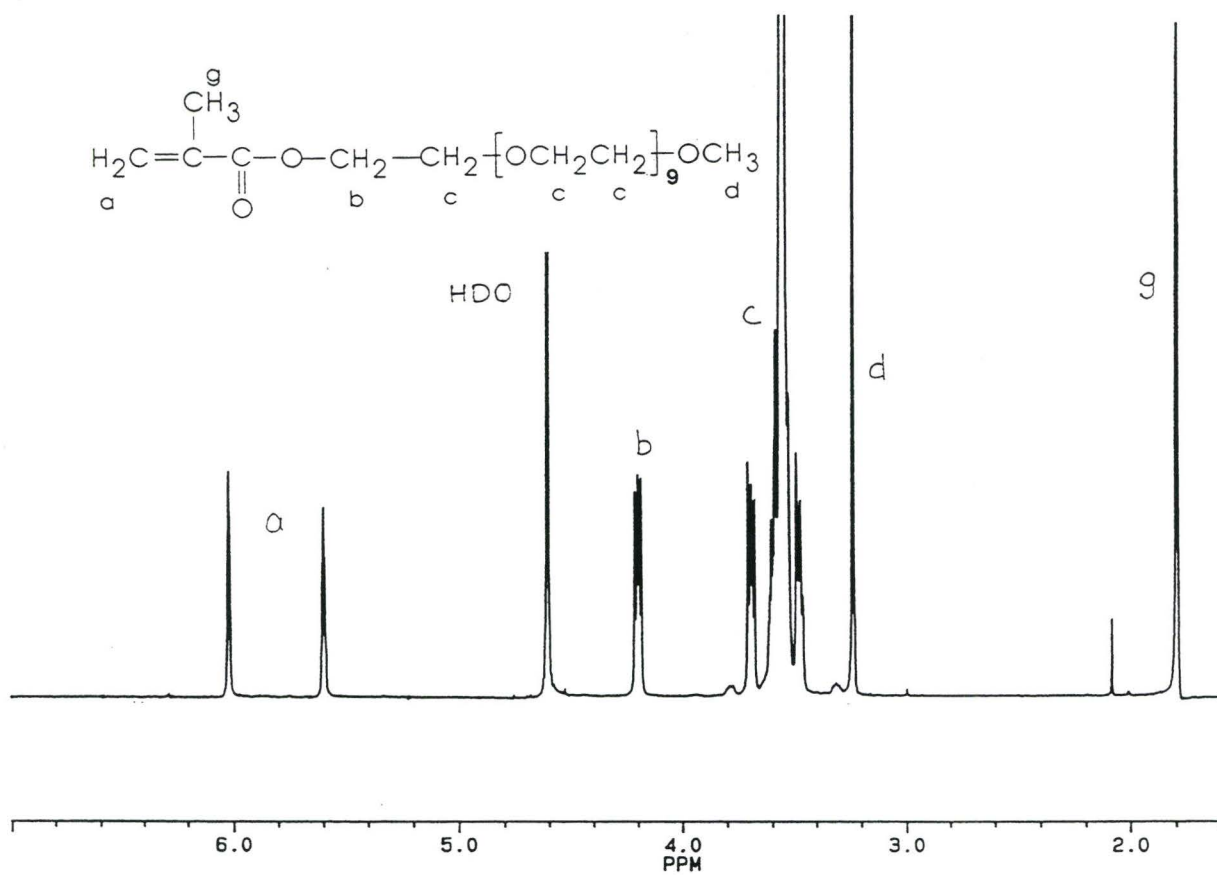


Figure A1-2. ^1H NMR spectrum for methoxy PEG monomethacrylate MA-9 macromonomer.

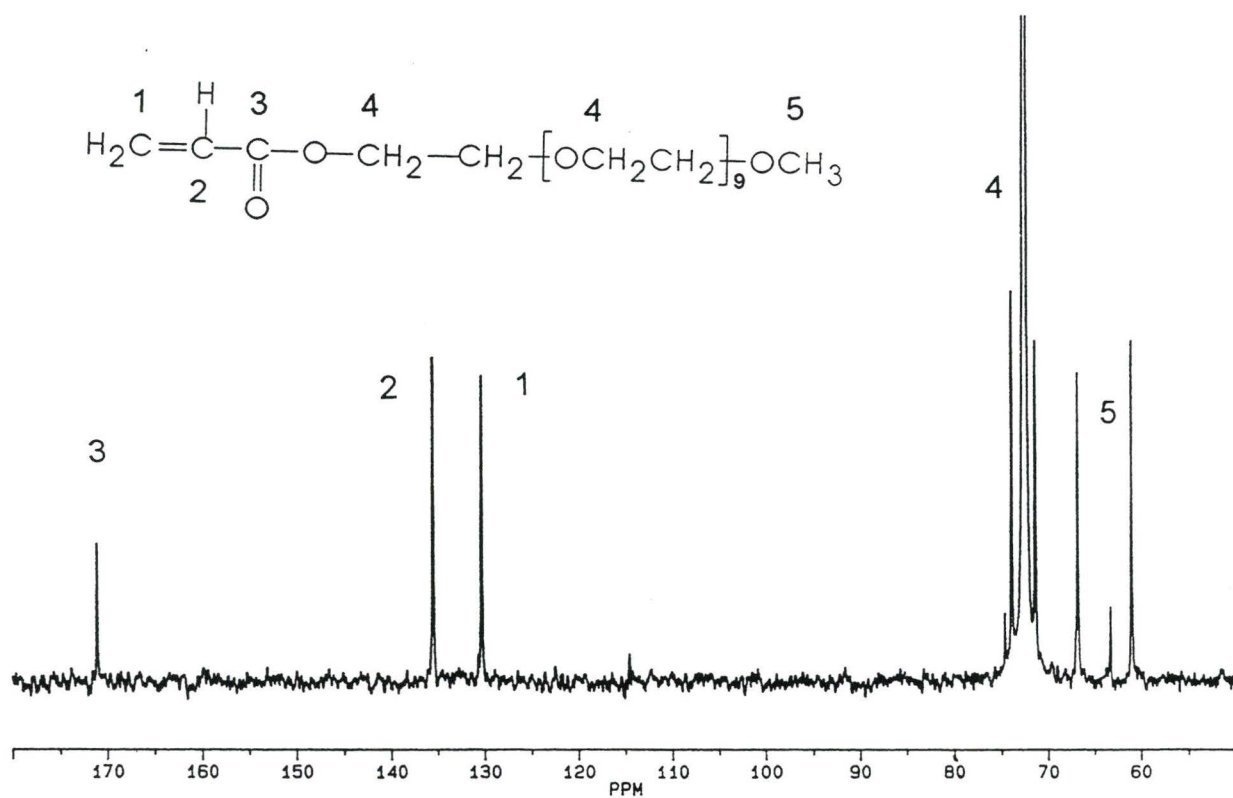


Figure A1-3. ^{13}C NMR spectrum for methoxy poly (ethyleneoxy) ethyl acrylate A-10 macromonomer.

The average degree of polymerization of PEG pendant chains in macromonomers, as shown in Table A1-1, was estimated from the peak areas of the OCH₂CH₂ protons relative to the area corresponding to the methoxy end group, OCH₃. The data in Table A1-1 indicate that PEG pendant chain lengths determined by NMR are in close agreement to the values given by suppliers.

Table A1-1 Average degree of polymerization, n, of PEG pendant chains in macromonomers. Standard deviation (Sd) was based on three duplicates.

Macromonomer	n (from NMR) ± Sd	n (from supplier)
MA-5	4.1 ± 0.3	5
MA-9	8.2 ± 0.4	9
MA-23	24.0 ± 1.3	23
A-10	11.1 ± 0.9	10
A-20	20.9 ± 1.2	20
A-40	40.8 ± 3.4	40

2. NMR characterization of copolymer compositions

Compositions of the copolymers were analyzed using proton NMR in terms of peak ratios of OCH₂CH₂ in PEG pendant chain to CH-CH₂ in copolymer backbones. The mole percentage of PEG macromonomers in copolymer was calculated by the following equation:

$$\text{mol\%} = \frac{\frac{A_{\text{CH}_2\text{CH}_2\text{O}}}{4n}}{\frac{A_{\text{CHCH}_2}}{3}}$$

where A is ^1H NMR peak area and n is the number of ether groups in PEG pendant chains.

Alternatively, a calibration method can be used in characterizing the composition of copolymers. The calibration curve was made from the mixtures of polyacrylamide (PAM) and macromonomers with different pendant chain lengths. An example NMR spectrum for the mixtures is given in Figure A1-4. Compared with the NMR spectra for copolymers, the vinylic protons are still observed in NMR Spectrum for the mixture. It was assumed that PAM represented the total CH-CH_2 backbone in the copolymer. The contribution to CH-CH_2 or $-\text{C-CH}_2$ backbone from macromonomers was negligible due to the feed mole ratio of macromonomer to acrylamide being extremely low, normally only 1 % or less. The ratios of peak areas of OCH_2CH_2 in PEG pendant chain to CH-CH_2 in PAM were recorded with ^1H NMR as a function of the weight ratios of macromonomer to polyacrylamide to give a calibration.

In order to generalize the calculation, a normalized calibration curve (Figure A1-5) was made from sequence NMR measurements for the mixtures of PAM and different macromonomers. The calibration curve chooses MA-9 (theoretical $n = 9$) as reference. The straight dashed line in Figure A1-5 is based on a formula:

$$P_m/P_p = C_n W_m/W_p$$

where P_m and P_p are OCH_2CH_2 and CH-CH_2 peak areas, respectively; W_m and W_p are weight amounts of macromonomer and PAM in mixtures;

$$C_n = 71 \times 4n / 3(44n + 100) = 1.718 \text{ when } n = 9.$$

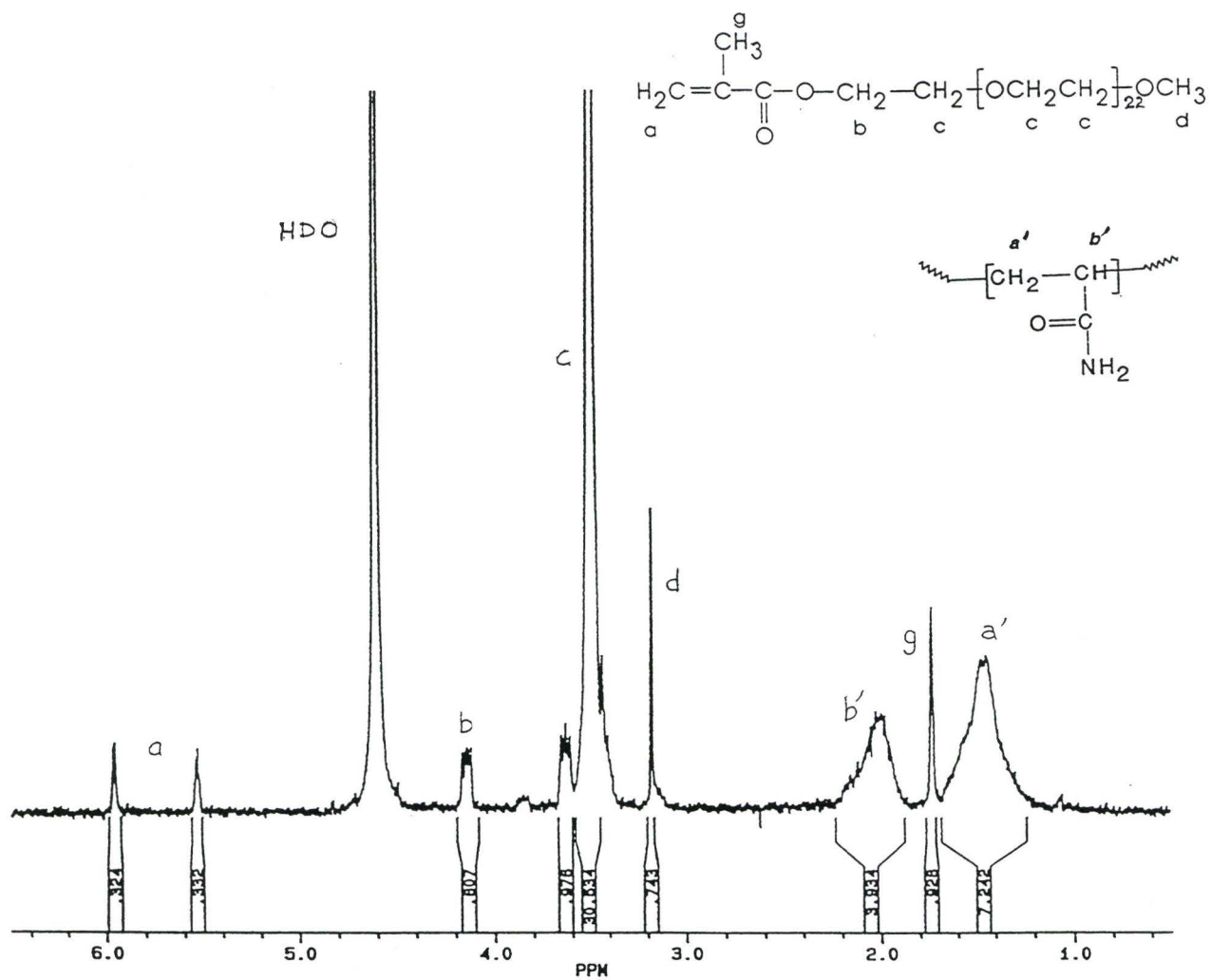


Figure A1-4 ^1H NMR spectrum for a mixture of PAM (Molecular weight 5,000,000) and PEG macromonomer MA-23.

Since each macromonomer contained different percentage of OCH_2CH_2 relative to total molecular weight, a correction factor $F_n (= 1.718/C_n)$ was introduced to normalize all calibration data for different macromonomers. The corrected experimental peak ratio $Y_n (= F_n P_m/P_p)$ are plotted as a function of weight ratios of macromonomer to PAM (see Figure A1-5). The results indicate that the experimental data were well fitted with the reference curve, especially at lower weight ratio (< 0.5) of macromonomer to PAM. Therefore, the composition of copolymers can be either determined from analysis NMR spectra or converted from the calibration curve.

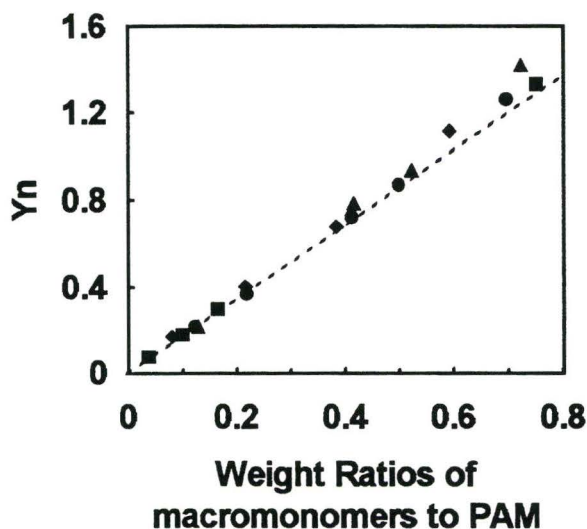


Figure A1-5. A normalized ^1H NMR calibration curve for the mixtures of PEG macromonomer and polyacrylamide homopolymer. The points represent different macromonomers (■ MA-9; ● MA-23; ◆ A-10; and ▲ A-40).

3. HPLC measurements of acrylamide conversion

HPLC samples were diluted with water to a concentration less than 100 mg/L, and filtered through 0.2 μm sterile Millex-GS (Millipore) filter to separate any precipitates. Below the 100 mg/L, AM concentrations were proportional to AM absorbed peak areas in HPLC measurement. The initial AM peak area (A_0) multiplied by the dilution factor (D_{t_0}) was chosen as a reference, the conversion of AM was calculated according to the following equation:

$$\text{Conversion of AM \%} = [(A_0 \times D_{t_0}) - (A_i \times D_{t_i})] / (A_0 \times D_{t_0}) \times 100$$

where A_i is the HPLC peak area of the samples which were collected at time t_i , and D_{t_i} is the dilution factor for the corresponding sample before being injected into HPLC. The standard deviation based on 4 duplicates was less than 2 % of the mean value.

When the conversion of acrylamide in a copolymerization was known, the corresponding macromonomer conversion was estimated from both AM conversion values and the copolymer composition determined from NMR measurement.

4. Summary of Copolymerization

Table A1-2 summarized the recipes of copolymerizations which were conducted in aqueous solution at constant initiator concentration ($[\text{K}_2\text{S}_2\text{O}_8] = 3 \times 10^{-3}$ mol/L and different temperatures. The corresponding conversion data for acrylamide and macromonomers are summarized in Table A1-3 which provided the database for the estimation of macromonomer reactivities in the copolymerizations. The structure of A-1 monomer is $\text{H}_2\text{C}=\text{CHCH}_2\text{OC}_2\text{H}_5$.

Table A1-2 Copolymerization Recipes

Sample No.	Wt. of AM(g)	Wt. of (M)A-n(g)	Mole Ratio AM/(M)A-n	Type of (M)A-n	H ₂ O mL	Temp. °C
43-36	9.20	2.84	50	MA-23	300	40
56-35	1.6	0.31	60	MA-23	35	40
43-176	12.8	0.99	200	MA-23	286	25
43-51	10.65	1.65	100	MA-23	300	40
43-55	11.08	0.858	200	MA-23	300	40
56-48	2.16	0.259	130	MA-23	40	20
43-48	8.25	5.28	25	MA-23	300	40
43-128	8.93	1.68	83	MA-23	300	20.5
43-129	12.8	1.998	99	MA-23	300	25
43-149	6.45	0.199	500	MA-23	140	25
56-51	2.21	0.177	88	MA-9	40	25
56-59-E	2.25	0.18	88	MA-9	40	40
56-59-F	1.95	0.201	68	MA-9	40	40
43-63	10.65	1.622	46	MA-9	300	40
43-71	11.08	0.798	100	MA-9	300	40
43-134	10.7	0.856	95	MA-9	250	25
56-49	2.19	0.166	56	MA-5	40	25
43-92	0.344	0.182	8.1	MA-5	10	40
43-93	0.496	0.109	19.4	MA-5	10	40
43-133	7.95	0.563	60	MA-5	200	23.5
43-3	11.36	12.08	25	A-40	300	40
43-16	11.36	6.07	50	A-40	400	40
23-170	16.0	8.44	50	A-40	475	40
43-104	1.02	0.265	100	A-40	40	40
43-131	11.38	3.06	98	A-40	300	25
56-36	1.61	0.369	60	A-20	35	40
56-1	12.82	0.968	200	A-20	285	25
43-22	12.78	1.99	50	A-10	385	40
56-36-2	1.61	0.441	29	A-10	40	40
23-160	16.0	9.99	14	A-10	500	40
56-70	2.14	0.111	23.3	A-1*	40	40

Table A1-3. Conversion data for AM and Macromonomers

Sample No.	Time (min.)	Conversion AM %(X_1)	Conversion PEG-n %(X_2)	Type of PEG-n
56-36-2	18	7.01	5.27	A-10
43-22-9	35	24.9	18.4	A-10
43-22-10	40	25.5	19.76	A-10
23-160-3	60	28.4	18.6	A-10
23-170-2	20	29.3	13.1	A-40
23-170-3	40	48.3	17.3	A-40
23-170-4	80	55.1	18.6	A-40
23-170-5	190	63.7	28.4	A-40
43-104-1	15	3.68	1.63	A-40
43-16-12	210	83.7	50.8	A-40
43-16-1	10	14.7	7.23	A-40
56-1-3	60	13.4	7.88	A-20
56-1-4	130	38.6	23.2	A-20
56-48-2	120	17	10.1	MA-23
43-176-2	30	19.3	13.4	MA-23
43-176-4	215	60.5	51.8	MA-23
43-36-3	30	27.0	19.6	MA-23
43-36-5	60	48.0	33.05	MA-23
43-36-6	90	58.6	42.6	MA-23
56-35-1-1	20	13.8	9.65	MA-23
56-35-1-2	50	4.79	3.0	MA-23
43-92	30	20.7	14.6	MA-5
56-49-2	60	15.5	12.4	MA-5
56-51-1	90	7.83	6.42	MA-9
56-51-2	280	19.3	14.1	MA-9
43-63-2	30	25.8	17.8	MA-9
43-63-8	250	69.9	53.0	MA-9
43-71-4	60	36.0	32.8	MA-9
43-71-6	330	77.6	66.3	MA-9

Recipes for inverse microemulsion copolymerization

Sample 23-119

Recipe:	AM:	31.64 g
	A-40:	8.36 g
	H ₂ O:	220 mL
	Isopar-M:	200 mL
	SMS:	18.5 g
	K ₂ S ₂ O ₈ :	1.08 g

Polymerization was conducted at 50°C with mechanical stirring at 350 rpm. Sorbitan monostearate (SMS, Aldrich) was used as a surfactant. The acrylamide conversion in the copolymerization is given in Figure A1-6.

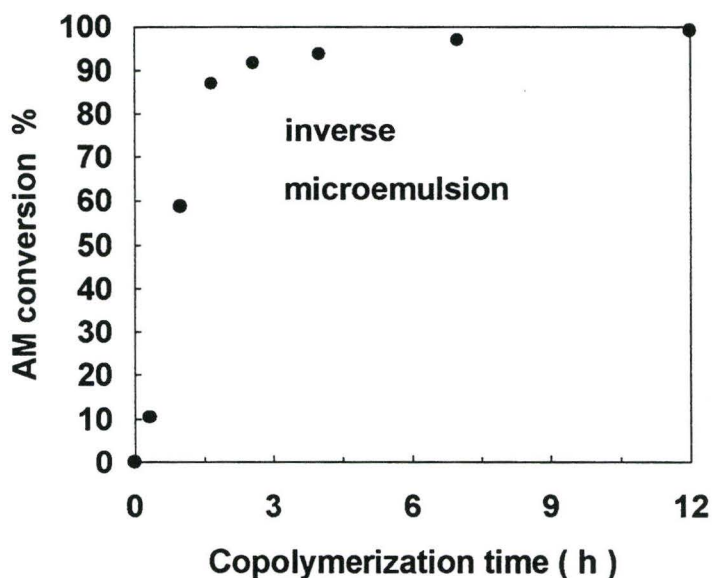


Figure A1-6 AM conversion in inverse microemulsion polymerization

The results indicate that AM conversion in inverse microemulsion polymerization was much higher than that in aqueous solution polymerization.

Grafting polymerization of PEG and AM in microemulsion polymerization

Inverse microemulsion copolymerization, as shown in the following recipe (43-30), was carried out using methoxy polyethylene glycol 2000 (PEG 2000, Union Carbide) instead of macromonomer. The objective is to graft PEG onto PAM during the radical polymerization of acrylamide. In other words, radical grafting reaction may occur simultaneously with acrylamide polymerization.

Sample 43-30

Recipe:	AM:	10	g
	PEG 2000:	5.0	g
	H ₂ O:	50	mL
	Toluene:	75	mL
	SMS:	7.5	g
	K ₂ S ₂ O ₈ :	3.0	mmol/L
	Ce ₂ SO ₄ :	1.0	mmol/L

Polymerization was conducted at 40°C with mechanical stirring at 250 rpm. However, the resulting emulsion was not stable.

Semi-Batch Aqueous Solution Copolymerizations

Policy II for semi-batch reactor:

A mixture of AM and macromonomer at desired concentration levels was added to reactor at time zero. The addition rate was controlled at a low level so that copolymer composition was approximately equal to the feed composition of monomers. This approach is called a starve policy. The recipes and copolymer compositions are presented in Table A1-4.

Table A1-4 recipes for semi-batch polymerization

Sample no.	Feed		molar ratio AM to (M)A-n	Dropping rate (g/min.)	Type (M)A-n	Time (min.)	(M)A-n in copolymer mol %
	in 50 mL	Phase water					
	AM (g)	(M)A-n (g)					
43-94	7.51	0.581	200	0.18	MA-23	135	
						280	0.479
43-96	7.504	0.294	180	0.17	MA-9	180	0.562
						410	0.621
43-97	7.224	1.094	46	0.17	MA-9	110	2.54
						220	2.24
						390	2.06

The copolymerizations were conducted at 40°C with mechanical stirring at 130 rpm. 161 mg potassium persulfate was dissolved in 100 mL distilled and deionized water and fed into the reactor before the mixtures of acrylamide and macromonomers were dropped. The results indicate that the drift of copolymer compositions were less than that in batch polymerization.

Policy I for semi-batch reactor:

All macromonomer and 30 % (wt) of acrylamide were added to the reactor; then, the remaining 70 % (wt) of acrylamide was dropped into the reactor at an average rate of 0.8 g/min.

Recipes: Sample no. **43-114**

1st addition:

AM: 3.181 g

A-40: 2.526 g

K₂S₂O₈: 0.241 g

H₂O: 100 mL

2nd addition(dropping part):

AM: 6.395 g

H₂O: 190 mL

The polymerization was conducted at 40°C with mechanical stirring at 133 rpm. Dropping rate: 0.77 g/min. The accumulated composition of the copolymer as a function of dropping time is given in following Table:

Table A1-5 Copolymer compositions

Time (min.)	A-40 % (mole) in copolymer
60	0.684
210	0.461
480	0.331

Therefore, to obtain the uniform composition of copolymers, policy II appeared to be better than policy I.

Appendix A2: Supplementary materials for chapter 2

1. UV calibration curve of PFR

The absorbencies of phenolic resin (PFR) were measured by a HP 8452A UV Spectrophotometer (Hewlett-Packard) at a wavelength of 286 nm. The relationship between the absorbency and phenolic resin (PFR) concentration is shown in the Figure A2-1. The equation in the Figure was used to estimate the PFR precipitation isotherms in complex formation between PEO/PFR and copolymer/PFR. The relationship was also used in estimating the PFR adsorption onto polystyrene latex surfaces which were described in chapter 4 in flocculation mechanism studies.

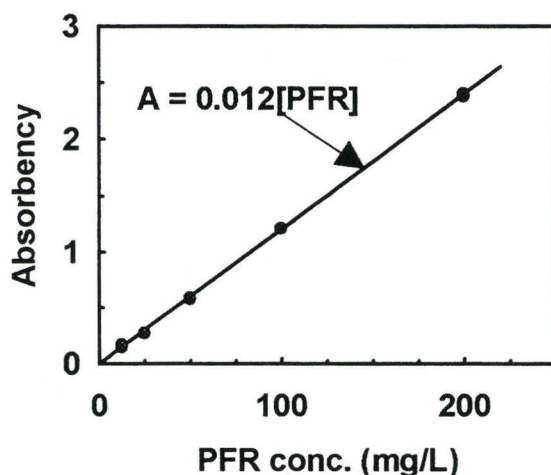


Figure A2-1. UV absorbency of PFR at 286 nm versus PFR concentration.

2. DSC measurement on estimating amounts of bound water in polymer systems

Applications of differential scanning calorimeter (DSC) have been used to study PEO hydration,¹ to determine the PEG concentration in the aqueous solution,² and to analyze the bound water contents in the microdomains of polyelectrolyte complexes.³ In this work, DSC measurements were conducted to estimate the amounts of the bound water in PEO and PEO/PFR complexes.

A Du Pont 910 differential scanning calorimeter was used with a cooling apparatus. Samples for DSC were hermetically sealed in aluminum pans in a sample encapsulating press. An empty pan was used as a reference. DSC was purged with nitrogen during measurements. To determine the amount of bound water measurements, the polymer aqueous solution was cooled by liquid nitrogen below -30°C . The DSC curves were obtained at a scanning rate of $10^{\circ}\text{C}/\text{min}$. from -30°C to 95°C . The fusion enthalpy was recorded and used to estimate the free water content in the system.

In DSC measurement for solid polymer samples, the PEO powder was used as received from the supplier. PFR solution was dried at the ambient temperature, and further dried in a desiccator over 72 hours. The same drying procedure was used for the complex solution. DSC curves, for the PEO/PFR complex and the PEO/PFR blend, were recorded at a scanning rate of $2^{\circ}\text{C}/\text{min}$. from 30°C till 150°C . Figure A2-2 shows the DSC results for PEO/PFR complex and blend. As can be seen, the blend sample exhibited individual transition temperatures corresponding to PEO and PFR respectively. By contrast, after complex formation, one broad and a combined two transition temperature was observed.

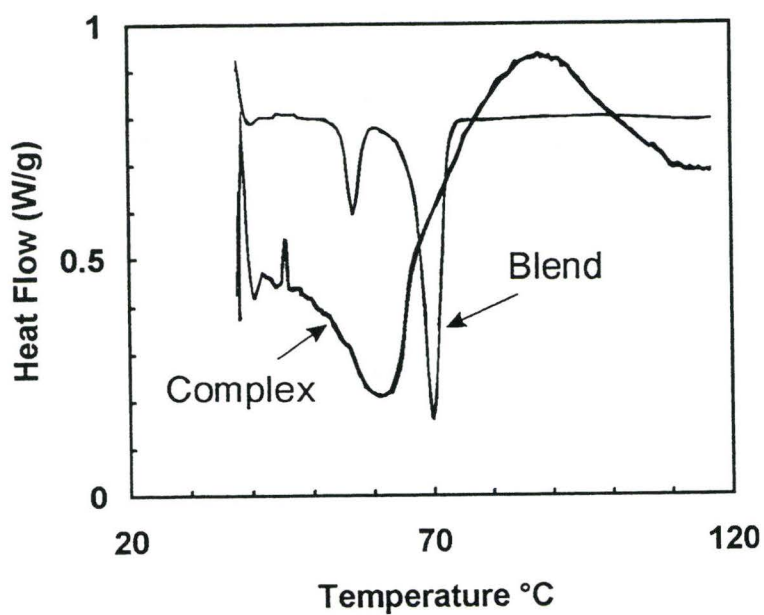


Figure A2-2 Transition Temperature measured by DSC; Solid line: Blends of PEO-309 and PFR C-271; Dashed line: Complex precipitate of PEO-309 and PFR C-271. DSC was conducted at constant heat rate of 2°C/min. and scanning from 30 to 150°C.

Figure A2-3 shows a schematic of the DSC thermogram for PEO solution (concentration 0.13 %). Another curve for the 30 % PEG solution, reported by Antonsen et al.⁴, is also presented as a comparison. Only one peak, which corresponds with the melt of ice, was observed in this work due to an extremely low polymer concentration. Whereas two peaks were found for the 30 % PEG solution.

Figure A2-4 shows the results of the enthalpy changes as function of polymer (PEO-309) concentrations, measured by DSC in this work. The results indicated that the heat fusion of pure water is 362 J/g, which is slightly higher than the literature data (334 J/g).⁵ At extremely low concentration (8.4 mg/L of PEO), the heat fusion of PEO solution is close to that of the pure water. Higher PEO concentrations in solution led to a lower fusion enthalpy. Only 302 J/g of heat was released at a PEO concentration of 0.13 % (wt). By contrast, the fusion enthalpy of PFR was 350.7 J/g at a concentration of 0.10 % (wt). This value was closer to the pure water value compared with the PEO solution at a similar concentration. The result suggested that the PFR was more hydrophobic than the PEO so that fewer water molecules were bound with the PFR.

After the complex formation between the PEO and the PFR, the fusion enthalpy of complex solution was dramatically changed. For example, the PEO solution at a concentration of 1.3 g/L exhibited a fusion heat of 302 J/g, when this PEO solution was mixed with the same amount of PFR at a concentration of 1.01 g/L at pH 5, the complex solution produced a higher fusion enthalpy (= 348 J/g). This result indicated that the greater bound water became free as the complex formation occurred.

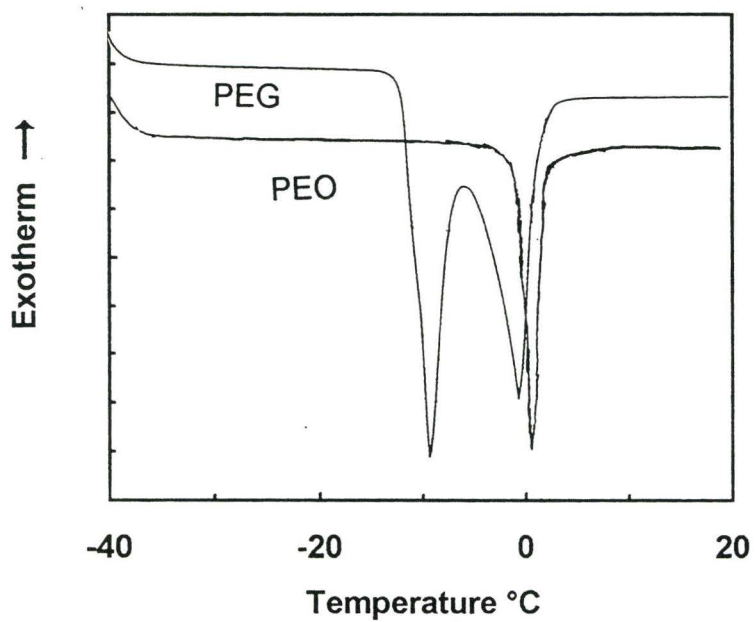


Figure A2-3. A schematic of DSC thermogram for PEO solution. PEG solution curve was reported by Antonsen et al.⁴

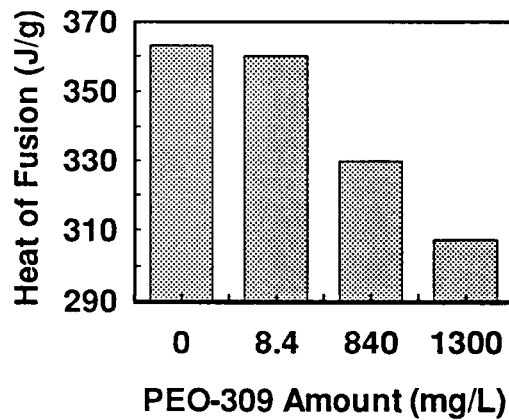


Figure A2-4. Influence of PEO 309 concentration in aqueous solution on the fusion enthalpy

The dependence of the complex formation on pH was also observed in the enthalpy measurements. Figure A2-5 shows that the heat of fusion as a function of pH for the PEO/PFR complex systems. The results indicated that at pH 4 fusion enthalpy of the system was close to the pure water value, however, at pH 10 a significantly lower enthalpy was recorded. To quantitatively describe amounts of bound water on the PEO/PFR complex, the difference between the heat of fusion for the complex solution and pure water was assumed completely due to the bound water. As a result, the bound water content of fraction was calculated from the following equation:

$$\varphi = 1 - \Delta H_S / (\Delta H_W f)$$

where φ is the bound water content or fraction; f is the total water weight fraction in the complex solution. ΔH_S is the enthalpy change of the complex aqueous solution. ΔH_W is the fusion heat of pure water at freezing point.

In the present systems, f is approximately equal to one due to very diluted complex solution. The estimated fraction of the bound water in the complex solutions are also shown in Figure A2-5.

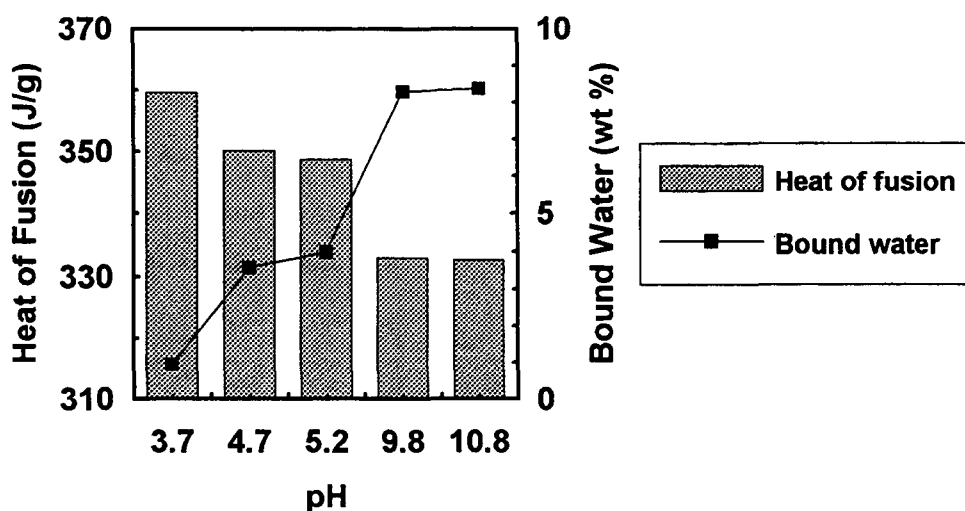


Figure A2-5. pH effects on fusion enthalpy for PEO/PFR complex aqueous solution. [PEO] = 840 mg/L; weight ratio of PEO/PFR = 1:1.

Antonsen et al.⁴, based on DSC measurements, found that the number of bound water ranged 2.3 to 3.8 per PEG repeat units, and the bound number risen with the increase of PEG molecular weight. By contrast, the number of water bound to the ether unit in PEO for the present system was too high (over thousand) based on results in Figure A2-5. There were two factors which significantly distinguished the current system with that studied by Antonsen et al. First, the number of bound water per polymer repeat unit is MW dependent. The

highest MW of PEO used by Antonsen et al. was 2×10^5 . This sample gave the number of bound water at approximately 3.8 per repeat unit. Molecular weight of the PEO used in the present work was 8×10^6 . Therefore, the higher number of bound water would be expected. Second, possibly there exist two types of bound water in the diluted aqueous solution of high MW PEO. One is the conventional bound water as in PEG, association occurs through hydrogen bonding; another is the water enclosed by the entanglements of long polymer chains. The latter situation is similar to the water bound in a crosslinked polymer hydrogel.

As complex formation occurs, PFR not only displaces the bound water via a hydrogen bond, but also changes the conformation of PEO chains in the aqueous solution. The more compact and hydrophobic complex formation allows the water initially bound in PEO "hydrogel" to be free. Therefore, the heat of fusion for the PEO/PFR complex solution was much higher than that of the PEO solution at the same concentration.

In spite of the difficulty in accurately estimating the enthalpy involved in complexation in the present system, DSC would be an useful technique to characterize the bound water associated with the polymer complexation processes if the instrumental accuracy was further improved.

References:

- 1 Hey, M.J. and Llett, S.M., J. Chem. Soc. Faraday Trans., **87**, 3671(1991).
- 2 Yamauchi, T. and Hasegawa, A., J. App. Polym. Sci. **49**, 1653(1993).
- 3 Ohno, H., Shibayama, M. and Tsuchida, E., Makromol. Chem. **184**,1017(1983).
- 4 Antonsen, K.P. and Hoffman, A.S., in Poly(ethylene Glycol) Chem., Ed. by Harris, J.M. Plenum Press, New York and London, 1992.
- 5 Vringer, T.de, Joosten, H.J. and Junginger, H.E., Colloid & Polymer Sci., **264**, 623(1986).

Appendix A3: Supplementary materials for chapter 3

1. Calibration of polystyrene latex concentration in the turbidity measurement

The amount of latex removed in polymer induced flocculation was characterized using UV spectrometry to measure the latex turbidity changes during the flocculation.

Light scattering of diluted latex was described by Beer-Lambert law:

$$T_c = T_o 2.3 \exp(-\epsilon c l)$$

where T_o is the initial transmittance for pure water, T_c is the transmittance of the radiation after passing through a length l of the latex dispersion, ϵ is extinction coefficient and c is the latex concentration. Turbidity τ is defined as $\tau = \epsilon c$.

If the latex particles were assumed to be monodispersed, the identical ϵ values for latex particles would be expected. Therefore, the latex suspension turbidity is proportional to the latex concentration. Figure A3-1 shows a calibration curve of $\log (T_o/T_c)$ ($\propto \tau$) versus polystyrene latex concentrations. Where T_o (= 100 %) was the transmittance of water, and T_c (i.e. T) was the transmittance of latex dispersions. The latex size was 0.69 μm in weight average diameter, measured by a disc centrifuge particle sizer. The linear relationship between latex turbidity and latex concentration (up to 120 mg/L) suggested that the amounts of latex removal can be estimated from the turbidity measurements.

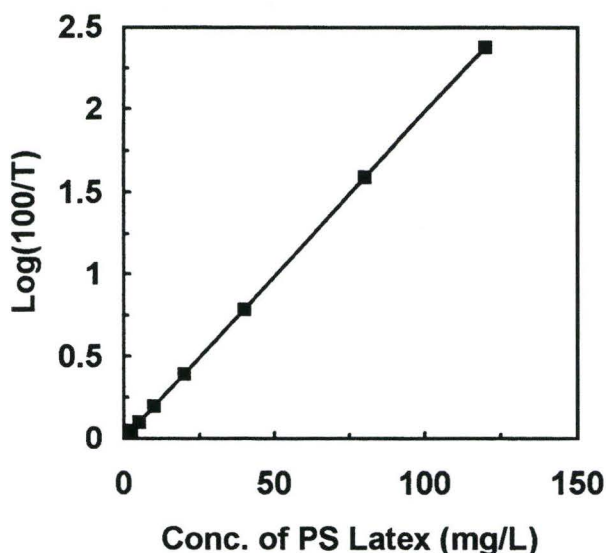


Figure A3-1. Calibration curve of the latex concentrations versus $\log(T_o/T_c)$

Details regarding the definition of the relative turbidity have been discussed in chapters 3 and 4 in this thesis.

2. Experimental data for aggression equation

To relate the latex flocculation efficiency and structures of copolymers, an empirical equation was derived to fit the experimental data. Formula of the empirical equation is as follows:

$$\tau_R = 0.078C^{-0.48} + 0.005C + 0.156(n/10)^{-0.65} + 0.006(n/10) + 0.19(M/X)^{-0.91}$$

where τ_R is the relative turbidity; C is the mole % of macromonomer in the copolymers; n is the number of repeat units of PEG pendant chain in the macromonomers; and M is molecular weight of the copolymers; and X is a scaling parameter equal to 1×10^6 Dalton.

Figure A3-2 shows the results of the evaluation database which consists of two relative turbidity data, one predicted by the empirical equation and another observed from experiments at the 21 grids. The correlation coefficient for the predicted data and observed data was 0.96, which indicated that the significant correlation between two group data. The original database for aggression analysis is given in Table A3-1.

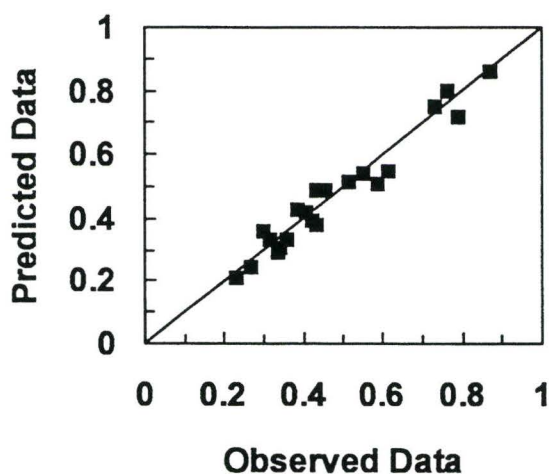


Figure A3-2. Correlation between the experimental observed data of the latex relative turbidity after flocculation and the data predicted by the empirical equation.

Table A3-1. Database for estimating the empirical equation; the correlation coefficient constant between the experimental and the prediction data (in the last two rows) was 0.96.

Samples	Molecular Weight (Mw)	PEG chain density (mole %)	PEG pendant chain length (# repeat unit)	Relative Turbidity (experimental)	Relative Turbidity (prediction)
43-131	4.2 x10 ⁵	0.38	40	0.613	0.545
56-109	2.5 x10 ⁵	0.23	40	0.730	0.750
56-117	1.3 x10 ⁶	0.80	40	0.336	0.294
56-110	3.7 x10 ⁶	1.4	23	0.231	0.209
43-36	1.2 x10 ⁶	0.85	23	0.357	0.334
56-48	4.5 x10 ⁶	0.47	23	0.270	0.246
43-149	5.1 x10 ⁶	0.14	23	0.337	0.292
56-112	1.9 x10 ⁶	0.65	20	0.344	0.303
43-22	6.3 x10 ⁵	1.1	10	0.587	0.508
56-113	2.1 x10 ⁶	0.70	10	0.299	0.356
23-141	1.1 x10 ⁶	0.8	10	0.387	0.423
43-134	9.0 x10 ⁵	0.50	9	0.435	0.485
56-108	4.6 x10 ⁶	0.69	9	0.316	0.250
43-97	6.0 x10 ⁵	1.7	9	0.514	0.510
43-63	7.0 x10 ⁵	1.5	9	0.455	0.483
43-116	1.2 x10 ⁶	0.85	9	0.407	0.421
43-71	7.0 x10 ⁵	0.41	9	0.550	0.538
56-49	3.7 x10 ⁶	1.6	5	0.432	0.376
43-133	4.5 x10 ⁵	0.60	5	0.791	0.713
56-72	2.3 x10 ⁶	2.3	1	0.874	0.856
56-71	4.7 x10 ⁶	2.7	1	0.767	0.799

3. Latex flocculation induced by copolymer in the special cases

1) Flocculation induced by the copolymer in the absence of cofactor

High molecular weight PEO alone has almost no ability to flocculate the latex in the present latex/fiber flocculation system at concentration of 1 to 2 mg/L. Whereas the copolymers exhibited limited flocculation ability in the absence of phenolic resins. Table A3-2 shows the relative turbidity values obtained by two copolymers and PEO-309 in the absence of phenolic resin. Although the latex flocculation efficiency with copolymer alone was much worse than that in the presence of phenolic resin, the results implied some different features between the comb copolymer and PEO homopolymer. The improved flocculation was possibly arisen from a result of the branched structure of the copolymer.

Table A3-2. Flocculation of the latex by polymers in the absence of phenolic resin. The features of the copolymers have been given in Table 1 in Chapter 3.

Sample	Concentration (mg/L)	Relative Turbidity
56-110	1.0	0.714
56-121	3.4	0.767
PEO-309	1.0	0.954

2) Latex flocculation induced by ter-polymers

A ter-polymer based on copolymerization of acrylamide, PEG macromonomers and acrylic acid was prepared. The polymerization recipe for the sample 43-135 is given as follows:

Acrylamide:	9.25	g
MA-23:	1.414	g
Acrylic acid:	0.478	g
$K_2S_2O_8$:	4.0	mmol/L
K_2HPO_4	54	mg
H ₂ O:	300	mL

Polymerization was carried out at 40°C for 10 hours. The relative turbidity of the latex was 0.58 when the ter-polymer was used in latex flocculation in conjunction with PFR.

Appendix A4: Supplementary materials for chapter 4

1. Flocculation conducted in the absence of the fibers

Table A4-1 shows that the polystyrene latex flocculation induced by PEO/PFR in the absence of fibers. Polymer and latex concentrations as well as latex sizes are given in the Table.

Table A4-1. Latex flocculation in the absence of the fibers

[Latex] mg/L	Size of latex μm	[PEO] mg/L	[PFR] mg/L	Relative Turbidity
50	0.69	1	2	0.57
9	1.09	10	20	0.79

2. Flocculation of PS latex in the presence of silica beads

The silica beads have been used as the substrates in the latex flocculation induced by PEO/PFR, which was discussed in Chapter 4. The following data summarizes the effects of the pretreatment of the silica bead surface on the latex flocculation. Size of the silica beads was 715 μm in diameter as indicated by supplier. The beads were pretreated at two level pH and then rinsed by distilled and deionized. water. Flocculation results are shown in Table A4-2.

The morphology of latex flocs formed onto the silica bead surfaces was observed under optical microscopy. One result is presented in Figure A4-1 as an example. Morphology of the flocs was similar to the flocs formed in fibers. The results suggested that the floc morphologies were not significantly affected by the types of substrates.

Table A4-2. Flocculation of PS latex in the presence of silica beads. PEO-309 and phenolic resin were added in different order and at 2 mg/L for all measurements. pH = 5 and [NaCl] = 10⁻³ M.

Amount of beads (g)	pH in pretreatment	1 st added polymer	2 nd added polymer	Relative Turbidity
2.91	2.2	PEO-309	C-271	0.93
3.02	2.2	C-271	PEO-309	0.52
3.01	10.3	PEO-309	C-271	0.68
3.15	10.3	C-271	PEO-309	0.43

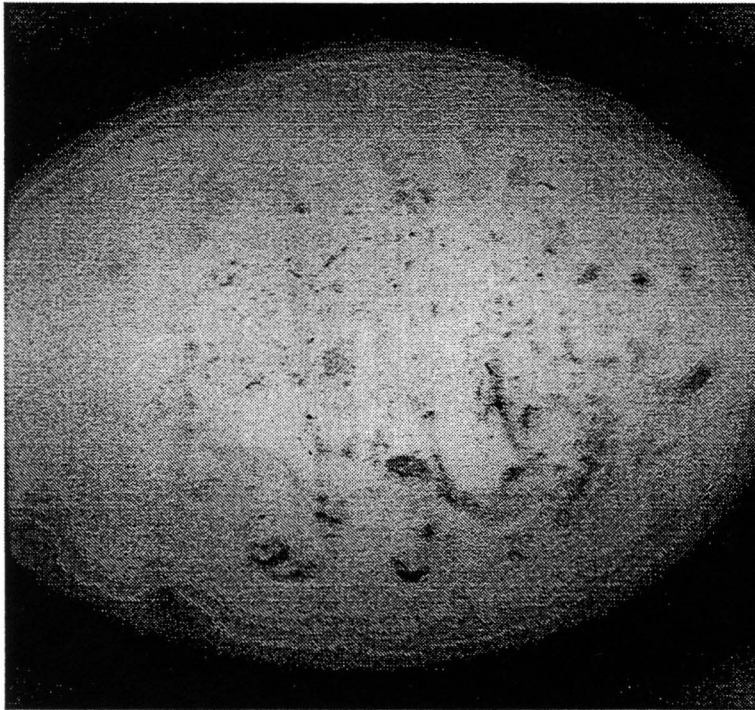


Figure A4-1. Morphology of latex flocs formed by PEO/PFR flocculation system in the presence of silica beads

3. Titanium dioxide (TiO₂) flocculation induced by PFR and PEO or copolymer

PEO/PFR and copolymer/PFR flocculation systems were also used in removal of titanium dioxide (TiO₂) fine particles. The results are given in Table A4-3. Data in the Table shows that the copolymer appeared more effective than PEO-309. The relative turbidity appeared to be time dependent. Much more latex was flocculated 4 hour after polymer additions than after 1 hours. It should be noted that the specific gravity of TiO₂ is approximately 4.2 g/cm³, which is much higher than that of PS latex (= 1.05 g/cm³). The sedimentation of the TiO₂ particles was not negligible.

Table A4-3 Flocculation of by dual-polymer systems. Concentration of TiO₂ = 48 mg/L. Phenolic resin was used as cofactor at 2 mg/L for all measurements. pH = 5 and [NaCl] = 10⁻³ M.

Polymer	Addition amounts (mg/L)	τ_R 1 h after flocculation	τ_R 4 h after flocculation
PEO-309	1	0.41	0.21
PEO-309	2	0.49	0.33
56-108-2	2	0.33	0.13
56-108-2	4	0.26	0.21

The morphology images of the TiO₂ particle flocs formed by PEO and copolymers are given in Figures A4-2 and A4-3. Both pictures show that the TiO₂ particles were flocculated and attached onto the fibers.

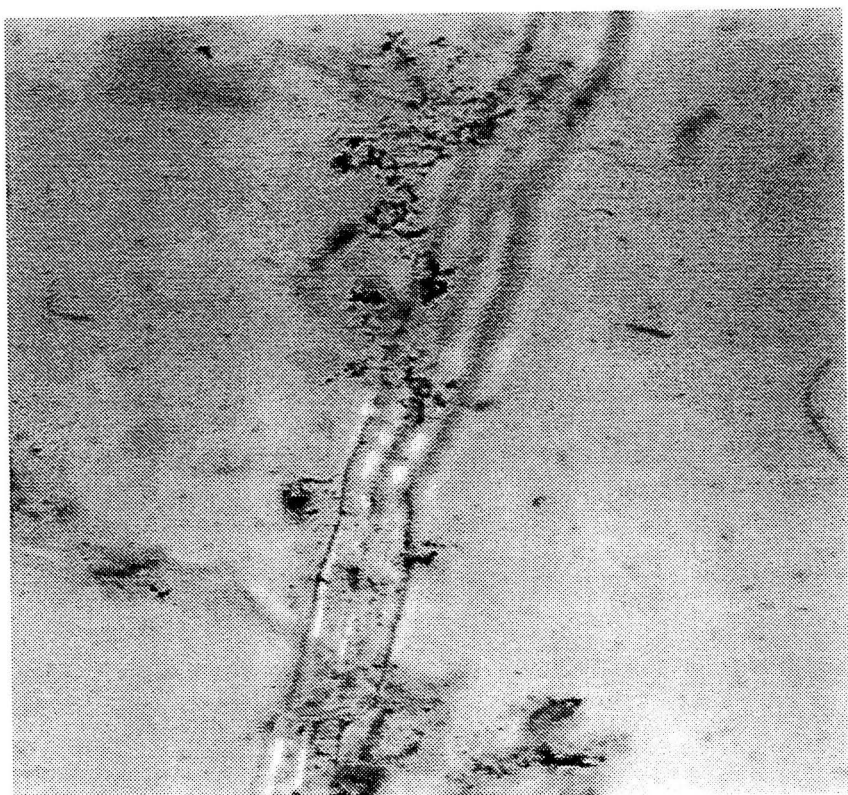


Figure A4-2. TiO₂ flocs formed by PEO-309 and PFR

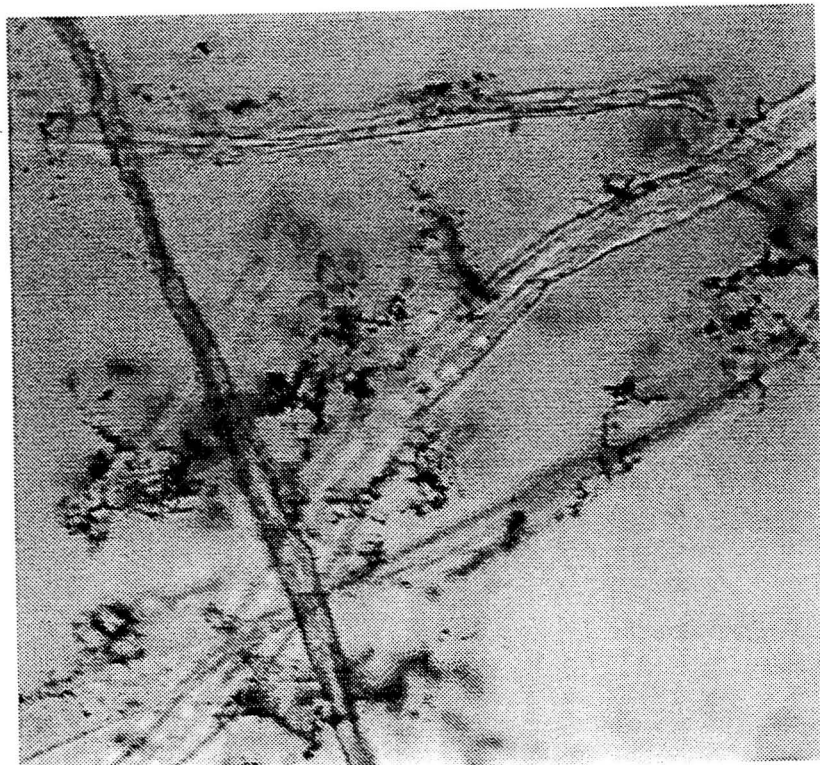


Figure A4-3. TiO_2 flocs formed by copolymer 56-108 and PFR

Appendix A5: Supplementary materials for chapter 5

The relationship between the first-pass retention of pulp fines and the relative turbidity of polystyrene latex particles are shown in the Figure A5-1. The squares were the experimental results shown in Table 2 in chapter 5. The fitting line was estimated based on the linear least square method, and is expressed in the equation shown in the Figure A5-1.

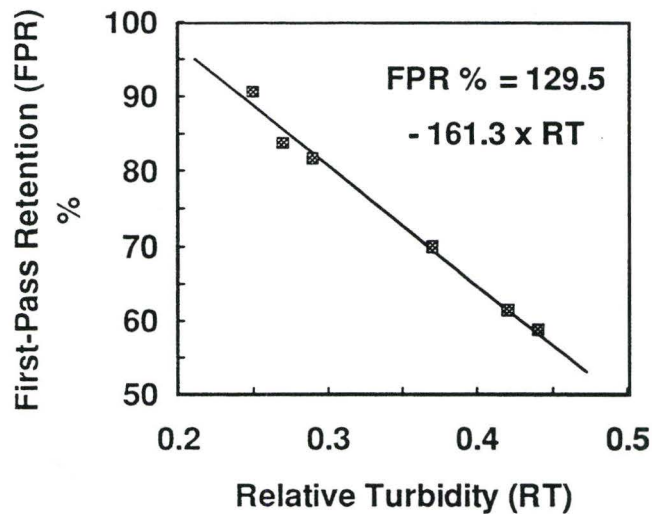


Figure A5-1 Correlation between PFR and relative turbidity

The correlation coefficient is calculated as follows:

$$\text{Correlation coefficient} = \frac{L_{xy}}{\sqrt{L_{xx} \cdot L_{yy}}}$$

where x = relative turbidity; y = FPR %; and $L_{xx} = \sum_{i=1}^n (x_i - \bar{X})^2$, similar expressions for L_{xy} and L_{yy} . The correlation coefficient between relative turbidity and first-pass retention was 0.995 based on the data in the Table .

Appendix A6: Supplementary materials for chapter 6

Observation on the morphology of polystyrene latex flocs

Confocal microscopic observations were conducted in an Micro LSM10 (Zeiss) system. Transmittance laser mode (Argon laser with wavelength 488 nm as light source) was used with the magnification of 40 lens and zoom factor 50 to observe the morphology of the fibers. The latex was observed under a confocal model with scanning 10 to 15 times at different latex floc sections. The pictures (see Figure A6-1) consisted of overlay transmittance observation on fibers and confocal observations on latex flocs.

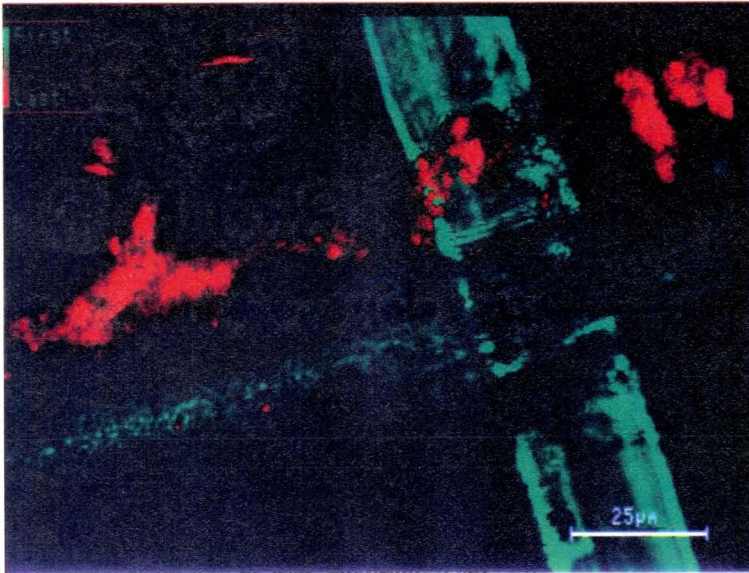
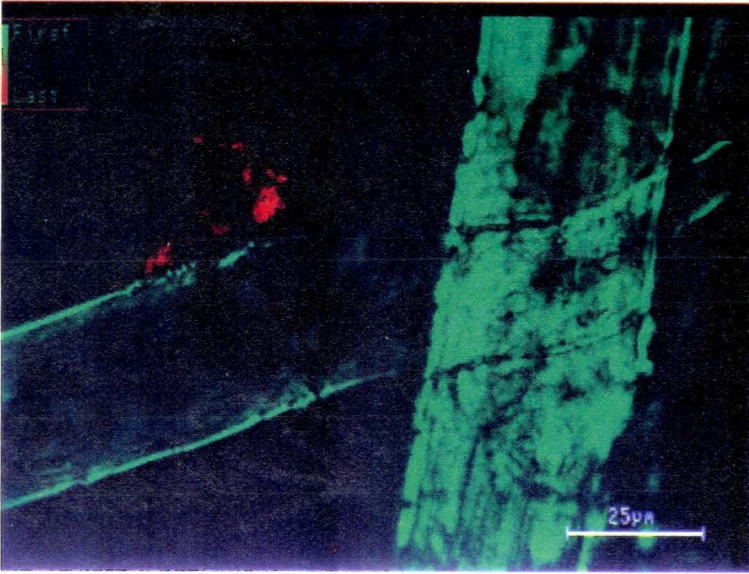


Figure A6-1. Morphology of polystyrene latex floccs formed by PEO/PVPh flocculation system in the presence of bleached fibers. The floccs appear as the red aggregations.